

Kasner bounces and fluctuating collapse inside hairy black holes with charged matter

Warren Li and Maxime Van de Moortel

January 9, 2025

Abstract

We study the interior of black holes in the presence of charged scalar hair of small amplitude ϵ on the event horizon and show their terminal boundary is a crushing Kasner-like singularity. These spacetimes are spherically symmetric, spatially homogeneous and they differ significantly from the hairy black holes with uncharged matter previously studied in [M. Van de Moortel, *Violent nonlinear collapse inside charged hairy black holes*, *Arch. Rational. Mech. Anal.*, 248, 89, 2024] in that the electric field is dynamical and subject to the backreaction of charged matter. We prove this charged backreaction causes drastically different dynamics compared to the uncharged case that ultimately impact the formation of the spacelike singularity, exhibiting novel phenomena such as

- Collapsed oscillations: oscillatory growth of the scalar hair, nonlinearly induced by the collapse
- A fluctuating collapse: The final Kasner exponents' dependency in ϵ is via an expression of the form $|\sin(\omega_0 \cdot \epsilon^{-2} + O(\log(\epsilon^{-1})))|$.
- A Kasner bounce: a transition from an unstable Kasner metric to a different stable Kasner metric

The Kasner bounce occurring in our spacetime is reminiscent of the celebrated BKL scenario in cosmology.

We additionally propose a construction indicating the relevance of the above phenomena – including Kasner bounces – to spacelike singularities inside more general (asymptotically flat) black holes, beyond the hairy case.

While our result applies to all values of $\Lambda \in \mathbb{R}$, in the $\Lambda < 0$ case, our spacetime corresponds to the interior region of a charged asymptotically Anti-de-Sitter stationary black hole, also known as a *holographic superconductor* in high-energy physics, and whose exterior region was rigorously constructed in the recent mathematical work [W. Zheng, *Asymptotically Anti-de Sitter Spherically Symmetric Hairy Black Holes*, arXiv.2410.04758].

Contents

1	Introduction	3
1.1	Rough version of our main result	5
1.2	Differences and connections with non-hairy black holes	10
1.3	Comparison with hairy black hole interiors for other matter models	14
1.4	The collapsed oscillations resulting from the charge of the scalar field	16
1.5	Kasner bounces and connections to cosmology	17
1.6	Holographic superconductors in the AdS-CFT correspondence	20
1.7	Outline of the paper and the different regions of Figure 6	22

2	Geometric set-up and preliminaries	23
2.1	Einstein-Maxwell-Klein-Gordon in double null coordinates	23
2.2	The Reissner-Nordström(-dS/AdS) interior metric	25
2.3	Black hole interiors with charged scalar hair	27
2.4	System of ODEs for spatially homogeneous solutions	30
2.5	Linear scattering in the Reissner-Nordström interior	32
3	Precise statement of the main theorems	33
3.1	Definition of the spacetime sub-regions	33
3.2	First statement: formation of a spacelike singularity	34
3.3	Second statement: Kasner asymptotics in the \mathcal{PK} and \mathcal{K} regions	37
4	Almost formation of a Cauchy horizon	39
4.1	Estimates up to the no-shift region	39
4.2	Estimates on the early blue-shift region	42
4.3	Estimates on the late blue-shift region	45
5	The collapsed oscillations	47
5.1	Bootstraps and preliminary estimates	50
5.2	Scalar field oscillations	51
5.3	Precise estimates for Q and Ω^2	54
6	The Proto-Kasner Region	59
6.1	Estimates beyond the oscillatory region – statement of Proposition 6.1	59
6.2	Proof of Proposition 6.1	60
6.3	The onset of the Kasner-like geometry	63
7	Construction of the sets E_η and $E'_{\eta,\sigma}$ for further quantitative estimates	65
7.1	Improved estimates on $\Theta(\epsilon)$	66
7.2	The measure of the set E_η	72
8	Kasner regimes and bounces	73
8.1	Background on Kasner bounces	74
8.2	The bootstraps, preliminary estimates and statement of Proposition 8.1	74
8.3	The dynamical system for Ψ and the proof of Proposition 8.1	77
8.4	Geometric features of the region \mathcal{K} in the bounce case $ \Psi_i < 1$	83
9	Quantitative Kasner-like asymptotics	86
9.1	Asymptotics for Ψ near the $\{r = 0\}$ singularity	89
9.2	First case: absence of Kasner bounce	90
9.3	Second case: presence of a Kasner bounce	91
9.4	Kasner-like asymptotics in synchronous coordinates in both cases	94
A	Bessel functions	96

1 Introduction

We are interested in the following two fundamental problems in astrophysics and cosmology:

- A. What does the interior of a black hole look like, and how strong is the (potential) singularity within it?
- B. How does the universe behave near its initial time, and is there a “Big Bang” singularity?

As it turns out, these two questions are intimately connected, loosely speaking because a black hole interior’s terminal boundary corresponds to the time-reverse of an initial-time singularity (at least locally).

In the present manuscript, we analyze a class of spatially homogeneous singular spacetimes, with the goal to shed some light on Problem A as our underlying motivation. We will also emphasize the deep connections between Problem A and Problem B: The common theme to both problems are *spacelike singularities* and whether they are stable dynamically. A very important example of such a spacelike singularity at $\{\tau = 0\}$ is given by the so-called Kasner metrics [56], i.e. spatially homogeneous (but potentially anisotropic) spacetimes of the form¹

$$g_K = -d\tau^2 + \tau^{2p_1} dx_1^2 + \tau^{2p_2} dx_2^2 + \tau^{2p_3} dx_3^2, \text{ with } p_1 + p_2 + p_3 = 1. \quad (1.1)$$

The main conjectured dynamics of spacelike singularities (in (3+1)-dimensional vacuum, or for gravity coupled to a reasonable matter model), corresponding respectively to Problem A and Problem B are as follows:

Conjecture A (Spacelike singularity conjecture, [26, 60, 65, 79]). *In the setting of gravitational collapse (one-ended data, left picture in Figure 1), the terminal boundary of a generic asymptotically flat black hole consists of*

- *a null piece emanating from infinity i^+ – the Cauchy horizon \mathcal{CH}_{i^+} , as depicted in Figure 1.*
- *a non-empty spacelike singularity S , such that, for all $p \in S$, the causal past of p has relatively compact intersection with the initial data hypersurface Σ .*

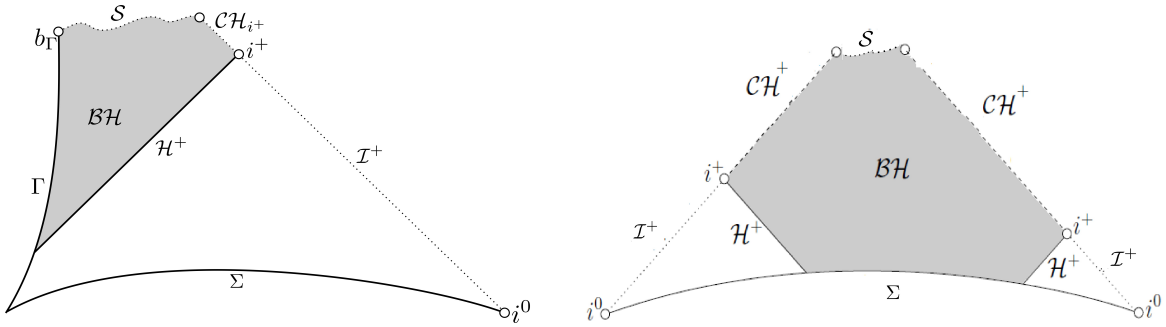


Figure 1: Penrose diagram of a (non-hairy) black hole interior with a Cauchy horizon \mathcal{CH}_{i^+} and a spacelike singularity S . Left: one-ended black hole (gravitational collapse case). Right: two-ended black hole.

The following conjecture regroups a series of heuristics [7, 9, 10, 64] and somewhat imprecise statements regarding the typical behavior near spacelike singularities, and is often termed the “BKL scenario”. In what follows, we imprecisely use the term “Kasner regime” to denote a region of spacetime in which the metric resembles (1.1), in a sense which will be made more precise in Section 1.5 (see also (1.16) and the surrounding discussion).

¹Note that in the original work of Kasner [56], (1.1) is a solution of the Einstein vacuum equations and satisfies the additional condition $p_1^2 + p_2^2 + p_3^2 = 1$. (1.1), however, refers to a Kasner solution in the presence of matter where this constraint is relaxed, see Section 1.5.

Conjecture B. [BKL proposal.] *The dynamics near a generic spacelike, initial cosmological singularity S , once restricted to a region sufficiently close to S , are described as follows.*

1. Asymptotically velocity term dominated behavior. *The causal future $J^+(p)$ of any given point $p \in S$ on the singularity is well-described by a nonlinear system of ODEs, once one is sufficiently close to S . Solutions to these ODEs resemble a sequence of Kasner-like regimes, which may be stable or unstable.*
2. Kasner bounces. *Any unstable Kasner regime transitions towards a (stable or unstable) different Kasner regime.*
- 3.a. (For stiff matter models only) Monotonic regime. *There are finitely many Kasner bounces: ultimately the spacetime only approaches a single (stable) Kasner metric with monotonic dynamics.*
- 3.b. (For vacuum or non-stiff matter) Chaotic regime. *There are infinitely many Kasner bounces between unstable Kasner-like regimes in any generic $J^+(p)$.*

Here, a stiff matter model is either a stiff fluid or scalar field, see [3, 7, 10] for a discussion.

Our objective is to study a class of *spatially homogeneous solutions* of a stiff-matter model: the Einstein–Maxwell–Klein–Gordon equations, in which a *charged* scalar field ϕ is coupled to electromagnetism and gravity.

$$Ric_{\mu\nu}(g) - \frac{1}{2}R(g)g_{\mu\nu} + \Lambda g_{\mu\nu} = \mathbb{T}_{\mu\nu}^{EM} + \mathbb{T}_{\mu\nu}^{KG}, \quad (1.2)$$

$$\mathbb{T}_{\mu\nu}^{EM} = 2 \left(g^{\alpha\beta} F_{\alpha\nu} F_{\beta\mu} - \frac{1}{4} F^{\alpha\beta} F_{\alpha\beta} g_{\mu\nu} \right), \quad \nabla^\mu F_{\mu\nu} = iq_0 \left(\frac{\phi \overline{D_\nu \phi} - \overline{\phi} D_\nu \phi}{2} \right), \quad F = dA, \quad (1.3)$$

$$\mathbb{T}_{\mu\nu}^{KG} = 2 \left(\operatorname{Re}(D_\mu \phi \overline{D_\nu \phi}) - \frac{1}{2} (g^{\alpha\beta} D_\alpha \phi \overline{D_\beta \phi} + m^2 |\phi|^2) g_{\mu\nu} \right), \quad D_\mu = \nabla_\mu + iq_0 A_\mu, \quad (1.4)$$

$$g^{\mu\nu} D_\mu D_\nu \phi = m^2 \phi, \quad (1.5)$$

with $\Lambda \in \mathbb{R}$ the cosmological constant, $m^2 \in \mathbb{R}$ the Klein–Gordon mass, and $q_0 \neq 0$ the scalar field charge.

Our study is based on the evolution of initial data posed on bifurcate characteristic hypersurfaces \mathcal{H}_L and \mathcal{H}_R emulating the event horizons of a two-ended black hole, and we show they lead to a spacelike singularity. Our main Theorem I will also provide a precise near-singularity behavior in terms of one or two Kasner metrics of the form (1.1). In cosmological terms, the spacetimes we construct in Theorem I are so-called Kantowski–Sachs metrics, namely spatially homogeneous, but anisotropic cosmological spacetimes with spatial topology $\mathbb{R} \times \mathbb{S}^2$.

We shall also view each of our constructed spacetimes as the interior region of a so-called *hairy black hole* (see Section 1.6), namely a stationary black hole with non-trivial matter fields (the “hair(s)”) on the horizon (see [23, 52, 82] and references therein for a review of various types of hairy black holes). While our result holds² for any $\Lambda \in \mathbb{R}$, in the $\Lambda < 0$ case, a large class of asymptotically Anti-de-Sitter (AdS) hairy black holes has recently been constructed [84, 83] and their interior region corresponds to the spacetime we construct in our Theorem I (see Section 1.6). Although we only expect to be able to construct an exterior region to our spacetime in the asymptotically AdS case, we nonetheless name our spacetimes hairy black holes for all choices of $\Lambda \in \mathbb{R}$.

Furthermore, for $\Lambda = 0$, our construction from Theorem I has bearings on the interior of (non-hairy) *asymptotically flat black holes* as well, as we explain in Section 1.2. To summarize: the domain of dependence property allows to consider the black hole interior region independently from the black hole exterior (see Figure 4); thus the repercussions of Theorem I extend significantly beyond asymptotically AdS hairy black holes.

²We also note the existence of exponentially growing modes for charged scalar fields on Reissner–Nordström–de Sitter and Kerr–Newman–de Sitter obtained in [11], which might suggest compatibility with the existence of hairy black hole solutions in the $\Lambda > 0$ setting.

1.1 Rough version of our main result

Before explaining the relevance to Conjectures A and B of these novel hairy black hole interiors that we construct, we will first give a rough (but detailed) version of our main result immediately below. To this effect, we recall the well-known interior region of the Reissner–Nordström-(dS/AdS) black hole (see also Section 2.2).

$$g_{RN} = - \left(1 - \frac{2M}{r} + \frac{\mathbf{e}^2}{r^2} - \frac{\Lambda r^2}{3} \right) dt^2 + \left(1 - \frac{2M}{r} + \frac{\mathbf{e}^2}{r^2} - \frac{\Lambda r^2}{3} \right)^{-1} dr^2 + r^2 d\sigma_{\mathbb{S}^2}$$

with parameters (M, \mathbf{e}, Λ) . The hairy black hole constructed in the following Theorem I has initial data (1.6), (1.7) that are $O(\epsilon^2)$ -perturbations of g_{RN} , with scalar hair of initial size ϵ .

Theorem I. [Rough version] *Fix the following characteristic initial data on bifurcate event horizons $\mathcal{H}_L \cup \mathcal{H}_R$:*

$$\phi \equiv \epsilon, \tag{1.6}$$

$$g = g_{RN} + O(\epsilon^2), \tag{1.7}$$

where g_{RN} is a Reissner–Nordström-(dS/AdS) metric with sub-extremal parameters (M, \mathbf{e}, Λ) and $\mathbf{e} \neq 0$.

Define $(\mathcal{M} = \mathbb{R} \times (-\infty, s_\infty) \times \mathbb{S}^2, g, F, \phi)$ to be the maximal globally hyperbolic future development of this data. (\mathcal{M}, g) is a spatially homogeneous, spherically symmetric spacetime, and we write g , F , and ϕ in a suitable gauge as

$$g = \Omega^2(s)[-ds^2 + dt^2] + r^2(s)d\sigma_{\mathbb{S}^2}, \quad F = \frac{Q(s)}{r^2(s)}\Omega^2(s)ds \wedge dt, \quad \phi = \phi(s), \tag{1.8}$$

solving (1.2)–(1.5) with $q_0 \neq 0$ and initial data given by (1.6), (1.7) and $Q|_{\mathcal{H}_L \cup \mathcal{H}_R} \equiv \mathbf{e} \neq 0$.

Let $\eta > 0$ be sufficiently small. Then there exists $\epsilon_0(M, \mathbf{e}, \Lambda, m^2, q_0, \eta) > 0$ and a set $E_\eta \subset (-\epsilon_0, \epsilon_0) \setminus \{0\}$, satisfying $\frac{|(-\delta, \delta) \setminus E_\eta|}{2\delta} = O(\eta)$ for all $0 < \delta \leq \epsilon_0$, such that for all $\epsilon \in E_\eta$, the spacetime (\mathcal{M}, g) terminates at a **spacelike singularity** $\mathcal{S} = \{r = 0\}$, asymptotically described by a Kasner metric of positive exponents $(p_1, p_2, p_3) \in (0, 1)^3$. The spacetime (M, g) may be partitioned into several regions, as illustrated by the Penrose diagram of Figure 2, and has the following features:

1. Almost formation of a Cauchy horizon. In the early regions, (g, F, ϕ) are uniformly close to those of the Reissner–Nordström-(dS/AdS) background, and the scalar field is approximated by a linearly-oscillating profile:

$$\phi(s) = B(M, \mathbf{e}, \Lambda, m^2, q_0) \cdot \epsilon \cdot e^{i\omega_{RN}(q_0, M, \mathbf{e}, \Lambda)s} + \overline{B}(M, \mathbf{e}, \Lambda, m^2, q_0) \cdot \epsilon \cdot e^{-i\omega_{RN}(q_0, M, \mathbf{e}, \Lambda)s} + O(\epsilon^2), \tag{1.9}$$

where $B(M, \mathbf{e}, \Lambda, m^2, q_0) \in \mathbb{C} \setminus \{0\}$ is a linear scattering parameter, and $\omega_{RN}(M, \mathbf{e}, \Lambda, q_0) = |q_0 \mathbf{e}| \cdot \left(\frac{1}{r_-} - \frac{1}{r_+} \right) > 0$. Here $r_\pm(M, \mathbf{e}, \Lambda) > 0$ are respectively the radii of the event and Cauchy horizons of the background Reissner–Nordström-(dS/AdS) metric as defined in Section 2.2.

2. Collapsed oscillations. The scalar field experiences **growing** oscillations while r shrinks towards 0 in the sense described in Section 1.4. More precisely, there exists $C(M, \mathbf{e}, \Lambda, m^2, q_0) \neq 0$ and $\omega_0(M, \mathbf{e}, \Lambda, m^2, q_0) > 0$ and

$$\alpha(\epsilon) = C \cdot \sin(\omega_0 \cdot \epsilon^{-2} + O(\log(\epsilon^{-1}))) + O(\epsilon^2 \log(\epsilon^{-1})) \quad \text{as } |\epsilon| \rightarrow 0, \tag{1.10}$$

so that, on the future boundary of the collapsed oscillations region

$$\phi = \alpha(\epsilon) \text{ and } r \approx \epsilon. \quad (1.11)$$

Note that $\phi|_{r \approx \epsilon} = O(1)$ despite the ϕ initial data being $O(\epsilon)$.

3. Formation of the first Kasner regime. A Kasner regime starts developing with Kasner exponents

$$p_1 = P(\alpha) = \frac{\alpha^2 - 1}{3 + \alpha^2}, \quad p_2 = p_3 = \frac{2}{3 + \alpha^2}, \quad (1.12)$$

where p_1 is the Kasner exponent in the t -direction and $p_2 = p_3$ are the exponents in the \mathbb{S}^2 directions in (1.8).

4. The final Kasner regime. For any fixed $\sigma \in (0, 1)$, we introduce the following disjoint subsets of E_η .

- (Non-bounce case) $\epsilon \in E'_{\eta, \sigma}{}^{Nbo} \subset E_\eta$ if $|\alpha(\epsilon)| \geq 1 + \sigma$ (i.e. $p_1 > 0$). When $\epsilon \in E'_{\eta, \sigma}{}^{Nbo}$, the first Kasner regime is also the final Kasner regime and continues all the way to $\mathcal{S} = \{r = 0\}$ in a monotonic fashion.
- (Kasner bounce case) $\epsilon \in E'_{\eta, \sigma}{}^{bo} \subset E_\eta$ if $\eta \leq |\alpha(\epsilon)| \leq 1 - \sigma$. We have $|E'_{\eta, \sigma}{}^{bo}| > 0$ (in particular $E'_{\eta, \sigma}{}^{bo} \neq \emptyset$). When $\epsilon \in E'_{\eta, \sigma}{}^{bo}$, the above Kasner regime eventually transitions towards a (different) final Kasner regime with positive Kasner exponents

$$p_1 = P\left(\frac{1}{\alpha}\right) = \frac{1 - \alpha^2}{1 + 3\alpha^2}, \quad p_2 = p_3 = \frac{2\alpha^2}{1 + 3\alpha^2}. \quad (1.13)$$

The final Kasner regime then continues all the way to $\mathcal{S} = \{r = 0\}$ in a monotonic fashion.

5. Charge retention of the Kasner singularity. The charge $Q(s)$ admits a limit $Q_\infty \neq 0$ as $r \rightarrow 0$. More precisely

$$Q_\infty = (1 - \nu(M, \mathbf{e}, \Lambda)) \cdot \mathbf{e} + O(\epsilon) \text{ with } \nu(M, \mathbf{e}, \Lambda) \in \left(0, \frac{1}{2}\right), \quad (1.14)$$

$$\text{and } \nu(M, \mathbf{e}, \Lambda) \begin{cases} = \frac{1}{4} & \text{if } \Lambda = 0, \\ \in (0, \frac{1}{4}) & \text{if } \Lambda > 0, \\ \in (\frac{1}{4}, \frac{1}{2}) & \text{if } \Lambda < 0. \end{cases} \quad (1.15)$$

In the above Theorem I, a Kasner regime with Kasner exponents $(p_1, p_2, p_3 = p_2)$ means the metric takes the following approximate spherically symmetric form, where $\chi, \mathcal{R} > 0$ are constants and $\mathcal{E}_R(\tau), \mathcal{E}_R(\tau)$ are errors with a small amplitude of size $O(\epsilon^2)$, which moreover decay as $\tau \rightarrow 0$ (see already (3.26) in Theorem 3.2):

$$g = -d\tau^2 + \chi \cdot (1 + \mathcal{E}_X(\tau))\tau^{2p_1} dt^2 + \mathcal{R} \cdot (1 + \mathcal{E}_R(\tau))\tau^{2p_2} (r_-^2 d\sigma_{\mathbb{S}^2}), \quad (1.16)$$

Metrics of the form (1.16) are called “Kasner-like”, see Section 1.5. Theorem I is a rough version of our main results later stated as Theorem 3.1 and Theorem 3.2. The content of Theorem 3.1 covers the statements 1, 2 and 5 in Theorem I, together with some preliminary estimates towards the statements 3-4. Theorem 3.2 is specifically dedicated to Kasner regimes (including the Kasner bounce phenomenon) and covers the statements 3 and 4 in Theorem I.

Remark 1.1. While Theorem I is in the setting of spherically symmetric spatially homogeneous spacetimes (also known as Kantowski–Sachs cosmologies), it also applies to spatially homogeneous spacetimes with planar sym-

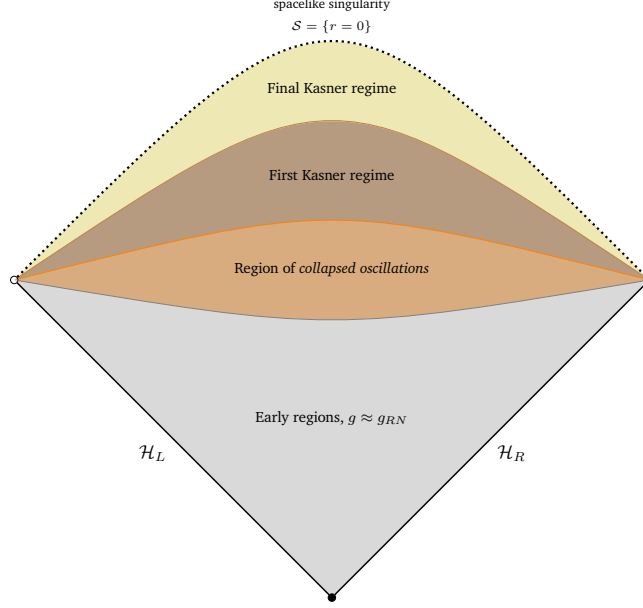


Figure 2: Penrose diagram of the hairy black hole interior from Theorem I. If $|\alpha| \geq 1 + \sigma > 1$, then the first Kasner regime matches the final Kasner regime and continues to $\{r = 0\}$. If $0 < \eta \leq |\alpha| \leq 1 - \sigma < 1$, then there is a Kasner bounce between the first and final Kasner regimes. A more detailed breakdown is given in Figure 6.

metry. While (1.2)–(1.5) take a slightly different form in the planar symmetric setting, our analysis still carries³ through, and the conclusions of Theorem I hold mutatis mutandis, see Remark 2.1.

Remark 1.2. The constants $\eta, \sigma > 0$, presumed small throughout this article, are present to ensure that $\alpha(\epsilon)$ is bounded away from $\{0, 1\}$. Note that we do not obtain a statement for every sufficiently small ϵ , but only for a set E_η , which features an $O(\eta)$ loss in the sense given above. However, the methods used to prove Theorem I allow for $|1 - \alpha|\epsilon^{-0.01} > 1$ or $|\alpha|\epsilon^{-0.01} > 1$, with only minor adjustments. Understanding what happens when say $|1 - \alpha| \ll \epsilon^2$ or $|\alpha| \ll \epsilon^2$, is an interesting open problem (see Section 1.5 and 1.6).

We will now discuss the relations between Theorem I, Problem A and Problem B. The following paragraphs provide short summaries of the subsequent sections in the introduction. One of the main features is the existence of a *Kasner bounce*: we provide the first rigorous example of a spacetime in which **an unstable Kasner regime forms dynamically, and then disappears under the Kasner bounce**.

Differences and connections with non-hairy black holes The hairy black holes of Theorem I and the uncharged-matter ones from [81] have a spacelike singularity $S = \{r = 0\}$ and no Cauchy horizon (see Section 1.2) and, in that, differ globally from the non-hairy black holes corresponding to Conjecture A (compare Figure 1 and Figure 2). However, the domain of dependence property (in two-ended black holes⁴) shows that the spacelike singularity S in non-hairy black holes can arise from initial data that is locally similar to the data of Theorem I, see Figure 4. Therefore, our new theorem on hairy black holes may also dictate the qualitative behavior of the spacelike singularity S inside the *non-hairy black holes* of Conjecture A (see Section 1.2 for a discussion). Lastly, our proof opens the door to studying spacelike singularity beyond the spatially homogeneous case in subsequent

³Note, however, that the only known planar symmetric analog of the Reissner–Nordström black hole is a solution of (1.2)–(1.5) with $\Lambda < 0$, so the planar symmetric equivalent of Theorem I is restricted to the negative cosmological constant setting.

⁴The differences between one-ended and two-ended black holes in Figure 1 will be elaborated upon in Section 1.2. For now, let us note that the *appearance of the spacelike singularity*, i.e. $S \neq \emptyset$, crucially depends on whether the black hole is one-ended or two-ended [79]. However, numerics indicate that the quantitative behavior near the spacelike singularity is similar in the one or two ended case.

works – notably in spherical symmetry – see Open Problem a.

Comparison with hairy black hole interiors for other matter models The Kasner exponents’ dependency on $\sin(\omega_0 \cdot \epsilon^{-2} + O(\log(\epsilon^{-1})))$ found in Theorem I gives rise to fluctuations near $\epsilon = 0$: we term this phenomenon the *fluctuating collapse*. The fluctuating collapse and Kasner bounces from Theorem I contrast with the *violent nonlinear collapse* of the *uncharged* hairy black holes ((1.2)-(1.5) with $q_0 = 0$, also a stiff model) found in [81] (see Section 1.3). Recall from [81] that in the $q_0 = 0$ case, *there is no Kasner bounce*, and the final Kasner exponents and curvature are of the form

$$(p_1, p_2, p_3) = (1 - O(\epsilon^2), O(\epsilon^2), O(\epsilon^2)), K(r) \approx r^{-O(\epsilon^{-2})}.$$

The name “violent collapse” in the $q_0 = 0$ comes from the $O(\epsilon^{-2})$ power in the blow-up rate of the curvature $K(r)$, which becomes *more singular* as $\epsilon \rightarrow 0$. This is an example of a singular limit, since $\epsilon = 0$ corresponds to Reissner–Nordström, while we can make sense of the $\epsilon \rightarrow 0$ (weak) limit in the appropriate region using

$$\lim_{\epsilon \rightarrow 0} (p_1, p_2, p_3)(\epsilon) = (1, 0, 0), \text{ which corresponds to a subset of Minkowski.}$$

In contrast, in the $q_0 \neq 0$ case newly studied in our Theorem I, there is *not even a weak limit* as $\epsilon \rightarrow 0$, since $(p_1, p_2, p_3)(\epsilon)$ depends on $\sin(\omega_0 \cdot \epsilon^{-2} + O(\log(\epsilon^{-1})))$ as discussed above. Also, in the $q_0 \neq 0$ case, any neighborhood of $\epsilon = 0$ contains all (positive) Kasner exponents (away from the degenerate cases), whereas in the $q_0 = 0$ case of [81] a neighborhood of $\epsilon = 0$ is mapped into a neighborhood of $(p_1, p_2, p_3) = (1, 0, 0)$.

Lastly, we mention that previous numerics in the physics literature also predicted the presence of Kasner bounces in the interior of Einstein–Yang–Mills hairy black holes [36, 14, 82]. It is a very interesting open problem to compare these Kasner bounces with the one obtained in the setting of Theorem I.

Collapsed oscillations and charge retention The main new phenomenon driving the dynamics of Theorem I are what we term *collapsed oscillations*. Even at the linear level, a (spatially homogeneous) charged scalar field has (infinite) linear oscillations of the form (1.9) near the Cauchy horizon of the Reissner–Nordström interior spacetime [59]. In the nonlinear setting, such linear oscillations appear in some “early regions” in the dynamics (namely \mathcal{EB} and \mathcal{LB} in Figure 6). Subsequently, these oscillations start interacting nonlinearly with the collapse process (as r gets closer to 0), leading to a Bessel-function type behavior in terms of $\frac{r}{\epsilon}$. Because $\frac{r}{\epsilon}$ is a *decreasing* function of time, this Bessel behavior leads to *growth of the scalar field* which transitions from amplitude ϵ to amplitude $\alpha(\epsilon) = O(1)$. We will elaborate on collapsed oscillations and their mechanism in Section 1.4.

Another important question relating to Problem A is whether spacelike singularities can retain charge/angular momentum. This issue is puzzling, as the only explicit black hole solution with a spacelike singularity is the Schwarzschild interior, which is uncharged and non-rotating. In point 5 of Theorem I, we exhibit a *mechanism of discharge* of the black hole, passing from e at the event horizon $\mathcal{H} = \mathcal{H}_L \cup \mathcal{H}_R$ to $(1 - \delta)e$ at the spacelike singularity \mathcal{S} , where $\delta \in (0, \frac{1}{2})$. Note that the *discharge is not complete* and the spacelike singularity retains a non-zero final charge $(1 - \delta)e$. It is remarkable that, for $\Lambda = 0$, the discharge ratio $\delta = \frac{1}{4}$ is independent of the black hole parameters. To the best of our knowledge, the spacetime of Theorem I is the first example of a spacelike singularity retaining⁵ charge. The main mechanism of discharge and charge retention occurs at the

⁵We note that the charged hairy black holes with uncharged matter from [81] also had non-zero charge, but it is not dynamical.

same time as the collapsed oscillations, and the charge varies little past the collapsed oscillations region (see Figure 1) until the spacelike singularity, see Remark 1.9.

Kasner bounces In Theorem I, we show that if $|\alpha(\epsilon)| = C \cdot |\sin(\omega_0 \epsilon^{-2} + O(\log(\epsilon^{-1})))| + O(\epsilon^2 \log(\epsilon^{-1})) < 1$, then there will be a Kasner bounce. For $(M, e, \Lambda, m^2, q_0)$ such that $C(M, e, \Lambda, m^2, q_0) > 1$, the bounce condition $C \cdot |\sin(\omega_0 \epsilon^{-2} + O(\log(\epsilon^{-1})))| < 1$ holds for all $\epsilon \in E_\eta^{bo} \cap (0, \epsilon_0)$, where E_η^{bo} has non-zero measure: in fact $|E_\eta^{bo} \cap (0, \epsilon_0)| \approx \frac{\epsilon_0}{C}$ if $C \gg 1$. On the other hand, if $C(M, e, \Lambda, m^2, q_0) < 1$, then the bounce condition always holds. These Kasner bounces have the following features:

1. For some range of proper time $\{e^{-b^2(\alpha) \cdot \epsilon^{-2}} \ll \tau < \epsilon^{q^2(\alpha)}\}$ with $q(\alpha) > 0$, $b(\alpha) > 0$, the metric is uniformly close to a $(p_1, \frac{1-p_1}{2}, \frac{1-p_1}{2})$ Kasner-(like) metric, where $p_1(\epsilon) \approx \frac{\alpha^2-1}{3+\alpha^2} < 0$.
2. In the smallest values of proper time from the singularity $\{0 < \tau \ll e^{-b^2(\alpha) \cdot \epsilon^{-2}}\}$, the metric is uniformly close to, and indeed converges as $\tau \rightarrow 0$ towards, a $(\dot{p}_1, \frac{1-\dot{p}_1}{2}, \frac{1-\dot{p}_1}{2})$ Kasner-(like) metric, where $\dot{p}_1(\epsilon) \approx \frac{1-\alpha^2}{1+3\alpha^2} > 0$.

Remark 1.3. When writing (imprecisely) $e^{-b^2(\alpha) \cdot \epsilon^{-2}} \ll \tau$, we mean $\epsilon^{-N_1} \cdot e^{-b^2(\alpha) \cdot \epsilon^{-2}} < \tau$ for some $N_1 > 0$, and similarly $\tau \ll e^{-b^2(\alpha) \cdot \epsilon^{-2}}$ means $\tau < \epsilon^{N_2} \cdot e^{-b^2(\alpha) \cdot \epsilon^{-2}}$ for $N_2 > 0$, so that the transition region in between the two Kasner regimes has size $O(\log(\epsilon^{-1}))$ in terms of $\log(\tau^{-1})$, while $\log(\tau^{-1}) \approx \epsilon^{-2}$ at the times where the bounce is occurring. We interpret this to mean that the bounce occurs very quickly in terms of proper time τ .

We note that the final (post-bounce) Kasner regime has $(\dot{p}_1, \dot{p}_2, \dot{p}_3) \in (0, 1)^3$, while the pre-bounce Kasner has $p_1 < 0$. This is consistent with the early predictions of BKL [7, 9, 10] that Kasner metrics with positive Kasner exponents are stable, while those with at least one negative exponent are unstable (see Section 1.5 for an extended discussion).

Holographic superconductors in the AdS-CFT correspondence The numerical study [47] already predicted the scenario of Theorem I and the presence of Kasner bounces in this context. Beyond the setting of Theorem I (which features zero, or one Kasner bounce depending on ϵ), [47] also discusses the possibility of having *two* (or more) Kasner bounces. The original motivation of [47] is related to a body of work on the physical significance of the hairy black hole (including its asymptotically AdS exterior region) of Theorem I, claimed to be the model for a *holographic superconductor* in the context of the AdS-CFT theory (see Section 1.6).

Outline of the rest of the Introduction

- In Section 1.2, we will first extend our discussion of Problem A and Conjecture A and elaborate on the links between non-hairy black holes and Theorem I. We will also review, in this context, the existing literature on the interior of black holes, and discuss some open problems.
- In Section 1.3, we will compare our new hairy black holes with charged matter from Theorem I to hairy black holes arising from other matter models. We will, in particular, discuss the charged hairy black holes with uncharged matter from [81], whose setting and model are very similar to that of Theorem I, but the late-time spacetime dynamics end up being very different.
- In Section 1.4, we will discuss one of the two primary nonlinear mechanisms governing the dynamics of the spacetime of Theorem I: *the collapsed oscillations*, which lead to the growth of the scalar field. We

will explain in particular how this phenomenon arises from the interaction between the linear oscillatory behavior for charged scalar fields at the Reissner–Nordström Cauchy horizon on the one hand, and the tendency of the Einstein equations to form a spacelike singularity $\{r = 0\}$ on the other hand.

- In Section 1.5, we will discuss the other primary nonlinear mechanism at play: the occurrence of *Kasner bounces*. This phenomenon has previously been investigated in depth in the cosmological setting, and we will elaborate on the connection with the pre-existing literature regarding such phenomena.
- In Section 1.6, we will discuss the *exterior region* corresponding to the black hole interior of Theorem I, the most physically relevant case of which is asymptotically Anti-de-Sitter. We will emphasize the physical motivation in studying these spacetimes, called *holographic superconductors*, which have been discovered and studied in the high-energy physics literature most notably in the context of the AdS-CFT correspondence.
- In Section 1.7, we give an outline of the paper and introduce the different regions of Figure 6.

1.2 Differences and connections with non-hairy black holes

The spacetimes constructed in Theorem I are spatially homogeneous and we interpret them as the interior region of so-called “hairy black holes”. The main distinctive feature of “hairy black holes” is the presence of so-called *scalar hair*, meaning that the scalar field ϕ in (1.5) *does not decay on the event horizon* \mathcal{H}^+ and tends to a non-zero constant instead. (In the case of the hairy black holes of Theorem I, ϕ is identically equal to this constant on $\mathcal{H} = \mathcal{H}_L \cup \mathcal{H}_R$, see (1.6)).

We have already explained that it is not possible to obtain an asymptotically flat spherically symmetric hairy black hole exterior solution of (1.2)–(1.5) with $\Lambda = 0$; however, as we will discuss in Section 1.6, the construction of a such hairy black hole exterior is possible for asymptotically-AdS data, with $\Lambda < 0$ in (1.2). Such a construction will necessarily involve a static exterior region, while the corresponding interior is spatially homogeneous, see Section 2 for a proof of this claim. This is due to the fact that for a t -independent black hole, t is a timelike coordinate in the exterior which, by definition, becomes a spacelike coordinate in the black hole interior.

Nonetheless, one may also wish to consider asymptotically flat (where $\Lambda = 0$) spacetimes which are relevant to the study of astrophysical black holes. In this context, one anticipates that solutions of (1.2)–(1.5) with regular Cauchy data *decay* towards a Reissner–Nordström exterior solution, in particular ϕ tends to 0 on \mathcal{H}^+ (in spherical symmetry, see [27, 66] for (1.2)–(1.5) with $q_0 = m^2 = 0$, and also [75] for small $|q_0\mathbf{e}|$ on a fixed Reissner–Nordström exterior). The resulting black holes thus feature ϕ decaying on \mathcal{H}^+ at the following rate: for all $v > 1$,

$$|\phi|_{|\mathcal{H}^+}(v) + |D_v\phi|_{|\mathcal{H}^+}(v) \lesssim v^{-s}, \quad (1.17)$$

where v is a standard Eddington–Finkelstein type advanced-time coordinate and $s > \frac{1}{2}$. We will call such black holes “non-hairy” in the sequel, to mark the contrast with the black holes from Theorem I.

The interior of the non-hairy black hole solving (1.2)–(1.5) in spherical symmetry was studied in [59, 76, 77, 79, 78] and their Penrose diagram was completely characterized (modulo issues related to locally naked singularities, see the second paragraph below). In this section, we will briefly explain these results and provide contrast with our hairy black hole interiors from Theorem I. We also comment that one can use our hairy black hole interiors as a tool to retrieve information on non-hairy black holes, connecting Theorem I to Conjecture A, see the third paragraph below.

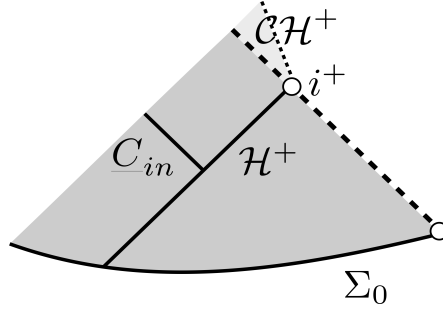


Figure 3: Penrose diagram of the spacetime corresponding to Theorem 1.1

Local structure of the non-hairy black hole interior near infinity i^+ We discuss the terminal boundary of the black hole interior. In the case of the hairy black holes of Theorem I, it is entirely spacelike $\mathcal{S} = \{r = 0\}$. In contrast, for (spherically symmetric) non-hairy black holes solutions of, the terminal boundary is *not* entirely spacelike and admits a null component near i^+ – called the Cauchy horizon $\mathcal{CH}^+ \neq \emptyset$. This fact constitutes the most important difference between hairy and non-hairy black holes.

Theorem 1.1 ([76]). *Consider regular spherically symmetric characteristic data on $\mathcal{H}^+ \cup \underline{C}_{in}$, where $\mathcal{H}^+ := [1, +\infty)_v \times \mathbb{S}^2$, converging to a sub-extremal Reissner–Nordström exterior as (1.17). Then, restricting \underline{C}_{in} to be sufficiently short, the future domain of dependence of $\mathcal{H}^+ \cup \underline{C}_{in}$ is bounded by a Cauchy horizon \mathcal{CH}^+ , namely a null boundary emanating from i^+ and foliated by spheres of strictly positive area-radius r , as depicted in Figure 3.*

Remark 1.4. We note that the presence of a Cauchy horizon $\mathcal{CH}^+ \neq \emptyset$ in the interior of dynamical black holes is not specific to spherical symmetry: for instance, it has been obtained for perturbations of Kerr for the Einstein vacuum equations (without symmetry) in [26]. Whether Theorem 1.1 can be generalized to (1.2)-(1.5) without spherical symmetry is an interesting open problem, in view of the particularly slow decay of the form (1.17) one has to assume in the presence of matter (see [58, 65, 77] for an extended discussion of slow decay).

Global structure of non-hairy black hole interiors Theorem 1.1 only gives information on a local region located near i^+ (see Figure 3). The *global nature of the terminal boundary*, as it turns out (see Theorem 1.2), depends on the topology of the initial data; we distinguish two important cases:

- The two-ended case (topology of time-slices: $\mathbb{R} \times \mathbb{S}^2$). The maximally-extended Schwarzschild/Reissner–Nordström/Kerr spacetimes, and our hairy black holes from Theorem I possess the two-ended topology.
- The one-ended case (topology of time-slices: \mathbb{R}^3) is the topology suitable to studying the gravitational collapse of a star into a black hole [19, 60, 65, 79] (referred to as “gravitational collapse” for short).

In the one-ended case b, the following is known about the terminal boundary.

Theorem 1.2 (Black hole interior in gravitational collapse, [79, 75, 78]). *We consider a one-ended black hole interior, under the assumptions of Theorem 1.1 and additional inverse-polynomial lower bounds on ϕ consistent with (1.17). Then, assuming the absence of locally naked singularities emanating from the center Γ , there is a (non-empty) spacelike singularity $\mathcal{S} = \{r = 0\}$ and the Penrose diagram is given by the left-most of Figure 1.*

Remark 1.5. A locally naked singularity is an (outgoing) null boundary \mathcal{CH}_Γ emanating from the center Γ . Assuming their absence in Theorem 1.2 is unavoidable, since examples of locally naked singularities have been

constructed [21] for (1.2)-(1.5). However, for (1.2)-(1.5) with $F \equiv 0$, such locally naked singularities are non-generic within spherical symmetry [20, 22] and one may conjecture the same statement in the more general situation where $F \neq 0$. See [60, 79] for an extended discussion of this delicate issue.

For two-ended black holes (irrelevant, however, to gravitational collapse), Theorem 1.2 is false because small perturbations of Reissner–Nordstrom obeying (1.17) feature no spacelike singularity [25]. However, it is conjectured [25, 29, 60] that, even in the two-ended case, large perturbations would yield a spacelike singularity $\mathcal{S} = \{r = 0\} \neq \emptyset$ and a Penrose diagram corresponding to the rightmost in Figure 1.

Remark 1.6. Note that for a two-ended black hole as in the rightmost Penrose diagram of Figure 1, the causal past of any compact subset of \mathcal{S} intersects the event horizon \mathcal{H}^+ on a set with compact closure. This observation will be important in the discussion of the next paragraph, see Figure 4.

We conclude this section by mentioning previous works providing a pretty detailed characterization of spacelike singularities in spherical symmetry [1, 2, 18, 19, 20, 22] in the uncharged case (i.e. (1.2)-(1.5) with $F \equiv 0$).

Connections between hairy and non-hairy black holes and related open problems We come back to our original motivation: Conjecture A and understanding spacelike singularities inside black holes. Our goal is to construct a large class of (asymptotically flat) black holes with *both* a spacelike singularity $\mathcal{S} = \{r = 0\}$ and a null Cauchy horizon \mathcal{CH}^+ , with precise quantitative information on (at least part of) $\mathcal{S} = \{r = 0\}$.

It is an open problem to provide a quantitative description of the spacelike singularity inside any charged⁶ or rotating black hole (note indeed that Theorem 1.2 does not describe \mathcal{S} quantitatively). In the two-ended case, however, we propose a construction of a black hole featuring both a null Cauchy horizon $\mathcal{CH}^+ \neq \emptyset$, and a spacelike singularity \mathcal{S} which is partially described by the terminal boundary in Theorem I.

Parameterize the two event horizons by $\mathcal{H}_R = \{(-\infty, v), v \in \mathbb{R}\}$, $\mathcal{H}_L = \{(u, -\infty), u \in \mathbb{R}\}$.

- i. Fix $\phi|_{\mathcal{H}_R^+}(v) \equiv \epsilon$ for $v \leq A$, and $\phi|_{\mathcal{H}_L^+}(u) \equiv \epsilon$ for $u \leq A$, for some large A depending on ϵ . We evolve (non-uniquely) this characteristic data on $(\mathcal{H}_R \cap \{v \leq A\}) \cup (\mathcal{H}_L \cap \{u \leq A\})$ towards the past in the following fashion:

- Attach a small past-directed ingoing (respectively outgoing) cone \underline{C}_R^+ (respectively C_L^+) to the future-endpoint of $\mathcal{H}_R \cap \{v \leq A\}$ (respectively $(\mathcal{H}_L \cap \{u \leq A\})$).
- By local well-posedness, the past domain of influence of $\mathcal{H}_R \cap \{v \leq A\} \cup \underline{C}_R^+$ (respectively $\mathcal{H}_L \cap \{u \leq A\} \cup C_L^+$) is the causal rectangle with past ingoing boundary \underline{C}_R^- (respectively C_L^-).
- Evolving the initial data on $\underline{C}_R^- \cup C_L^-$ towards the past and appealing to local well-posedness again provides another smaller causal rectangle. This rectangle combines with the two previously-constructed rectangles into the (future) domain of influence of some $C_{out} \cup \underline{C}_{in}$.

We obtain a (non-unique) solution to (1.2)–(1.5) up to the bifurcate null cones $C_{out} \cup \underline{C}_{in}$ (see Figure 4).

- ii. Extend C_{out} (respectively \underline{C}_{in}) into an outgoing (respectively ingoing) cone which is asymptotically flat using a standard truncation argument (see [21, 69]). The bifurcate null cones $\tilde{C}_{out} \cup \tilde{C}_{in}$ thus obtained intersect (what should be thought of as) future null infinity $\mathcal{I}^+ = \mathcal{I}_L^+ \cup \mathcal{I}_R^+$, and $\phi|_{\tilde{C}_{out} \cup \tilde{C}_{in}}$ decays towards \mathcal{I}^+ .

⁶Note, however, that it is possible to describe asymptotically Schwarzschild one-ended uncharged spherically symmetric black holes [1].

Open problem a. Construct a (one or two)-ended black hole with a Cauchy horizon $\mathcal{CH}^+ \neq \emptyset$ and a spacelike singularity $\mathcal{S} \neq \emptyset$, which coincides with the hairy black hole singularity \mathcal{S} from Theorem I away from $\mathcal{CH}^+ \cap \mathcal{S}$.

Our road-map towards a resolution of Open Problem a shows that the fluctuations and Kasner bounces of Theorem I **can play a role in the interior of asymptotically flat, non-hairy black holes**. We find it striking that, even when restricted to spherical symmetry, the spacelike singularity inside a black hole can obey such intricate dynamics. It is an interesting open problem to study the stability of these dynamics outside of any symmetry assumption and thus gauge their relevance to generic black hole solutions.

To understand a larger class of black holes with both a Cauchy horizon $\mathcal{CH}^+ \neq \emptyset$ and a spacelike singularity $\mathcal{S} \neq \emptyset$, it is of interest to perturb the hairy black hole of Theorem I within spherical symmetry but relaxing spatial homogeneity. Subsequently following steps i-iv, where g_ϵ is replaced by a perturbed spacetime, will yield even more general insights than Open Problem a into spherically symmetric spacelike inside black holes, which we formalize in the following open problem (note Open Problem b is the charged ($q_0 \neq 0$) version of Open Problem v in [81]).

Open problem b. Consider (two-ended) initial data on \mathcal{H}^+ such that, instead of (1.6):

$$|\phi|_{\mathcal{H}^+}(v) - \epsilon \leq |\epsilon|^N \cdot e^{-C_0 v} \quad (1.18)$$

for $\epsilon \in E_\eta$, as defined in Theorem I, with $N > 0$ and $C_0 > 0$ sufficiently large constants. Prove (or disprove) that the terminal boundary is spacelike, and provide (reasonably) precise quantitative estimates.

Then, construct a (one or two)-ended black hole with a Cauchy horizon $\mathcal{CH}^+ \neq \emptyset$ and a spacelike singularity $\mathcal{S} \neq \emptyset$, which coincides with the above perturbed hairy black hole singularity \mathcal{S} away from $\mathcal{CH}^+ \cap \mathcal{S}$.

We finally want to emphasize that our quantitative methods give hope to transpose some results of Theorem I to towards Open Problem b. We hope to return to these very interesting questions in future work.

1.3 Comparison with hairy black hole interiors for other matter models

The charged hairy black holes with uncharged matter from [81] An alternative to studying (1.2)-(1.5) with a charged scalar field ($q_0 \neq 0$) is to study the uncharged scalar field case $q_0 = 0$ where the Maxwell field $F \neq 0$ does not interact with ϕ . This was first done numerically in [46] and then rigorously by the second author [81] and qualified as “violent nonlinear collapse”. It is remarkable that the behavior in the $q_0 = 0$ case differs drastically from what we found in the $q_0 \neq 0$ case in Theorem I, as the following result shows.

Theorem 1.3 ([81]). *We make the same assumptions as Theorem I, except that now $q_0 = 0$, hence $F = \frac{\mathbf{e}}{r^2(s)} \Omega^2 ds \wedge dt$, where $\mathbf{e} \neq 0$. Then, for almost all sub-extremal parameters $(M, \mathbf{e}, \Lambda, m^2)$, there exists $\epsilon_0(M, \mathbf{e}, \Lambda, m^2) > 0$ such that, for all $0 < |\epsilon| < \epsilon_0$, the spacetime (\mathcal{M}, g) ends at a spacelike singularity $\mathcal{S} = \{r = 0\}$ asymptotically described by a Kasner metric with exponents $(p_1, p_2, p_3) = (1, 0, 0) + O(\epsilon^2) \in (0, 1)^3$ and given by Figure 5. Moreover, the Kretschmann scalar $\mathcal{K} = R^{\alpha\beta\gamma\delta} R_{\alpha\beta\gamma\delta}$ blows up at a rate $r^{-C \cdot \epsilon^{-2} + O(\epsilon^{-1})}$ on $\mathcal{S} = \{r = 0\}$ for $C(M, \mathbf{e}, \Lambda, m^2) > 0$.*

We point out the following similarities and differences between Theorem 1.3 and Theorem I.

1. In both cases, the terminal boundary is a spacelike singularity $\mathcal{S} = \{r = 0\}$ approximately described by a Kasner metric (1.1) with positive Kasner exponents (compare Figure 2 and Figure 5).

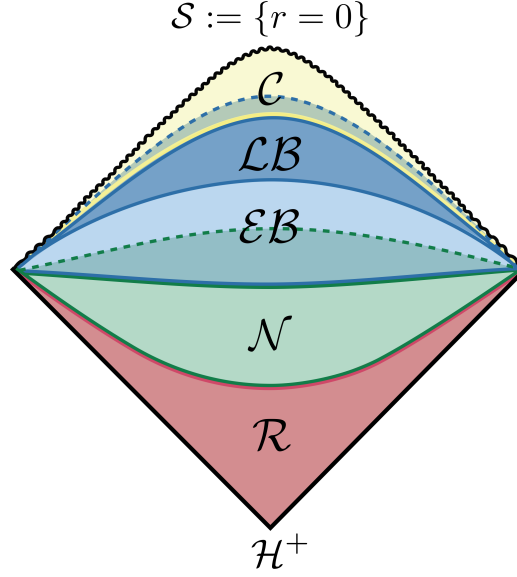


Figure 5: The Penrose diagram of the hairy black hole interiors constructed in Theorem 1.3.

2. In both cases, the early regions are similar and governed by the almost formation of a Cauchy horizon.
3. In both cases, the Maxwell charge Q is uniformly bounded away from 0: in Theorem 1.3, this is trivial ($Q = e \neq 0$ is constant), in Theorem I, this is item 5, a surprising property that we call “charge retention”.
4. Even at the linear level (i.e. (1.5) on a fixed Reissner–Nordström interior), (1.9) is not true if $q_0 = 0$: the scalar field does not oscillate, it grows instead like $\phi \approx \epsilon \cdot s$, where $\mathcal{CH}^+ = \{s = \infty\}$ (except possibly for an exceptional set of (M, e, Λ, m^2) of 0-Lebesgue measure that leads to the absence of growth, see [57, 81], which is why one restricts to *almost* every parameter in Theorem 1.3).
5. The oscillating profile (1.9) turns it a Bessel-type growing oscillation as $r \rightarrow 0$, after which $|\phi|$ becomes $O(1)$ around $r \approx \epsilon$ (collapsed oscillations). There is no such mechanism in Theorem 1.3.
6. The final Kasner exponent $p_1 \in (0, 1)$ in Theorem I is related to $|\sin(\omega_0 \epsilon^{-2} + O(\log(\epsilon^{-1})))|$, but we restrict ϵ so that p_1 is bounded away from 0 and 1, so there is no overlap (by our assumptions) with any of the Kasner exponents obtained in Theorem 1.3 where $|p_1 - 1| \lesssim \epsilon^2$.
7. As a consequence, the collapse in Theorem I is *not violent* but instead rapidly fluctuating in ϵ : one can easily see that \mathcal{K} blows up at a rate r^{-q} , where q depends on $\sin(\omega_0 \cdot \epsilon^{-2} + O(\log(\epsilon^{-1})))$.
8. There is no Kasner bounce in the $q_0 = 0$ setting: in fact, in Theorem 1.3 one proves that the final exponent p_1 lies in $(0, 1)$, so there is no mechanism triggering a Kasner bounce. In contrast, in Theorem I, in the regimes where $|\sin(\omega_0 \cdot \epsilon^{-2} + O(\log(\epsilon^{-1})))|$ is too small, a Kasner regime with $\dot{p}_1 < 0$ forms, which is unstable, and ultimately disappears under Kasner bounce, giving rise to a second Kasner regime with $p_1 \in (0, 1)$.

We also remark that Theorem I restricts ϵ to a subset of $(-\epsilon_0, \epsilon_0) \setminus \{0\}$, which is the complement of a set of small measure, while Theorem 1.3 does not have this restriction. The restriction is to ensure that the final p_1 is bounded away from $\{0, 1\}$ in Theorem I, as we explained above.

Finally, we note that Theorem 1.3 should lead to a resolution of Open Problem a in the case of an uncharged, massive scalar field (i.e. (1.2)-(1.5) with $q_0 = 0, m^2 \neq 0$), upon the proof of (1.17) for $m^2 \neq 0$ (i.e. step iv in the

last paragraph of Section 1.2).

Other hairy black holes The study of spatially homogeneous hairy black holes has been abundant both in the mathematics and physics literature: we first mention the important examples of Einstein–Yang–Mills hairy black holes [13, 14, 16, 36, 72, 73]. For the Einstein–Yang–Mills black holes, the above work suggest the presence of a spacelike singularity preceded by (potentially many) Kasner bounces, although the qualitative behavior is different than what we obtained for charged scalar fields in Theorem I. Finally, we mention the existence of rotating hairy black holes with massive Klein–Gordon fields [17, 34, 51]; The study of the interior of these rotating hairy black holes remains an open problem.

We refer the reader to the introductions of [17, 81] for an extended discussion of various hairy black holes.

1.4 The collapsed oscillations resulting from the charge of the scalar field

The collapsed oscillations occur in a region $\mathcal{O} = \{\epsilon \lesssim r \lesssim r_-\}$ (see Figure 2). The key point is that, schematically, ϕ will be shown to obey the following Bessel equation of order 0 in \mathcal{O} , with respect to a new variable which is the renormalized square of the area-radius $z := \frac{r^2}{\epsilon^2}$:

$$\frac{d}{dz} \left(z \frac{d\phi}{dz} \right) + \xi_0^2 z \phi = \text{error}. \quad (1.19)$$

Here $\xi_0 \neq 0$ is a constant proportional⁷ to q_0 . To simplify the discussion here, we normalize $\xi_0 = 1$. Since $1 \lesssim z \lesssim \epsilon^{-2}$, we need to understand the behavior for large z : it is given by damped oscillations of the form

$$Y_0(z) \sim \sqrt{\frac{2}{\pi z}} \cos\left(z - \frac{\pi}{4}\right) \text{ or } J_0(z) \sim \sqrt{\frac{2}{\pi z}} \sin\left(z - \frac{\pi}{4}\right) \text{ as } z \rightarrow +\infty. \quad (1.20)$$

Note, however, that z is a past-directed timelike variable, so the damping is “backwards-in-time”. Thus $|Y_0(z)|, |J_0(z)| \lesssim \epsilon$ on the past boundary $z \sim \epsilon^{-2}$ of \mathcal{O} , but $|Y_0(z)|, |J_0(z)| \lesssim 1$ on the future boundary $z \approx 1$ of \mathcal{O} ; modulo the oscillations, this means that *the scalar field amplitude has experienced growth of size ϵ^{-1} in \mathcal{O} .*

Remark 1.8. Note that, as long as r is bounded away from 0, (1.19) is consistent with (linear) oscillations giving rise to (1.9): it is only as r gets close to 0 that these oscillations provide growth, hence the name “collapsed oscillations”. We will show, however, that as soon as $r \ll \epsilon$, ϕ no longer oscillates, see Section 1.5.

The algebraic relations connecting (1.20) to the ODE initial conditions $\phi(r \approx r_-)$ will ultimately show that ϕ has the following schematic form at the exit of the collapsed oscillations region \mathcal{O} :

$$\phi(r) \approx C_J \cos(\omega_0 \cdot \epsilon^{-2} + O(\log(\epsilon^{-1}))) J_0\left(\xi_0 \frac{r^2}{\epsilon^2}\right) + C_Y \sin(\omega_0 \cdot \epsilon^{-2} + O(\log(\epsilon^{-1}))) Y_0\left(\xi_0 \frac{r^2}{\epsilon^2}\right). \quad (1.21)$$

Contrary to appearances, (1.21) is not symmetric in J_0 and Y_0 : when $r \ll \epsilon$, the function $Y_0\left(\xi_0 \frac{r^2}{\epsilon^2}\right)$ dominates $J_0\left(\xi_0 \frac{r^2}{\epsilon^2}\right)$, since the Bessel functions $J_0(z)$ and $Y_0(z)$ obey the asymptotics

$$J_0(z) = O(1) \text{ and } Y_0(z) \sim \log(z^{-1}) \text{ as } z \rightarrow 0. \quad (1.22)$$

⁷One sees, as predicted by Theorem 1.3 (see [81]), that in the $q_0 = 0$ case, we have $\frac{d}{dr} \left(r \frac{d\phi}{dr} \right) \approx 0$, hence $r \frac{d\phi}{dr} \approx \text{constant} = \epsilon^{-1}$, which is why in the $q_0 = 0$ case, the behavior is violent, and not fluctuating as in the $q_0 \neq 0$ case, see also the discussion in Section 1.3.

Hence, for $e^{-\delta_0 \epsilon^{-2}} \ll r \ll \epsilon$ (the lower bound will be explained in Section 1.5), we schematically show

$$\phi(r) \approx C_Y \sin(\omega_0 \cdot \epsilon^{-2} + O(\log(\epsilon^{-1}))) \log\left(\xi_0^{-1} \frac{\epsilon^2}{r^2}\right) \approx C_Y \sin(\omega_0 \cdot \epsilon^{-2} + O(\log(\epsilon^{-1}))) \log\left(\frac{\epsilon}{r}\right). \quad (1.23)$$

Since on a fixed Kasner metric (1.1), we find $\phi = p_\phi \log(\tau^{-1})$, where τ is roughly a power of r , and p_ϕ is chosen so that $p_1^2 + p_2^2 + p_3^2 + 2p_\phi^2 = 1$ (see already (1.29)), the expression (1.23) explains why we obtain final Kasner exponents that depend on $\sin(\omega_0 \cdot \epsilon^{-2} + O(\log(\epsilon^{-1})))$.

Remark 1.9. Most other quantities, such as the charge Q , already determine their final values at $r = 0$ inside \mathcal{O} (up to $O(\epsilon)$ -errors). Therefore, the charge retention mechanism from Theorem I results from an explicit computation in \mathcal{O} , see Lemma 5.7.

For more details on Bessel equations and functions, we refer the reader to our Appendix A.

1.5 Kasner bounces and connections to cosmology

We now relate the results of this paper to the heuristic observations of BKL [7, 9, 10, 64] regarding problems in relativistic cosmology, and explain how these heuristics manifest themselves rigorously in our work.

The BKL heuristics and Kasner bounces In [64], Khalatnikov and Lifschitz propose an asymptotic form of the metric for a spacetime obeying the vacuum Einstein equations in the vicinity of a spacelike singularity. Assuming $\mathcal{M} \cong I \times \Sigma = (0, T) \times \Sigma$ for some spatial 3-manifold Σ , they suggest that g locally takes the form

$$g \approx -d\tau^2 + \sum_{I=1}^3 \tau^{2p_I(x)} \omega_I(x) \otimes \omega_I(x). \quad (1.24)$$

Here, the exponents $p_I(x)$ are smooth functions on Σ , the $\omega_I(x)$ form a (local) basis of 1-forms on Σ , and the metric is ‘synchronized’ so that the singularity is located at $\tau = 0$. The exponents $p_I(x)$ are further constrained to obey the following two so-called *Kasner relations*:

$$\sum_{I=1}^3 p_I(x) = \sum_{I=1}^3 p_I^2(x) = 1. \quad (1.25)$$

However, [64] argues that generically, there is an inconsistency in the ansatz (1.24), so long as near $\tau = 0$, one fails to obey the *subcriticality condition*:

$$\tau^{p_I - p_J - p_K} \ll \tau^{-1} \text{ for all } I, J, K \in \{1, 2, 3\} \text{ with } J \neq K. \quad (1.26)$$

Further, in 1+3-dimensional vacuum, the relations (1.25) mean that the subcriticality condition (1.26) can never hold, outside of the exceptional case where $(p_1, p_2, p_3) = (1, 0, 0)$ or a permutation thereof. [64] thus concludes that singularities of the form (1.24) are not generic.

Subsequently, in [9], the authors suggest that the metric (1.24) may be valid in some interval $(\tau_1, \tau_2) \subset I$, but as τ decreases further towards 0, there must be a transition to a new modified Kasner-like regime. If we order

$p_1 < p_2 \leq p_3$, then [9] calculates this transition⁸ explicitly to be:

$$g \approx -d\tau^2 + \sum_{I=1}^3 \tau^{2\dot{p}_I(x)} \dot{\omega}_I(x) \otimes \dot{\omega}_I(x),$$

$$\dot{p}_1 = \frac{-p_1}{1+2p_1}, \quad \dot{p}_2 = \frac{p_2+2p_1}{1+2p_1}, \quad \dot{p}_3 = \frac{p_3+2p_1}{1+2p_1}. \quad (1.27)$$

Such a transition is what we call a *Kasner bounce*, and also may be described in the literature as a Kasner inversion (see [47]) or oscillation.

The new Kasner exponents \dot{p}_I also obey the Kasner relations (1.25), and as such, will also fail to obey the subcriticality condition. Hence, [9] predicts that the generic behavior in the vicinity of a spacelike singularity *in vacuum* is an infinite cascade of such transitions, which they term as the *oscillatory approach* to singularity, and is expected to be highly chaotic in nature, see again Conjecture B.

To avoid this infinite cascade of transitions occurring in vacuum, the authors of [7] then consider gravity coupled to a massless scalar field ϕ , and modify the ansatz (1.24) and relations (1.25) to

$$g \approx -d\tau^2 + \sum_{I=1}^3 \tau^{2p_I(x)} \omega_I(x) \otimes \omega_I(x), \quad \phi \approx p_\phi(x) \log \tau, \quad (1.28)$$

$$\sum_{I=1}^3 p_I(x) = \sum_{I=1}^3 p_I^2(x) + 2p_\phi^2(x) = 1. \quad (1.29)$$

For particular choices of generalized exponents (p_1, p_2, p_3, p_ϕ) , it is now possible for the subcriticality condition (1.26) to hold near $\tau = 0$, and as such the ansatz (1.28) is consistent, and moreover, conjecturally stable. We note that in this context, the condition (1.26) is identical to $\min\{p_I(x)\} > 0$, i.e. all Kasner exponents being positive. There still exist, of course, choices of exponents that violate (1.26); the corresponding spacetimes are then subject to an instability with the same Kasner transition map (1.27), to which we append the transition of the scalar field coefficient: $p_\phi \mapsto \dot{p}_\phi = \frac{p_\phi}{1+2p_1}$. After a finite number of such transitions [7], one will reach a tuple of generalized Kasner coefficients obeying (1.26). Hence, a scalar field is often referred to as a stiff matter model, as in Conjecture B.

We make one final observation. The source of the instability in [7, 9] is a spatial curvature term, which is actually suppressed in spherical symmetry. However, in [8], the authors argue that one can alternatively use an electromagnetic field to source the instability, and that the transition map (1.27) between different regimes of Kasner exponents is identical. This is consistent with the stability of the Schwarzschild interior in spherical symmetry for electromagnetism-free matter models [1, 19], in contrast with Theorem I and Theorem 1.3.

For further discussions regarding the BKL ansatz in relativistic cosmology, including generalization to higher dimension and other matter models, see also [6, 30, 31, 50].

Rigorous constructions and stability results of Kasner metrics Beyond the heuristics of [7, 8, 9, 10, 64], one may ask the following questions – can one actually construct a large class of spacetimes containing a spacelike singularity, obeying the asymptotics (1.25) and (1.29), and what does one know about their stability? For the first problem, [3] constructs a large class of *real analytic* solutions to the Einstein-scalar field system obeying the asymptotics (1.28). Beyond the real analytic regime, [38] recently constructed a reasonably general class of

⁸We remark that we exclude the particular case $p_1 = p_2$ corresponding to the degenerate exponents $(p_1, p_2, p_3) = (0, 0, 1)$.

vacuum spacetimes obeying (1.24), which are moreover allowed to be only C^k , for large k .

Regarding stability, the state of the art is due to Fournodavlos–Rodnianski–Speck [39] and a recent generalization by Oude Groeniger–Petersen–Ringström [42]. Loosely speaking, the former proves the stability of exact generalized Kasner spacetimes on $(0, +\infty) \times \mathbb{T}^3$ obeying the subcriticality condition (1.26), while the latter both permits more general closed spatial topologies and greater inhomogeneity in the initial data, so long as the inhomogeneity is compensated by prescribing the data “sufficiently close to the singularity”. For other related results, we refer the reader to [70, 71, 74, 12, 37].

In particular, [42] provides evidence for stability, *including outside of symmetry*, of the spacetimes constructed in Theorem I and Theorem 1.3; there only remains the technical issue of extending the stability arguments to non-compact spatial topologies, for instance by localizing the analysis of [39, 42]. We also mention several works of the first author. In [61], it is shown that all spacelike singularities, including spatially inhomogeneous singularities, in the spherically symmetric Einstein–scalar field model exhibit Kasner-like behavior, as does a class of singularities in the spherically symmetric Einstein–Maxwell–(uncharged) scalar field model obeying certain a priori assumptions. In [62], the first author constructs a large class of (inhomogeneous) data in this latter model such that the corresponding spacetime achieves these a priori assumptions, but so that the spacetime also exhibits nonlinear dynamics reminiscent of Kasner bounces (1.27). See also [63] concerning similar results in Gowdy symmetry.

Finally, we mention the work of Ringström [68] and Béguin–Dutilleul [4] on Bianchi IX cosmologies, containing a rigorous study of a large class of spatially homogeneous spacetimes. Among other things, [68] provides examples of spacetimes with infinitely many Kasner bounces in vacuum and, in contrast, proves the convergence to a stable Kasner-like regime in the presence of stiff matter.

The Kasner bounce mechanism for charged scalar fields We will now explain the schematic mechanism behind the Kasner bounce phenomenon as obtained in our Theorem I, which is the second main novelty compared to the $q_0 = 0$ case of [81]. We will show that the Kasner bounce, *in the regimes where it occurs* (namely, for $\epsilon \in E'_{\eta, \sigma}{}^{bo}$ of positive measure), is located in a region of the following form; for constants $D > 0$, $N > 0$:

$$\mathcal{K}_{bo} \subset \{e^{-D \cdot \epsilon^{-2}} \epsilon^N \lesssim r \lesssim e^{-D \cdot \epsilon^{-2}} \epsilon^{-N}\}. \quad (1.30)$$

We define the key quantity Ψ , which is a dimensionless derivative of ϕ : for $r_-(M, \mathbf{e}, \Lambda) > 0$ and $\delta_0(M, \mathbf{e}, \Lambda) > 0$ to be defined later, let

$$\Psi := -r \frac{d\phi}{dr}, \text{ and define } \Psi_i := \Psi|_{r=e^{-\delta_0 \cdot \epsilon^{-2}} r_-}. \quad (1.31)$$

The condition for the presence of a bounce will end up being

$$\eta \leq |\Psi_i| \leq 1 - \sigma, \text{ for some } \eta, \sigma > 0 \text{ independent of } \epsilon. \quad (\text{bo})$$

The reason for assuming $\eta \leq |\Psi_i|$ is that, based on numerics (see Section 1.6), there could be multiple Kasner bounces when $|\Psi_i|$ is close to 0, and the dynamics would be even more complicated. If $|\Psi_i|$ is too close to 1, though we are still able to produce a spacelike singularity (see already Theorem 3.1), we do not claim further quantitative estimates, as some Kasner exponents degenerate towards 0 in this case

As a consequence of (1.23), we find that, for some $C(M, \mathbf{e}, \Lambda, m^2, q_0) \neq 0$,

$$|\Psi_i| \approx |C| \cdot |\sin(\omega_0 \cdot \epsilon^{-2} + O(\log(\epsilon^{-1})))|. \quad (1.32)$$

Combining (bo) and (1.32) explains heuristically why the presence of a bounce depends on ϵ and why any small neighborhood of 0 of the form $(-\delta, \delta)$ still contains infinitely many spacetimes featuring a bounce.

Our non-bounce condition in Theorem I is not the complement of (bo), it is instead

$$|\Psi_i| \geq 1 + \sigma, \text{ for some } \sigma > 0 \text{ independent of } \epsilon, \quad (\text{no-bo})$$

where, as above, we arrange that $|\Psi_i|$ is not too close to 1 to avoid the Kasner exponents degenerating.

We now explain why it is that if (bo) is satisfied, there is a bounce, whereas if (no-bo) is satisfied then there is no bounce. Since the wave equation is second-order, Ψ should satisfy a first-order ODE. Though our system is highly nonlinear, this ODE surprisingly turns out to be presentable in a simple form, written schematically⁹ as follows:

$$\frac{d\Psi}{dR} = -\Psi(\Psi - \Psi_i)(\Psi - \Psi_i^{-1}) + \text{error}, \text{ where } R := \log\left(\frac{r_-}{r}\right), \quad (1.33)$$

where the error terms are of size $O(e^{-\delta_0 \epsilon^{-2}})$ for some $\delta_0 > 0$ and, thus, have no impact on the qualitative behavior of the ODE. The dynamics of Ψ relies on the linearized stability of (1.33) near $\Psi = \Psi_i$ of the schematic form

$$\frac{d(\delta\Psi)}{dR} = -(\Psi_i^2 - 1) \cdot \delta\Psi + \text{error}.$$

If $|\Psi_i| > 1$, then $\Psi = \Psi_i$ is a stable fixed point as $R \rightarrow +\infty$ (corresponding to $r \rightarrow 0$): this is what happens if (no-bo) is true and then, there is no bounce and $\Psi \approx \Psi_i$ up to $r = 0$. In contrast, if $|\Psi_i| < 1$, then $\Psi = \Psi_i$ is an *unstable* fixed point, but $\Psi = \Psi_i^{-1}$ is a stable fixed point. If (bo) is true, then we find that Ψ gets inverted from Ψ_i to Ψ_i^{-1} in the region (1.30), over which the change in R is $\Delta R = O(\log(\epsilon^{-1}))$.

Once the behavior of Ψ has been quantified, one can immediately retrieve the Kasner exponents from Theorem I using similar techniques as in [81]. The most important (but algebraically trivial) feature of these relations is that $p_1 = P(\alpha) > 0$ if and only if $|\alpha| > 1$, see the formula (1.12), (1.13) (where $\alpha \approx \Psi_i$): thus, the final Kasner regime always has $p_1 > 0$ in Theorem I. Hence, the final Kasner regime indeed lies in the subcritical regime of exponents as explained earlier in Section 1.5.

1.6 Holographic superconductors in the AdS-CFT correspondence

In this section, we will discuss two separate questions, which end up being connected by a vast literature.

- In what sense is the spacetime of Theorem I the interior of a hairy black hole, i.e. can we construct a corresponding “hairy black hole exterior”?
- What do numerics tell us about the hairy black hole interior of Theorem I?

Note that Theorem I is valid for any value of the cosmological constant $\Lambda \in \mathbb{R}$. However, in the $\Lambda = 0$ case, there are no non-trivial static, spherically symmetric solutions of (1.2)-(1.5), see [5] (although [5] assumes $q_0 = 0$).

⁹Note that the discussion of the ODE (1.33) and its solutions was already present in [47] at the heuristic and numerical level.

On the other hand, in the $\Lambda < 0$ case, recent works of Zheng [84, 83] construct asymptotically Anti-de-Sitter hairy black hole exteriors bifurcating off of (a large subset of) sub-extremal Reissner–Nordström–AdS spacetimes. The interior of these black holes corresponds to the spacetimes considered in Theorem I (in the $q_0 \neq 0$ case) and Theorem 1.3 (in the $q_0 = 0$ case), thereby resolving Open Problem iv in [81].

Anti-de-Sitter asymptotics impose that, for a negative cosmological constant $\Lambda < 0$ in (1.2):

$$g = \left(1 - \frac{2M}{r} - \frac{\Lambda r^2}{3} + o(r^{-1})\right) [-dt^2 + ds^2] + r^2(s) d\sigma_{\mathbb{S}^2}, \quad (1.34)$$

which gives the following asymptotics on ϕ in (1.5), for $m^2 < 0$, there exists constants $\phi_{(0)}, \phi_{(1)}$ such that

$$\phi(r) = \phi_{(0)} \cdot u_D(r) + \phi_{(1)} \cdot u_N(r), \text{ where } u_D(r) \sim r^{-\frac{3}{2} + \sqrt{\frac{9}{4} - m^2}} \text{ and } u_N(r) \sim r^{-\frac{3}{2} - \sqrt{\frac{9}{4} - m^2}} \text{ as } r \rightarrow +\infty. \quad (1.35)$$

Here $\phi_{(0)} = 0$ corresponds to Dirichlet-type boundary conditions, while $\phi_{(1)} = 0$ is Neumann-type. Both boundary conditions are allowed in [84, 83]. We note that the Dirichlet case is the $\Lambda < 0$ analogue of asymptotic flatness in the $\Lambda = 0$ case and thus truly corresponds to what should be called an asymptotically-AdS “hairy black hole”.

Previous works in physics already argued for the existence of such stationary asymptotically-AdS black holes [43, 44, 45] as part of the broader field of AdS/CMT (for Condensed Matter Theory) aiming at improving the understanding of condensed matter on flat spacetime by embedding it in a higher-dimensional AdS spacetime (see e.g. [49] or the related discussion in [81]). In the charged scalar field case ($q_0 \neq 0$), such black holes represent holographic analogues of superconductors due to a spontaneous breaking of the $\mathbb{U}(1)$ -symmetry that the charged scalar field is associated with. The presence of black hole hair (meaning a non-trivial stationary black hole) reflects the phenomenon of condensation, with Dirichlet boundary condition $\phi_{(0)} \neq 0$ corresponding to a so-called stimulated emission, and $\phi_{(0)} = 0$ to spontaneous emission, in analogy with real-life superconductors (see e.g. [53] for more details).

In summary, the first question is answered in the affirmative: the regions considered in Theorem I and Theorem 1.3 indeed correspond to the interior of an asymptotically-AdS black hole (with Dirichlet or Neumann boundary conditions) recently rigorously constructed in [84, 83], whose existence had already been speculated in physics works [43, 45] in view of their importance as holographic models of superconductors.

We turn to the second question, regarding previous numerical works in the interior of asymptotically-AdS hairy black holes. Prior to discussing (1.2)–(1.5) with $q_0 \neq 0$ as studied in Theorem I, let us mention that the black hole interior for (1.2)–(1.5) with $F \equiv 0$ (uncharged black hole) was studied in [40], and (1.2)–(1.5) with $F \neq 0$, $q_0 = 0$ (uncharged matter) in [46], see [81] for an extended discussion. We also mention the interesting follow-up works [15, 32, 33, 41, 48] for different matter models. Turning to the case (1.2)–(1.5) with $q_0 \neq 0$, we start by remarking that the collapsed oscillations and Kasner bounces from Theorem I were previously anticipated¹⁰ numerically in [47]. This scenario was verified numerically and is entirely consistent with our findings from Theorem I. The motivation to investigate the interior of holographic superconductors in [40, 46, 47] is two-fold: at first, it originates as a rudimentary model for quantum effects in the interior of black holes, following the AdS/CFT paradigm. In this context, the authors of [47] promote a *holographic*

¹⁰While [47] is in the setting of planar symmetry which obeys slightly different equations, it happens to make no difference to the fluctuating collapse and Kasner bounce phenomena and the conclusion of Theorem I also hold in this setting, as we already noted in Remark 1.1.

version of *Strong Cosmic Censorship* roughly asserting that generic *stationary*¹¹ (asymptotically-AdS) black holes (corresponding to thermal states) possess an internal singularity. Secondly, another motivation originates in the paradigm of AdS/CMT to understand real-life superconductors using holographic models (as already formulated in [43, 45, 44] and pursued in [40, 46, 47]). In this context, an analogy was established between the oscillations found inside holographic superconductors and the (AC) Josephson effect inside a “real-life” superconductor, see [54, 55], ultimately causing the Kasner bounce in some regime. The physical interpretation of these Kasner bounces inside holographic superconductors is still being debated [47].

Finally, note that, by the formula (1.12), when $\alpha \approx \Psi_i$ gets close to 0, then the Kasner exponents $p_2 = p_3$ get close to 0: when this happens, [47] numerically observes a *second Kasner bounce* and have also mentioned the possibility of arbitrarily many Kasner bounces. These very interesting aspects are not covered by Theorem I, since its assumptions *specifically require to choose* ϵ so that $\alpha(\epsilon)$ is bounded away from 0 (at the cost, of course, of reducing the measure of the set of eligible ϵ by an arbitrarily small amount $\eta > 0$). It would be of great interest to prove rigorous results confirming the numerical breakthroughs of [47].

Open problem c. *Generalize the conclusion of Theorem I for a larger set of $\epsilon \in (-\epsilon_0, \epsilon_0) \setminus \{0\}$ such that $|\Psi_i| \lesssim \epsilon^N$ are allowed for a suitably chosen $N > 0$, where Ψ_i defined in (1.31) is schematically of the form (1.32). In the $|\Psi_i| \lesssim \epsilon^N$ situation, control the occurrence of two (or more) Kasner bounces.*

We finally note that the techniques of Theorem I still allow to control quantitatively the spacetime up to the Proto-Kasner region (see Figure 6 and Section 6), even if $|\Psi_i|$ is close to $\{0, 1\}$, but not beyond.

1.7 Outline of the paper and the different regions of Figure 6

The paper (and the proof) will follow the various regions \mathcal{R} , \mathcal{N} , \mathcal{EB} , \mathcal{LB} , \mathcal{O} , \mathcal{PK} and \mathcal{K} depicted on Figure 6.

- In Section 2, we give some geometric preliminaries, and explain the gauge used in Theorem I.
- In Section 3, we give a precise statement of the main result corresponding to Theorem I, together with the precise definition of the regions \mathcal{R} , \mathcal{N} , \mathcal{EB} , \mathcal{LB} , \mathcal{O} , \mathcal{PK} and \mathcal{K} .
- In Section 4, we prove estimates in the red-shift region \mathcal{R} , the no-shift region \mathcal{N} , the early blue-shift region \mathcal{EB} , and the late blue-shift region \mathcal{LB} . These estimates are similar to the ones appearing in [81] and feature the almost formation of a Cauchy horizon.
- In Section 5, we prove estimates in the oscillation region \mathcal{O} . This section corresponds to the collapsed oscillations discussed in Section 1.4.
- In Section 6, we prove estimates in the proto-Kasner region \mathcal{PK} . In this section, we demonstrate the onset of a Kasner geometry transitioning from the collapsed oscillations in \mathcal{O} to the Kasner behavior in \mathcal{K} .
- In Section 7, we linearize the system of Einstein equations to control precisely the phase $\Theta(\epsilon) = \omega_0 \epsilon^{-2} + O(\log(\epsilon^{-1}))$ appearing in (1.32); this step is essential in constructing the set E_η of acceptable ϵ in Theorem I.

¹¹In contrast, the usual notion of Strong Cosmic Censorship is not tied to stationary solutions and formulates genericity considerations inside a moduli space of initial data leading to a large class of dynamical spacetimes, see, for instance, the discussion in [80].

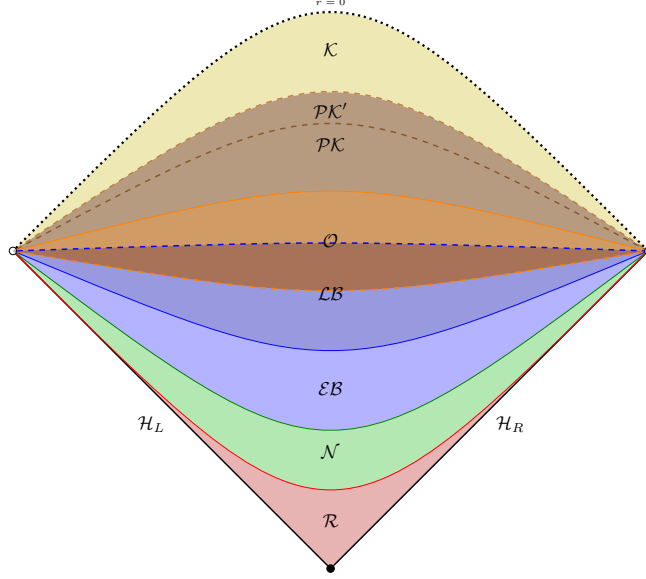


Figure 6: A more detailed version of Figure 2, partitioning the hairy black hole interior into the different regions $\mathcal{R}, \mathcal{N}, \mathcal{EB}, \mathcal{LB}, \mathcal{O}, \mathcal{PK}, \mathcal{K}$, to be precisely defined in Section 3.1.

- In Section 8, we prove estimates in the Kasner region \mathcal{K} . In particular, we prove the Kasner bounce phenomenon discussed in Section 1.5.
- In Section 9, we conclude the proof of (the precise version of) Theorem I by providing precise geometric estimates characteristic of the Kasner behavior in a sub-region of $\mathcal{PK} \cup \mathcal{K}$.

We will also introduce the following regions that overlap with some of the regions of Figure 6: the restricted proto-Kasner region \mathcal{PK}' , the first Kasner region \mathcal{K}_1 , the second Kasner region \mathcal{K}_2 and the Kasner-bounce region \mathcal{K}_{bo} (see Figure 7 and Section 3). Note, however, that in the absence of a Kasner bounce, $\mathcal{K}_2 = \mathcal{K}_{bo} = \emptyset$.

Acknowledgements We are grateful to Mihalis Dafermos for suggesting the construction of Figure 4 and for useful comments on the manuscripts. We also would like to thank Grigorios Fournodavlos, Jonathan Luk and Yakov Shlapentokh-Rothman for useful comments on the manuscript, and Jorge Santos for helpful discussions, as well as an anonymous referee for extremely detailed and thorough suggestions which have vastly improved the manuscript.

2 Geometric set-up and preliminaries

2.1 Einstein-Maxwell-Klein-Gordon in double null coordinates

We consider a spherically symmetric Lorentzian metric (M, g) with a choice of double null coordinates (u, v) :

$$g = -g_{\mathcal{Q}} + r^2(u, v)d\sigma_{\mathbb{S}^2} = -\Omega^2(u, v)dudv + r^2(u, v)d\sigma_{\mathbb{S}^2}. \quad (2.1)$$

Here (u, v) are coordinates on the quotient manifold $\mathcal{Q} = M/SO(3)$ and $d\sigma_{\mathbb{S}^2} = d\theta^2 + \sin^2 \theta d\varphi^2$ is the standard metric on the unit sphere. We call $r = r(u, v)$ the *area-radius* function.

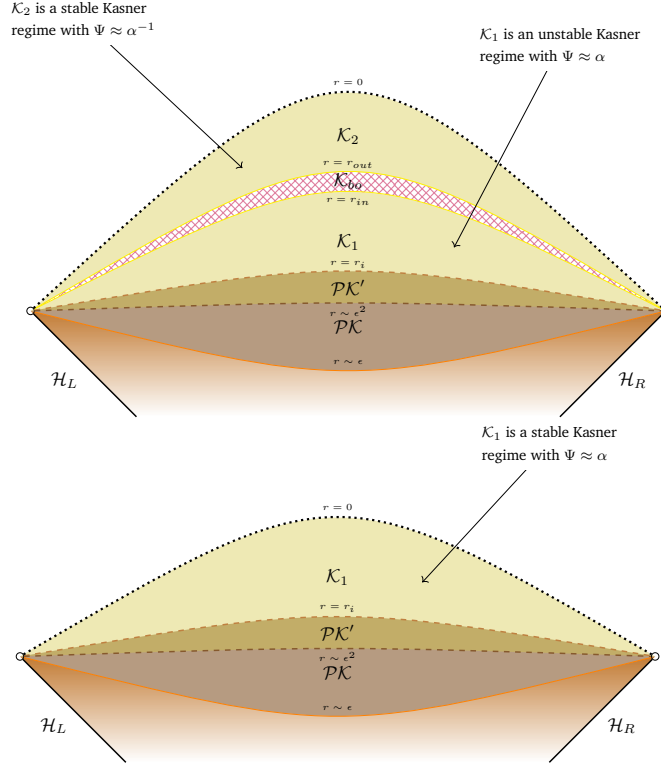


Figure 7: A zoom on $\mathcal{PK} \cup \mathcal{K}$ in Figure 6, with the top picture representing the bounce case ($\mathcal{K}_2, \mathcal{K}_{bo} \neq \emptyset$) and the bottom picture the no bounce case ($\mathcal{K}_2, \mathcal{K}_{bo} = \emptyset$). Note the inclusion $\mathcal{PK}' \subset \mathcal{PK}$.

Due to the presence of charged scalar matter, the Maxwell field will itself be dynamical, and is described via the following function $Q(u, v)$ on \mathcal{Q} :

$$F = \frac{Q\Omega^2}{2r^2} du \wedge dv. \quad (2.2)$$

To describe the coupling to the scalar field, we must choose a gauge for the Maxwell field. In spherical symmetry, we specify the gauge using a one-form $A = A_u du + A_v dv$ on \mathcal{Q} which satisfies $dA = F$.

Define the covariant derivative by $D_\mu = \nabla_\mu + iq_0 A_\mu$. Then the scalar field ϕ is a complex-valued function on \mathcal{Q} satisfying the following covariant wave equation:

$$g^{\mu\nu} D_\mu D_\nu \phi = 0. \quad (2.3)$$

Recall that the whole system of equations must be invariant under the gauge transformation $A \mapsto A + df$, $\phi \mapsto \phi e^{-iq_0 f}$, where f is any smooth function on \mathcal{Q} .

We make a few more standard definitions. The *Hawking mass* ρ is given by

$$\rho := \frac{r}{2}(1 - g_{\mathcal{Q}}(\nabla r, \nabla r)) = \frac{r}{2}(1 - 4\Omega^{-2}\partial_u r \partial_v r). \quad (2.4)$$

In the presence of the Maxwell field and the cosmological constant, we further define the renormalized Vaidya mass ϖ and the r -constant surface gravity $2K$ as

$$\varpi = \rho + \frac{Q^2}{2r} - \frac{\Lambda r^3}{6}, \quad 2K = \frac{2}{r^2} \left(\varpi - \frac{Q^2}{r} - \frac{\Lambda r^3}{3} \right). \quad (2.5)$$

Suppose that (M, g, F, ϕ) are a solution to the Einstein-Maxwell-Klein-Gordon system (1.2)–(1.5). In the double-null coordinates of (2.1), the quantities $(r, \Omega^2, Q, A, \phi)$ then satisfy the following system of PDEs:

$$\partial_u(\Omega^{-2}\partial_u r) = -\Omega^{-2}r|D_u\phi|^2, \quad (2.6)$$

$$\partial_v(\Omega^{-2}\partial_v r) = -\Omega^{-2}r|D_v\phi|^2, \quad (2.7)$$

$$\partial_u\partial_v r = -\frac{\Omega^2}{4r} - \frac{\partial_u r \partial_v r}{r} + \frac{\Omega^2 Q^2}{4r^3} + \frac{\Omega^2 r(m^2|\phi|^2 + \Lambda)}{4}, \quad (2.8)$$

$$\partial_u\partial_v \log(\Omega^2) = \frac{\Omega^2}{2r^2} + \frac{2\partial_u r \partial_v r}{r^2} - \frac{\Omega^2 Q^2}{r^4} - 2\Re(D_u\phi \overline{D_v\phi}), \quad (2.9)$$

$$\partial_u Q = -q_0 r^2 \Im(\phi \overline{D_u\phi}), \quad (2.10)$$

$$\partial_v Q = +q_0 r^2 \Im(\phi \overline{D_v\phi}), \quad (2.11)$$

$$D_u D_v \phi = -\frac{\partial_u r \cdot D_v \phi}{r} - \frac{\partial_v r \cdot D_u \phi}{r} + \frac{iq_0 Q \Omega^2}{4r^2} \phi - \frac{m^2 \Omega^2}{4} \phi, \quad (2.12)$$

$$\partial_u A_v - \partial_v A_u = \frac{Q \Omega^2}{2r^2}. \quad (2.13)$$

The equations (2.6) and (2.7) are the celebrated *Raychaudhuri equations*, the equations (2.8) and (2.9) can be viewed as wave equations for the geometric quantities r and Ω^2 on \mathcal{Q} , and the remaining equations describe the dynamics of the coupled Maxwell field and charged scalar field.

We recall also the transport equations for the Vaidya mass ϖ :

$$\partial_u \varpi = -2r^2(\Omega^{-2}\partial_v r)^{-1}|D_u\phi|^2 + \frac{m^2}{2}r^2|\phi|^2\partial_u r - q_0 Q r \Im(\phi \overline{D_u\phi}), \quad (2.14)$$

$$\partial_v \varpi = -2r^2(\Omega^{-2}\partial_u r)^{-1}|D_v\phi|^2 + \frac{m^2}{2}r^2|\phi|^2\partial_v r + q_0 Q r \Im(\phi \overline{D_v\phi}). \quad (2.15)$$

Remark 2.1. In the case of planar symmetry, the only changes to the equations are that the first term on the right hand sides of (2.8) and (2.9) are removed. Our results remain valid in this symmetry class.

2.2 The Reissner-Nordström(-dS/AdS) interior metric

We are interested in charged hairy perturbations of sub-extremal Reissner-Nordström interiors. To define sub-extremality, given some parameters $M > 0$, $e, \Lambda \in \mathbb{R}$, consider the polynomial

$$P_{M,e,\Lambda}(X) = X^2 - 2MX + e^2 - \frac{1}{3}\Lambda X^4. \quad (2.16)$$

Then the set of subextremal-parameters (M, e, Λ) is $\mathcal{P}_{se} = \mathcal{P}_{se}^{\Lambda < 0} \cup \mathcal{P}_{se}^{\Lambda = 0} \cup \mathcal{P}_{se}^{\Lambda > 0}$, where $\mathcal{P}_{se}^{\Lambda < 0}$ is such that $\Lambda < 0$ and the polynomial $P_{M,e,\Lambda}(X)$ has two distinct positive real roots $r_- < r_+$, $\mathcal{P}_{se}^{\Lambda = 0}$ is such that $\Lambda = 0$ and the polynomial $P_{M,e,\Lambda}(X)$ has two distinct positive real roots $r_- < r_+$, while $\mathcal{P}_{se}^{\Lambda > 0}$ is such that $\Lambda > 0$ and $P_{M,e,\Lambda}(X)$ has three distinct positive real roots $r_- < r_+ < r_c$.

The Reissner-Nordström(-dS/AdS) spacetime is a solution to (1.2)–(1.5) in electrovacuum (i.e. $\phi \equiv 0$), and

can be written in standard (t, r) coordinates as

$$g_{RN} = - \left(1 - \frac{2M}{r} + \frac{\mathbf{e}^2}{r^2} - \frac{\Lambda r^2}{3} \right) dt^2 + \left(1 - \frac{2M}{r} + \frac{\mathbf{e}^2}{r^2} - \frac{\Lambda r^2}{3} \right)^{-1} dr^2 + r^2 d\sigma_{\mathbb{S}^2}. \quad (2.17)$$

In particular, the Reissner-Nordström(-dS/AdS) interior metric is given by (2.17), restricted to the coordinate range $r_- < r < r_+$, $t \in \mathbb{R}$. Note that, in the interior, t is a spacelike coordinate while r is a timelike coordinate.

The Maxwell field is given by setting $Q \equiv \mathbf{e}$ in (2.2), and $\Omega^2 = \Omega_{RN}^2$ will be defined shortly. One choice of gauge field A which will be consistent with the remainder of this article is

$$A = - \left(\frac{\mathbf{e}}{r_+} - \frac{\mathbf{e}}{r} \right) dt. \quad (2.18)$$

To recast the metric (2.17) into the double null form (2.1), we define

$$\frac{dr}{dr^*} := \frac{\Omega_{RN}^2}{4}, \quad \Omega_{RN}^2 := -4 \left(1 - \frac{2M}{r} + \frac{\mathbf{e}^2}{r^2} - \frac{\Lambda r^2}{3} \right), \quad (2.19)$$

$$u := \frac{r^* - t}{2}, \quad v := \frac{r^* + t}{2}. \quad (2.20)$$

In this (u, v) coordinate system, the metric can now be written as

$$g_{RN} = -\Omega_{RN}^2 du dv + r^2 d\sigma_{\mathbb{S}^2}. \quad (2.21)$$

In the sequel, we denote the Reissner-Nordström area-radius function by r_{RN} .

Recalling the definition of $2K$ in (2.5), we define the surface gravity of the event horizon $2K_+$, and the surface gravity of the Cauchy horizon $2K_-$ by

$$2K_{\pm} = 2K(r = r_{\pm}) = \frac{2}{r_{\pm}^2} \left(M - \frac{\mathbf{e}^2}{r_{\pm}} - \frac{\Lambda r_{\pm}^3}{3} \right). \quad (2.22)$$

It is then a well-known fact that the null lapse Ω_{RN}^2 obeys the following asymptotics, where $\alpha_{\pm} > 0$ are fixed constants depending on the black hole parameters:

$$\log \left(\frac{\Omega_{RN}^2}{\alpha_+ e^{2K_+(M, \mathbf{e}, \Lambda) \cdot r^*}} \right) = O(e^{2K_+(M, \mathbf{e}, \Lambda) \cdot r^*}) \quad \text{as } r^* = u + v \rightarrow -\infty, \quad (2.23)$$

$$\log \left(\frac{\Omega_{RN}^2}{\alpha_- e^{2K_-(M, \mathbf{e}, \Lambda) \cdot r^*}} \right) = O(e^{2K_-(M, \mathbf{e}, \Lambda) \cdot r^*}) \quad \text{as } r^* = u + v \rightarrow +\infty. \quad (2.24)$$

We note that, for subextremal black hole parameters, one has $2K_+ > 0$ while $2K_- < 0$.

Introducing the following “regular coordinates”,

$$U = e^{2K_+ u}, \quad V = e^{2K_+ v}, \quad (2.25)$$

it is well-known that in the coordinate system (U, v) , the metric g_{RN} can be smoothly extended beyond $U = 0$, and the right event horizon $\mathcal{H}_R = \{(U, v) : U = 0, v \in [-\infty, +\infty)\}$ is realised as a smooth null hypersurface. A similar construction can be made for the coordinates (u, V) , with $\mathcal{H}_L = \{(u, V) : u \in [-\infty, +\infty), V = 0\}$.

Indeed, using the coordinate system (U, V) , the metric g_{RN} is defined for $0 \leq U, V < +\infty$, and can be

smoothly beyond both \mathcal{H}_R and \mathcal{H}_L , including the bifurcation sphere $\mathcal{H}_R \cap \mathcal{H}_L = \{U = 0, V = 0\}$.

2.3 Black hole interiors with charged scalar hair

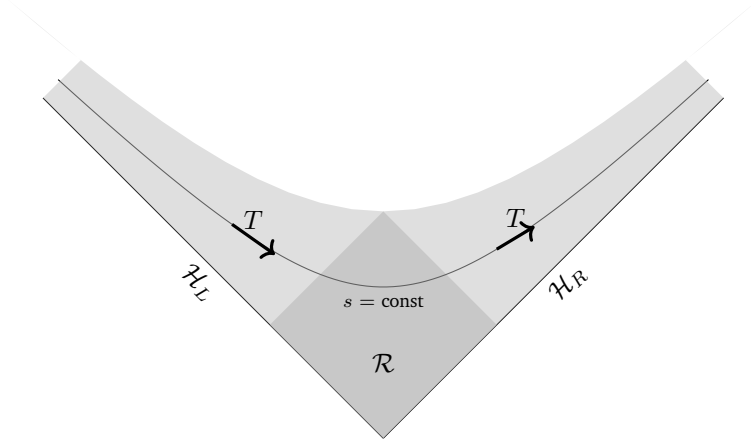


Figure 8: The local solution to the characteristic initial value problem for a spatially homogeneous black hole interior with charged scalar hair

Consider the characteristic initial value problem with initial data given on the two affine complete null hypersurfaces $\mathcal{H}_L = \{(U, V) : U \geq 0, V = 0\} = \{(u, v) : u \in [-\infty, +\infty), v = -\infty\}$ and $\mathcal{H}_R = \{(U, V) : U = 0, V \geq 0\} = \{(u, v) : u = -\infty, v \in [-\infty, +\infty)\}$, intersecting at the bifurcation sphere $(U, V) = (0, 0)$.

We normalize the regular coordinates (U, V) , which are related to the usual interior coordinates (u, v) via (2.25), using the following gauge choice:

$$\Omega_R^2(U, v)|_{\mathcal{H}_R} = \frac{1}{2K_+} e^{-2K_+(M, \mathbf{e}, \Lambda) \cdot u} \Omega^2(u, v)|_{\mathcal{H}_R} = \frac{\alpha_+}{2K_+} e^{2K_+(M, \mathbf{e}, \Lambda) \cdot v}, \quad (2.26)$$

$$\Omega_L^2(u, V)|_{\mathcal{H}_L} = \frac{1}{2K_+} e^{-2K_+(M, \mathbf{e}, \Lambda) \cdot v} \Omega^2(u, v)|_{\mathcal{H}_L} = \frac{\alpha_+}{2K_+} e^{2K_+(M, \mathbf{e}, \Lambda) \cdot u}, \quad (2.27)$$

These choices are made such that, with respect to the *generalized Kruskal-Szekeres* coordinate system (U, V) , Ω^2 is normalized as follows on $\mathcal{H} = \mathcal{H}_R \cup \mathcal{H}_L$:

$$\Omega_{reg}^2(U, V)|_{\mathcal{H}} = \frac{\alpha_+}{(2K_+)^2}. \quad (\Omega\text{-data})$$

In the context of this article, we pose the following characteristic initial data:

$$r|_{\mathcal{H}} = r_+(M, \mathbf{e}, \Lambda), \quad (r\text{-data})$$

$$\varpi|_{\mathcal{H}} = M > 0, \quad (\varpi\text{-data})$$

$$Q|_{\mathcal{H}} = \mathbf{e} \in \mathbb{R} \setminus \{0\}, \quad (Q\text{-data})$$

$$\phi|_{\mathcal{H}} = \epsilon \in \mathbb{R} \setminus \{0\}, \quad (\phi\text{-data})$$

as well as a gauge for the Maxwell field such that the components A_V, A_U vanish on $\mathcal{H}_R, \mathcal{H}_L$ respectively. In particular $D_V \phi$ and $D_U \phi$ will vanish on their respective horizon pieces. As a result, this data is compatible with the null constraints (2.6), (2.7).

In the following proposition, we show that the data $(\Omega\text{-data})$, $(r\text{-data})$, $(Q\text{-data})$, $(\phi\text{-data})$ uniquely specifies a solution to the Einstein-Maxwell-Klein-Gordon system, which is moreover spatially homogeneous. Of course, in order to have uniqueness we must impose a gauge for the Maxwell field A . In our setting, for the purpose of reducing the Einstein-Maxwell-Klein-Gordon system to a system of ODEs (see already Section 2.4 and (2.35)), it will be convenient to choose

$$UA_U + VA_V = 0. \quad (A\text{-gauge})$$

We now identify the spacetime describing the hairy black hole interior spacetimes studied in this article, which we firstly describe in the regular coordinate system (U, V) .

Proposition 2.1. Consider characteristic initial data $(\Omega\text{-data})$, $(r\text{-data})$, $(Q\text{-data})$, $(\phi\text{-data})$ to the Einstein-Maxwell-Klein-Gordon system (2.6)–(2.13), with u, v replaced by U, V respectively. Then imposing also $(A\text{-gauge})$, there exists a unique maximal future development¹² of the system $(\Omega^2, r, \phi, Q, A_U, A_V)$ that is smooth up to and including the horizon $\mathcal{H} = \mathcal{H}_L \cup \mathcal{H}_R$.

Furthermore, the domain of definition of this maximal development is given by $\{(U, V) : 0 \leq UV < D_{max}\}$ for some $D_{max}(M, \mathbf{e}, \Lambda, m^2, q_0, \epsilon) \in (0, +\infty]$, and letting T be the vector field (see Figure 8)

$$T := 2K_+ \left(-U \frac{\partial}{\partial U} + V \frac{\partial}{\partial V} \right), \quad (2.28)$$

one finds that T is a Killing vector field, satisfying $Tr = T\Omega^2 = TQ = T\phi = T(UA_U) = 0$. In particular, the spacetime is foliated by Cauchy hypersurfaces $UV = \text{const}$, which are each spatially homogeneous with isometry group $\mathbb{R} \times SO(3)$.

Proof. We wish to appeal to a local existence result, for instance [60, Proposition 4.1], with the caveat that our gauge choice $(A\text{-gauge})$ is not well-suited to such local well-posedness statements. Following [60], we firstly instead find a solution with respect to the Maxwell gauge choice:

$$A_V^{(0)}(U, V) = 0, \quad A_U^{(0)}(U, 0) = 0. \quad (A\text{-gauge}')$$

[60] asserts that there exists a unique solution to (2.6)–(2.13) for $(U, V) \in [0, \delta] \times [0, \delta]$ with δ sufficiently small (see the darker shaded region of Figure 8), attaining the prescribed data and using the gauge $(A\text{-gauge}')$, with A replaced by $A^{(0)}$ in the equations. In particular, Maxwell gauge-independent quantities such as Ω_{reg}^2, r, Q are already uniquely determined.

We seek a gauge transformation that relates an $A^{(0)}$ satisfying $(A\text{-gauge}')$ to an A satisfying $(A\text{-gauge})$. The correct gauge transformation is $A = A^{(0)} - dh$, with h given by

$$h(U, V) := \int_0^1 UA^{(0)}(Ux, Vx) dx. \quad (2.29)$$

The reason is that this choice of h implies that

$$\begin{aligned} U \frac{\partial h}{\partial U} + V \frac{\partial h}{\partial V} &= \int_0^1 \left(UA^{(0)}(Ux, Vx) + U^2 x \frac{\partial A^{(0)}}{\partial U}(Ux, Vx) + UVx \frac{\partial A^{(0)}}{\partial V}(Ux, Vx) \right) dx, \\ &= \int_0^1 \frac{d}{dx} (Ux A^{(0)}(Ux, Vx)) dx = UA^{(0)}(U, V), \end{aligned}$$

¹²Maximality is meant in the sense that there is no larger causal region of the (U, V) -plane where one may smoothly extend the solution.

so that

$$UA_U + VA_V = UA^{(0)} - U \frac{\partial h}{\partial U} - V \frac{\partial h}{\partial V} = 0,$$

as required. Furthermore, the h chosen in (2.29) is the unique such gauge transformation that is regular at $(0, 0)$: If \tilde{h} was another such function, then the difference $g = h - \tilde{h}$ would satisfy

$$U \frac{\partial g}{\partial U} + V \frac{\partial g}{\partial V} = 0,$$

whose general solution is of the form $g(U, V) = G(U/V)$. So regularity at $(0, 0)$ implies that G , and thus g , is constant, and $dh = d\tilde{h}$ after all.

Hence we have constructed a unique regular solution in the characteristic rectangle $[0, \delta] \times [0, \delta]$. We next show that the vector field T defined in (2.28) annihilates all the relevant quantities. For this purpose, we argue geometrically as follows: let $a > 0$ be any positive real number, and consider the double null coordinate transformation $U \mapsto U' = aU, V \mapsto V' = a^{-1}V$. Then in the (U', V') coordinate system, we note that it still holds that on $\mathcal{H} = \{(U', V') : U' = 0 \text{ or } V' = 0\}$, we have

$$\Omega_{reg}'^2(U', V') = \frac{\alpha_+}{(2K_+)^2},$$

$$r = r_+,$$

$$Q = \mathbf{e},$$

$$\phi = \epsilon,$$

$$U' A_{U'} + V' A_{V'} = 0.$$

Hence by the aforementioned existence and uniqueness result, we have a unique solution in the characteristic rectangle $(U', V') \in [0, \delta] \times [0, \delta]$. Furthermore, this agrees with the solution in the original (U, V) coordinates, so that, for $f \in \{\Omega^2, r, Q, \phi, UA_U\}$, we have

$$f(U', V') = f(aU, a^{-1}V) = f(U, V). \quad (2.30)$$

Allowing a to vary across all positive reals, it is clear that we have a solution in the whole of $\{(U, V) \in \mathbb{R}_{\geq 0}^2 : 0 \leq UV \leq \delta^2\}$, i.e. the lighter shaded region in Figure 8 that arises from sweeping out the darker shaded region for different choices of $a > 0$. Furthermore, it is immediate from (2.30) that T annihilates all such quantities f .

The extension to the region $\{0 \leq UV < D_{max}\}$ is then straightforward using standard extension principle arguments for nonlinear waves and again appealing to this geometric trick. \square

Remark 2.2. By the generalized extension principle of [60], if the quantity D_{max} of Proposition 2.1 is finite, then one must have $r \rightarrow 0$ as $UV \rightarrow D_{max}$. However, Proposition 2.1 is qualitative in nature and says little about quantitative properties of the interior, or if and how any spacelike singularity is formed.

Following Proposition 2.1, we would also like to understand the transversal derivatives of r and ϕ along \mathcal{H} , for which we shall need the full system of equations (2.6)–(2.13). For r , we see that using (2.8) on \mathcal{H}_R ,

$$\partial_V \partial_U r = \frac{\alpha_+}{4(2K_+)^2} \left(-\frac{1}{r_+} + \frac{\mathbf{e}^2}{r_+^3} + r_+ \Lambda + r_+ m^2 \epsilon^2 \right). \quad (2.31)$$

Since $r_+ = r_+(M, \mathbf{e}, \Lambda)$ satisfies the equation

$$P_{M, \mathbf{e}, \Lambda}(r_+) = r_+^2 - 2Mr_+ + \mathbf{e}^2 - \frac{1}{3}\Lambda r_+^4 = 0,$$

it is readily checked that the expression in the parentheses in (2.31) is equal to $-2K_+ + r_+ m^2 \epsilon^2$. We then integrate (2.31), noting that $\partial_U r = 0$ at the bifurcation sphere $(U, V) = (0, 0)$, to find

$$\partial_U r|_{\mathcal{H}_R} = \frac{\alpha_+ V}{8K_+} \left(-1 + \frac{r_+ m^2 \epsilon^2}{2K_+} \right).$$

Returning to (u, v) coordinates, and performing a similar procedure on \mathcal{H}_L , we deduce

$$\lim_{u \rightarrow -\infty} \frac{-4\partial_u r}{\Omega^2}(u, v) = \lim_{v \rightarrow -\infty} \frac{-4\partial_v r}{\Omega^2}(u, v) = 1 - \frac{r_+ m^2 \epsilon^2}{2K_+}. \quad (2.32)$$

We remark here that due to the presence of the Klein-Gordon mass, there is already an $O(\epsilon^2)$ deviation from the corresponding Reissner-Nordström quantity. A similar procedure applied to (2.12) will yield

$$\frac{2K_+}{\alpha_+ V} \cdot D_U \phi(0, V) = \lim_{u \rightarrow -\infty} \frac{D_u \phi}{\Omega^2}(u, v) = \beta_+ \epsilon, \quad (2.33)$$

$$\frac{2K_+}{\alpha_+ U} \cdot D_V \phi(U, 0) = \lim_{v \rightarrow -\infty} \frac{D_v \phi}{\Omega^2}(u, v) = \beta_+ \epsilon, \quad (2.34)$$

where $\beta_+ = \beta_+(M, \mathbf{e}, \Lambda, m)$ is some fixed constant we do not explicitly determine.

2.4 System of ODEs for spatially homogeneous solutions

Define $s = u + v$, $t = v - u$, where the null coordinates (u, v) are fixed by the gauge choices (2.26), (2.27), (2.25). Since $\partial_t = \frac{1}{2}(\partial_v - \partial_u) = \frac{1}{2}T$, Proposition 2.1 proves that the maximal future development arising from the characteristic data of Section 2.3 obeys $\partial_t r = 0$, $\partial_t \Omega^2 = 0$, $\partial_t Q = 0$, $\partial_t \phi = 0$. So we may consider these just as functions of s .

Of course, this is only true after imposing (A -gauge). In the (u, v) coordinate system, we notice that

$$A = A_U dU + A_V dV = 2K_+(UA_U du + VA_V dv) =: \tilde{A}(du - dv) = -\tilde{A}dt, \quad (2.35)$$

where, due to Proposition 2.1, $\tilde{A} = UA_U(s)$ is a real-valued function of s , with $\lim_{s \rightarrow -\infty} \tilde{A}(s) = 0$. We next show that this choice of gauge will in fact constrain the scalar field ϕ to be real.

Lemma 2.2. With the gauge choice (2.35) and the initial data of Section 2.3, $\phi = \phi(s)$ is everywhere real.

Proof. Consider the transport equations (2.10), (2.11) for the quantity Q . Since $\partial_t Q = \frac{1}{2}(\partial_v - \partial_u)Q = 0$,

$$q_0 r^2 \Im(\phi \overline{D_s \phi}) = \frac{1}{2} q_0 r^2 \Im(\phi(\overline{D_u \phi} + \overline{D_v \phi})) = 0.$$

Hence by (2.35) we must have $\Im(\phi \overline{D_s \phi}) = \Im(\phi \overline{\partial_s \phi}) = 0$.

Next, we decompose ϕ into its modulus and argument; $\phi = \Phi e^{i\theta}$. Then

$$\Im(\phi \overline{\partial_s \phi}) = -\Phi^2 \partial_s \theta = 0,$$

so that the phase θ is constant whenever ϕ is nonzero. But as ϕ is smooth in the variable s , it does not change phase when it reaches 0, hence ϕ is real everywhere. \square

Using the identities $\partial_u = \partial_s - \partial_t$, $\partial_v = \partial_s + \partial_t$, we have that, for $f \in \{r(s), \Omega(s), \phi(s), Q(s), \tilde{A}(s)\}$, one has

$$\partial_u f = \partial_v f = \frac{df}{ds} =: \dot{f}.$$

We now proceed to rewrite the Einstein-Maxwell-Klein-Gordon system (2.6)–(2.13) as a system of ODEs.

Firstly, the Raychaudhuri equation becomes

$$\frac{d}{ds}(-\Omega^{-2}\dot{r}) = \Omega^{-2}r(|\dot{\phi}|^2 + |\tilde{A}|^2 q_0^2 |\phi|^2). \quad (2.36)$$

Defining the quantity $\kappa = -\frac{1}{4}\Omega^2\dot{r}^{-1}$, which is exactly 1 in Reissner-Nordström(-dS/AdS), we may rewrite this as

$$\frac{d}{ds}\kappa^{-1} = 4\Omega^{-2}r(|\dot{\phi}|^2 + |\tilde{A}|^2 q_0^2 |\phi|^2). \quad (2.37)$$

We also at times appeal to (2.36) in the form:

$$\frac{d}{ds}(-\dot{r}) - \frac{d}{ds}\log(\Omega^2) \cdot (-\dot{r}) = r(|\dot{\phi}|^2 + |\tilde{A}|^2 q_0^2 |\phi|^2). \quad (2.38)$$

The wave equation for r is now written as

$$\ddot{r} = -\frac{\Omega^2}{4r} - \frac{\dot{r}^2}{r} + \frac{\Omega^2}{4r^3}Q^2 + \frac{\Omega^2 r}{4}(m^2|\phi|^2 + \Lambda), \quad (2.39)$$

which may be conveniently rewritten as

$$\frac{d}{ds}(-r\dot{r}) = \frac{\Omega^2}{4} - \frac{\Omega^2 Q^2}{4r^2} - \frac{\Omega^2 r^2}{4}(m^2|\phi|^2 + \Lambda). \quad (2.40)$$

The wave equation (2.9) for the null lapse Ω^2 becomes

$$\frac{d^2}{ds^2}\log(\Omega^2) = \frac{\Omega^2}{2r^2} + 2\frac{\dot{r}^2}{r^2} - \frac{\Omega^2}{r^4}Q^2 - 2\dot{\phi}^2 + 2|\tilde{A}|^2 q_0^2 |\phi|^2, \quad (2.41)$$

or alternatively

$$\frac{d^2}{ds^2}\log(r\Omega^2) = \frac{\Omega^2}{4r^2} - \frac{3}{4}\frac{\Omega^2 Q^2}{r^4} - 2|\dot{\phi}|^2 + 2|\tilde{A}|^2 q_0^2 |\phi|^2 + \frac{\Omega^2 m^2}{4}|\phi|^2. \quad (2.42)$$

For the Maxwell field Q and the gauge field \tilde{A} , the equations (2.10), (2.11), (2.13) become

$$\dot{Q} = \tilde{A}q_0^2 r^2 |\phi|^2, \quad (2.43)$$

$$\dot{\tilde{A}} = -\frac{Q\Omega^2}{4r^2}. \quad (2.44)$$

Finally, the wave equation (2.12) for the scalar field may be written as the second order ODE

$$\ddot{\phi} = -\frac{2\dot{r}\dot{\phi}}{r} - q_0^2 |\tilde{A}|^2 \phi - \frac{m^2 \Omega^2}{4}\phi, \quad (2.45)$$

which we often use in the form

$$\frac{d}{ds}(r^2\dot{\phi}) = -r^2q_0^2|\tilde{A}|^2\phi - \frac{m^2\Omega^2r^2}{4}\phi. \quad (2.46)$$

We also reformulate the initial data of Section 2.3 so as to satisfy the ODE system (2.36)–(2.46). Data is posed at the limit $s \rightarrow -\infty$, and is given by

$$\lim_{s \rightarrow -\infty} r(s) = r_+, \quad \lim_{s \rightarrow -\infty} Q(s) = \mathbf{e}, \quad \lim_{s \rightarrow -\infty} \phi(s) = \epsilon, \quad (2.47)$$

$$\lim_{s \rightarrow -\infty} \Omega^2(s) \cdot e^{-2K_+s} = \alpha_+, \quad (2.48)$$

$$\lim_{s \rightarrow -\infty} -4\Omega^{-2}(s)\dot{r}(s) = 1 - \frac{r_+m^2\epsilon^2}{2K_+}, \quad (2.49)$$

$$\lim_{s \rightarrow -\infty} \frac{d}{ds} \log(\Omega^2)(s) = 2K_+, \quad (2.50)$$

$$\lim_{s \rightarrow -\infty} \Omega^{-2}(s)\tilde{A}(s) = -\frac{\mathbf{e}}{8K_+r_+^2}, \quad (2.51)$$

$$\lim_{s \rightarrow -\infty} \Omega^{-2}(s)\dot{\phi}(s) = \beta_+\epsilon. \quad (2.52)$$

This concludes the set-up for the analytical problem considered in this paper.

2.5 Linear scattering in the Reissner-Nordström interior

We will often need to make comparisons to various quantities in exact Reissner-Nordström(-dS/AdS). While this is straightforward for (r, Ω^2, Q) , the scalar field ϕ vanishes in Reissner-Nordström, and we instead compare ϕ to solutions to the linear (*charged*) covariant Klein-Gordon equation in the Reissner-Nordström interior:

$$g_{RN}^{\mu\nu} D_\mu D_\nu \phi = m^2 \phi. \quad (2.53)$$

Here g_{RN} and D are the metric and covariant derivative in Reissner-Nordström(-dS/AdS), with A as specified in Section 2.2, and $m^2 \in \mathbb{R}$ and $q_0 \neq 0$ are fixed.

Since we are interested in the spatially homogeneous problem, we consider only solutions $\phi = \phi_{\mathcal{L}}$ to (2.53) that satisfy $T\phi_{\mathcal{L}} = 0$, $S\phi_{\mathcal{L}} = 0$, where $T = \partial_t$ is the Killing vector field of Reissner-Nordström(-dS/AdS) associated to stationarity and S is any vector field on the sphere.

Then denoting $\psi(s) = \phi_{\mathcal{L}}(t = 0, r^* = s)$, where r^*, t are as defined in Section 2.2, it can be checked that ψ satisfies the following second order ODE in s (see, for instance, the equation (2.45)):

$$\ddot{\psi} = \frac{\Omega_{RN}^2(s)}{4} \frac{\dot{\psi}}{2r_{RN}(s)} - \frac{\Omega_{RN}^2(s)}{4} m^2 \psi - q_0^2 \left(\frac{\mathbf{e}}{r_+} - \frac{\mathbf{e}}{r_{RN}(s)} \right)^2 \psi. \quad (2.54)$$

We define the quantities

$$\tilde{A}_{RN,\infty} = \frac{\mathbf{e}}{r_+} - \frac{\mathbf{e}}{r_-} \neq 0, \quad \omega_{RN} := |q_0 \tilde{A}_{RN,\infty}| > 0. \quad (2.55)$$

Then, following [59], we define four functions solving (2.54): $\psi_{\mathcal{H},1}, \psi_{\mathcal{H},2}, \psi_{\mathcal{CH},1}$ and $\psi_{\mathcal{CH},2}$. These satisfy the

following asymptotics towards the event horizon $\mathcal{H} = \{s = -\infty\}$ and the Cauchy horizon $\mathcal{CH} = \{s = +\infty\}$

$$\psi_{\mathcal{H},1}(s) = 1 + o(1) \quad \text{as } s \rightarrow -\infty, \quad (2.56)$$

$$\psi_{\mathcal{H},2}(s) = s + o(1) \quad \text{as } s \rightarrow -\infty, \quad (2.57)$$

$$\psi_{\mathcal{CH},1}(s) = e^{i\omega_{RN}s} + o(1) \quad \text{as } s \rightarrow +\infty, \quad (2.58)$$

$$\psi_{\mathcal{CH},2}(s) = \overline{\psi_{\mathcal{CH},1}}(s) = e^{-i\omega_{RN}s} + o(1) \quad \text{as } s \rightarrow +\infty. \quad (2.59)$$

The results of [59] then imply the following:

Proposition 2.3. Recalling the definition of $2K_-(M, \mathbf{e}, \Lambda) < 0$ from (2.22), and $\alpha_-(M, \mathbf{e}, \Lambda) > 0$ from (2.24), there exists some constant $C > 0$ such that

$$|\psi_{\mathcal{CH},1}(s) - e^{i\omega_{RN}s}| + \left| \frac{d\psi_{\mathcal{CH},1}}{ds}(s) - i\omega_{RN}e^{i\omega_{RN}s} \right| \leq C\Omega_{RN}^2(s) \leq 2C\alpha_-e^{2K_-s}, \quad (2.60)$$

$$|\psi_{\mathcal{CH},2}(s) - e^{-i\omega_{RN}s}| + \left| \frac{d\psi_{\mathcal{CH},2}}{ds}(s) + i\omega_{RN}e^{-i\omega_{RN}s} \right| \leq C\Omega_{RN}^2(s) \leq 2C\alpha_-e^{2K_-s}. \quad (2.61)$$

Furthermore, there exists a scattering coefficient $B = B(M, q_0, \mathbf{e}, \Lambda) \in \mathbb{C} \setminus \{0\}$ such that

$$\psi_{\mathcal{H},1}(s) = B\psi_{\mathcal{CH},1}(s) + \overline{B}\psi_{\mathcal{CH},2}(s) = 2\Re(B\psi_{\mathcal{CH},1}(s)). \quad (2.62)$$

Corollary 2.4. Let $\phi_{\mathcal{L}}$ be the solution to (2.53) with constant data $\phi = \epsilon$ on the event horizon $\mathcal{H} = \{s = -\infty\}$. Then there exists $C(M, \mathbf{e}, \Lambda, m^2, q_0) > 0$ and $\tilde{S}(M, \mathbf{e}, \Lambda, m^2, q_0) > 0$ such that, for $s \geq \tilde{S}$, one has

$$|\phi_{\mathcal{L}}(s) - B\epsilon e^{i\omega_{RN}s} - \overline{B}\epsilon e^{-i\omega_{RN}s}| \leq C\epsilon e^{2K_-s}. \quad (2.63)$$

$$\left| \dot{\phi}_{\mathcal{L}}(s) - i\omega_{RN}B\epsilon e^{i\omega_{RN}s} + i\omega_{RN}\overline{B}\epsilon e^{-i\omega_{RN}s} \right| \leq C\epsilon e^{2K_-s}. \quad (2.64)$$

3 Precise statement of the main theorems

3.1 Definition of the spacetime sub-regions

We now give a precise definition of the regions in Figure 6. Using the gauge choice (Ω -data), the following regions are part of the spacetime described in Proposition 2.1. The following regions, which each correspond to s being inside a non-empty interval $I \subset \mathbb{R}$, are such that, for ϵ chosen sufficiently small, their union covers the entire spacetime of Theorem 3.1.

- The red-shift region is $\mathcal{R} := \{-\infty < s \leq -\Delta_{\mathcal{R}}\}$ for some $\Delta_{\mathcal{R}} \gg 1$: Here, we make strong use of the positive surface gravity of the event horizon (red-shift effect, see [24, 28] and subsequent works).
- The no-shift region is $\mathcal{N} := \{-\Delta_{\mathcal{R}} \leq s \leq S\}$ for some $S \gg 1$: Here, we use a Cauchy stability argument and Grönwall's inequality to show that quantities are still ϵ^2 -close to their Reissner-Nordström values.
- The early blue-shift region is $\mathcal{EB} := \{S \leq s \leq s_{lin}(\epsilon) := |2K_-|^{-1} \log(\nu\epsilon^{-1})\}$ for $\nu > 0$: Here, we begin to exploit the *blue-shift* effect of the Cauchy horizon of Reissner-Nordström, which is due to negative surface gravity $2K_- < 0$.

- The late blue-shift region is $\mathcal{LB} := \{s_{lin}(\epsilon) \leq s \leq \Delta_B \epsilon^{-1}\}$ for some $\Delta_B > 0$: Here, the spacetime geometry begins to depart from that of Reissner-Nordström, and we provide the key ingredients to help us with the analysis of subsequent regions. In particular, this region starts to see a growth of the Hawking mass (a relic of mass inflation, see [67, 78] and the introduction of [81]).
- The oscillation region is $\mathcal{O} := \{s_O(\epsilon) := 50s_{lin}(\epsilon) \leq s \leq s_{PK}(\epsilon)\}$ where $r(s_{PK}) = 2|B|\mathfrak{W}r_- \epsilon$ for $\mathfrak{W} = \mathfrak{W}(M, \mathbf{e}, \Lambda, q_0) > 0$ defined in (4.51): Here, the Bessel-type behavior kicks in, leading to the collapsed oscillations discussed in Section 1.4.
- The proto-Kasner region is $\mathcal{PK} := \{s_{PK}(\epsilon) \leq s \leq s_i(\epsilon)\}$ where $r(s_i) = e^{-\delta_0 \epsilon^{-2}}$ for $\delta_0 = \delta_0(M, \mathbf{e}, \Lambda, q_0) > 0$ defined in (6.1): Here, the Bessel-type behavior continues but exhibits logarithmic growth rather than oscillations.

We also define the sub-region $\mathcal{PK}' := \{s_{K_1}(\epsilon) \leq s \leq s_i(\epsilon)\} \subset \mathcal{PK}$ where $r(s_{K_1}) = 2|B|\mathfrak{W}r_- \epsilon^2$. In this sub-region, we will establish that Kasner-type behavior starts to take place.

- The Kasner region is $\mathcal{K} := \{s_i(\epsilon) \leq s < s_\infty(\epsilon)\}$, where $\lim_{s \rightarrow s_\infty} r(s) = 0$. In this region, we prove that the metric is described by either one Kasner regime, or two Kasner regimes connected by a bounce. In \mathcal{K} , the scalar field is governed by a first-order ODE.

We also introduce the additional sub-regions of $\mathcal{PK} \cup \mathcal{K}$ depicted in Figure 7, where Ψ is defined in (1.31) and α in (1.10).

- The first Kasner region $\mathcal{K}_1 \subset \mathcal{PK}' \cup \mathcal{K}$ overlaps with \mathcal{PK} and \mathcal{K} . In this region, we will show the metric is in a Kasner regime. Anticipating Theorem 3.2, we will find that $\mathcal{K}_1 = \mathcal{PK}' \cup \mathcal{K}$ in the no Kasner bounce case (3.22) (i.e. the first Kasner regime is the final Kasner regime, with all Kasner exponents being positive) and $\mathcal{K}_1 = \{s_{K_1} \leq s \leq s_{in}\} \neq \mathcal{PK}' \cup \mathcal{K}$ in the Kasner bounce case (3.21) (with one negative Kasner exponent, which is thus expected to be unstable). Here $s_{in} := \min\{s \in \mathcal{K} : |\Psi(s)| = |\alpha| + \epsilon^2\}$.
- The Kasner bounce region $\mathcal{K}_{bo} \subset \mathcal{K}$. We have $\mathcal{K}_{bo} = \emptyset$ in the no Kasner bounce case (3.22), and $\mathcal{K}_{bo} = \{s_{in} \leq s \leq s_{out}\}$ in the Kasner bounce case (3.21), where $s_{out} := \min\{s \in \mathcal{K} : |\Psi(s)| = |\alpha|^{-1} - \epsilon^2\}$. We have weaker control of the metric in \mathcal{K}_{bo} , but we show that it is very short in terms of proper time.
- The second Kasner region $\mathcal{K}_2 \subset \mathcal{K}$. We will have $\mathcal{K}_2 = \emptyset$ in the no Kasner bounce case (3.22), and $\mathcal{K}_2 = \{s_{out} \leq s < s_\infty\}$ in the Kasner bounce case (3.21), where we exhibit a second Kasner regime (with positive Kasner exponents, in contrast to the first Kasner regime \mathcal{K}_1).

3.2 First statement: formation of a spacelike singularity

We first start with our main result, which covers part of Theorem I (namely the formation of the spacelike singularity). We reiterate that Theorem 3.1 contains the statements 1, 2, 5 of our rough Theorem I; more precisely statement 1 of Theorem I corresponds to statement i of Theorem 3.1, while statements 2 and 5 of Theorem I are covered by statement ii of Theorem 3.1 as well as the estimate (3.15).

The statements iii and iv of Theorem 3.1 will also lay the groundwork towards proving the more specific Kasner asymptotics claimed in statements 3 and 4 of Theorem I; the precise nature of these asymptotics will be covered in Theorem 3.2, upon further restricting ϵ .

In the following theorem and the rest of the paper, for $A, B \geq 0$ we will use the notation $A \lesssim B$ to denote that there exists $C(M, \mathbf{e}, \Lambda, q_0, m^2, \eta) > 0$ such that $A \leq CB$.

Theorem 3.1. *Let $(M, \mathbf{e}, \Lambda) \in \mathcal{P}_{se}$ with $\mathbf{e} \neq 0$, $q_0 \neq 0$, $m^2 \in \mathbb{R}$ be subextremal Reissner-Nordström(-dS/AdS) parameters (see Section 2.2). Then, for $\eta > 0$ chosen sufficiently small, there exists $\epsilon_0(M, \mathbf{e}, \Lambda, q_0, m^2, \eta) > 0$ and a subset $E_\eta \subset (-\epsilon_0, \epsilon_0) \setminus \{0\}$ satisfying $\frac{|(-\delta, \delta) \setminus E_\eta|}{2\delta} = O(\eta)$ for any $0 < \delta \leq \epsilon_0$, such that the following holds: For all $\epsilon \in E_\eta$, the maximal future development \mathcal{M} for (1.2)-(1.5) of the characteristic data from Section 2 (i.e. $(\Omega$ -data), $(r$ -data), $(Q$ -data), and $(\phi$ -data)) terminates at a spacelike singularity S on which r extends continuously to 0, and the Penrose diagram is given by Figure 6.*

More precisely, there exists a foliation of \mathcal{M} by spacelike hypersurfaces Σ_s , with $s \in (-\infty, s_\infty(\epsilon))$, where s is defined in $(\Omega$ -data), and $s_\infty = \frac{|K_-|}{4|B|^2\omega_{RN}^2}\epsilon^{-2} + O(\log(\epsilon^{-1}))$, where $B(M, \mathbf{e}, \Lambda, m^2, q_0) \neq 0$ is defined in (2.62), and $2K_-(M, \mathbf{e}, \Lambda) < 0$, $\omega_{RN}(M, \mathbf{e}, \Lambda, q_0) > 0$ are defined in Section 2.2. The subsequent spacetime dynamics are described as follows:

- i. (Almost formation of a Cauchy horizon). In the late blue-shift region $\mathcal{LB} := \{s_{lin}(\epsilon) \leq s \leq \Delta_B \epsilon^{-1}\}$, we have the following stability estimates with respect to the Reissner-Nordström(-dS/AdS) metric:

$$\begin{aligned} \epsilon^{-1}|\phi(s) - 2\epsilon \operatorname{Re}(Be^{i\omega_{RN}s})| + \epsilon^{-1} \left| \frac{d}{ds}[\phi(s) - 2\epsilon \operatorname{Re}(Be^{i\omega_{RN}s})] \right| + |r(s) - r_-| \\ + |Q(s) - \mathbf{e}| + \left| \frac{d}{ds} \log(\Omega^2)(s) - 2K_- \right| \lesssim \epsilon^2 s \lesssim \epsilon. \end{aligned} \quad (3.1)$$

For $s \in \mathcal{LB}$, we find also the following estimate for $-r\dot{r}(s)$:

$$\left| -r\dot{r}(s) - \frac{4|B|^2\omega_{RN}^2\epsilon^2 r_-^2}{2|K_-|} \right| \lesssim e^{2K_-s} + \epsilon^4 s. \quad (3.2)$$

- ii. (Collapsed oscillations and loss of charge). In the oscillation region $\mathcal{O} := \{s_O(\epsilon) \leq s \leq s_{PK}(\epsilon)\}$, we have the following Bessel-type oscillations for the scalar field: for some $\xi_0 = \frac{|K_-|}{4|B|^2\omega_{RN}} + O(\epsilon^2 \log(\epsilon^{-1}))$,

$$\left| \phi(s) - \left(C_J(\epsilon) J_0 \left(\frac{\xi_0 r^2(s)}{r_-^2 \epsilon^2} \right) + C_Y(\epsilon) Y_0 \left(\frac{\xi_0 r^2(s)}{r_-^2 \epsilon^2} \right) \right) \right| \lesssim \epsilon^2 \log(\epsilon^{-1}), \quad (3.3)$$

$$\left| \frac{d}{ds} \left(\phi(s) - \left(C_J(\epsilon) J_0 \left(\frac{\xi_0 r^2(s)}{r_-^2 \epsilon^2} \right) + C_Y(\epsilon) Y_0 \left(\frac{\xi_0 r^2(s)}{r_-^2 \epsilon^2} \right) \right) \right) \right| \lesssim \epsilon^2 \log(\epsilon^{-1}), \quad (3.4)$$

where the constants $C_J(\epsilon)$, $C_Y(\epsilon)$ are highly oscillatory in ϵ ; namely for $\mathfrak{W}(M, \mathbf{e}, q_0, \Lambda) > 0$ given by

$$\mathfrak{W}(M, \mathbf{e}, \Lambda, q_0) = \sqrt{\frac{\omega_{RN}}{2|K_-|}} = \sqrt{\frac{|q_0 \mathbf{e}|}{|\frac{\mathbf{e}^2}{r_-^2} - \frac{\Lambda}{3} r_+(r_+ + 2r_-)|}} > 0, \quad (3.5)$$

one finds that

$$\left| C_J(\epsilon) - \frac{\sqrt{\pi}}{2} \mathfrak{W}^{-1} \cos(\Theta(\epsilon)) \right| + \left| C_Y(\epsilon) - \frac{\sqrt{\pi}}{2} \mathfrak{W}^{-1} \sin(\Theta(\epsilon)) \right| \lesssim \epsilon^2 \log(\epsilon^{-1}), \quad (3.6)$$

$$\left| \Theta(\epsilon) - \frac{\epsilon^{-2}}{8|B|^2 \mathfrak{W}} \right| \lesssim \log(\epsilon^{-1}). \quad (3.7)$$

For $s \in \mathcal{O}$, one has (note this improves upon (3.2) in $\mathcal{LB} \cap \mathcal{O}$):

$$\left| -r\dot{r}(s) - \frac{4|B|^2\omega_{RN}^2\epsilon^2r_-^2}{2|K_-|} \right| \lesssim \epsilon^4 \log(\epsilon^{-1}). \quad (3.8)$$

Moreover, the charge Q transitions from \mathbf{e} to $Q_\infty(M, \mathbf{e}, \Lambda) := \frac{3}{4}\mathbf{e} + \Lambda \frac{r_-^2 r_+ (2r_- + r_+)}{12\mathbf{e}}$ (up to $O(\epsilon^{2-})$ errors), and

$$\left| Q(s) - \mathbf{e} + (\mathbf{e} - Q_\infty) \left(1 - \frac{r_-^2(s)}{r_-^2} \right) \right| \lesssim \epsilon^2 \log(\epsilon^{-1}) \text{ for all } s \in \mathcal{O}, \quad (3.9)$$

$$\frac{Q_\infty(M, \mathbf{e}, 0)}{\mathbf{e}} = \frac{3}{4}, \quad (3.10)$$

$$\left\{ \frac{Q_\infty(M, \mathbf{e}, \Lambda)}{\mathbf{e}} : (M, \mathbf{e}, \Lambda) \in \mathcal{P}_{se}, \Lambda < 0 \right\} = \left(\frac{1}{2}, \frac{3}{4} \right), \quad (3.11)$$

$$\left\{ \frac{Q_\infty(M, \mathbf{e}, \Lambda)}{\mathbf{e}} : (M, \mathbf{e}, \Lambda) \in \mathcal{P}_{se}, \Lambda > 0 \right\} = \left(\frac{3}{4}, 1 \right). \quad (3.12)$$

iii. (Logarithmic Bessel-type divergence). In the proto-Kasner region $\mathcal{PK} := \{s_{PK}(\epsilon) \leq s \leq s_i(\epsilon)\}$, the Bessel-type behavior persists with modified coefficients, namely there exist

$$C_{YK}(\epsilon) = C_Y(\epsilon) + O(\epsilon^2 \log(\epsilon^{-1})), \quad C_{JK}(\epsilon) = C_J(\epsilon) + O(\epsilon^2 \log(\epsilon^{-1})), \quad \xi_K = \xi_0 + O(\epsilon^2 \log(\epsilon^{-1})),$$

such that (3.3), (3.4) remain true for all $s \in \mathcal{PK}$, after replacing $(C_Y(\epsilon), C_J(\epsilon), \xi_0)$ by $(C_{YK}(\epsilon), C_{JK}(\epsilon), \xi_K)$.

Consequently, we have the following logarithmic growth: for all $s \in \mathcal{PK}$,

$$\left| \phi(s) + \frac{2}{\pi} C_{YK}(\epsilon) \log\left(\frac{r_-^2 \epsilon^2}{\xi_K r^2(s)}\right) - C_{YK}(\epsilon) - 2\pi^{-1}(\gamma - \log 2) C_{JK}(\epsilon) \right| \lesssim \epsilon^2 \log(\epsilon^{-1}), \quad (3.13)$$

$$\left| \frac{d}{ds} \left(\phi(s) + \frac{2}{\pi} C_{YK} \log\left(\frac{r_-^2 \epsilon^2}{\xi_K r^2(s)}\right) \right) \right| \lesssim \epsilon^2 \log(\epsilon^{-1}). \quad (3.14)$$

Moreover, (3.8) still holds for $s \in \mathcal{PK}$, while the charge Q remains close to its value at s_{PK} ; for all $s \in \mathcal{PK}$:

$$|Q(s) - Q_\infty| \lesssim \epsilon^2 \log(\epsilon^{-1}). \quad (3.15)$$

Finally, in the sub-region $\mathcal{PK}' = \{s_{K_1}(\epsilon) \leq s \leq s_i(\epsilon)\} \subset \mathcal{PK}$, the quantity $\Psi(s)$ defined by

$$\Psi(s) := -r(s) \frac{d\phi}{dr}(s) = \frac{r(s)}{-\frac{dr}{ds}(s)} \frac{d\phi}{ds}(s)$$

obeys the estimates:

$$\left| \Psi(s) + \frac{2}{\sqrt{\pi}} \mathfrak{W}^{-1} \sin(\Theta(\epsilon)) \right| \lesssim \epsilon^2 \log(\epsilon^{-1}). \quad (3.16)$$

$$|\Psi(s) - \Psi(s_i)| \lesssim r^2(s) \log(\epsilon^{-1}) \lesssim \epsilon^4 \log(\epsilon^{-1}). \quad (3.17)$$

iv. In the Kasner region $\mathcal{K} := \{s_i \leq s < s_\infty(\epsilon)\}$, $-r\dot{r}(s)$ obeys the lower bound

$$-r\dot{r}(s) \geq \frac{4|B|^2\omega_{RN}^2\epsilon^2r_-^2}{2|K_-|} \cdot \frac{1}{2}\eta^2. \quad (3.18)$$

The quantity Ψ obeys the following ODE: introducing $R := \log\left(\frac{r_-}{r}\right)$,

$$\frac{d\Psi}{dR} = -\Psi(\Psi - \alpha)(\Psi - \alpha^{-1}) + \mathcal{F}, \quad (3.19)$$

$$|\alpha - \Psi(s_i)| \lesssim e^{-\delta_0 \epsilon^{-2}}, \quad \mathcal{F}(R) \lesssim e^{-\delta_0 \epsilon^{-2}} r(R). \quad (3.20)$$

Finally, the charge retention remains in the sense that (3.15) is also valid for all $s \in \mathcal{K}$.

3.3 Second statement: Kasner asymptotics in the \mathcal{PK} and \mathcal{K} regions

We now enter into the details of the regions $\mathcal{PK}' \cup \mathcal{K}$, in which the Kasner-like behavior manifests. The following theorem requires a (slightly) stronger assumption on ϵ than Theorem 3.1.

Theorem 3.2. *Let $(M, \mathbf{e}, \Lambda) \in \mathcal{P}_{se}$ with $\mathbf{e} \neq 0$, $q_0 \neq 0$, $m^2 \in \mathbb{R}$. Then, for any sufficiently small $\eta, \sigma > 0$, there exists $\epsilon_0(M, \mathbf{e}, \Lambda, q_0, m^2, \eta, \sigma) > 0$ such that there exists a subset $E'_{\eta, \sigma} \subset E_\eta$ satisfying $\frac{|(-\delta, \delta) \setminus E'_{\eta, \sigma}|}{2\delta} = O(\eta + \sigma)$ for any $0 < \delta \leq \epsilon_0$, and such that $E'_{\eta, \sigma}$ may be expressed as a disjoint union $E'_{\eta, \sigma} = E'_{\eta, \sigma}{}^{bo} \cup E'_{\eta, \sigma}{}^{Nbo}$, where*

$$\epsilon \in E'_{\eta, \sigma}{}^{bo} \text{ if } |\Psi(s_i)| = \frac{2}{\sqrt{\pi}} \mathfrak{W}^{-1} |\sin(\Theta(\epsilon))| + O(\epsilon^2 \log(\epsilon^{-1})) \leq 1 - \sigma < 1. \quad (3.21)$$

$$\epsilon \in E'_{\eta, \sigma}{}^{Nbo} \text{ if } |\Psi(s_i)| = \frac{2}{\sqrt{\pi}} \mathfrak{W}^{-1} |\sin(\Theta(\epsilon))| + O(\epsilon^2 \log(\epsilon^{-1})) \geq 1 + \sigma > 1. \quad (3.22)$$

We call these respectively the Kasner bounce case and the no bounce inversion case.

Moreover, we have the following two possibilities.

- If $\mathfrak{W}(M, \mathbf{e}, \Lambda, q_0) \geq \frac{2}{\sqrt{\pi}}$, then $E'_{\eta, \sigma}{}^{Nbo} = \emptyset$, and therefore $\frac{|(-\epsilon, \epsilon) \setminus E'_{\eta, \sigma}{}^{bo}|}{2\epsilon} = O(\eta + \sigma)$, for η, σ small.
- If $\mathfrak{W}(M, \mathbf{e}, \Lambda, q_0) < \frac{2}{\sqrt{\pi}}$, then $|E'_{\eta, \sigma}{}^{Nbo}|, |E'_{\eta, \sigma}{}^{bo}| > 0$, and for η, σ small:

$$\begin{aligned} \frac{|E'_{\eta, \sigma}{}^{Nbo} \cap (-\epsilon, \epsilon)|}{2\epsilon} &= \frac{2}{\pi} \arcsin\left(1 - \frac{\sqrt{\pi}}{2} \mathfrak{W}\right) + O(\sigma), \\ \frac{|E'_{\eta, \sigma}{}^{bo} \cap (-\epsilon, \epsilon)|}{2\epsilon} &= 1 - \frac{2}{\pi} \arcsin\left(1 - \frac{\sqrt{\pi}}{2} \mathfrak{W}\right) + O(\eta + \sigma). \end{aligned}$$

Then, for all $\epsilon \in E'_{\eta, \sigma}$, we have the following Kasner-like behavior, where, in what follows, $b_- = \frac{|B| \omega_{RN}}{|K_-|}$.

1. In the first Kasner region \mathcal{K}_1 , we have the following, recalling α from (3.20).

(a) In the no Kasner bounce case (3.22), we have $|\alpha| > 1$, $\mathcal{K}_1 = \mathcal{PK}' \cup \mathcal{K}$, and for all $s \in \mathcal{K}_1$,

$$|\Psi(s) - \alpha| \lesssim \epsilon^2 \cdot \left(\frac{r(s)}{r(s_{PK})} \right)^\beta, \quad (3.23)$$

where we define $\beta := \min\{\frac{1}{2}, \alpha^2 - 1\} > 0$. Moreover, the metric takes the following Kasner-like form

$$g = -d\tau^2 + \mathcal{X}_1 \cdot (1 + \mathfrak{E}_{X,1}(\tau)) \tau^{\frac{2(\alpha^2-1)}{\alpha^2+3}} dt^2 + \mathcal{R}_1 \cdot (1 + \mathfrak{E}_{R,1}(\tau)) r_-^2 \tau^{\frac{4}{\alpha^2+3}} d\sigma_{\mathbb{S}^2}, \quad (3.24)$$

$$\left| \log \mathcal{X}_1 + \frac{\alpha^2 + 1}{\alpha^2 + 3} \frac{4|K_-|^2}{|B|^2} \epsilon^{-2} \right| + \left| \log \mathcal{R}_1 - \frac{1}{\alpha^2 + 3} \frac{4|K_-|^2}{|B|^2} \epsilon^{-2} \right| \lesssim \log(\epsilon^{-1}), \quad (3.25)$$

$$|\mathfrak{E}_{X,1}(\tau)| + |\mathfrak{E}_{R,1}(\tau)| \lesssim \epsilon^2 \cdot \left(\frac{\tau}{\tau(s_{K_1})} \right)^{\frac{2\beta}{\alpha^2+3}}, \quad (3.26)$$

where τ is the proper time¹³, and we call $(p_1, p_2, p_3) = (\frac{\alpha^2-1}{\alpha^2+3}, \frac{2}{\alpha^2+3}, \frac{2}{\alpha^2+3}) \in (0, 1)^3$ the Kasner exponents.

(b) In the Kasner bounce case (3.21), we have $|\alpha| < 1$, $\mathcal{K}_1 = \{s_{K_1} \leq s \leq s_{in}\} \subset \mathcal{PK}' \cup \mathcal{K}$, and for all $s \in \mathcal{K}_1$,

$$|\Psi(s) - \alpha| \lesssim \epsilon^2, \quad (3.27)$$

where $s_{in} = \frac{b_-^{-2}}{4|K_-|} + O(\log(\epsilon^{-1}))$ is such that

$$r(s_{in}) = r_- \cdot \exp\left(-\frac{\epsilon^{-2}}{2b_-^2 \cdot (1-\alpha^2)} + O(\log(\epsilon^{-1}))\right). \quad (3.28)$$

Moreover, the metric takes the following Kasner-like form, where $\tau_0 > 0$ is a constant.

$$g = -d\tau^2 + \mathcal{X}_1 \cdot (1 + \mathfrak{E}_{X,1}(\tau)) (\tau - \tau_0)^{\frac{2(\alpha^2-1)}{\alpha^2+3}} dt^2 + \mathcal{R}_1 \cdot (1 + \mathfrak{E}_{R,1}(\tau)) r_-^2 (\tau - \tau_0)^{\frac{4}{\alpha^2+3}} d\sigma_{\mathbb{S}^2}. \quad (3.29)$$

We call $(p_1, p_2, p_3) = (\frac{\alpha^2-1}{\alpha^2+3}, \frac{2}{\alpha^2+3}, \frac{2}{\alpha^2+3}) \in (-\frac{1}{3}, 0) \times (\frac{1}{2}, \frac{2}{3})^2$ the first Kasner exponents.

Moreover, \mathcal{X}_1 and \mathcal{R}_1 obey (3.25), and for all $\tau(s_{K_1}) \leq \tau \leq \tau(s_{in})$:

$$|\mathfrak{E}_{X,1}(\tau)| + |\mathfrak{E}_{R,1}(\tau)| \lesssim \epsilon^2. \quad (3.30)$$

2. In the Kasner bounce region \mathcal{K}_{bo} (only in the Kasner bounce case (3.21)), we have for all $s \in \mathcal{K}_{bo}$,

$$r(s) = r_- \cdot \exp\left(-\frac{\epsilon^{-2}}{2b_-^2 \cdot (1-\alpha^2)} + O(\log(\epsilon^{-1}))\right). \quad (3.31)$$

Moreover, in terms of proper time, we have

$$0 < \tau(s_{in}) - \tau(s_{out}) \lesssim \exp\left(-\frac{\epsilon^{-2}}{b_-^2 \cdot (1-\alpha^2)} + O(\log(\epsilon^{-1}))\right). \quad (3.32)$$

3. In the second Kasner region \mathcal{K}_2 (only in the Kasner bounce case (3.21)), we define $\beta := \min\{\frac{1}{2}, \alpha^{-2} - 1\} > 0$ (since $|\alpha| < 1$). We have for all $s \in \mathcal{K}_1$:

$$|\Psi(s) - \alpha^{-1}| \lesssim \epsilon^2 \cdot \left(\frac{r(s)}{r(s_{out})} \right)^\beta. \quad (3.33)$$

Moreover, the metric takes the following Kasner-like form, for all $0 < \tau \leq \tau(s_{out})$

$$g = -d\tau^2 + \mathcal{X}_2 \cdot (1 + \mathfrak{E}_{X,2}(\tau)) \tau^{\frac{2(1-\alpha^2)}{1+3\alpha^2}} dt^2 + \mathcal{R}_2 \cdot (1 + \mathfrak{E}_{R,2}(\tau)) r_-^2 \tau^{\frac{4\alpha^2}{1+3\alpha^2}} d\sigma_{\mathbb{S}^2}. \quad (3.34)$$

$$\left| \log \mathcal{X}_2 + \frac{1 + \alpha^{-2}}{1 + 3\alpha^2} \frac{4|K_-|^2}{|B|^2} \epsilon^{-2} \right| + \left| \log \mathcal{R}_2 - \frac{1}{1 + 3\alpha^2} \frac{4|K_-|^2}{|B|^2} \epsilon^{-2} \right| \lesssim \log(\epsilon^{-1}), \quad (3.35)$$

$$|\mathfrak{E}_{X,2}(\tau)| + |\mathfrak{E}_{R,2}(\tau)| \lesssim \epsilon^2 \cdot \left(\frac{\tau}{\tau(s_{out})} \right)^{\frac{2\beta}{\alpha^{-2}+3}}. \quad (3.36)$$

¹³More precisely, τ is a past-directed timelike variable, orthogonal to the hypersurfaces Σ_s , and normalized such that $g(d\tau, d\tau) = -1$ and $\tau = 0$ at the spacelike singularity $\{r = 0\}$.

We call $(p_1, p_2, p_3) = (\frac{1-\alpha^2}{1+3\alpha^2}, \frac{2\alpha^2}{1+3\alpha^2}, \frac{2\alpha^2}{1+3\alpha^2}) \in (0, 1)^3$ the second Kasner exponents.

Finally, in terms of proper time, we have (recalling that τ is normalized so that $\lim_{s \rightarrow s_\infty} \tau(s) = 0$):

$$\exp\left(-\frac{1+\alpha^{-2}}{2b_-^2 \cdot (1-\alpha^2)} \epsilon^{-2} + O(\log(\epsilon^{-1}))\right) \lesssim \tau(s_{out}) \lesssim \exp\left(-\frac{1+\alpha^{-2}}{2b_-^2 \cdot (1-\alpha^2)} \epsilon^{-2} + O(\log(\epsilon^{-1}))\right). \quad (3.37)$$

Without loss of generality, we will choose $\epsilon > 0$ in all the subsequent sections.

4 Almost formation of a Cauchy horizon

In this section, we provide estimates up to a region $s \sim \epsilon^{-1}$. The analysis will be perturbative in nature, and we always bear in mind the comparison to the linear charged scalar field problem in Reissner-Nordström, see Section 2.5. The analysis will largely follow [81], with minor modifications due to the now dynamical nature of the charge Q and the charge term for the scalar field.

As in [81], the estimates up to $s \sim \epsilon^{-1}$ will be divided into the four regions \mathcal{R} , \mathcal{N} , \mathcal{EB} , and \mathcal{LB} (see Figure 6 and Figure 1). Where differences from [81] are minor, we aim to be relatively brief, and focus on the new techniques required to deal with the charge and the scalar field.

4.1 Estimates up to the no-shift region

We begin with some notation. As the arguments of this section are perturbative, it will help to introduce differences between the quantities $(r, \Omega^2, \phi, Q, \tilde{A})$ and their Reissner-Nordström(-dS/AdS) values. Therefore define

$$\begin{aligned} \delta r(s) &= r(s) - r_{RN}(s), & \delta \Omega^2(s) &= \Omega^2(s) - \Omega_{RN}^2(s), \\ \delta \phi(s) &= \phi(s) - \phi_{\mathcal{L}}(s), \\ \delta Q(s) &= Q(s) - \mathbf{e}, & \delta \tilde{A}(s) &= \tilde{A}(s) + \left(\frac{\mathbf{e}}{r_+} - \frac{\mathbf{e}}{r_{RN}(s)} \right), \end{aligned}$$

where we used (2.18) to provide the Maxwell gauge field \tilde{A}_{RN} to which we compare, and $\phi_{\mathcal{L}}$ is the solution to the linear charged scalar field scattering problem in Reissner-Nordström, see Corollary 2.4.

We also use the quantity $\delta \log \Omega^2(s) = \log \Omega^2(s) - \log \Omega_{RN}^2(s)$. We commonly use that for $\delta \log \Omega^2(s) \lesssim 1$,

$$\delta \Omega^2(s) \lesssim \Omega^2(s) \delta \log \Omega^2(s) \lesssim \delta \Omega^2(s). \quad (4.1)$$

We now proceed to the estimates in the red-shift region \mathcal{R} .

Proposition 4.1. There exist $D_R(M, \mathbf{e}, \Lambda, m^2, q_0) > 0$ and $\Delta_{\mathcal{R}}(M, \mathbf{e}, \Lambda) \gg 1$ such that, in the red-shift region $\mathcal{R} = \{-\infty < s < -\Delta_R\}$, the following estimates hold:

$$|\phi| + |\Omega^{-2} \dot{\phi}| \leq D_R \epsilon, \quad (4.2)$$

$$|\kappa^{-1} - 1| \leq D_R \epsilon^2, \quad (4.3)$$

$$|\varpi - M| \leq D_R \epsilon^2, \quad (4.4)$$

$$\left| \frac{d \log(\Omega^2)}{ds} - 2K(s) \right| + |\log(\alpha_+^{-1} \Omega^2) - 2K_+ s| \leq D_R \Omega^2 \ll 1, \quad (4.5)$$

$$|\delta \log(\Omega^2)| + |\delta r| + |\delta \dot{r}| + |\delta \tilde{A}| \Omega^{-2} + |\delta Q| \leq D_R \epsilon^2, \quad (4.6)$$

$$|\delta \phi| + |\delta \dot{\phi}| \leq D_R \epsilon^3. \quad (4.7)$$

Proof. We provide a short sketch. For more details, see Proposition 4.5 in [76] or Lemma 4.1 in [81]. We make the following bootstrap assumptions:

$$\left| \frac{d}{ds} \log(\Omega^2) - 2K_+ \right| \leq K_+, \quad (\text{RS1})$$

$$|\phi| \leq 4\epsilon, \quad (\text{RS2})$$

$$|Q - \mathbf{e}| \leq \frac{\mathbf{e}}{2}, \quad (\text{RS3})$$

$$|r - r_+| \leq \frac{r_+}{2}. \quad (\text{RS4})$$

These will hold in neighborhood of $s = -\infty$ due to the asymptotic data (2.47) and (2.50). The bootstrap assumption (RS1) will give the important estimate

$$\int_{-\infty}^s \Omega^2(s') ds' \lesssim \int_{-\infty}^s \frac{d}{ds} \log(\Omega^2) \cdot \Omega^2(s') ds' = \int_{-\infty}^s \frac{d}{ds} \Omega^2(s') = \Omega^2(s). \quad (4.8)$$

The evolution equation (2.44) for \tilde{A} will immediately yield that $|\tilde{A}| \lesssim \Omega^2$. Therefore, turning to the equation (2.46), we use (4.8) to see that

$$|r^2 \dot{\phi}| \lesssim \int_{-\infty}^s \Omega^2(s') \epsilon ds' \lesssim \Omega^2(s) \epsilon,$$

which, after another round of integration, gives $|\phi| \leq \epsilon + C\Omega^2(s)\epsilon$, for some positive constant C .

Since the right hand side of the equation (2.37) is now bounded by $C\Omega^2\epsilon^2$, the estimate (4.3) is straightforward, and from this point (4.4) and (4.5) are also immediate. In particular, the remaining bootstraps are all improved, so long as $\Delta_{\mathcal{R}}$ is chosen large enough that $\Omega^2(s) < C^{-1}$ and ϵ is sufficiently small.

In order to get the difference estimates (4.6), (4.7), we make yet another bootstrap assumption:

$$|\delta r| + |\delta \dot{r}| + |\delta \log(\Omega^2)| + |\delta \tilde{A}| + \epsilon^{-1} |\delta \phi| + \epsilon^{-1} |\delta \dot{\phi}| \leq \epsilon^2. \quad (\text{RS5})$$

The claim is that we can then use the ODEs for differences (found by subtracting from the relevant ODE in Section 2.4 the analogous ODE in Reissner-Nordström) to then improve the RHS of (RS5) by $C\Omega^2\epsilon^2$, hence improving the bootstrap for $\Delta_{\mathcal{R}} > 0$ sufficiently large.

We demonstrate this for the $\delta\phi$ estimate as an illustration. Taking the differences of (2.45), we have

$$|\delta \ddot{\phi}| \lesssim |\delta \dot{r}| |\dot{\phi}| + |\dot{r}| |\delta \dot{\phi}| + |\dot{r} \dot{\phi}| |\delta r| + |\delta \tilde{A}| |\tilde{A}| |\phi| + (\tilde{A}^2 + \Omega^2) |\delta \phi| + |\delta \Omega^2| |\phi|.$$

Using (4.2)–(4.5) as well as (RS5) to estimate the RHS by appropriate powers of ϵ and Ω^2 ((4.1) is also useful here), we see that

$$|\delta \ddot{\phi}| \lesssim \Omega^2 \epsilon^3,$$

so that, integrating this from $s = -\infty$ once and then twice, using (4.8) we indeed get

$$|\delta\dot{\phi}| + |\delta\phi| \leq C\Omega^2\epsilon^3$$

as claimed. A similar procedure can be executed for the remaining equations of Section 2.4. This improves (RS5) and completes the proof of this proposition. \square

In the sequel, we fix $\Delta_{\mathcal{R}}$ such that Proposition 4.1 applies. Next, we use a Grönwall argument to provide estimates in the no-shift region \mathcal{N} .

Proposition 4.2. Take $S > 0$ to be any fixed real number. Then there exists some $C(M, \mathbf{e}, \Lambda, m^2, q_0) > 1$ and $D_N(M, \mathbf{e}, \Lambda, m^2, q_0) > 0$ such that, in the region $\mathcal{N} = \{-\Delta_{\mathcal{R}} \leq s \leq S\}$, the following estimates hold for ϵ sufficiently small:

$$|\phi| + |\dot{\phi}| \leq D_N C^s \epsilon, \quad (4.9)$$

$$|\kappa^{-1} - 1| \leq D_N C^s \epsilon^2, \quad (4.10)$$

$$|Q - \mathbf{e}| \leq D_N C^s \epsilon^2, \quad (4.11)$$

$$|\varpi - M| \leq D_N C^s \epsilon^2, \quad (4.12)$$

$$|\delta r| + |\delta \dot{r}| + |\delta \log(\Omega^2)| + \left| \frac{d}{ds} \delta \log(\Omega^2) \right| + |\delta \tilde{A}| \leq D_N C^s \epsilon^2, \quad (4.13)$$

$$|\delta\phi| + |\delta\dot{\phi}| \leq D_N C^s \epsilon^3. \quad (4.14)$$

In the sequel, we only apply these estimates at $s = S$, so that allowing D_N to depend also on S , the terms involving C^s can be absorbed into D_N – indeed we define $D'_N = C^S D_N$ for convenience.

Proof. Here, we begin with some bootstrap assumptions on the geometry and the Maxwell field which clearly hold in a neighborhood of $s = -\Delta_{\mathcal{R}}$:

$$|Q| \leq 2|\mathbf{e}|, \quad (\text{NS1})$$

$$|\tilde{A}| \leq \frac{2|\mathbf{e}|}{r_+}, \quad (\text{NS2})$$

$$|\kappa^{-1} - 1| \leq \frac{1}{2}, \quad (\text{NS3})$$

$$r \geq \frac{r_-}{2}, \quad (\text{NS4})$$

$$\Omega^2 \leq 2\Omega_{\max}^2(M, \mathbf{e}, \Lambda) := 2 \sup_{s \in \mathbb{R}} \Omega_{RN}^2(s). \quad (\text{NS5})$$

Using these bootstraps and (2.45), it is straightforward to see that

$$\left| \frac{d}{ds}(\phi, \dot{\phi}) \right| \leq C_1(M, \mathbf{e}, \Lambda, q_0, m^2) |(\phi, \dot{\phi})|,$$

which immediately yields (4.9). Using the evolution equation (2.43) for Q then gives (4.11), improving (NS1) – in fact we have $|Q - \mathbf{e}| \lesssim C_1^{2s} \epsilon^2$.

Next, we consider the following tuple of geometric and gauge quantities:

$$\mathbf{X} = (\delta r, \delta \dot{r}, \delta \log \Omega^2, \frac{d}{ds} \delta \log \Omega^2, \delta \tilde{A}).$$

Taking the differences from Reissner-Nordström for the equations (2.39), (2.41), (2.44), along with the bootstrap assumptions, for some $C_2(M, \mathbf{e}, \Lambda, m^2, q_0) > 0$, we get

$$\left| \frac{d\mathbf{X}}{ds} \right| \leq C_2(|\mathbf{X}| + C_1^{2s} \epsilon^2). \quad (4.15)$$

Thus, using Grönwall, we deduce (4.13) for some C with appropriate dependence on C_1, C_2 . For ϵ small, this improves (NS2), (NS4), (NS5).

Next, for $s \geq -\Delta_{\mathcal{R}}$, we know $\Omega^{-2} \leq C_3 e^{-2K-s}$ for some $C_3(M, \mathbf{e}, \Lambda, m^2, q_0) > 0$. Hence, (2.37),

$$|\kappa^{-1}(s) - \kappa^{-1}(-\Delta_{\mathcal{R}})| \lesssim C_3 e^{-2K-s} C_1^{2s} \epsilon^2. \quad (4.16)$$

So, for C chosen sufficiently large, we get (4.10) and improve (NS3). The final estimate (4.14) is straightforward. \square

Corollary 4.3. Let $S' > S$ be another arbitrarily chosen real number. Then for $S \leq s \leq S'$ and for ϵ sufficiently small, there exists some $D_-(M, \mathbf{e}, \Lambda, m^2, q_0, S, S') > 0$ such that:

$$|r(s) - r_-| \leq D_-(\epsilon^2 + e^{2K-s}), \quad (4.17)$$

$$\left| \tilde{A} + \frac{\mathbf{e}}{r_+} - \frac{\mathbf{e}}{r_-} \right| \leq D_-(\epsilon^2 + e^{2K-s}), \quad (4.18)$$

$$D_-^{-1} e^{2K-s} \leq \Omega^2 \leq D_- e^{2K-s}, \quad (4.19)$$

$$|\phi - B\epsilon e^{i\omega_{RN}s} - \bar{B}\epsilon e^{-i\omega_{RN}s}| + |\dot{\phi} - i\omega_{RN}B\epsilon e^{i\omega_{RN}s} + i\omega_{RN}\bar{B}\epsilon e^{-i\omega_{RN}s}| \leq D_-(\epsilon^3 + \epsilon e^{2K-s}), \quad (4.20)$$

$$\left| \frac{d \log(\Omega^2)}{ds} - 2K_- \right| \leq D_-(\epsilon^2 + e^{2K-s}) \leq \frac{|K_-|}{100}. \quad (4.21)$$

Proof. Note the previous proposition holds in the same way for S replaced by S' . Therefore, the corollary follows from the difference estimates of that proposition, Corollary 2.4, and some further basic computations on Reissner-Nordström such as

1. $r_{RN}(s) - r_- \lesssim e^{2K-s}$ for $s \geq S \gg 1$.
2. $\Omega_{RN}^2 \sim e^{2K-s}$ for $s \geq S \gg 1$.

The final part of (4.21) clearly follows by taking S large and ϵ small. In the sequel, we will take advantage of the fact that S and S' can be taken to be as large as required. \square

4.2 Estimates on the early blue-shift region

The early blue-shift \mathcal{EB} is defined by $\mathcal{EB} = \{S \leq s \leq s_{lin} = (|2K_-|)^{-1} \log(\nu \epsilon^{-2})\}$, where $\nu(M, \mathbf{e}, \Lambda, m^2, q_0) > 0$ is chosen such that (4.28) holds. In the blue-shift regions, we begin to exploit the fact that Ω^2 is exponentially decaying in s .

Proposition 4.4. Take the quantity S in Proposition 4.2 to be sufficiently large, and $\nu(M, \mathbf{e}, \Lambda, m^2, q_0) > 0$ to be

sufficiently small. Then there exists some $D_E(M, \mathbf{e}, \Lambda, m^2, q_0) > 0$ such that the following hold:

$$|\delta \log(\Omega^2)| + s \left| \frac{d}{ds} \delta \log(\Omega^2) \right| \leq D_E \epsilon^2 s^2, \quad (4.22)$$

$$|\phi| + |\dot{\phi}| \leq D_E |B| \epsilon, \quad (4.23)$$

$$|\delta r| s^{-1} + |\delta \dot{r}| + |\delta \tilde{A}| \leq D_E \epsilon^2, \quad (4.24)$$

$$|\kappa^{-1} - 1| \leq \frac{1}{100}, \quad (4.25)$$

$$|\varpi - M| + |Q - \mathbf{e}| \leq D_E \epsilon^2 s, \quad (4.26)$$

$$|\delta \phi| + |\delta \dot{\phi}| \leq D_E \epsilon^3 s. \quad (4.27)$$

Proof. Recall the quantities D'_N from Proposition 4.2 and $B \in \mathbb{C}$ from Proposition 2.3. We bootstrap the following estimates:

$$|\delta \log \Omega^2| \leq 4D'_N \epsilon^2 s^2, \quad (\text{EB1})$$

$$|\phi| + \omega_{RN}^{-1} |\dot{\phi}| \leq 20|B| \epsilon, \quad (\text{EB2})$$

$$r \geq \frac{r_-}{2}, \quad (\text{EB3})$$

$$|\tilde{A}| \leq \frac{2\mathbf{e}}{r_+}. \quad (\text{EB4})$$

To start with, note that, by (EB1) and the Reissner-Nordström asymptotics, we have that, for some $C > 0$,

$$C^{-1} e^{2K_- s} \leq \Omega^2 \leq C e^{2K_- s}.$$

Note also that $|\delta Q| \lesssim \epsilon^2 s$ is immediate from (4.11) and the bootstraps.

Next, we use (EB2) along with the Raychaudhuri equation (2.37) to get the estimate on κ :

$$|\kappa^{-1} - 1| \leq D'_N \epsilon^2 + C|B|^2 \epsilon^2 e^{2|K_-|s} \leq \frac{1}{100}, \quad (4.28)$$

where ν is chosen such that the second inequality holds. One can rewrite the left hand side of this expression as

$$|\kappa^{-1} - 1| = 4\Omega_{RN}^{-2} |\delta \dot{r} + \dot{r}(e^{-\delta \log \Omega^2} - 1)|.$$

Hence, we can use (4.28) and (EB1) to produce a preliminary estimate on $\delta \dot{r}$:

$$|\delta \dot{r}| \lesssim \Omega^2 |\delta \log \Omega^2| + e^{2K_- s} \epsilon^2 + |B|^2 \epsilon^2 \lesssim e^{2K_- s} (D'_N + D'_N s^2) \epsilon^2 + |B|^2 \epsilon^2. \quad (4.29)$$

Integrating this up¹⁴ from $s = S$, we get $|\delta r| \lesssim \epsilon^2 s$, or to be more specific we have the following, where C depends on the black hole parameters, m^2 and q_0 but not the choice of S (unlike the quantity $D'_N = C^S D_N$ which does have exponential dependence on S):

$$|\delta r| \leq C \epsilon^2 (|B|^2 s + D'_N + D'_N S^2 e^{2K_- S}) \leq C \epsilon^2 (|B|^2 s + D'_N). \quad (4.30)$$

¹⁴We use here a straightforward calculus lemma: given $\alpha > 0$ and $N \in \mathbb{N}$, then for $s_0 \in \mathbb{R}$ large, $\int_{s_0}^{\infty} s^N e^{-\alpha s} ds \lesssim_{\alpha, N} s_0^N e^{-\alpha s_0}$.

Here, we use that $S^2 e^{2K-S}$ is uniformly bounded for $S > 0$.

We wish to improve the bootstrap (EB1). So we use the equation (2.41) and take differences from Reissner-Nordström, leading to following inequality

$$\begin{aligned} \left| \frac{d^2}{ds^2} \delta \log \Omega^2 \right| &\lesssim \Omega^2 (|\delta \log \Omega^2| + |\delta r| + |\delta \dot{r}| + |\delta Q|) + |\phi|^2 + |\dot{\phi}|^2, \\ &\lesssim e^{2K-s} (D'_N s^2 + |B|^2 s + D'_N) \epsilon^2 + |B|^2 \epsilon^2. \end{aligned}$$

Integrating this expression up from $s = S$ twice, we get

$$\begin{aligned} \left| \frac{d}{ds} \delta \log \Omega^2 \right| &\lesssim D'_N \epsilon^2 + |B|^2 \epsilon^2 s, \\ |\delta \log \Omega^2| &\lesssim D'_N \epsilon^2 s + |B|^2 \epsilon^2 s^2. \end{aligned}$$

So, for S sufficiently large, we improve the bootstrap (EB1) – note that $D'_N = C^S D_N$ grows exponentially in S so that $D'_N \gg |B|^2$ for S large.

Then taking differences between our ODEs and the Reissner-Nordström ODEs will lead to the estimates (4.24) and (4.26), thus improving upon the bootstraps (EB3) and (EB4).

We now turn to the estimates on the charged scalar field. We shall use the equation (2.46) and consider the quantity

$$H = r^4 \dot{\phi}^2 + r^4 q_0^2 |\tilde{A}|^2 \phi^2. \quad (4.31)$$

As we already control r and $|\tilde{A}|$ from below in this region, producing an upper bound for H would give us desired estimates on $|\phi|, |\dot{\phi}|$. Using (2.46) as well as (2.44), we compute

$$\frac{dH}{ds} = -\frac{m^2 \Omega^2 r^4}{2} \phi \dot{\phi} - \frac{r^2 q_0^2 \tilde{A} Q \Omega^2}{2} \phi^2 + 4r^3 \dot{r} q_0^2 |\tilde{A}|^2 \phi^2.$$

The last term is negative since $\dot{r} < 0$, so we can apply Cauchy-Schwarz (again recalling the lower bounds on r and $|\tilde{A}|$) to see that

$$\frac{dH}{ds} \leq C_H \Omega^2 H,$$

for some $C_H = C_H(M, e, \Lambda, m^2, q_0) > 0$. Therefore, by Grönwall, so long as we pick S large enough such that

$$\int_S^{s_{lin}} C_H \Omega^2 ds \leq C C_H \int_S^\infty e^{2K-s} ds < \log 2,$$

we deduce that $H(s) \leq 2H(S) \leq 16r_-^4 \omega_{RN}^2 |B|^2 \epsilon^2$, where the latter estimate for $H(S)$ is computed using (4.20). This improves (EB2).

Finally, for the difference estimate on the scalar field we use the modified quantity \tilde{H} , given by

$$\tilde{H} = r^4 |\delta \dot{\phi}|^2 + r^4 q_0^2 |\tilde{A}|^2 |\delta \phi|^2. \quad (4.32)$$

To find the analogous differential inequality here, we first need to find the difference version of (2.45):

$$\delta \ddot{\phi} = -\frac{2\dot{r}}{r} \delta \dot{\phi} - q_0^2 |\tilde{A}|^2 \delta \phi - \frac{m^2 \Omega^2}{4} \delta \phi + \mathcal{E}_{EB}, \quad (4.33)$$

where the error¹⁵ term \mathcal{E}_{EB} is estimated by $|\mathcal{E}_{EB}| \lesssim \epsilon^3(1 - s\dot{r} + s^2\Omega_{RN}^2)$.

Using a similar procedure as before, one can use this equation to get the differential inequality:

$$\frac{d\tilde{H}}{ds} \lesssim \Omega^2 \tilde{H} + \epsilon^3(1 - s\dot{r} + s^2\Omega_{RN}^2)\sqrt{\tilde{H}}. \quad (4.34)$$

Rewriting this expression as a differential inequality in terms of $\sqrt{\tilde{H}}$ and using the usual Grönwall inequality with a (nondecreasing) inhomogeneous term, we get

$$\sqrt{\tilde{H}}(s) \lesssim \sqrt{\tilde{H}}(S) + \int_S^s \epsilon^3(1 - s\dot{r} + s^2\Omega_{RN}^2) ds \lesssim \epsilon^3 s$$

as required. This concludes the proof of (4.27) and the proposition. \square

4.3 Estimates on the late blue-shift region

To close this section, we give the estimates on the late blue-shift region. Here, we leave the regime where Cauchy stability holds, in particular showing that \dot{r} remains at size $O(\epsilon^2)$ rather than continuing to decay exponentially.

Proposition 4.5. Choose $\Delta_B > 0$ sufficiently small, and define $b_- = \frac{2|B|\omega_{RN}}{2|K_-|}$. Then, in the region $\mathcal{LB} = \{s_{lin} \leq s \leq \Delta_B \epsilon^{-1}\}$, there exists some $D_L(M, \mathbf{e}, \Lambda, m^2, q_0) > 0$ such that the following estimates hold, recalling the quantity α_- from (2.24):

$$|r(s) - r_-| \leq D_L \epsilon^2 s, \quad (4.35)$$

$$\left| -\dot{r} - \frac{4|B|^2 \omega_{RN}^2 \epsilon^2 r(s)}{2|K_-|} \right| \leq D_L(\Omega^2 + \epsilon^4 s), \quad (4.36)$$

$$\left| \frac{d}{ds} \log(\Omega^2) - 2K_- \right| \leq D_L \epsilon^2 s, \quad (4.37)$$

$$\left| \frac{d}{ds} \log\left(r(s)^{-b_-^2 \epsilon^{-2}} \cdot \Omega^2(s)\right) \right| \leq D_L(\epsilon^{-2} \Omega^2 + \epsilon^2 s), \quad (4.38)$$

$$\left| \log\left(\frac{\Omega^2}{\alpha_- e^{2K_- s}}\right) \right| \leq D_L \epsilon^2 s^2, \quad (4.39)$$

$$|\phi| + |\dot{\phi}| \leq D_L \epsilon, \quad (4.40)$$

$$|Q - \mathbf{e}|s^{-1} + |\delta \tilde{A}| \leq D_L \epsilon^2, \quad (4.41)$$

$$|\phi - B\epsilon e^{i\omega_{RN}s} - \overline{B}\epsilon e^{-i\omega_{RN}s}| + |\dot{\phi} - i\omega_{RN}B\epsilon e^{i\omega_{RN}s} + i\omega_{RN}\overline{B}\epsilon e^{-i\omega_{RN}s}| \leq D_L \epsilon^3 s. \quad (4.42)$$

Proof. We use the following bootstrap assumptions, where the constant $B_1(M, \mathbf{e}, \Lambda, m^2, q_0) > 0$ will be described later in the proof:

$$\left| \frac{d}{ds} \log \Omega^2 - 2K_- \right| \leq |K_-|, \quad (\text{LB1})$$

$$|\tilde{A}| \leq \frac{2|\mathbf{e}|}{r_+}, \quad (\text{LB2})$$

$$-\dot{r} \leq \frac{8|B|^2 \omega_{RN}^2 r_-}{2|K_-|} \epsilon^2, \quad (\text{LB3})$$

¹⁵In this expression for the error term, our estimates in the region \mathcal{EB} show that both $-s\dot{r}$ and $s^2\Omega_{RN}^2$ are $O(1)$. Nonetheless, we choose to write it in this form both for clarity and because we shall use the same expression again in the late blue-shift region, where both of these are still $O(1)$ but for different reasons.

$$|Q| \leq 2|e|, \quad (\text{LB4})$$

$$|\delta \log \Omega^2| \leq B_1 \epsilon^2 s^2. \quad (\text{LB5})$$

From (LB3), we have the trivial estimate $|\delta \dot{r}| \lesssim \epsilon^2$, and thus $|\delta r| \lesssim \epsilon^2 s$.

Due to (LB1), we have that in \mathcal{LB} ,

$$\int_{s_{lin}}^s \Omega^2(s') ds' \leq |K_-|^{-1} \Omega^2(s_{lin}) \lesssim \epsilon^2,$$

So given all the bootstrap assumptions, we may proceed exactly as in the proof of Proposition 4.4 to recover the estimates (4.40) and (4.42). Note that the error \mathcal{E}_{LB} in (4.33) is replaced by \mathcal{E}_{LB} which still satisfies the same estimate

$$|\mathcal{E}_{LB}| \lesssim \epsilon^3 (1 - s\dot{r} + s^2 \Omega_{RN}^2) \lesssim \epsilon^3,$$

so the proof follows in an identical fashion.

We also get the estimate (4.41) just as in Proposition 4.4, improving the two bootstraps (LB2) and (LB4).

Using the difference version of (2.42), we get the inequality

$$\left| \frac{d^2}{ds^2} \delta \log(r\Omega^2) \right| \lesssim B_1 \Omega^2 \epsilon^2 s^2 + \epsilon^2. \quad (4.43)$$

Integrating once, we deduce that

$$\left| \frac{d}{ds} \delta \log(r\Omega^2) \right| \lesssim B_1 \epsilon^2 s_{lin}^2(\epsilon) \cdot \epsilon^2 + \epsilon^2 s \lesssim \epsilon^2 s. \quad (4.44)$$

Therefore, in light of the previous estimates on $\delta r, \delta \dot{r}$, for ϵ sufficiently small we have

$$\left| \frac{d}{ds} \log(r\Omega^2)(s) - 2K_- \right| + \left| \frac{d}{ds} \log(\Omega^2)(s) - 2K_- \right| \leq C \epsilon^2 s \leq \frac{|K_-|}{10}, \quad (4.45)$$

where the final inequality follows for Δ_B taken sufficiently small.

This improves the bootstrap (LB1), and moreover, integrating (4.44) once again will yield

$$|\delta \log(r\Omega^2)| \leq C(\epsilon^2 s_{lin}^2(\epsilon) + B_1 \epsilon^4 s_{lin}^2(\epsilon) + \epsilon^2 s^2), \quad (4.46)$$

which improves (LB5) after once again accounting for δr , so long as B_1 is chosen sufficiently large (i.e. larger than $4C$ for the C appearing in (4.46)).

It remains to improve upon the bootstrap (LB3). For this, as in the uncharged scalar field model of [81], we use the Raychaudhuri equation in the convenient form (2.38). We begin by estimating the expression involving the scalar field; using (4.42) and (4.41), we have

$$|\dot{\phi}|^2 + |\tilde{A}|^2 q_0^2 |\phi|^2 = |B \omega_{RN} \epsilon e^{i\omega_{RN} s} - \bar{B} \omega_{RN} \epsilon e^{-i\omega_{RN} s}|^2 + \omega_{RN}^2 |B \epsilon e^{i\omega_{RN} s} + \bar{B} \epsilon e^{-i\omega_{RN} s}|^2 + \mathcal{E}_B.$$

Expanding out the trigonometric expressions on the right, we can see this can be rewritten as

$$|\dot{\phi}|^2 + |\tilde{A}|^2 q_0^2 |\phi|^2 = 4|B|^2 \omega_{RN}^2 \epsilon^2 + \mathcal{E}_B, \quad (4.47)$$

where the error term is bounded by $|\mathcal{E}_B| \lesssim \epsilon^4 s$.

Therefore, using also (4.35) and (4.44), one finds that (2.38) may be written in the form

$$\frac{d}{ds}(-\dot{r}) - 2K_-(-\dot{r}) = 4|B|^2 \omega_{RN}^2 r_- \epsilon^2 + \mathcal{E}_B(s), \quad (4.48)$$

with the error $\mathcal{E}_B(s)$ once again satisfying $|\mathcal{E}_B(s)| \lesssim \epsilon^4 s$.

We now use a classical integrating factor of e^{-2K_-s} to integrate (4.48) between s_{lin} and s , yielding

$$-\dot{r}(s) = -e^{2K_-(s-s_{lin})} \dot{r}(s_{lin}) + \int_{s_{lin}}^s 4|B|^2 \omega_{RN}^2 r_- \epsilon^2 e^{2K_-(s-s')} + \mathcal{E}_B(s') e^{2K_-(s-s')} ds'. \quad (4.49)$$

Using $|\mathcal{E}_B(s')| \lesssim \epsilon^4 s'$ and computing these integrals, we find that

$$\left| -\dot{r}(s) - \frac{4|B|^2 \omega_{RN}^2 r_- \epsilon^2}{|2K_-|} \right| \lesssim e^{2K_-(s-s_{lin})} \left| -\dot{r}(s_{lin}) - \frac{4|B|^2 \omega_{RN}^2 r_- \epsilon^2}{|2K_-|} \right| + \epsilon^4 s. \quad (4.50)$$

From this and prior estimates, we yield (4.36), thus improving the remaining bootstrap (LB3).

The estimate (4.38) simply comes from combining (4.36) and (4.37). Finally, (4.39) follows from combining (2.24) with (LB5), plus using that $e^{2K_-s} \leq e^{2K_-s_{lin}} \lesssim \epsilon^2$ for $s \in \mathcal{LB}$. \square

We conclude this section with a straightforward corollary concerning quantities evaluated at a specific point $s = s_O(\epsilon) := 50s_{lin}(\epsilon)$ that will be useful in the next region. For ease of notation, we first define the dimensionless parameter $\mathfrak{M}(M, \mathbf{e}, \Lambda, q_0) > 0$ as:

$$\mathfrak{M} := \sqrt{\frac{\omega_{RN}(M, \mathbf{e}, \Lambda, q_0)}{|2K_-(M, \mathbf{e}, \Lambda)|}}. \quad (4.51)$$

Corollary 4.6. Let $s_O(\epsilon) = 50s_{lin}(\epsilon) \in \mathcal{LB}$. Then, upon defining the quantities

$$r_0 = r(s_O), \quad \omega_0 = |q_0 \tilde{A}(s_O)|, \quad \xi_0 = \omega_0 \left(-\frac{d}{ds} \left(\frac{r^2}{r_-^2 \epsilon^2} \right) \right)^{-1}(s_O), \quad Q_0 = Q(s_O), \quad (4.52)$$

we have the following estimates:

$$|r_0 - r_-| + \log(\epsilon^{-1}) |\omega_0 - \omega_{RN}| + \left| \xi_0 - \frac{1}{8|B|^2 \mathfrak{M}^2} \right| + |Q_0 - \mathbf{e}| \leq D_L \epsilon^2 \log(\epsilon^{-1}). \quad (4.53)$$

In particular, the following upper and lower bounds hold for ξ_0 .

$$\xi_0 \leq \frac{1}{4|B|^2 \mathfrak{M}^2}, \quad \xi_0^{-1} \leq 16|B|^2 \mathfrak{M}^2. \quad (4.54)$$

Finally, one has

$$|\phi(s_O)| + |\dot{\phi}(s_O)| \leq D_L \epsilon. \quad (4.55)$$

5 The collapsed oscillations

From this point, the results begin to differ from that of [81]. We next study the region of ‘collapsed oscillations’ (see Section 1.11), a region where r eventually becomes $O(\epsilon)$ small. The dynamics in this section are largely

driven by the charged scalar field, which remains oscillatory but also exhibits a slowly growing behavior, in that the amplitude grows from $O(\epsilon)$ at start of the regime to $O(1)$ at the end of the regime. Indeed, after a change of variables, the behavior of ϕ will be well approximated by a *Bessel function* of order 0. Schematically, in the region $\epsilon \lesssim r \ll r_-$, the scalar field behaves as

$$\phi(r) \approx \frac{C\epsilon}{r} \cdot \cos\left(\frac{r^2 - r_-^2}{\epsilon^2} + O(\log(\epsilon^{-1}))\right). \quad (5.1)$$

We will, in fact, need to track the growth-oscillatory behavior more precisely using the explicit Bessel functions $J_0(x)$ and $Y_0(x)$, defined as the two linearly independent solutions of Bessel's equation of order 0:

$$\frac{d}{dz} \left(z \frac{df}{dz} \right) + zf = 0. \quad (5.2)$$

They exhibit the following asymptotic behavior (see also Facts A.1, A.2 and A.4 in Appendix A for more detailed asymptotics):

$$J_0(z) = \begin{cases} \sqrt{\frac{2}{\pi z}} \cos\left(z - \frac{\pi}{4}\right) + O(z^{-3/2}) & \text{as } z \rightarrow +\infty, \\ 1 + O(z) & \text{as } z \rightarrow 0, \end{cases} \quad (5.3)$$

$$Y_0(z) = \begin{cases} \sqrt{\frac{2}{\pi z}} \sin\left(z - \frac{\pi}{4}\right) + O(z^{-3/2}) & \text{as } z \rightarrow +\infty, \\ \frac{2}{\pi} \left(\ln\left(\frac{z}{2}\right) + \gamma \right) + O(z) & \text{as } z \rightarrow 0, \end{cases} \quad (5.4)$$

where $\gamma \approx 0.577$ is the Euler-Mascheroni constant. We see, therefore, that the Bessel functions $J_0(z)$ and $Y_0(z)$ both oscillate and decay¹⁶ at a slow inverse polynomial rate as $z \rightarrow \infty$, but exhibit very different behavior in the $z \rightarrow 0$ regime. We later show the schematic estimate (5.1) takes the following more precise form involving the renormalized variable $z = \frac{r^2}{\epsilon^2}$ and the frequency ξ_0 defined in Corollary 4.6:

$$\phi(r) \approx C_J(\epsilon) \cdot J_0\left(\frac{\xi_0}{r_-^2} \cdot \frac{r^2}{\epsilon^2}\right) + C_Y(\epsilon) \cdot Y_0\left(\frac{\xi_0}{r_-^2} \cdot \frac{r^2}{\epsilon^2}\right),$$

$$C_J(\epsilon) \approx \sqrt{2\pi\xi_0} \cdot |B| \cdot \cos(\xi_0 \cdot \epsilon^{-2}), \quad C_Y(\epsilon) \approx \sqrt{2\pi\xi_0} \cdot |B| \cdot \sin(\xi_0 \cdot \epsilon^{-2}).$$

In light of (5.3)–(5.4), tracking the size of the coefficients $C_J(\epsilon)$ and $C_Y(\epsilon)$ precisely will be important in later sections.

The main objective of Section 5 is to prove these schematic estimates. In view of the logarithmic growth of $Y_0(z)$ for $z \ll 1$, the precise value of the coefficient $C_Y(\epsilon)$ will be crucial in the geometry of the later regions where $r \ll \epsilon$ (see Section 6).

Once the scalar field asymptotics are understood, we also account for the scalar field *backreaction* onto both the Maxwell field and the geometry. In this region, the backreaction on the spacetime geometry is minimal; however the backreaction on the Maxwell field has a rather curious effect. That is, within the oscillatory region, the charge $Q(s)$ will decrease in absolute value from (approximately) e to (approximately) Q_∞ , where $Q_\infty(M, e, \Lambda)$ depends on the black hole parameters and lies strictly between $\frac{e}{2}$ and e , see (5.13) and Lemma 5.7. Q_∞ being bounded away from 0 is causing the *charge retention* in Theorem I, see Section 1.4.

We now state the main result of this section, where $\mathcal{O} = \{s \geq s_O(\epsilon) : r(s) \geq 2|B|\mathfrak{W}\epsilon r_-\}$ and we recall that

¹⁶As z is decreasing in s in our setting, and we are interested in behavior as z decreases, the decay of Bessel functions exhibits itself as inverse polynomial growth of the amplitude of the scalar field ϕ .

\mathfrak{W} was defined in (4.51).

Proposition 5.1. For $s \in \mathcal{O}$, the lapse Ω^2 obeys the following upper bound, where we recall α_- from (2.24).

$$\Omega^2(s) \leq \alpha_- \exp(K_- s). \quad (5.5)$$

There exists some $D_O(M, \mathbf{e}, \Lambda, m^2, q_0) > 0$ such that, for $s \in \mathcal{O}$, we have the following estimates:

$$| -r\dot{r}(s) - 4|B|^2 \mathfrak{W}^2 r_-^2 \epsilon^2 \omega_{RN} | \leq D_O \epsilon^4 \log \epsilon^{-1}, \quad (5.6)$$

$$\left| \frac{d}{ds} \log \Omega^2 - 2K_- \right| \leq D_O \epsilon^2 (\log(\epsilon^{-1}) + r^{-2}(s)). \quad (5.7)$$

$$|q_0 \tilde{A}(s) - q_0 \tilde{A}_{RN, \infty}| \leq D_O \epsilon^2, \quad (5.8)$$

$$\left| Q(s) - \mathbf{e} + \frac{1}{4} \frac{2K_-}{\tilde{A}_{RN, \infty}} (r_-^2 - r^2(s)) \right| \leq D_O \epsilon^2 \log(\epsilon^{-1}). \quad (5.9)$$

Finally, there exist coefficients $C_J(\epsilon)$ and $C_Y(\epsilon)$ determined via the formula (5.28) and satisfying (5.29) and (5.30) such that we have the following two estimates on the scalar field: for all $s \in \mathcal{O}$,

$$\left| \phi(s) - \left(C_J(\epsilon) J_0 \left(\frac{\xi_0 r^2(s)}{r_-^2 \epsilon^2} \right) + C_Y(\epsilon) Y_0 \left(\frac{\xi_0 r^2(s)}{r_-^2 \epsilon^2} \right) \right) \right| \leq D_O \epsilon^2 \log(\epsilon^{-1}), \quad (5.10)$$

$$\left| \dot{\phi}(s) - \omega_0 \left(C_J(\epsilon) J_1 \left(\frac{\xi_0 r^2(s)}{r_-^2 \epsilon^2} \right) + C_Y(\epsilon) Y_1 \left(\frac{\xi_0 r^2(s)}{r_-^2 \epsilon^2} \right) \right) \right| \leq D_O \epsilon^2 \log(\epsilon^{-1}). \quad (5.11)$$

Here, ξ_0 and ω_0 are as defined in Corollary 4.6.

Later, it will be convenient to refer to (5.9), (5.10) and (5.11) evaluated at the right endpoint of \mathcal{O} .

Corollary 5.2. Let $s_{PK}(\epsilon) > 0$ be such that $r(s_{PK}) = 2|B|\mathfrak{W}\epsilon r_-$. Then

$$|s_{PK} - (8|B|^2 \mathfrak{W}^2 \omega_{RN})^{-1} \epsilon^{-2}| \leq D_O \log(\epsilon^{-1}). \quad (5.12)$$

Further, if one defines Q_∞ as

$$Q_\infty(M, \mathbf{e}, \Lambda) := \mathbf{e} - \frac{2K_-(M, \mathbf{e}, \Lambda) \cdot r_-^2(M, \mathbf{e}, \Lambda)}{4\tilde{A}_{RN, \infty}(M, \mathbf{e}, \Lambda)}, \quad (5.13)$$

one may infer the following estimates at $s = s_{PK}$.

$$|Q(s_{PK}) - Q_\infty| \leq D_O \epsilon^2 \log(\epsilon^{-1}), \quad (5.14)$$

$$|\phi(s_{PK}) - (C_J(\epsilon) J_0(4\xi_0|B|^2 \mathfrak{W}^2) + C_Y(\epsilon) Y_0(4\xi_0|B|^2 \mathfrak{W}^2))| \leq D_O \epsilon^2 \log(\epsilon^{-1}), \quad (5.15)$$

$$\left| \dot{\phi}(s_{PK}) - \omega_0 (C_J(\epsilon) J_1(4\xi_0|B|^2 \mathfrak{W}^2) + C_Y(\epsilon) Y_1(4\xi_0|B|^2 \mathfrak{W}^2)) \right| \leq D_O \epsilon^2 \log(\epsilon^{-1}). \quad (5.16)$$

This section will be organized into three parts. In Section 5.1, we introduce the main bootstrap assumptions for the region \mathcal{O} , and make several preliminary observations. In Section 5.2, we derive the main scalar field estimates, establishing the aforementioned Bessel type behavior. In Section 5.3, we use the results on the scalar field to improve the bootstrap assumptions, proving in particular the estimates (5.5), (5.7) and (5.9) regarding

$\Omega^2(s)$ and $Q(s)$, then complete the proof of Proposition 5.1.

5.1 Bootstraps and preliminary estimates

Throughout the proof of Proposition 5.1, we make reference to the following three bootstrap assumptions:

$$\Omega^2 \leq \epsilon^{40}, \quad (\text{O1})$$

$$|\phi| + |\dot{\phi}| \leq \epsilon^{-1}, \quad (\text{O2})$$

$$|Q| \leq \epsilon^{-2}. \quad (\text{O3})$$

By Proposition 4.5 and Corollary 4.6, these hold within a neighborhood of $s = s_O(\epsilon)$. It will be convenient to define the bootstrap region \mathcal{O}_{boot} as the connected component of $\{s \in \mathcal{O} : s \leq \epsilon^{-4}, (\text{O1})\text{--}(\text{O3}) \text{ apply}\}$ such that $s_O \in \mathcal{O}_{boot}$. We now make some preliminary estimates using these bootstraps and Proposition 4.5. Morally, the following lemma will allow us to treat $-r\dot{r}$ and \tilde{A} as constant inside \mathcal{O} , at least up to an extremely small error.

Lemma 5.3. Any $s \in \mathcal{O}_{boot}$ satisfies $s \lesssim \epsilon^{-2}$. Furthermore, there exists some constant $D_O(M, \mathbf{e}, \Lambda, m^2, q_0) > 0$ such that, for $s \in \mathcal{O}_{boot}$,

$$\left| \frac{d}{ds}(-r\dot{r}) \right| + |r\dot{r}(s) - r\dot{r}(s_O)| \leq D_O \epsilon^{30}, \quad (5.17)$$

$$|-r\dot{r}(s) - 4|B|^2 \mathfrak{W}^2 \omega_{RN} r_-^2 \epsilon^2| \leq D_O \epsilon^4 \log(\epsilon^{-1}), \quad (5.18)$$

$$|q_0 \tilde{A}(s) - q_0 \tilde{A}(s_O)| \leq D_O \epsilon^{30}, \quad (5.19)$$

$$||q_0 \tilde{A}(s) - \omega_{RN}| \leq D_O \epsilon^2. \quad (5.20)$$

Proof. These estimates are immediate from (2.40) and (2.44). Indeed, letting f be either $-r\dot{r}$ or \tilde{A} , we see that

$$\left| \frac{df}{ds} \right| \leq \Omega^2 \cdot P_f(|\phi|, |Q|, |\dot{\phi}|, r^{-2})$$

for some polynomial P_f of degree less than 2. Then, using that (O1) provides a large power of ϵ , the remaining bootstraps plus the fact that $r(s) \gtrsim \epsilon$ give the estimates (5.17) and (5.19). The other two estimates then follow straightforwardly from Proposition 4.5, (5.17) and (5.19).

As $-r\dot{r} \gtrsim \epsilon^2$ and $r^2(s_O) = r_-^2 + O(\epsilon^2 \log(\epsilon^{-1}))$, it is immediate that $s \lesssim \epsilon^{-2}$ for $s \in \mathcal{O}_{boot}$. \square

We use Lemma 5.3 to rewrite several of the equations of Section 2.4 as simplified equations with constant coefficients, plus an error term. Recalling ξ_0 from (4.52), to simplify notation, we denote

$$x = x(s) := \frac{r^2(s)}{r_-^2 \epsilon^2}, \text{ so that } \xi_0 = \left| \left(-\frac{dx}{ds} \right)^{-1} \cdot q_0 \tilde{A} \right| (s = s_O). \quad (5.21)$$

We then proceed to rewrite (2.46) and (2.43) in terms of the new variable x . Performing this change of variables, one gets the two equations:

$$\frac{d}{dx} \left(x \frac{d\phi}{dx} \right) + \xi_0^2 x \phi = \mathcal{E}_\phi, \quad (5.22)$$

$$\frac{dQ}{dx} = \text{sgn}(\mathbf{e}) q_0 r_-^2 \xi_0 \epsilon^2 x |\phi|^2 + \mathcal{E}_Q. \quad (5.23)$$

We should like to estimate the error terms \mathcal{E}_ϕ and \mathcal{E}_Q . To do so, we apply Lemma 5.3 extensively to prove the following corollary.

Corollary 5.4. Recall x and ξ_0 from (5.21). Then, for $s \in \mathcal{O}_{boot}$, one finds

$$\left| \xi_0 - \left(-\frac{dx}{ds} \right)^{-1} \cdot |q_0 \tilde{A}|(s) \right| \leq D_O \epsilon^{25}. \quad (5.24)$$

Furthermore, in the equations (5.22) and (5.23), one has the following control on the error terms:

$$|\mathcal{E}_\phi| + |\mathcal{E}_Q| \leq D_O \epsilon^{20}.$$

Proof. For (5.24), we first use that, from (2.40),

$$\left| \frac{d^2 x}{ds^2} \right| = \frac{2}{r_-^2 \epsilon^2} \left| \frac{d}{ds}(-r\dot{r}) \right| = \frac{\Omega^2}{2r_-^2 \epsilon^2} \left| 1 - \frac{Q^2}{r^2} - r^2 |\phi|^2 - r^2 \Lambda \right| \lesssim \epsilon^{25}, \quad (5.25)$$

where the final estimate comes from the bootstrap assumptions (O1)–(O3). Integrating this once between s_O and $s \in \mathcal{O}_{boot}$, and combining with (5.21), (5.24) follows.

For the error terms, making the substitution $s \mapsto x$ in (2.46) and (2.43) yields:

$$|\mathcal{E}_\phi| + |\mathcal{E}_Q| \lesssim \left(\Omega^2 + \left| \frac{d^2 x}{ds^2} \right| + \left| \xi_0 - \left(-\frac{dx}{ds} \right)^{-1} |q_0 \tilde{A}| \right| \right) \cdot P(\epsilon^{-1}, r^{-1}, |\phi|, |\dot{\phi}|),$$

for some polynomial P of degree less than five. Upon inserting (O1), (5.25) and (5.24), the corollary follows. \square

5.2 Scalar field oscillations

The focus of this subsection will be understanding the behavior of the *charged* scalar field $\phi(s)$ via the equation (5.22). This equation is a Bessel type ODE that we would like to understand as x decreases from $\epsilon^{-2} + O(\log(\epsilon^{-1}))$ to $r^2(s_{PK})(r_-^2 \epsilon^2)^{-1} = 4|B|^2 \mathfrak{W}^2$.

Proposition 5.5. For $s \in \mathcal{O}_{boot}$, there exists a constant $D_O > 0$, and coefficients $C_J(\epsilon)$ and $C_Y(\epsilon)$ such that¹⁷

$$|\phi - C_J(\epsilon)J_0(\xi_0 x) - C_Y(\epsilon)Y_0(\xi_0 x)| \leq D_O \epsilon^{10}, \quad (5.26)$$

$$\left| \frac{d\phi}{dx} + \xi_0 C_J(\epsilon)J_1(\xi_0 x) + \xi_0 C_Y(\epsilon)Y_1(\xi_0 x) \right| \leq D_O \epsilon^{10}. \quad (5.27)$$

Defining $x_B = x(s_O)$, the coefficients $C_J(\epsilon)$ and $C_Y(\epsilon)$ are determined by

$$\begin{bmatrix} C_J(\epsilon) \\ C_Y(\epsilon) \end{bmatrix} = \frac{\pi x_B}{2} \begin{bmatrix} -\xi_0 Y_1(\xi_0 x_B) & -Y_0(\xi_0 x_B) \\ \xi_0 J_1(\xi_0 x_B) & J_0(\xi_0 x_B) \end{bmatrix} \begin{bmatrix} \phi(x_B) \\ \frac{d\phi}{dx}(x_B) \end{bmatrix}. \quad (5.28)$$

The coefficients obey the estimates

$$\left| C_J(\epsilon) - \frac{\sqrt{\pi}}{2} \mathfrak{W}^{-1} \cos(\Theta(\epsilon)) \right| \leq D_O \epsilon^2 \log(\epsilon^{-1}), \quad (5.29)$$

¹⁷For a definition of the Bessel functions $J_\nu(z)$ and $Y_\nu(z)$, see Appendix A and Fact A.3.

$$\left| C_Y(\epsilon) - \frac{\sqrt{\pi}}{2} \mathfrak{W}^{-1} \sin(\Theta(\epsilon)) \right| \leq D_O \epsilon^2 \log(\epsilon^{-1}), \quad (5.30)$$

where the phase function $\Theta(\epsilon)$ is given by

$$\Theta(\epsilon) = |q_0 \tilde{A}(s) \cdot r^2(s) \cdot \left(-\frac{d}{ds} r^2(s) \right)^{-1} + \omega_{RN} s + \arg B - \frac{\pi}{4} \Big|_{s=s_O}. \quad (5.31)$$

Finally, one has the following upper bounds for $\phi(s)$ and $\dot{\phi}(s)$:

$$\max\{|\phi|, \omega_{RN}^{-1} |\dot{\phi}|\} \leq \frac{100|B|\epsilon r_-}{r}. \quad (5.32)$$

Proof. Ignoring the error term \mathcal{E}_ϕ , the equation (5.22) is exactly Bessel's equation of order 0 after a rescaling $z = \xi_0 x$. We should like to separate the analysis of the linear behavior arising from Bessel's equation and analysis of the error term.

For this purpose, we recast the equation (5.22) as a first-order linear evolution equation in the variables $(\phi, \frac{d\phi}{dx})$, treating the error term as an inhomogeneity. We get the following (see also the discussion preceding Lemma A.6):

$$\frac{d}{dx} \begin{bmatrix} \phi(x) \\ \frac{d\phi}{dx}(x) \end{bmatrix} = \begin{bmatrix} 0 & 1 \\ -\xi_0^2 & -\frac{1}{x} \end{bmatrix} \begin{bmatrix} \phi(x) \\ \frac{d\phi}{dx}(x) \end{bmatrix} + \begin{bmatrix} 0 \\ \frac{1}{x} \mathcal{E}_\phi \end{bmatrix}. \quad (5.33)$$

The analysis of this first-order system then follows from Lemma A.6, or more precisely Corollary A.7. Following these, we aim to write the solution using Duhamel's principle; let $\mathbf{S}(z_1; z_0)$ be the linear solution operator for the usual Bessel's equation defined in Lemma A.6, and $\mathbf{S}_{\xi_0}(x_1; x_0) := \mathbf{Q}_{\xi_0} \circ \mathbf{S}(\xi_0 x_1; \xi_0 x_0) \circ \mathbf{Q}_{\xi_0}^{-1}$ as in Corollary A.7, where $\mathbf{Q}_\chi : \mathbb{R}^2 \rightarrow \mathbb{R}^2$ is the linear stretching operator $\mathbf{Q}_\chi : (A, B) \mapsto (A, \chi B)$.

Then, following Corollary A.7, $\mathbf{S}_{\xi_0}(x_1; x_0)$ can be interpreted as the linear solution (semigroup) operator for the first-order system (5.33) without the inhomogeneous term \mathcal{E}_ϕ . Defining x_B as in the statement of the proposition, we have from Corollary 4.6 that $|x_B - \epsilon^{-2}| \lesssim \log(\epsilon^{-1})$. Duhamel's principle (i.e. Corollary A.7) applied to first-order systems¹⁸ gives that

$$\begin{bmatrix} \phi \\ \frac{d\phi}{dx} \end{bmatrix} (x) = \mathbf{S}_{\xi_0}(x; x_B) \begin{bmatrix} \phi \\ \frac{d\phi}{dx} \end{bmatrix} (x_B) + \int_{x_B}^x \mathbf{S}_{\xi_0}(x; \tilde{x}) \begin{bmatrix} 0 \\ \frac{1}{\tilde{x}} \mathcal{E}_\phi(\tilde{x}) \end{bmatrix} d\tilde{x}. \quad (5.34)$$

We define:

$$\begin{bmatrix} \phi_B \\ \frac{d\phi_B}{dx} \end{bmatrix} (x) := \mathbf{S}_{\xi_0}(x; x_B) \begin{bmatrix} \phi \\ \frac{d\phi}{dx} \end{bmatrix} (x_B), \quad \begin{bmatrix} \phi_e \\ \frac{d\phi_e}{dx} \end{bmatrix} (x) := \int_{x_B}^x \mathbf{S}_{\xi_0}(x; \tilde{x}) \begin{bmatrix} 0 \\ \frac{1}{\tilde{x}} \mathcal{E}_\phi(\tilde{x}) \end{bmatrix} d\tilde{x}. \quad (5.35)$$

Thus $\phi_B(x)$ represents exactly the solution of the homogeneous linear Bessel ODE with data given at $x = x_B$, while $\phi_e(x)$ is to be treated as an error term due to the small inhomogeneity. To treat $\phi_B(x)$ and $\phi_e(x)$, we shall use parts (1) and (2) of Corollary A.7 respectively.

As $\phi_B(x)$ must be a solution to (a rescaled) Bessel's equation, the solution must be exactly (using Fact A.3 to

¹⁸Note that in this section, we are always integrating backwards in x . Nonetheless, the standard theory of first order systems will still apply, with the usual convention that $\int_{x_0}^{x_1} = -\int_{x_1}^{x_0}$.

justify the appearance of $J_1(\xi_0 x)$ and $Y_1(\xi_0 x)$ in the derivatives):

$$\phi_B(x) = C_J J_0(\xi_0 x) + C_Y Y_0(\xi_0 x), \quad (5.36)$$

$$\frac{d\phi_B}{dx}(x) = -\xi_0 C_J J_1(\xi_0 x) - \xi_0 C_Y Y_1(\xi_0 x). \quad (5.37)$$

In these equations, the coefficients $C_J = C_J(\epsilon)$ and $C_Y = C_Y(\epsilon)$ are chosen such that $\phi(x_B) = \phi_B(x_B)$ and $\frac{d\phi}{dx}(x_B) = \frac{d\phi_B}{dx}(x_B)$, i.e. so that $\phi_B(x)$ agrees with $\phi(x)$ to first order at $x = x_B$. (It is immediate from (5.35) that $\phi_e(x)$ vanishes to first order at $x = x_B$.) Part (1) of Corollary A.7 then implies (5.28).

In order to deal with $\phi_e(x)$, we recall part 2 of Corollary A.7. Using Corollary 5.2, in particular the upper and lower bounds for ξ_0 in (4.54), the operator norm of the rescaled solution operator satisfies

$$\|\mathbf{S}_{\xi_0}(x_1; x_0)\|_{l^2 \rightarrow l^2} \leq \max \left\{ \frac{1}{4|B|^2 \mathfrak{M}^2}, 16|B|^2 \mathfrak{M}^2 \right\} \cdot \max \left\{ 1, \frac{x_0}{x_1} \right\}.$$

Integrating backwards in the variable x , i.e. $x < \bar{x}$ in (5.34), we can see that upon defining the l^∞ norm on \mathbb{R}^2 as $\|(x, y)\|_{l^\infty} = \max\{|x|, |y|\}$,

$$\left\| \mathbf{S}_{\xi_0}(x, \tilde{x}) \begin{bmatrix} 0 \\ \frac{1}{\tilde{x}} \mathcal{E}_\phi(\tilde{x}) \end{bmatrix} \right\|_{l^\infty} \lesssim \max \left\{ \frac{1}{|B|^2 \mathfrak{M}^2}, |B|^2 \mathfrak{M}^2 \right\} \cdot \frac{1}{x} \sup |\mathcal{E}_\phi| \lesssim \epsilon^{20},$$

where we apply Corollary 5.4 and $x \geq 4|B|^2 \mathfrak{M}^2$ in the last step. Furthermore, the length of the interval of integration in (5.34) is bounded by $x_B - x \leq x_B \lesssim 2\epsilon^{-2}$, so we have

$$\left\| \begin{bmatrix} \phi_e(x) \\ \frac{d\phi_e}{dx}(x) \end{bmatrix} \right\|_{l^\infty} = \left\| \int_{x_B}^x \mathbf{S}_{\xi_0}(x; \tilde{x}) \begin{bmatrix} 0 \\ \frac{1}{\tilde{x}} \mathcal{E}_\phi(\tilde{x}) \end{bmatrix} dx' \right\|_{l^\infty} \lesssim \epsilon^{10} \quad (5.38)$$

as required. Combining (5.36), (5.37) and (5.38) then gives both (5.26) and (5.27).

We now recover the precise form for the coefficients $C_J(\epsilon), C_Y(\epsilon)$. We carefully compute $C_J(\epsilon)$; the other coefficient $C_Y(\epsilon)$ shall follow in an analogous manner. By (5.28), we have the formula

$$C_J(\epsilon) = \frac{\pi x_B}{2} \left[-\xi_0 Y_1(\xi_0 x_B) \phi(x_B) - Y_0(\xi_0 x_B) \frac{d\phi}{dx}(x_B) \right]. \quad (5.39)$$

We therefore obtain a precise expression for $C_J(\epsilon)$ using the large- z asymptotics for the Bessel function $Y_\nu(z)$, and the scalar field estimates at the comparison point $s = s_O$ given by (4.42) in Proposition 4.5. By Fact A.4 and $x_B = \epsilon^{-2} + O(\log(\epsilon^{-1}))$,

$$Y_0(\xi_0 x_B) = \sqrt{\frac{2}{\pi \xi_0 x_B}} \sin \left(\xi_0 x_B - \frac{\pi}{4} \right) + O(\epsilon^3), \quad (5.40)$$

$$Y_1(\xi_0 x_B) = -\sqrt{\frac{2}{\pi \xi_0 x_B}} \cos \left(\xi_0 x_B - \frac{\pi}{4} \right) + O(\epsilon^3). \quad (5.41)$$

On the other hand, writing B as $B = |B|(\cos \arg B + i \sin \arg B)$ in (4.42) gives for $\phi(x_B) = \phi(s)|_{s=s_O}$:

$$\phi(x_B) = 2|B|\epsilon \cos(\omega_{RN} s_O + \arg B) + O(\epsilon^3 \log(\epsilon^{-1})). \quad (5.42)$$

For $\frac{d\phi}{dx}$, we proceed in several steps, using in particular Lemma 5.3, (5.24), (5.21) and (4.53):

$$\begin{aligned}
\frac{d\phi}{dx}(x_B) &= \left(\frac{dx}{ds} \right)^{-1} \dot{\phi} \Big|_{s=s_O} \\
&= -2|B|\epsilon \omega_{RN} \left(\frac{dx}{ds} \right)^{-1} \sin(\omega_{RN}s + \arg B) \Big|_{s=s_O} + O(\epsilon^3 \log(\epsilon^{-1})) \\
&= +2|B|\epsilon \omega_{RN} (8|B|^2 \mathfrak{W}^2 \omega_{RN})^{-1} \sin(\omega_{RN}s_O + \arg B) + O(\epsilon^3 \log(\epsilon^{-1})) \\
&= 2|B|\epsilon \xi_0 \sin(\omega_{RN}s_O + \arg B) + O(\epsilon^3 \log(\epsilon^{-1})).
\end{aligned} \tag{5.43}$$

Substituting all of (5.40), (5.41), (5.42), (5.43) into (5.39), one deduces that

$$C_J(\epsilon) = \frac{\pi x_B}{2} \sqrt{\frac{2\xi_0}{\pi x_B}} \cdot 2|B|\epsilon \cos\left(\xi_0 x_B - \frac{\pi}{4} + \omega_{RN}s_O + \arg B\right) + O(\epsilon^2 \log(\epsilon^{-1})). \tag{5.44}$$

To conclude, one uses Corollary 4.6 and $x_B = \epsilon^{-2} + O(\log(\epsilon^{-1}))$ to yield, since $\sqrt{8\xi_0}|B| = \mathfrak{W} + O(\epsilon \log(\epsilon^{-1}))$:

$$C_J(\epsilon) = \frac{\sqrt{\pi}}{2} \mathfrak{W}^{-1} \cos(\Theta(\epsilon)) + O(\epsilon^2 \log(\epsilon^{-1})), \tag{5.45}$$

where by the definition of ξ_0 in Corollary 4.6, $\Theta(\epsilon)$ is as in (5.31).

Finally, to obtain the upper bound (5.32), note first of all that $\xi_0 x \geq \xi_0 4|B|^2 \mathfrak{W}^2 \geq 1/4$ by Corollary 4.6. Since one can check that, for $z \geq \frac{1}{4}$,

$$\max\{|J_0(z)|, |J_1(z)|, |Y_0(z)|, |Y_1(z)|\} \leq 10z^{-1/2},$$

one can use (5.26) and (5.27) along with (5.29) and (5.30) to deduce that

$$\max\left\{|\phi(x)|, \xi_0^{-1} \left| \frac{d\phi}{dx} \right| \right\} \leq \sqrt{\pi} \mathfrak{W}^{-1} \cdot 10(\xi_0 x)^{-1/2} + O(\epsilon^2 \log(\epsilon^{-1})) \leq \frac{60|B|\epsilon r_-}{r}. \tag{5.46}$$

Then, one can use Lemma 5.3 to change the x -derivative to an s -derivative, with negligible error, and thus find (5.32). \square

5.3 Precise estimates for Q and Ω^2

Note that while (O2) has already been improved by (5.26), it remains to estimate Q and Ω^2 in the region \mathcal{O}_{boot} , and close the remaining bootstraps (O3) and (O1). We shall show that Q changes to (a value close to) the quantity Q_∞ , while Ω^2 remains exponentially decaying in s .

Proposition 5.6. For $s \in \mathcal{O}_{boot}$, we have the following estimates for $Q(s)$ and $\Omega^2(s)$, where $D_O > 0$ may be larger than that of Lemma 5.3 and Proposition 5.5 if necessary.

$$\left| Q(s) - \mathbf{e} + \frac{1}{4} \frac{2K_-}{\tilde{A}_{RN,\infty}} (r_-^2 - r^2(s)) \right| \leq D_O \epsilon^2 \log(\epsilon^{-1}), \tag{5.47}$$

$$\left| \frac{d}{ds} \log \Omega^2 - 2K_- \right| \leq D_O \epsilon^2 (\log(\epsilon^{-1}) + r^{-2}(s)). \tag{5.48}$$

Proof. We shall prove (5.47) using (5.23) and Proposition 5.5. By Corollary 4.6, particularly the estimate $|Q_0 - \mathbf{e}| \lesssim \epsilon^2 \log(\epsilon^{-1})$ from (4.53), it remains to estimate the integral:

$$\text{sgn}(\mathbf{e}) \int_{x_B}^x q_0 r_-^2 \xi_0 \epsilon^2 \tilde{x} |\phi|^2(\tilde{x}) d\tilde{x}, \quad (5.49)$$

where we recall for convenience that $x = (\frac{r_-}{r_-})^2 \epsilon^{-2}$.

Firstly, using (5.26), (5.29), (5.30), and the Bessel function asymptotics in (5.3), (5.4), one may find that

$$\left| \phi - \sqrt{\frac{1}{2\xi_0 x}} \mathfrak{W}^{-1} \cos(\xi_0 x - \pi/4 - \Theta(\epsilon)) \right| \lesssim \epsilon^2 \log(\epsilon^{-1}) x^{-1/2} + x^{-3/2}, \quad (5.50)$$

which we may use to deduce the estimate

$$\left| \xi_0 x \phi^2 - \frac{\mathfrak{W}^{-2}}{2} \cos^2(\xi_0 x - \pi/4 - \Theta(\epsilon)) \right| \lesssim \epsilon^2 \log(\epsilon^{-1}) + x^{-1}. \quad (5.51)$$

Therefore, recalling that $\mathfrak{W}^{-2} = \frac{|2K_-|}{\omega_{RN}} = \frac{|2K_-|}{q_0 |\tilde{A}_{RN,\infty}|}$ by definition, we can integrate this to estimate (5.49) by

$$\begin{aligned} \left| \int_{x_B}^x q_0 r_-^2 \xi_0 \epsilon^2 \tilde{x} |\phi|^2(\tilde{x}) d\tilde{x} - \frac{2|K_-| r_-^2}{2|\tilde{A}_{RN,\infty}|} \epsilon^2 \int_{x_B}^x \cos^2(\xi_0 \tilde{x} - \pi/4 - \Theta(\epsilon)) d\tilde{x} \right| \\ \lesssim \epsilon^2 (\epsilon^2 \log(\epsilon^{-1}) x_B + \log(x_B/x)) \lesssim \epsilon^2 \log(\epsilon^{-1}). \end{aligned} \quad (5.52)$$

Then integrating $\cos^2(\xi_0 x - \pi/4 - \Theta(\epsilon)) = \frac{1}{2}(1 + \cos(2\xi_0 x - \pi/2 - 2\Theta(\epsilon)))$ in the usual manner,

$$\left| \int_{x_B}^x q_0 r_-^2 \xi_0 \epsilon^2 \tilde{x} |\phi|^2(\tilde{x}) d\tilde{x} - \frac{1}{4} \frac{2|K_-|}{|\tilde{A}_{RN,\infty}|} (r^2(x) - r^2(x_B)) \right| \lesssim \epsilon^2 \log(\epsilon^{-1}). \quad (5.53)$$

By replacing $r^2(x_B)$ by r_-^2 (which carries an error of $O(\epsilon^2 \log(\epsilon^{-1}))$), we get the estimate (5.47) – to ensure we have the right sign in (5.47), recall that \mathbf{e} and $\tilde{A}_{RN,\infty}$ have opposite signs, while $2K_-$ is negative.

We now move onto the estimates for Ω^2 . For this, we consider (2.42), and integrate by parts using (2.45) as follows, where we use (O1) to control error terms involving Ω^2 :

$$\begin{aligned} \left| \frac{d}{ds} \log(r\Omega^2) - 2K_- \right| (s) &\lesssim \left| \frac{d}{ds} \delta \log(r\Omega^2) \right| (s_O) + \left| \int_{s_O}^s (-|\dot{\phi}|^2 + q_0^2 |\tilde{A}|^2 |\phi|^2) ds \right| + \epsilon^{30} \\ &\lesssim \epsilon^2 \log(\epsilon^{-1}) + |\phi \dot{\phi}(s)| + |\phi \dot{\phi}(s_O)| + \left| \int_{s_O}^s \phi(\ddot{\phi} + q_0^2 |\tilde{A}|^2 \phi) ds \right| \\ &\lesssim \epsilon^2 \log(\epsilon^{-1}) + |\phi \dot{\phi}(s)| + \left| \int_{s_O}^s \frac{-\dot{r} \phi \dot{\phi}}{r} ds \right|. \end{aligned} \quad (5.54)$$

In the third line, we used Corollary 4.6 to absorb $|\phi \dot{\phi}(s_O)|$ into the $\epsilon^2 \log(\epsilon^{-1})$ error.

By (5.32) in Proposition 5.5, for $s \in \mathcal{O}_{boot}$, one has

$$|\phi \dot{\phi}(s)| \leq \frac{10^4 |B|^2 \omega_{RN} \epsilon^2 r_-^2}{r^2}.$$

Inserting this estimate into all instances of $\phi \dot{\phi}$ in (5.54) and then evaluating the integral, one eventually arrives

at the estimate (5.48), after applying (5.18) again. Indeed, one has

$$\left| \frac{d}{ds} \log \Omega^2 - 2K_- \right| \leq \left| \frac{d}{ds} \log(r\Omega^2) - 2K_- \right| + \frac{-\dot{r}}{r} \lesssim \epsilon^2 [\log(\epsilon^{-1}) + r^{-2}(s)].$$

This completes the proof of the proposition. \square

Proof of Proposition 5.1 and Corollary 5.2. Suppose the bootstrap assumptions (O1), (O3), (O2) hold in $\mathcal{O}_{boot} \subset \mathcal{O}$. Then the conclusions of Lemma 5.3 and Propositions 5.5 and 5.6 hold. In particular, (5.32) and (5.47) show that (O2) and (O3) are indeed improved in the bootstrap region. Since, by Lemma 5.3, we know that $s \lesssim \epsilon^{-2}$ for all $s \in \mathcal{O}_{boot}$, in order to show $\mathcal{O} = \mathcal{O}_{boot}$ it remains only to improve (O1).

For this purpose, we simply need to integrate (5.48). By (5.18), we know that $-\dot{r}r \gtrsim \epsilon^2$, hence due to (4.39) and $s \geq s_O \gtrsim \log(\epsilon^{-1})$, one has

$$\begin{aligned} |\log \Omega^2(s) - 2K_-s - \log \alpha_-| &\lesssim \epsilon^2 \log(\epsilon^{-1})^2 + \int_{s_O}^s \left(\epsilon^2 \log(\epsilon^{-1}) - \frac{\dot{r}}{r} \right) \\ &\lesssim \epsilon^2 \log(\epsilon^{-1})s + \log \frac{r(s_O)}{r(s)}. \end{aligned} \quad (5.55)$$

In fact, the final term on the right hand side is also bounded by $\epsilon^2 \log(\epsilon^{-1})s$. To see this, note that if s is such that $r(s) \geq \frac{r_-}{2}$, then (5.18) implies that

$$\log \frac{r(s_O)}{r(s)} = \int_{s_O}^s \frac{-\dot{r}(\tilde{s})}{r(\tilde{s})} d\tilde{s} \lesssim \int_{s_O}^s \frac{\epsilon^2}{r(\tilde{s})^2} d\tilde{s} \lesssim \epsilon^2 s.$$

On the other hand, if $r(s) \leq \frac{r_-}{2}$ then (5.18) implies that $s \gtrsim \epsilon^{-2}$, and thus $\log\left(\frac{r(s_O)}{r(s)}\right) \lesssim \log(\epsilon^{-1}) \lesssim \epsilon^2 \log(\epsilon^{-1})s$.

Hence, (5.55) implies that

$$\Omega^2 \leq \alpha_- e^{(2K_- + D_O \epsilon^2 \log(\epsilon^{-1}))s}, \quad (5.56)$$

which clearly implies (5.5) for ϵ small. Moreover, since $e^{K_- \cdot s_O(\epsilon)} \lesssim \epsilon^{50}$, we have improved the final bootstrap (O1). Therefore, $\mathcal{O}_{boot} = \mathcal{O}$ and its right endpoint is $s = s_{PK}$, where $r(s_{PK}) = 2|B|\mathfrak{W}\epsilon r_-$.

Integrating (5.18) in the region \mathcal{O} , one gets:

$$\left| \frac{1}{2}r^2(s_O) - \frac{1}{2}r^2(s_{PK}) - 4|B|^2\mathfrak{W}^2\omega_{RN}r_-^2\epsilon^2(s_{PK} - s_O) \right| \lesssim \epsilon^2 \log(\epsilon^{-1}),$$

which simplifies after applying the estimates of Proposition 4.5 to

$$|r_-^2 - 8|B|^2\mathfrak{W}^2\omega_{RN}r_-^2\epsilon^2s_{PK}| \lesssim \epsilon^2 \log(\epsilon^{-1}).$$

This yields the estimate (5.12) for s_{PK} . The remaining parts of both Proposition 5.1 and Corollary 5.2 are straightforward. \square

Remarkably, (5.14) shows that the spacetime exhibits a nonzero, yet controlled *discharge* within the oscillatory region \mathcal{O} . We conclude this section with a (purely algebraic) lemma revealing that the final charge $Q_\infty(M, \mathbf{e}, \Lambda)$ lies strictly between \mathbf{e} and $\mathbf{e}/2$.

Lemma 5.7. Define Q_∞ as in (5.13). Then one has the following alternative form for Q_∞ , where we recall

$\mathcal{P}_{se} = \mathcal{P}_{se}^{\Lambda < 0} \cup \mathcal{P}_{se}^{\Lambda = 0} \cup \mathcal{P}_{se}^{\Lambda > 0}$ from Section 2.2.

$$Q_\infty = \frac{3}{4}\mathbf{e} + \frac{\Lambda r_-^2 r_+ (2r_- + r_+)}{12\mathbf{e}}. \quad (5.57)$$

From this, we make the following observations regarding Q_∞ :

- (i) If $\Lambda = 0$, then $Q_\infty = \frac{3}{4}\mathbf{e}$.
- (ii) If $\Lambda < 0$, then Q_∞ lies strictly between $\frac{1}{2}\mathbf{e}$ and $\frac{3}{4}\mathbf{e}$. Furthermore, as (M, \mathbf{e}, Λ) varies across the sub-extremal parameter space $\mathcal{P}_{se}^{\Lambda < 0}$, Q_∞/\mathbf{e} achieves all values in $(\frac{1}{2}, \frac{3}{4})$.
- (iii) If $\Lambda > 0$, then Q_∞ lies strictly between $\frac{3}{4}\mathbf{e}$ and \mathbf{e} . Furthermore, as (M, \mathbf{e}, Λ) varies across the sub-extremal parameter space $\mathcal{P}_{se}^{\Lambda > 0}$, Q_∞/\mathbf{e} achieves all values in $(\frac{3}{4}, 1)$.

In particular, in all cases, one has $|Q_\infty| > \frac{1}{2}|\mathbf{e}| > 0$.

Proof. To get (5.57), we need to find a clean expression for $2K_-$ in terms of the black hole parameters. For this purpose, recall the polynomial (2.16), and define the function $f(X)$ as

$$f(X) = X^{-2}P_{M, \mathbf{e}, \Lambda}(X) = X^{-2}(r_+ - X)(r_- - X) \left(\frac{\mathbf{e}^2}{r_+ r_-} - \frac{\Lambda}{3}(r_+ + r_-)X - \frac{\Lambda}{3}X^2 \right),$$

from which we may alternatively define the surface gravity $2K_-$ as:

$$2K_-(M, \mathbf{e}, \Lambda) = f'(X)|_{X=r_-} = r_-^{-2}(r_- - r_+) \left(\frac{\mathbf{e}^2}{r_+ r_-} - \frac{\Lambda}{3}r_-(r_+ + r_-) - \frac{\Lambda}{3}r_-^2 \right).$$

Recalling once more that $\tilde{A}_{RN, \infty}(M, \mathbf{e}, \Lambda) = \frac{\mathbf{e}}{r_+} - \frac{\mathbf{e}}{r_-} = \frac{\mathbf{e}(r_- - r_+)}{r_+ r_-}$, we therefore get (5.57).

Once we have (5.57), the case (i) is immediate. For the first statement of (iii), one may assume without loss of generality that $\mathbf{e} > 0$. Then, for $\Lambda > 0$, (5.57) gives $Q_\infty > \frac{3}{4}\mathbf{e}$, while (5.13) gives $Q_\infty < \mathbf{e}$, since $\tilde{A}_{RN, \infty} < 0$ and $2K_- < 0$. For the $\Lambda < 0$ case, we require one final observation, namely

$$0 = r_+^{-1}P_{M, \mathbf{e}, \Lambda}(r_+) - r_-^{-1}P_{M, \mathbf{e}, \Lambda}(r_-) = \mathbf{e}^2 \left(\frac{1}{r_+} - \frac{1}{r_-} \right) + (r_+ - r_-) - \frac{\Lambda}{3}(r_+^3 - r_-^3).$$

Dividing by $r_+ - r_-$ and multiplying by $r_+ r_-$, this gives

$$\frac{\Lambda}{3}r_+ r_- (r_+^2 + r_+ r_- + r_-^2) = -\mathbf{e}^2 + r_+ r_-.$$

In particular, in the case $\Lambda < 0$, we then have

$$0 < -\frac{\Lambda}{3}r_-^2 r_+ (2r_- + r_+) < -\frac{\Lambda}{3}r_+ r_- (r_+^2 + r_+ r_- + r_-^2) < \mathbf{e}^2.$$

Substituting this into (5.57), we get the first statement of (ii).

To prove the second statements of (ii), (iii), we first state without proof several facts about the sub-extremal parameter spaces. Without loss of generality, we fix \mathbf{e} to be positive. Then letting $\mathcal{P}_{se}^+ = \mathcal{P}_{se} \cap \{\mathbf{e} > 0\}$ be the space of subextremal parameters with positive \mathbf{e} ,

- \mathcal{P}_{se}^+ is an open, connected set in \mathbb{R}^3 .

- Define the set $\mathcal{P}_{ex}^{\Lambda < 0}$ to be the set of $(M, \mathbf{e}, \Lambda) \in \mathbb{R}^+ \times \mathbb{R} \times (-\infty, 0)$ such that the polynomial $P_{M, \mathbf{e}, \Lambda}(X)$ has a single repeated positive root $X = R$, and $\mathcal{P}_{ex}^{\Lambda > 0}$ to be the set of $(M, \mathbf{e}, \Lambda) \in \mathbb{R}^+ \times \mathbb{R} \times (0, +\infty)$ such that the polynomial $P_{M, \mathbf{e}, \Lambda}(X)$ has two positive roots $X = R$ and $X = R_C$, with $X = R$ having multiplicity 2 and $R < R_C$. Then, $\mathcal{P}_{ex}^+ := (\mathcal{P}_{ex}^{\Lambda < 0} \cup \mathcal{P}_{ex}^{\Lambda > 0}) \cap \{\mathbf{e} > 0\}$ is a subset of the boundary $\partial \mathcal{P}_{se}^+$.
- For $(M, \mathbf{e}, \Lambda) \in \mathcal{P}_{se}^+$, one must have $-\infty < \Lambda M^2 < \frac{2}{9}$, i.e. we are constrained to have $\Lambda M^2 < \frac{2}{9}$ in order for there to exist a choice of $\mathbf{e} > 0$ such that the polynomial $P_{M, \mathbf{e}, \Lambda}(X)$ has the correct number of distinct positive roots. Moreover, all these values are achieved when restricting to the extremal case i.e. $\{\Lambda M^2 : (M, \mathbf{e}, \Lambda) \in \mathcal{P}_{ex}^+\} = (-\infty, \frac{2}{9})$.
- The functions $r_+(M, \mathbf{e}, \Lambda)$ and $r_-(M, \mathbf{e}, \Lambda)$ are continuous in \mathcal{P}_{se}^+ . Furthermore, they may be continuously extended onto $\mathcal{P}_{ex}^+ \subset \partial \mathcal{P}_{se}^+$, upon defining $r_- = r_+ = R$ on \mathcal{P}_{ex}^+ .

In light of these facts, Q_∞ is a continuous function of (M, \mathbf{e}, Λ) in \mathcal{P}_{se}^+ , and may be continuously extended onto the space of extremal parameters \mathcal{P}_{ex}^+ , where we have

$$Q_\infty = \frac{3}{4}\mathbf{e} + \frac{\Lambda R^4}{4\mathbf{e}}. \quad (5.58)$$

We would like to estimate ΛR^4 . For extremal parameters, we must have $P_{M, \mathbf{e}, \Lambda}(R) = \frac{d}{dX}P_{M, \mathbf{e}, \Lambda}(R) = 0$, from which we can get the two identities¹⁹:

$$-2\Lambda R^3 + 3R - 3M = 0, \quad (5.59)$$

$$R^2 - 3MR + 2\mathbf{e}^2 = 0. \quad (5.60)$$

Using (5.59) and then (5.60) in (5.58), we then get

$$Q_\infty = \frac{3}{4}\mathbf{e} \left(1 + \frac{R(R-M)}{2\mathbf{e}^2} \right) = \frac{3}{4}\mathbf{e} \left(1 + \frac{R-M}{3M-R} \right) = \frac{3}{2}\mathbf{e} \cdot \frac{1}{3-R/M}. \quad (5.61)$$

It remains to work out the range of values that R/M can take. We rearrange (5.59) to get the equation:

$$1 - \frac{R}{M} + \frac{2}{3}\Lambda M^2 \left(\frac{R}{M} \right)^3 = 0. \quad (5.62)$$

As ΛM^2 varies between $-\infty$ and $\frac{2}{9}$, we can see that the unique positive root of this cubic expression in R/M varies between 0 and $\frac{3}{2}$, not including the endpoints. (Note that if $\Lambda M^2 > \frac{2}{9}$, then in fact there are no positive roots! This is why ΛM^2 must be upper bounded.)

Therefore, as ΛM^2 and thus R/M vary within their allowed ranges, from (5.61) we have that Q_∞ is allowed to take every value between $\mathbf{e}/2$ and \mathbf{e} , not including the endpoints.

Of course, this computation was done for extremal parameters in \mathcal{P}_{ex}^+ rather than the subextremal parameters in \mathcal{P}_{se}^+ . But \mathcal{P}_{se}^+ is connected, so it is straightforward to show that indeed $\{Q_\infty(M, \mathbf{e}, \Lambda) : (M, \mathbf{e}, \Lambda) \in \mathcal{P}_{se}^+\} = (\mathbf{e}/2, \mathbf{e})$ also. This concludes the proof of Lemma 5.7. \square

¹⁹These will arise from $\frac{d}{dX}P_{M, \mathbf{e}, \Lambda}(R) = 0$ and $\frac{d}{dX}(X^{-4}P_{M, \mathbf{e}, \Lambda})(R) = 0$ respectively.

6 The Proto-Kasner Region

6.1 Estimates beyond the oscillatory region – statement of Proposition 6.1

In the previous section, we considered the region $\mathcal{O} = \{s \geq s_O : r(s) \geq 2|B|\mathfrak{W}\epsilon r_-\} = \{s_O \leq s \leq s_{PK}\}$, where $s_O(\epsilon) = 50s_{lin}$ and we $s_{PK} = O(\epsilon^{-2})$ was defined such that $r(s_{PK}) = 2|B|\mathfrak{W}\epsilon r_-$. The reason it was necessary to end this region at $r \sim \epsilon r_-$ was twofold:

1. Considering the Bessel function form of ϕ ,

$$\phi = C_J(\epsilon)J_0\left(\frac{\xi_0 r^2}{r_-^2 \epsilon^2}\right) + C_Y(\epsilon)Y_0\left(\frac{\xi_0 r^2}{r_-^2 \epsilon^2}\right) + \text{error},$$

then the Bessel functions $J_0(z), Y_0(z)$ will change behavior from oscillatory (at large z) to convergent or logarithmically growing (at small z) once $r^2(s) \leq \xi_0^{-1} r_-^2 \epsilon^2 \approx 8|B|^2 \mathfrak{W}^2 \epsilon^2 r_-^2$. (See (5.3), (5.4))

2. We tackled many error terms using the smallness of $\Omega^2(s)$ to dominate polynomial powers of r^{-1} and $|\phi|$. At the start of the region \mathcal{O} , i.e. $s = s_O(\epsilon) = 50s_{lin}(\epsilon)$, we only had that $\Omega^2 \lesssim \epsilon^{100}$, so in order for the errors to be controlled we required r^{-1} to be at worst an inverse power of ϵ .

Nevertheless, we will show that we may extend many of the important estimates beyond $s = s_{PK}$ to a region $\mathcal{PK} = \{s \geq s_{PK} : r(s) \geq e^{-\delta_0 \epsilon^{-2}} r_-\}$, which for reasons that will later become clear we denote by the *proto-Kasner* region. Here, the dimensionless constant $\delta_0(M, \mathbf{e}, \Lambda, q_0)$ is selected to be (recall that $b_- = \frac{2|B|\omega_{RN}}{|2K_-|} = 2|B|\mathfrak{W}^2$)

$$\delta_0 := \frac{1}{2000} |B(M, \mathbf{e}, \Lambda)|^{-2} \mathfrak{W}^{-4}(M, \mathbf{e}, \Lambda, q_0) = \frac{1}{500} b_-^{-2}. \quad (6.1)$$

In the region \mathcal{PK} , we will overcome difficulty 1 by instead using new bootstrap assumptions that reflect the now monotonic behavior of ϕ and $\dot{\phi}$. The more fundamental difficulty 2 is dealt with by now using the fact that Ω^2 is now such that $-\log \Omega^2 \gtrsim -K_- s \gtrsim \epsilon^{-2}$ in regimes such as \mathcal{PK} where s is of order ϵ^{-2} .

Proposition 6.1. Choose $\delta_0(M, \mathbf{e}, \Lambda, q_0) > 0$ as in (6.1). Then, in the region $\mathcal{PK} = \{2|B|\mathfrak{W}\epsilon r_- \geq r(s) \geq e^{-\delta_0 \epsilon^{-2}} r_-\}$, there exists some $D_{PK}(M, \mathbf{e}, \Lambda, m^2, q_0) > 0$ such that that one has the following exponential behavior for the lapse $\Omega^2(s)$:

$$\Omega^2(s) \leq D_{PK} \exp(-50\delta_0 \epsilon^{-2}). \quad (6.2)$$

Recalling the quantity Q_∞ from (5.13), we have the following for all $s \in \mathcal{PK}$:

$$|-r\dot{r}(s) - 4|B|^2 \mathfrak{W}^2 \omega_{RN} r_-^2 \epsilon^2| \leq D_{PK} \epsilon^4 \log(\epsilon^{-1}), \quad (6.3)$$

$$|q_0 \tilde{A}(s) - q_0 \tilde{A}_{RN, \infty}| \leq D_{PK} \epsilon^2, \quad (6.4)$$

$$|Q(s) - Q_\infty| \leq D_{PK} \epsilon^2 \log(\epsilon^{-1}). \quad (6.5)$$

Using these, and recalling that $\omega_{RN} = |q_0 \tilde{A}_{RN, \infty}|$, we define the quantities ω_K and ξ_K by

$$\omega_K := |q_0 \tilde{A}|(s_{PK}) = \omega_{RN} + O(\epsilon^2), \quad (6.6)$$

$$\xi_K := \omega_K \left(-\frac{d}{ds} \frac{r^2}{r_-^2 \epsilon^2} \right)^{-1} (s_{PK}) = \frac{1}{8|B|^2 \mathfrak{W}^2} + O(\epsilon^2 \log(\epsilon^{-1})). \quad (6.7)$$

For the scalar field ϕ , there will exist coefficients $C_{JK}(\epsilon)$ and $C_{YK}(\epsilon)$ obeying, for $C_J(\epsilon)$ and $C_Y(\epsilon)$ as in Proposition 5.5, the estimates $|C_{JK}(\epsilon) - C_J(\epsilon)| + |C_{YK}(\epsilon) - C_Y(\epsilon)| \leq D_{PK}\epsilon^2 \log(\epsilon^{-1})$, such that for all $s \in \mathcal{PK}$:

$$\left| \phi(s) - \left(C_{JK}(\epsilon) J_0 \left(\frac{\xi_K r^2(s)}{r_-^2 \epsilon^2} \right) + C_{YK}(\epsilon) Y_0 \left(\frac{\xi_K r^2(s)}{r_-^2 \epsilon^2} \right) \right) \right| \leq D_{PK} \epsilon^2 \log(\epsilon^{-1}), \quad (6.8)$$

$$\left| \dot{\phi}(s) - \omega_K \left(C_{JK}(\epsilon) J_1 \left(\frac{\xi_K r^2(s)}{r_-^2 \epsilon^2} \right) + C_{YK}(\epsilon) Y_1 \left(\frac{\xi_K r^2(s)}{r_-^2 \epsilon^2} \right) \right) \right| \leq D_{PK} \epsilon^2 \log(\epsilon^{-1}). \quad (6.9)$$

Moreover, the following upper bounds for ϕ and $\dot{\phi}$ are satisfied for all $s \in \mathcal{PK}$:

$$|\phi(s)| \leq 100 \mathfrak{W}^{-1} \left(1 + \log \left(\frac{8|B|^2 \mathfrak{W}^2 r_-^2 \epsilon^2}{r^2} \right) \right), \quad (6.10)$$

$$|\dot{\phi}| \leq 100 \omega_{RN} \cdot \frac{8|B|^2 \mathfrak{W}^2 r_-^2 \epsilon^2}{r^2}. \quad (6.11)$$

Remark 6.1. Both the statement and the proof of Proposition 6.1 will show large similarities to Proposition 5.1 in Section 5. One notes, however, that, in order to obtain the necessary error estimates, such as those of Lemma 6.2, the quantities ξ_0 and ω_0 , which are defined as the values of certain quantities evaluated at $s = s_O$, to the quantities ξ_K and ω_K , which are the values of the same quantities but evaluated at $s = s_{PK}$ instead.

6.2 Proof of Proposition 6.1

We often make reference to the following four bootstrap assumptions in the region \mathcal{PK} .

$$\Omega^2 \leq \alpha_- \exp(-50\delta_0 \epsilon^{-2}), \quad (\text{PK1})$$

$$|\phi| \leq 100 \mathfrak{W}^{-1} \left(1 + \log \left(\frac{8|B|^2 \mathfrak{W}^2 r_-^2 \epsilon^2}{r^2} \right) \right), \quad (\text{PK2})$$

$$|\dot{\phi}| \leq 100 \omega_{RN} \cdot \frac{8|B|^2 \mathfrak{W}^2 r_-^2 \epsilon^2}{r^2}. \quad (\text{PK3})$$

$$|Q| \leq 2|e|. \quad (\text{PK4})$$

From Corollary 5.2 and Lemma 5.7, it follows that the bootstraps (PK2), (PK3), (PK4) hold in a neighborhood of $s = s_{PK}$. On the other hand, (PK1) holds in a neighborhood of $s = s_{PK}$ due to (5.5) and (5.12): note that, for ϵ chosen sufficiently small, using (6.1) and (5.12), we have

$$K_{-s_{PK}} \leq -\frac{2|K_-|}{\omega_{RN}} \frac{1}{32|B|^2 \mathfrak{W}^2} \epsilon^{-2} \leq -\frac{1}{32|B|^2 \mathfrak{W}^4} \epsilon^{-2} < -51\delta_0 \epsilon^{-2}. \quad (6.12)$$

We now proceed in largely the same manner as in the region \mathcal{O} . Always assuming the bootstraps, we begin as in Section 5.1 with some preliminary estimates on $-r\dot{r}$ and \tilde{A} , then as in Section 5.2 we use these together with the equation (2.46) written in Bessel-like form to find precise asymptotics for the scalar field ϕ . Finally one concludes using these Bessel asymptotics to close estimates for Q and Ω^2 as in Section 5.3. We shall aim to be rather terse, as modifications from the analysis of the region \mathcal{O} are generally minor.

Before proceeding, we briefly address how to deal with the difficulty 2 mentioned in Section 6.1. The idea is that the new bootstrap (PK1) now means the smallness of Ω^2 dominates by powers of r^{-1} , since $r^{-1} \lesssim e^{-\delta_0 \epsilon^{-2}}$

in the region under consideration. For instance, consider the following expression arising in (2.40); in light of the bootstrap assumptions (PK1)–(PK4), one estimates

$$\frac{\Omega^2}{4} \left(\frac{Q^2}{r^2} + m^2 r^2 |\phi|^2 \right) \lesssim e^{-48\delta_0 \epsilon^{-2}}.$$

We now proceed with the proof in a series of lemmas similar to those of Section 5. As in that section, it is convenient to define \mathcal{PK}_{boot} as the connected component of the set $\{s \in \mathcal{PK} : s \leq \epsilon^{-4}, \text{ (PK1)–(PK4) apply} \}$ such that $s_{PK} \in \mathcal{PK}_{boot}$. Then we have the following.

Lemma 6.2. For $s \in \mathcal{PK}_{boot}$, one finds

$$\left| \frac{d}{ds}(-r\dot{r})(s) \right| + |-r\dot{r}(s) + r\dot{r}(s_{PK})| \leq D_{PK} e^{-40\delta_0 \epsilon^{-2}}, \quad (6.13)$$

$$|q_0 \tilde{A}(s) - q_0 \tilde{A}(s_{PK})| \leq D_{PK} e^{-40\delta_0 \epsilon^{-2}}. \quad (6.14)$$

Further, (6.3) and (6.4) hold. Moreover, letting $x(s) = \frac{r^2(s)}{r_-^2 \epsilon^2}$, one finds that

$$\frac{d}{dx} \left(x \frac{d\phi}{dx} \right) + \xi_K^2 x f = \mathcal{E}_\phi, \quad (6.15)$$

where the error term \mathcal{E}_ϕ is bounded by

$$|\mathcal{E}_\phi(s)| \leq D_{PK} e^{-30\delta_0 \epsilon^{-2}}.$$

Proof. The proof is almost identical to that of Lemma 5.3 and 5.4, in light of the comments above. \square

Lemma 6.3. Recalling $x(s) = \frac{r^2(s)}{r_-^2 \epsilon^2}$, let $x_{PK} = x(s_{PK})$, and define the coefficients $C_{JK}(\epsilon)$ and $C_{YK}(\epsilon)$ via

$$\begin{bmatrix} C_{JK}(\epsilon) \\ C_{YK}(\epsilon) \end{bmatrix} = \begin{bmatrix} J_0(\xi_K x_{PK}) & Y_0(\xi_K x_{PK}) \\ -\xi_K J_1(\xi_K x_{PK}) & -\xi_K Y_1(\xi_K x_{PK}) \end{bmatrix}^{-1} \begin{bmatrix} \phi(x_{PK}) \\ \frac{d\phi}{dx}(x_{PK}) \end{bmatrix}. \quad (6.16)$$

Then one has that $|C_{JK}(\epsilon) - C_J(\epsilon)| + |C_{YK}(\epsilon) - C_Y(\epsilon)| \leq D_{PK} \epsilon^2 \log(\epsilon^{-1})$, and that, for $x = x(s)$ corresponding to $s \in \mathcal{PK}_{boot}$,

$$|\phi(x) - C_{JK}(\epsilon) J_0(\xi_K x) - C_{YK}(\epsilon) Y_0(\xi_K x)| \leq D_{PK} e^{-20\delta_0 \epsilon^{-2}}, \quad (6.17)$$

$$\left| \frac{d\phi}{dx}(s) + \xi_K C_{JK}(\epsilon) J_1(\xi_K x) + \xi_K C_{YK}(\epsilon) Y_1(\xi_K x) \right| \leq D_{PK} e^{-20\delta_0 \epsilon^{-2}}. \quad (6.18)$$

Proof. The idea is that in light of (6.15), we can use the equation (5.34) describing the solution for the scalar field using the solution operator to the linear Bessel equation, just as in Proposition 5.5. To get improved error estimates, however, we evolve the system from $x = x_{PK}$ as opposed to $x = x_B$, hence the appearance of the updated Bessel coefficients $C_{JK}(\epsilon)$ and $C_{YK}(\epsilon)$ in (6.16).

We first show these are close to the original coefficients as claimed; from Proposition 5.5, we have

$$\begin{bmatrix} \phi(x_{PK}) \\ \frac{d\phi}{dx}(x_{PK}) \end{bmatrix} = \begin{bmatrix} J_0(\xi_0 x_{PK}) & Y_0(\xi_0 x_{PK}) \\ -\xi_0 J_1(\xi_0 x_{PK}) & -\xi_0 Y_1(\xi_0 x_{PK}) \end{bmatrix} \begin{bmatrix} C_J(\epsilon) \\ C_Y(\epsilon) \end{bmatrix} + O(\epsilon^{10}).$$

Moreover, using $x_{PK} = 4|B|^2 \mathfrak{W}^2$, from (4.53) and Corollary 5.4, we know that $\xi_0 x_{PK}$ and $\xi_K x_{PK}$ lie within the

interval $(\frac{1}{4}, 1)$ and that $|\xi_0 x_{PK} - \xi_K x_{PK}| \lesssim \epsilon^{25} \lesssim \epsilon^2 \log(\epsilon^{-1})$. Thus, since the derivatives of $J_\nu(z)$ and $Y_\nu(z)$ are bounded for $1/4 \leq z \leq 1$, and $|C_J(\epsilon)|, |C_Y(\epsilon)| \lesssim 1$, we can modify the above formula to

$$\begin{bmatrix} \phi(x_{PK}) \\ \frac{d\phi}{dx}(x_{PK}) \end{bmatrix} = \begin{bmatrix} J_0(\xi_K x_{PK}) & Y_0(\xi_K x_{PK}) \\ -\xi_K J_1(\xi_K x_{PK}) & -\xi_K Y_1(\xi_K x_{PK}) \end{bmatrix} \begin{bmatrix} C_J(\epsilon) \\ C_Y(\epsilon) \end{bmatrix} + O(\epsilon^2 \log(\epsilon^{-1})). \quad (6.19)$$

Finally, since by Lemma A.5 the inverse matrix

$$\begin{bmatrix} J_0(\xi_K x_{PK}) & Y_0(\xi_K x_{PK}) \\ -\xi_K J_1(\xi_K x_{PK}) & -\xi_K Y_1(\xi_K x_{PK}) \end{bmatrix}^{-1} = \frac{2}{\pi x_{PK}} \begin{bmatrix} -\xi_K Y_1(\xi_K x_{PK}) & -Y_0(\xi_K x_{PK}) \\ \xi_K J_1(\xi_K x_{PK}) & J_0(\xi_K x_{PK}) \end{bmatrix}$$

has uniformly bounded entries, combining (6.19) with (6.16) shows, as claimed, the relation

$$\begin{bmatrix} C_{JK}(\epsilon) \\ C_{YK}(\epsilon) \end{bmatrix} = \begin{bmatrix} C_J(\epsilon) \\ C_Y(\epsilon) \end{bmatrix} + O(\epsilon^2 \log(\epsilon^{-1})).$$

The remainder of the proof is as in Proposition 5.5. Adopting the same notation from the proof of this proposition, we record the analogue of (5.34) again here:

$$\begin{bmatrix} \phi \\ \frac{d\phi}{dx} \end{bmatrix}(x) = \mathbf{S}_{\xi_K}(x; x_{PK}) \begin{bmatrix} \phi \\ \frac{d\phi}{dx} \end{bmatrix}(x_{PK}) + \int_{x_{PK}}^x \mathbf{S}_{\xi_K}(x; \tilde{x}) \begin{bmatrix} 0 \\ \frac{1}{\tilde{x}} \mathcal{E}_\phi(\tilde{x}) \end{bmatrix} d\tilde{x}. \quad (6.20)$$

The first term on the right hand side will correspond to a solution of the linear Bessel equation after a rescaling $z = \xi_K x$, just as before. Using once again part (1) of Corollary A.7 we see this corresponds to the objects on the left hand sides of (6.17) and (6.18).

For the second term on the right hand side of (6.20), we once again appeal to part (2) of Corollary A.7. From this corollary, the appearance of the operator $\mathbf{S}_{\xi_K}(x; x_{PK})$ will contribute at worst an additional factor of $x^{-1} \leq \epsilon^2 e^{2\delta_0 \epsilon^{-2}}$ in our l^∞ estimates. Since the length of the integration interval $|x - x_{PK}| \leq x_{PK}$ is uniformly bounded, (6.17) and (6.18) follow straightforwardly. \square

Completing the proof of Proposition 6.1. We are now in a position to close all the bootstraps and complete the proof. We first use Lemma 6.3 to improve (PK2) and (PK3). We shall only show the latter; the former follows in a similar fashion.

By Lemma 6.3 and the bounds on the coefficients in Proposition 5.5, within the region \mathcal{PK}_{boot} , one has

$$\left| \frac{d\phi}{dx} \right| \leq 2\sqrt{\pi} \mathfrak{W}^{-1} \xi_K \cdot (|J_1(\xi_K x)| + |Y_1(\xi_K x)|).$$

In light of Facts A.1 and A.2, one may check that $\left| \frac{d\phi}{dx} \right| \leq 4\sqrt{\pi} \mathfrak{W}^{-1} x^{-1}$. Hence, using $-\frac{dx}{ds} = 8|B|^2 \mathfrak{W}^2 \omega_{RN} + O(\epsilon^2 \log(\epsilon^{-1}))$ from Lemma 6.2, we improve (PK3). As mentioned, improving (PK2) is similar.

We now move onto Q and Ω^2 . For $Q(s)$, it remains to understand only how Q changes in the region \mathcal{PK} , in particular that it changes only by $O(\epsilon^2 \log(\epsilon^{-1}))$. Looking at (2.43), we need to study

$$\left| \int_{s_{PK}}^s \tilde{A} q_0^2 r^2 |\phi|^2(s') ds' \right|.$$

Now, we use (5.20) and (6.10) to estimate

$$\left| \int_{s_{PK}}^s \tilde{A} q_0^2 r^2 |\phi|^2(s') ds' \right| \lesssim \int_{s_{PK}}^s \epsilon^2 \cdot \frac{r^2}{r_-^2 \epsilon^2} \left(1 + \left| \log \left(\frac{\epsilon^2}{r^2} \right) \right| \right)^2 (s') ds'. \quad (6.21)$$

Substituting $x = \frac{r^2}{r_-^2 \epsilon^2}$ as usual, and noting that $-\frac{dx}{ds} \sim 1$, we therefore see that

$$\left| \int_{s_{PK}}^s \tilde{A} q_0^2 r^2 |\phi|^2(s') ds' \right| \lesssim \int_0^{4|B|^2 \mathfrak{W}^2} \epsilon^2 x (1 + |\log(x)|)^2 dx \lesssim \epsilon^2. \quad (6.22)$$

Combined with (5.14), this will yield (6.5), and hence improve the bootstrap (PK4).

Last of all, for the quantity Ω^2 , we proceed using that the Raychaudhuri equation (2.36) implies $-\Omega^{-2} \dot{r}(s)$ is nonincreasing. Therefore, for $s \in \mathcal{PK}_{boot}$,

$$\Omega^2(s) \leq \frac{\Omega^2(s_{PK})}{-\dot{r}(s_{PK})} \cdot (-\dot{r}(s)) = \Omega^2(s_{PK}) \cdot \frac{-r\dot{r}(s)}{-r\dot{r}(s_{PK})} \cdot \frac{r(s_{PK})}{r(s)}.$$

Therefore, one applies (6.3) and (5.5), alongside $r(s_{PK}) = 2|B|\mathfrak{W}r_- \epsilon$ and $r(s) \geq e^{-\delta_0 \epsilon^{-2}}$ for $s \in \mathcal{PK}$, to find

$$\Omega^2(s) \leq (1 + 2D_O \epsilon^2 \log(\epsilon^{-1})) \cdot \alpha_- e^{K-s_{PK}} \cdot 2|B|\mathfrak{W}r_- \epsilon \cdot e^{\delta_0 \epsilon^{-2}}. \quad (6.23)$$

By (6.12), this means that $\Omega^2(s) \leq \alpha_- e^{-50\delta_0 \epsilon^{-2}} \cdot (1 + 2D_O \epsilon^2 \log(\epsilon^{-1})) 2|B|\mathfrak{W}r_- \epsilon$. Thus, for ϵ chosen sufficiently small, it is straightforward to bound the right hand side such that we improve the final bootstrap (PK1). As a result, $\mathcal{PK}_{boot} = \mathcal{PK}$, and the remaining assertions of Proposition 6.1 are straightforward. \square

6.3 The onset of the Kasner-like geometry

Following the proof of Proposition 6.1, we mention a corollary of Proposition 6.1 that will be important in later sections, and in interpreting the subset $\mathcal{PK}' = \mathcal{K}_1 \cap \mathcal{PK} = \{2|B|\mathfrak{W}\epsilon^2 r_- \geq r(s) \geq e^{-\delta_0 \epsilon^{-2}} r_-\}$ as a genuine Kasner-like region. (Note that, for this step, we restrict to $r(s) \lesssim \epsilon^2 r_-$ rather than $r(s) \lesssim \epsilon r_-$ in order to ignore the $O(1)$ terms in the Bessel function asymptotics.)

Corollary 6.4. Consider the region $s \in \mathcal{PK}' = \{2|B|\mathfrak{W}\epsilon^2 r_- \geq r(s) \geq e^{-\delta_0 \epsilon^{-2}} r_-\}$. In this region, we have the following forms for $(\phi, \dot{\phi})$, where $c_1 = 1$ and $c_2 = 2\pi^{-1}(\gamma - \log 2)$ and $\gamma \approx 0.577$ is the Euler-Mascheroni constant.

$$\left| \phi(s) + \frac{2}{\pi} C_{YK}(\epsilon) \log \left(\frac{r_-^2 \epsilon^2}{r^2(s) \xi_K} \right) - c_1 C_{JK}(\epsilon) - c_2 C_{YK}(\epsilon) \right| \leq D_{PK} \epsilon^2 \log(\epsilon^{-1}), \quad (6.24)$$

$$\left| \dot{\phi}(s) + \frac{2}{\pi} C_{YK}(\epsilon) \frac{r_-^2 \omega_K \epsilon^2}{r^2(s) \xi_K} \right| \leq D_{PK} \epsilon^2 \log(\epsilon^{-1}). \quad (6.25)$$

Next, recall the function $\Theta(\epsilon)$ arising in (5.31). Then, defining $\Psi(s) := \frac{r^2 \dot{\phi}}{-r\dot{r}}(s)$ [see already (7.1) in the next section], one finds that

$$\left| \Psi(s) + \frac{2}{\sqrt{\pi}} \mathfrak{W}^{-1} \sin(\Theta(\epsilon)) \right| \leq D_{PK} \epsilon^2 \log(\epsilon^{-1}). \quad (6.26)$$

Furthermore, if we let $\Psi_i = \Psi(s_i)$, where $r(s_i) = e^{-\delta_0 \epsilon^{-2}}$, then for $s \in \mathcal{PK}'$,

$$|\Psi(s) - \Psi_i| \leq D_{PK} r^2(s) \log(\epsilon^{-1}) \leq D_{PK}^2 \epsilon^4 \log(\epsilon^{-1}). \quad (6.27)$$

Finally, one obtains the following estimates for the lapse Ω^2 :

$$\left| \frac{\frac{d}{ds} \log \Omega^2(s)}{\frac{d}{ds} \log r(s)} - \Psi_i^2 + 1 \right| \leq D_{PK} \epsilon^4 \log(\epsilon^{-1}), \quad (6.28)$$

$$\left| \log \left[\Omega^2(s) \left(\frac{r(s)}{r_-} \right)^{1-\Psi_i^2} \right] + \frac{1}{2} b_-^2 \epsilon^{-2} \right| \leq D_{PK} \log(\epsilon^{-1}). \quad (6.29)$$

Proof. The equations (6.24) and (6.25) follow immediately from (6.8), (6.9) and the Bessel function asymptotics in Facts A.1 and A.2. Indeed, by restricting $r(s) \leq 2|B|\mathfrak{W}\epsilon^2 r_-$, we guarantee that

$$\frac{\xi_K r^2(s)}{r_-^2 \epsilon^2} \leq \epsilon^2,$$

hence Facts A.1 and A.2 guarantee that

$$\begin{aligned} \left| J_0 \left(\frac{\xi_K r^2(s)}{r_-^2 \epsilon^2} \right) - 1 \right| &\lesssim \epsilon^4, \quad \left| J_1 \left(\frac{\xi_K r^2(s)}{r_-^2 \epsilon^2} \right) \right| \lesssim \epsilon^2, \\ \left| Y_0 \left(\frac{\xi_K r^2(s)}{r_-^2 \epsilon^2} \right) + \frac{2}{\pi} \log \frac{r_-^2 \epsilon^2}{\xi_K r^2(s)} - \frac{2}{\pi} (\gamma - \log 2) \right| &\lesssim \epsilon^4, \quad \left| Y_1 \left(\frac{\xi_K r^2(s)}{r_-^2 \epsilon^2} \right) + \frac{2}{\pi} \frac{r_-^2 \epsilon^2}{\xi_K r^2(s)} \right| \lesssim \epsilon^2 \log(\epsilon^{-1}). \end{aligned}$$

Substituting these into (6.8) and (6.9), we get (6.24) and (6.25) with $c_1 = 1$ and $c_2 = 2\pi^{-1}(\gamma - \log 2)$.

Next, combining (6.25) with the estimates (6.6) and (6.7) it is straightforward to get

$$\left| r^2 \dot{\phi}(s) + 16\pi^{-1} C_{YK}(\epsilon) |B|^2 \mathfrak{W}^2 \omega_{RN} r_-^2 \epsilon^2 \right| \lesssim \epsilon^4 \log(\epsilon^{-1}). \quad (6.30)$$

Hence from (6.3) we find that

$$\left| \Psi(s) + 4\pi^{-1} C_{YK}(\epsilon) \right| = \left| \frac{r^2 \dot{\phi}(s)}{-r \dot{r}(s)} + 4\pi^{-1} C_{YK}(\epsilon) \right| \lesssim \epsilon^2 \log(\epsilon^{-1}), \quad (6.31)$$

thus (6.26) follows from $|C_{YK}(\epsilon) - C_Y(\epsilon)| \lesssim \epsilon^2 \log(\epsilon^{-1})$ and (5.30).

To get (6.27), note that (6.25) will also yield $|r^2 \dot{\phi}(s) - r^2 \dot{\phi}(s_i)| \lesssim \epsilon^2 \log(\epsilon^{-1}) r^2(s)$, while we also know from (6.13) that $|-r \dot{r}(s) + r \dot{r}(s_i)| \lesssim e^{-40\delta_0 \epsilon^{-2}} \lesssim \epsilon^2 \log(\epsilon^{-1}) r^2(s)$ changes little in the region \mathcal{PK} . Since $-r \dot{r}(s) \sim \epsilon^2$ by (6.3), the computation

$$\left| \frac{r^2 \dot{\phi}(s)}{-r \dot{r}(s)} - \frac{r^2 \dot{\phi}(s_i)}{-r \dot{r}(s_i)} \right| \lesssim \frac{1}{-r \dot{r}(s)} \cdot \left[|r^2 \dot{\phi}(s) - r^2 \dot{\phi}(s_i)| + |-r \dot{r}(s) + r \dot{r}(s_i)| \right],$$

together with $r(s) \lesssim \epsilon^2$ for $s \in \mathcal{PK}'$, yields (6.27).

We now move on to the estimate (6.28) for the derivative of $\Omega^2(s)$. We proceed here using the Raychaudhuri equation in the form (2.38), which after multiplying by $r(s)(\dot{r}(s))^{-2}$ gives

$$\frac{r}{\dot{r}} \frac{d}{ds} \log \Omega^2 - \frac{r \ddot{r}}{\dot{r}^2} - \frac{r^2 \dot{\phi}^2}{\dot{r}^2} = \frac{r^2 |\tilde{A}|^2 q_0^2 |\phi|^2}{\dot{r}^2}.$$

Using (2.39) to substitute for \ddot{r} , and noticing that the rightmost term on the left hand side is exactly Ψ^2 , one

finds

$$\frac{r}{\dot{r}} \frac{d}{ds} \log \Omega^2 + 1 - \Psi^2 = (-r\dot{r})^{-2} \left[r^4 \tilde{A}^2 q_0^2 |\phi|^2 + \frac{\Omega^2}{4} (Q^2 - r^2 + r^4 \Lambda + r^4 m^2 |\phi|^2) \right].$$

From Proposition 6.1 and (6.24), the right hand side of this is bounded by a multiple of $\epsilon^{-4} (r^2 \log(\frac{1}{r^2}))^2 \lesssim \epsilon^4 \log(\epsilon^{-1})$, so that if we also use (6.27), then we get (6.28) as required.

Finally, for (6.29), one would like to integrate (6.28). However, one needs to first estimate $\Omega^2(s_{K_1})$, where $s = s_{K_1}$ is such that $r(s_{K_1}) = 2|B|\mathfrak{M}\epsilon^2 r_-$ (corresponding to the past boundary of \mathcal{PK}'). For this purpose, one finds exactly as in the proof of Proposition 5.1²⁰ that, for $s \in \mathcal{O} \cup (\mathcal{PK} \setminus \mathcal{PK}') = \{s_O \leq s \leq s_{K_1}\}$,

$$\left| \frac{d}{ds} \log \Omega^2(s) - 2K_- \right| \lesssim \epsilon^2 [\log(\epsilon^{-1}) + r^{-2}(s)]. \quad (6.32)$$

Integrating this for $s \in \mathcal{O} \cup (\mathcal{PK} \setminus \mathcal{PK}')$, using that the length of the integration interval is of $O(\epsilon^{-2})$, one gets

$$|\log \Omega^2(s_{K_1}) - 2K_{-s_{K_1}}| \lesssim \log(\epsilon^{-1}) + |\log \Omega^2(s_O)| \lesssim \log(\epsilon^{-1}).$$

We also need to estimate the expression $2K_{-s_{K_1}}$. This follows from an identical computation to that of s_{PK} as in (5.12), and one finds that

$$2K_{-s_{K_1}} = -\frac{|2K_-|}{8|B|^2 \mathfrak{M}^2 \omega_{RN} \epsilon^2} + O(\log(\epsilon^{-1})) = -\frac{1}{2} b_-^2 \epsilon^{-2} + O(\log(\epsilon^{-1})).$$

Since $\frac{r(s_{K_1})}{r_-} \sim \epsilon^2$, so that additional factors of $\log\left(\frac{r(s_{K_1})}{r_-}\right)$ may be added, we arrive at

$$\left| \log \left[\Omega^2(s_{K_1}) \left(\frac{r(s_{K_1})}{r_-} \right)^{1-\Psi_i^2} \right] + \frac{1}{2} b_-^2 \epsilon^{-2} \right| \lesssim \log(\epsilon^{-1}). \quad (6.33)$$

Finally, we rewrite (6.28) as

$$\left| \frac{d}{ds} \log \left[\Omega^2(s) \left(\frac{r(s)}{r_-} \right)^{1-\Psi_i^2} \right] \right| \lesssim \epsilon^2 \log(\epsilon^{-1}) \frac{-\dot{r}(s)}{r(s)}.$$

Integrating this for $s \in \mathcal{PK}'$, and using (6.33) to estimate the boundary term at $s = s_{K_1}$, we find (6.29). \square

7 Construction of the sets E_η and $E'_{\eta,\sigma}$ for further quantitative estimates

So far, we have a description of the hairy black hole interior up to the region \mathcal{PK} , where $s \approx (8|B|^2 \mathfrak{M}^2 \omega_{RN} \epsilon^2)^{-1}$ and $r(s) \geq \exp(-\delta_0 \epsilon^{-2}) r_-$. These estimates hold for $0 < \epsilon \leq \epsilon_0$, where $\epsilon_0(M, \mathbf{e}, \Lambda, m^2, q_0) > 0$ is taken sufficiently small, and δ_0 is a fixed quantity determined by (6.1). In particular, up to this point, we have placed no restriction on the value of ϵ , other than its smallness.

However, within the present article, to proceed further we will need to restrict attention to a smaller subset of values of ϵ verifying a certain condition. We define the following important quantity:

$$\Psi := \frac{r^2 \dot{\phi}}{-r\dot{r}} = -r \frac{d\phi}{dr}. \quad (7.1)$$

²⁰We need to extend from $r(s) \gtrsim \epsilon$ to $r(s) \gtrsim \epsilon^2$, but the proof still applies as we only needed $|\log(r/r_-)| \lesssim \log(\epsilon^{-1})$.

Then the precise condition on ϵ we shall use is that

$$|\Psi_i| := |\Psi(s_i)| \geq \eta > 0, \quad (\dagger)$$

where s_i marks the end of the region \mathcal{PK} , i.e. $r(s_i) = e^{-\delta_0 \epsilon^{-2}} r_-$, and $\eta > 0$ is an arbitrary small constant. Before using (\dagger) to analyse the spacetime beyond \mathcal{PK} in Section 8, we first quantitatively characterize the set of ϵ for which a condition such as (\dagger) holds. In light of Corollary 6.4, we are required to study the quantity $\Theta(\epsilon)$ defined in (5.31).

7.1 Improved estimates on $\Theta(\epsilon)$

From Proposition 4.5, $\Theta(\epsilon)$ is identified to have the following dependence on ϵ :

$$\Theta(\epsilon) = \frac{1}{8|B|^2 \mathfrak{M}^2 \epsilon^2} + O(\log(\epsilon^{-1})). \quad (7.2)$$

However, the $O(\log(\epsilon^{-1}))$ error prevents us from having any quantitative control on quantities such as $\sin(\Theta(\epsilon))$, i.e. given only the above expression, for any fixed $\eta > 0$, if $|\cdot|$ denotes Lebesgue measure, the *limiting density*

$$\limsup_{\epsilon_0 \rightarrow 0} \epsilon_0^{-1} |\{\epsilon \in (0, \epsilon_0] : |\sin(\Theta(\epsilon))| > \eta\}|$$

could be arbitrarily small, or even vanish asymptotically.

To overcome this issue, we instead consider the quantity:

$$\frac{d}{d\epsilon} \Theta(\epsilon) = \left(\frac{\partial}{\partial \epsilon} + \frac{ds_O(\epsilon)}{d\epsilon} \frac{\partial}{\partial s} \right) \left(|q_0 \tilde{A}(s) \cdot r^2(s) \cdot \left(-\frac{d}{ds} r^2(s) \right)^{-1} + \omega_{RN} s \right), \quad (7.3)$$

where to make sense of the right hand side, we now interpret $f(s) \in \{r(s), \log \Omega^2(s), Q(s), \tilde{A}(s), \phi(s), \dot{\phi}(s)\}$ as (smooth) functions of ϵ as well as s .

Denoting the ϵ -derivatives by using a subscript, i.e. $f_\epsilon = \frac{\partial}{\partial \epsilon} f$, while still using $\dot{f} = \frac{\partial}{\partial s} f$ to denote s -derivatives, we shall take an ϵ -derivative of the system (2.36)–(2.46) to find a system of *linear* evolution equations for the quantities $f_\epsilon(s)$. For instance, the ϵ -derivative of (2.44) is

$$\dot{A}_\epsilon = -\frac{\Omega^2}{4r^2} \left(Q_\epsilon + Q(\log \Omega^2)_\epsilon - \frac{2Qr_\epsilon}{r} \right),$$

while the corresponding evolution equations for the other linearized quantities are more complicated and will not be written explicitly. We can also perform this linearization for the difference quantities

$$\delta \phi_\epsilon = \frac{\partial}{\partial \epsilon} (\phi(s) - \phi_{\mathcal{L}}(s)), \quad \delta \dot{\phi}_\epsilon = \frac{\partial}{\partial s} \delta \phi_\epsilon.$$

Along with the evolution equations, one must pose data for the quantities $f_\epsilon(s)$ in the $s \rightarrow -\infty$ limit. For this purpose, one should return to the 1+1-dimensional formulation of the problem in the regular (U, V) coordinates

as in Section 2.3, and take the appropriate ϵ -derivatives there. The correct asymptotic data is

$$\lim_{s \rightarrow -\infty} r_\epsilon(s) = 0, \quad \lim_{s \rightarrow -\infty} Q_\epsilon(s) = 0, \quad \lim_{s \rightarrow -\infty} \phi_\epsilon = 1, \quad (7.4)$$

$$\lim_{s \rightarrow -\infty} (\log \Omega^2)_\epsilon = \lim_{s \rightarrow -\infty} \frac{d}{ds} (\log \Omega^2)_\epsilon = 0, \quad (7.5)$$

$$\lim_{s \rightarrow -\infty} \Omega^{-2} \tilde{A}_\epsilon(s) = 0, \quad (7.6)$$

$$\lim_{s \rightarrow -\infty} 4\Omega^{-2} \dot{r}_\epsilon(s) = \frac{2r_+ m^2 \epsilon}{2K_+}, \quad (7.7)$$

$$\lim_{s \rightarrow -\infty} \Omega^{-2} \dot{\phi}_\epsilon = \beta_+. \quad (7.8)$$

The plan is now to use a similar procedure to Section 4 to find sufficiently strong estimates for the quantities $f_\epsilon \in \{r_\epsilon, (\log \Omega^2)_\epsilon, Q_\epsilon, \tilde{A}_\epsilon, \phi_\epsilon\}$ up to the late blue shift region \mathcal{LB} , where we have nontrivial overlap with the oscillatory region \mathcal{O} , and compute $\frac{d}{d\epsilon} \Theta(\epsilon)$. The most crucial estimate will be to determine that \dot{r}_ϵ is comparable to ϵ .

Proposition 7.1. For $s \in \mathcal{EB} \cup \mathcal{LB} = \{S \leq s \leq \Delta_B \epsilon^{-1}\}$, there exists some constant $D_{LE}(M, \mathbf{e}, \Lambda, m^2, q_0)$ such that:

$$|\dot{r}_\epsilon| + s^{-1} |r_\epsilon| \leq D_{LE} \epsilon, \quad (7.9)$$

$$\left| \frac{d}{ds} (\log \Omega^2)_\epsilon \right| + s^{-1} |(\log \Omega^2)_\epsilon| \leq D_{LE} \epsilon s, \quad (7.10)$$

$$|\tilde{A}_\epsilon| + s^{-1} |Q_\epsilon| \leq D_{LE} \epsilon, \quad (7.11)$$

$$|\dot{\phi}_\epsilon| + |\phi_\epsilon| \leq D_{LE}, \quad (7.12)$$

$$|\delta \dot{\phi}_\epsilon| + |\delta \phi_\epsilon| \leq D_{LE} \epsilon^2 s. \quad (7.13)$$

Furthermore, we have the more precise estimate for $s_O = 50s_{lin} \leq s \leq \Delta_B \epsilon^{-1}$:

$$|-\dot{r}_\epsilon(s) - 8|B|^2 \mathfrak{W}^2 \omega_{RN} r_\epsilon| \leq D_{LE} \epsilon^3 s. \quad (7.14)$$

Corollary 7.2. Consider the expression (7.3). Then

$$\left| \frac{d}{d\epsilon} \Theta(\epsilon) + \frac{1}{4|B|^2 \mathfrak{W}^2 \epsilon^3} \right| \leq D_{LE} \epsilon^{-1} \log(\epsilon^{-1}). \quad (7.15)$$

Proof of Corollary 7.2 given Proposition 7.1. First consider the $\frac{\partial}{\partial s}$ derivative in (7.3). One checks from (2.40), (2.44) and Proposition 4.5, that one has

$$\left| \frac{\partial}{\partial s} \left(|q_0 \tilde{A}|(s) \cdot r^2(s) \cdot \left(-\frac{d}{ds} r^2(s) \right)^{-1} + \omega_{RN} s \right) \right| \lesssim \epsilon^{-4} \Omega^2 \cdot (1 + |\phi|^2) + |\omega_{RN} - |q_0 \tilde{A}|| \lesssim \epsilon^2$$

where the final step follows from $\Omega^2 \lesssim \epsilon^{100}$ at $s = s_O$ and Proposition 4.5. Hence even with the $\frac{ds_O}{d\epsilon} \sim \epsilon^{-1}$ factor in front, this term contributes at worst $O(\epsilon)$ and can be ignored.

The main term $(4|B|^2 \mathfrak{W}^2 \epsilon^3)^{-1}$ on the left hand side of (7.15) comes from taking the ϵ -derivative of

$(-\frac{d}{ds}r^2(s))^{-1}$. Indeed, the expression that arises from this is

$$I = |q_0 \tilde{A}|(s) \cdot r^2(s) \cdot \left(-\frac{d}{ds}r^2(s)\right)^{-2} \cdot 2(r_\epsilon(s)\dot{r}(s) + r(s)\dot{r}_\epsilon(s)).$$

Using Propositions 4.5 and 7.1, particularly (7.14), we can evaluate (note $\dot{r}(s)r_\epsilon(s) = O(\epsilon^3 s)$ is treated as part of the error):

$$\begin{aligned} I &= \frac{\omega_{RN} r_-^2}{(8|B|^2 \mathfrak{M}^2 r_-^2 \omega_{RN} \epsilon^2)^2} \cdot 2(-8|B|^2 \mathfrak{M}^2 \omega_{RN} r_-^2 \epsilon) + O(\epsilon^{-1} \log(\epsilon^{-1})) \\ &= -\frac{1}{4|B|^2 \mathfrak{M}^2 \epsilon^3} + O(\epsilon^{-1} \log(\epsilon^{-1})). \end{aligned}$$

Therefore, the ϵ -derivative on the left hand side of (7.15) can be evaluated using Proposition 7.1 as:

$$I + (|q_0 \tilde{A}|_\epsilon(s) r^2(s) + 2|q_0 \tilde{A}|(s) r(s) r_\epsilon(s)) \cdot \left(-\frac{d}{ds}r^2(s)\right)^{-1} = -\frac{1}{4|B|^2 \mathfrak{M}^2 \epsilon^3} + O(\epsilon^{-1} \log(\epsilon^{-1})),$$

completing the proof of the corollary. \square

Proof of Proposition 7.1. The first step will be to find the upper bounds. For this purpose, we will have to write out the full linear system of ODEs, however, as mentioned previously, this would be cumbersome, and we therefore only include upper bounds for $|\dot{f}_\epsilon|$, often using that $r \sim 1, -\dot{r} \lesssim 1, |\phi| \lesssim \epsilon, |\dot{\phi}| \lesssim \epsilon, Q \sim 1$ and $\tilde{A} \lesssim 1$ within this region. Differentiating (2.39)–(2.45) in ϵ , the appropriate inequalities and equations are:

$$|\ddot{r}_\epsilon| \lesssim \Omega^2(|r_\epsilon| + |(\log \Omega^2)_\epsilon| + |Q_\epsilon|) + (-\dot{r})(|r_\epsilon| + |\dot{r}_\epsilon|) + \Omega^2|\phi\phi_\epsilon|, \quad (7.16)$$

$$\left| \frac{d^2}{ds^2}(\log \Omega^2)_\epsilon \right| \lesssim \Omega^2(|r_\epsilon| + |(\log \Omega^2)_\epsilon| + |Q_\epsilon|) + (-\dot{r})(|r_\epsilon| + |\dot{r}_\epsilon|) + \tilde{A}|\phi\phi_\epsilon| + |\dot{\phi}\dot{\phi}_\epsilon| + |\tilde{A}_\epsilon||\phi|^2, \quad (7.17)$$

$$|\dot{Q}_\epsilon| \lesssim (|\tilde{A}_\epsilon| + |\tilde{A}r_\epsilon|)|\phi|^2 + |\tilde{A}\phi\phi_\epsilon|, \quad (7.18)$$

$$|\dot{\tilde{A}}_\epsilon| \lesssim \Omega^2(|r_\epsilon| + |(\log \Omega^2)_\epsilon| + |Q_\epsilon|), \quad (7.19)$$

$$\ddot{\phi}_\epsilon = -\frac{2\dot{r}\dot{\phi}_\epsilon}{r} - q_0^2 \tilde{A}^2 \phi_\epsilon - \frac{m^2 \Omega^2}{4} \phi_\epsilon + J_\phi, \quad |J_\phi| \lesssim |\dot{r}_\epsilon - \dot{r}r_\epsilon||\dot{\phi}| + |\tilde{A}_\epsilon||\phi| + \Omega^2(\log \Omega^2)_\epsilon |\phi|. \quad (7.20)$$

Note that, for the final equation (7.20), it is necessary to exactly keep the terms corresponding to ϕ being a solution of the linear charged scalar wave equation. We now proceed through the regions \mathcal{R} , \mathcal{N} , \mathcal{EB} and \mathcal{LB} exactly as in Section 4.

Step 1: The redshift region $\mathcal{R} = \{-\infty < s \leq -\Delta_{\mathcal{R}}\}$

In this region, we consider the following bootstrap assumptions, which hold in a neighborhood of $s = -\infty$ by the asymptotic data above:

$$|r_\epsilon| + |\dot{r}_\epsilon| + |(\log \Omega^2)_\epsilon| + |Q_\epsilon| + |\Omega^{-2} \tilde{A}_\epsilon| \leq \epsilon, \quad (7.21)$$

$$|\phi_\epsilon| + |\dot{\phi}_\epsilon| \leq 2. \quad (7.22)$$

Note that by Proposition 4.1, we know already that $-\dot{r}, |\tilde{A}| \lesssim \Omega^2$ and $|\phi|, |\dot{\phi}| \lesssim \epsilon$, so given these bootstrap

assumptions and the inequality (4.8) we may simply integrate up the equations (7.16)–(7.20) to get

$$|r_\epsilon| + |\dot{r}_\epsilon| + |(\log \Omega^2)_\epsilon| + \left| \frac{d}{ds}(\log \Omega^2)_\epsilon \right| + |Q_\epsilon| + |\Omega^{-2}\tilde{A}_\epsilon| \lesssim \epsilon \Omega^2, \quad (7.23)$$

$$|\phi_\epsilon - 1| + |\dot{\phi}_\epsilon| \lesssim \Omega^2. \quad (7.24)$$

(Recall that the asymptotic data for r_ϵ , \dot{r}_ϵ , $\log \Omega_\epsilon^2$ and Q_ϵ is 0.) Hence with a choice of $\Delta_{\mathcal{R}}$ large enough, the bootstraps are easily improved.

Step 2: The no-shift region $\mathcal{N} = \{-\Delta_{\mathcal{R}} \leq s \leq S\}$

Since we are integrating only in a finite s -region, the no-shift region is easily dealt with using Grönwall. To do this, let \mathbf{X}_ϵ and Φ_ϵ denote the tuples:

$$\mathbf{X}_\epsilon = \left(r_\epsilon, \dot{r}_\epsilon, (\log \Omega^2)_\epsilon, \frac{d}{ds}(\log \Omega^2)_\epsilon, Q_\epsilon, \tilde{A}_\epsilon \right), \quad \Phi_\epsilon = (\phi_\epsilon, \dot{\phi}_\epsilon),$$

then in light of Proposition 4.2, the system (7.16)–(7.20) can be translated into

$$|\dot{\mathbf{X}}_\epsilon| \lesssim |\mathbf{X}_\epsilon| + \epsilon |\Phi_\epsilon|, \quad |\dot{\Phi}_\epsilon| \lesssim |\Phi_\epsilon| + \epsilon |\mathbf{X}_\epsilon|.$$

Hence a straightforward use of Grönwall in the bounded s -region $s \in [-\Delta_{\mathcal{R}}, S]$ yields

$$\sup_{s \in \mathcal{N}} |\mathbf{X}_\epsilon|(s) \lesssim |\mathbf{X}_\epsilon|(-\Delta_{\mathcal{R}}) + \epsilon \sup_{s \in \mathcal{N}} |\Phi_\epsilon|(s) \lesssim |\mathbf{X}_\epsilon|(-\Delta_{\mathcal{R}}) + \epsilon |\Phi_\epsilon|(-\Delta_{\mathcal{R}}) + \epsilon^2 \sup_{s \in \mathcal{N}} |\mathbf{X}_\epsilon|(s)$$

So, for ϵ sufficiently small, we absorb the rightmost term into the left hand side, and repeat the argument for $\Phi_\epsilon(s)$, to derive that

$$\begin{aligned} \sup_{s \in \mathcal{N}} |\mathbf{X}_\epsilon|(s) &\lesssim |\mathbf{X}_\epsilon|(-\Delta_{\mathcal{R}}) + \epsilon |\Phi_\epsilon|(-\Delta_{\mathcal{R}}), \\ \sup_{s \in \mathcal{N}} |\Phi_\epsilon|(s) &\lesssim |\Phi_\epsilon|(-\Delta_{\mathcal{R}}) + \epsilon |\mathbf{X}_\epsilon|(-\Delta_{\mathcal{R}}). \end{aligned}$$

Inserting our bounds from the red-shift region \mathcal{R} , there exists $D_{NE}(M, \mathbf{e}, \Lambda, m^2, q_0)$ such that, for all $s \in \mathcal{N}$,

$$|\mathbf{X}_\epsilon|(s) \leq D_{NE}\epsilon, \quad |\Phi_\epsilon|(s) \leq D_{NE}. \quad (7.25)$$

Step 3: Upper bounds in the blue shift regions $\mathcal{EB} \cup \mathcal{LB} = \{S \leq s \leq \Delta_{\mathcal{B}}\epsilon^{-1}\}$.

This step will be much simpler than the corresponding nonlinear estimates in Sections 4.2 and 4.3. We use the bootstrap assumptions:

$$|\dot{r}_\epsilon| \leq 10D_{NE}\epsilon, \quad (7.26)$$

$$|(\log \Omega^2)_\epsilon| \leq 10D_{NE}\epsilon s^3, \quad (7.27)$$

$$|Q_\epsilon| \leq 10D_{NE}\epsilon s^2. \quad (7.28)$$

Note that the first of these trivially implies $|r_\epsilon| \leq 10D_{NE}\epsilon s$. Then integration of (7.19) gives that $|\tilde{A}_\epsilon| \lesssim D_{NE}\epsilon$.

We next use these bootstraps to estimate ϕ_ϵ and $\dot{\phi}_\epsilon$. Note that the expression J_ϕ in (7.20) now obeys the estimate $|J_\phi| \lesssim D_{NE}\epsilon^2$. We now follow the proof of Proposition 4.4 and consider the quantity

$$H^{(\epsilon)} = r^4 \dot{\phi}_\epsilon^2 + r^4 q_0^2 |\tilde{A}|^2 \phi_\epsilon^2.$$

Completely analogously to before, one finds that

$$\dot{H}^{(\epsilon)} \lesssim \Omega^2 H^{(\epsilon)} + |J_\phi| |\dot{\phi}| \lesssim \Omega^2 H^{(\epsilon)} + D_{NE}\epsilon^2 \sqrt{H^{(\epsilon)}}.$$

So, as $\int_S^{\Delta_B \epsilon^{-1}} \Omega^2(\tilde{s}) d\tilde{s} \lesssim 1$, one can apply Grönwall to the quantity $\sqrt{H^{(\epsilon)}}$ to yield

$$\sqrt{H^{(\epsilon)}}(s) \lesssim \sqrt{H^{(\epsilon)}}(S) + D_{NE}\epsilon^2 s \lesssim |\phi_\epsilon|(S) + |\dot{\phi}_\epsilon|(S) + D_{NE}\epsilon^2 s \lesssim D_{NE}.$$

Since $H^{(\epsilon)} \sim \phi_\epsilon^2 + \dot{\phi}_\epsilon^2$, one gets the estimate (7.12).

The next step is to integrate (7.16). Note that, by Propositions 4.4 and 4.5, we have $-\dot{r} \lesssim \max\{\Omega^2, \epsilon^2\}$, $|\phi| \lesssim \epsilon$ and $\Omega^2 \lesssim e^{2K-s}$, so

$$|\dot{r}_\epsilon| \leq D_{NE}\epsilon + CD_{NE} \int_S^{\Delta_B \epsilon^{-1}} (e^{2K-s'} s'^3 \epsilon + \epsilon^3 s') ds' \leq 2D_{NE}\epsilon,$$

where C is a constant independent of ϵ and D_{NE} . For the second inequality above, note that evaluating the integral gives a quantity bounded by a multiple of $\epsilon(e^{2K-S} S^3 + \Delta_B^2)$, hence the inequality follows for S chosen sufficiently large and Δ_B chosen sufficiently small. This improves (7.26) and in fact yields (7.9) after a further integration.

The estimates (7.10) and (7.11) then follow from integration of (7.17), (7.18) and (7.19), and this also improves the remaining two bootstrap assumptions.

Step 4: Precise bounds for the scalar field

We now move onto the estimate (7.13). Note that $\delta\phi_\epsilon = \phi_\epsilon - (\phi_\mathcal{L})_\epsilon$, but recall that since $\phi_\mathcal{L}$ is the exactly the solution to the linear charged wave equation in a Reissner-Nördstrom background having initial data $\lim_{s \rightarrow -\infty} \phi_\mathcal{L} = \epsilon$, it is clear that $(\phi_\mathcal{L})_\epsilon$ is exactly the solution to the linear charged wave equation in Reissner-Nördstrom with $\lim_{s \rightarrow -\infty} (\phi_\mathcal{L})_\epsilon(s) = 1$. Namely, we have

$$(\ddot{\phi}_\mathcal{L})_\epsilon = -\frac{2\dot{r}_{RN}(\dot{\phi}_\mathcal{L})_\epsilon}{r_{RN}} - q_0^2 \tilde{A}_{RN}^2 (\phi_\mathcal{L})_\epsilon - \frac{m^2 \Omega_{RN}^2}{4} (\phi_\mathcal{L})_\epsilon.$$

Hence subtracting this equation from (7.20), and using both the estimates of Section 4 and earlier within the proof of this proposition, one finds

$$\delta\dot{\phi}_\epsilon = -\frac{2\dot{r}\delta\dot{\phi}_\epsilon}{r} - q_0^2 \tilde{A}^2 \delta\phi - \frac{m^2 \Omega^2}{4} \delta\phi_\epsilon + J_\phi + \tilde{J}_\phi, \quad (7.29)$$

where J_ϕ is as in (7.20), \tilde{J}_ϕ arises from taking the differences of $r, \dot{r}, \tilde{A}, \Omega^2$ from their Reissner-Nordström quan-

tities, and one gets the estimate

$$|J_\phi(s)| + |\tilde{J}_\phi(s)| \lesssim \begin{cases} \epsilon^2 \Omega^2 & \text{for } s \in \mathcal{R}, \\ \epsilon^2 & \text{for } s \in \mathcal{N} \cup \mathcal{EB} \cup \mathcal{LB}. \end{cases}$$

We now proceed in the usual way using the quantity

$$\tilde{H}^{(\epsilon)} = r^4 |\delta \dot{\phi}_\epsilon|^2 + r^4 q_0^2 |\tilde{A}|^2 |\delta \phi_\epsilon|^2.$$

Then by using the equation (7.29), one finds that for all $s \in \mathcal{R} \cup \mathcal{N} \cup \mathcal{EB} \cup \mathcal{LB}$, we get

$$\frac{d}{ds} \tilde{H}^{(\epsilon)} \lesssim \Omega^2 \tilde{H}^{(\epsilon)} + (|J_\phi| + |\tilde{J}_\phi|) \sqrt{\tilde{H}^{(\epsilon)}}.$$

Using now the fact that $\lim_{s \rightarrow -\infty} \tilde{H}^{(\epsilon)}(s) = 0$ and $\int_{-\infty}^{\Delta_{\mathcal{B}} \epsilon^{-1}} \Omega^2$ is uniformly bounded in ϵ , Grönwall applied to this differential inequality gives:

$$\sqrt{\tilde{H}^{(\epsilon)}} \lesssim \int_{-\infty}^{\Delta_{\mathcal{B}} \epsilon^{-1}} (|J_\phi(\tilde{s})| + |\tilde{J}_\phi(\tilde{s})|) d\tilde{s} \lesssim \epsilon^2 s. \quad (7.30)$$

This of course will yield the estimate (7.13). Note that by Corollary 2.4, one then has for $s \in \mathcal{LB}$,

$$|\phi_\epsilon - B e^{i\omega_{RN}s} - \bar{B} e^{-i\omega_{RN}s}| \lesssim \epsilon^2 s, \quad (7.31)$$

$$|\dot{\phi}_\epsilon - i\omega_{RN} B e^{i\omega_{RN}s} + i\omega_{RN} \bar{B} e^{-i\omega_{RN}s}| \lesssim \epsilon^2 s. \quad (7.32)$$

Step 5: The precise estimate for \dot{r}_ϵ

We finally move to the estimate (7.14). We now use the differentiated version of the Raychaudhuri equation in the convenient form (2.38). We see that using (7.9), (7.10) and (7.11) we can find

$$\frac{d}{ds}(-\dot{r}_\epsilon) - \frac{d}{ds} \log(\Omega^2) \cdot (-\dot{r}_\epsilon) = 2r(\dot{\phi}_\epsilon \dot{\phi}_\epsilon + |\tilde{A}|^2 q_0^2 \phi_\epsilon \phi_\epsilon) + J_\Omega,$$

where the error J_Ω satisfies $|J_\Omega| \lesssim \epsilon^3 s$.

Now we use (7.31), (7.32), alongside the estimates (4.35), (4.37), (4.42), to find further that

$$\frac{d}{ds}(-\dot{r}_\epsilon) - 2K_-(-\dot{r}_\epsilon) = 8|B|^2 \omega_{RN}^2 r_- \epsilon + J_\Omega + \tilde{J}_\Omega,$$

where $|\tilde{J}_\Omega| \lesssim \epsilon^3 s$. We now use a standard integrating factor to integrate between s_{lin} and $s \in \mathcal{LB}$, yielding

$$-\dot{r}_\epsilon(s) = e^{2K_-(s-s_{lin})}(-\dot{r}_\epsilon)(s_{lin}) + \int_{s_{lin}}^s e^{2K_-(s-s')} (8|B|^2 \omega_{RN}^2 r_- \epsilon + J_\Omega(s') + \tilde{J}_\Omega(s')) ds'.$$

One may then simply compute the relevant integrals to find that

$$\left| -\dot{r}_\epsilon - \frac{8|B|^2 \omega_{RN}^2 r_- \epsilon}{2K_-} \right| \lesssim \epsilon^{-1} \Omega^2 + \epsilon^3 s.$$

But for $s \geq s_O$, we know $\Omega^2 \lesssim \epsilon^{100}$, and (7.14) follows immediately. \square

7.2 The measure of the set E_η

We now use Proposition 7.1, or more precisely Corollary 7.2, to control the measure of the set of values of ϵ such that condition (\dagger) holds. Let $\epsilon_0(M, \mathbf{e}, \Lambda, m^2, q_0) > 0$ be such that the results of Section 6 hold for $0 < |\epsilon| < \epsilon_0$. Then we have the following corollary:

Corollary 7.3. Let $\eta > 0$ be a sufficiently small constant. We define E_η to be the set of ϵ such that the hairy black hole interior corresponding to $\phi = \epsilon$ on \mathcal{H} obeys the condition (\dagger) at $s = s_i$:

$$E_\eta = \{\epsilon \in (0, \epsilon_0) : |\Psi_i| \geq \eta\}. \quad (7.33)$$

Then the set E_η is non-empty, has 0 as a limit point, and we have the following upper bound for the limiting density of values of ϵ violating (\dagger) : there exists some constant K such that

$$\limsup_{\tilde{\epsilon} \downarrow 0} \tilde{\epsilon}^{-1} |(0, \tilde{\epsilon}) \setminus E_\eta| \leq K \mathfrak{W} \eta. \quad (7.34)$$

Proof. We will estimate the measure of the set $F_{\eta, \tilde{\epsilon}} = (0, \tilde{\epsilon}) \setminus E_\eta = \{\epsilon \in (0, \tilde{\epsilon}) : |\Psi_i| < \eta\}$. We first use Corollary 6.4 to change variable from ϵ to $\tilde{\Theta} = \Theta(\epsilon)$. For ϵ_0 and η sufficiently small,

$$\begin{aligned} |F_{\eta, \tilde{\epsilon}}| &= \int_0^{\tilde{\epsilon}} \mathbb{1}_{\{|\Psi_i| < \eta\}} d\epsilon \\ &\leq \int_0^{\tilde{\epsilon}} \mathbb{1}_{\{|\sin(\Theta(\epsilon))| < \sqrt{\pi} \mathfrak{W} \eta\}} d\epsilon \\ &= \int_{\Theta(\tilde{\epsilon})}^{+\infty} \mathbb{1}_{\{|\sin \tilde{\Theta}| < \sqrt{\pi} \mathfrak{W} \eta\}} \left| \frac{d}{d\epsilon} \Theta(\epsilon) \right|_{\epsilon=\Theta^{-1}(\tilde{\Theta})}^{-1} d\tilde{\Theta}. \end{aligned}$$

We now apply Corollary 7.2 along with the previous estimate (7.2) for $\Theta(\epsilon)$. This will yield:

$$\frac{d}{d\epsilon} \Theta(\epsilon) = -4\sqrt{2}|B| \mathfrak{W} \Theta(\epsilon)^{3/2} + O(\Theta^{1/2} \log \Theta). \quad (7.35)$$

Combining with the above, we therefore see that

$$|F_{\eta, \tilde{\epsilon}}| \leq \int_{\Theta(\tilde{\epsilon})}^{+\infty} \mathbb{1}_{\{|\sin \tilde{\Theta}| < \sqrt{\pi} \mathfrak{W} \eta\}} \frac{1}{4|B| \mathfrak{W}} \tilde{\Theta}^{-3/2} d\tilde{\Theta}.$$

To evaluate this integral, note that if η is taken sufficiently small, then the set $\{|\sin \Theta| < \sqrt{\pi} \mathfrak{W} \eta\}$ is simply a union of intervals of width $2\sqrt{\pi} \mathfrak{W} \eta + O(\eta^2)$ and centered on the integer lattice $\pi\mathbb{Z}$. So the integral is akin to taking a discrete sum of the form $\sum_{n=\Theta(\tilde{\epsilon})}^{+\infty} \frac{\eta}{n^{3/2}}$, multiplied by appropriate weights. Keeping only the weights $|B|$ and \mathfrak{W} which depend on the background parameters, we have

$$|F_{\eta, \tilde{\epsilon}}| \lesssim |B|^{-1} \Theta(\tilde{\epsilon})^{-1/2} \eta \lesssim \mathfrak{W} \eta \tilde{\epsilon}, \quad (7.36)$$

using (7.2) again in the last step. This yields (7.34), and the remainder of the corollary follows easily. \square

Remark 7.1. Recalling Theorem 3.2, as well as studying the values of ϵ obeying (\dagger) , we also need to investigate the measure of the set of values of ϵ obeying the ‘bounce’ condition $\eta \leq |\Psi_i| \leq 1 - \sigma$ or the ‘non-bounce’ condition

$|\Psi_i| \geq 1 + \sigma$. This can be done in the same way as the proof of Corollary 7.3.

8 Kasner regimes and bounces

Now, assuming the condition (\dagger) , i.e that ϵ lies in E_η as defined in Theorem 3.1, we will complete the proof of Theorem 3.1. In particular, we claim there exists some $\epsilon_0(\eta) > 0$ depending on η as well as the usual parameters M, e, Λ, m^2, q_0 , such that if $0 < \epsilon \leq \epsilon_0 = \epsilon_0(\eta)$ **and** (\dagger) holds, then our corresponding hairy black hole interior contains a crushing spacelike singularity, with more quantitative Kasner-like asymptotics to follow.

Firstly, we briefly describe the expected dynamics between the end of the region \mathcal{PK} and the eventual spacelike singularity at $s = s_\infty$. It turns out the intermediate dynamics will be highly sensitive to the value of $\Psi(s_i)$, often denoted as Ψ_i in the sequel, where $\Psi(s)$ is given by (7.1).

Following the discussion of the introduction, particularly Section 1.5, if $|\Psi_i| > 1$, then the region $\mathcal{PK}' \subset \mathcal{PK}$ (see Corollary 6.4) should already lie in a regime associated with positive Kasner exponents. For ϵ sufficiently small, we will show that many of the estimates of Proposition 6.1 will persist all the way to the spacelike singularity $\{s = s_\infty\}$, meaning a single (stable) Kasner-like regime.

On the other hand, if $\eta \leq |\Psi_i| < 1$, then initially, the spacetime lies in a regime associated with one negative and two positive Kasner exponents – known to be unstable in the cosmological setting. In this case, we shall observe the aforementioned *Kasner bounce* phenomenon. In simplified terms, between $s = s_i$ and $s = s_\infty$, the quantity Ψ will *invert* from its initial value $\Psi_i = \Psi(s_i)$ to a final value $\Psi_f \approx \Psi_i^{-1}$ satisfying $|\Psi_f| > 1$. The spacetime in turn evolves into a regime associated with positive Kasner exponents, which in turn persists up to the singularity.

The cause and nature of such Kasner bounces, as well as why this allows for spacelike singularity formation, will be the focus of this section. Denote by \mathcal{K} the region $\{s \geq s_i\} = \{s : r(s) \leq e^{-\delta_0 \epsilon^{-2}} r_-\}$. The section will be organized as follows:

- In Section 8.1, we give further background into why we distinguish between $|\Psi| < 1$ and $|\Psi| > 1$, and hence the need to study Kasner bounces. We will also introduce new renormalized quantities and the equations that they obey.
- In Section 8.2, we state the main Proposition 8.1 regarding the quantity Ψ in the region \mathcal{K} . We then state the main bootstrap assumptions used in this proof, and prove some preliminary results used in the proof of Proposition 8.1.
- In Section 8.3, we provide the proof of Proposition 8.1. This will entail a detailed estimate for all the error terms involved in deriving an ODE of the form (1.33). Once completed, this proof shows that the spacetime will exist up to a spacelike singularity at some $s = s_\infty$ with $r(s_\infty) = 0$.
- In Section 8.4, we apply our results regarding Ψ in Proposition 8.1 to find quantitative estimates on geometric quantities such as Ω^2 . This will be crucial in showing quantitative closeness to Kasner spacetimes in Section 9.

8.1 Background on Kasner bounces

In this section, we briefly explore the important role played by the quantity Ψ , and the differing evolutionary dynamics that occur when $|\Psi_i| = |\Psi(s_i)|$ is greater than or less than 1. The two key equations are the evolution equation (2.40) for $-r\dot{r}$ and the Raychaudhuri equation (2.36). It will be useful to rewrite (2.36) as an evolution equation for $\log(\Omega^2/(-\dot{r}))$, and express the first term on the right hand side in terms of the quantity Ψ :

$$\frac{d}{ds} \log \left(\frac{\Omega^2}{-\dot{r}} \right) = \frac{\dot{r}}{r} \Psi^2 + \frac{r^2}{r\dot{r}} |\tilde{A}|^2 q_0^2 |\phi|^2. \quad (8.1)$$

Supposing for now that the rightmost term is integrable and small, one sees that the value of Ψ^2 determines the leading order behavior of Ω^2 in r . Letting $\alpha^2 = \inf \Psi^2$ and $\beta^2 = \sup \Psi^2$ in our region of interest, integrating (8.1) gives:

$$C_{lower} r^{\beta^2} \leq \frac{\Omega^2}{-\dot{r}} \leq C_{upper} r^{\alpha^2}. \quad (8.2)$$

For this heuristic discussion, it is only important to note that C_{lower} and C_{upper} are independent of r , indeed the important feature will be the powers of r .

In light of (8.2), we turn to the evolution equation for $-r\dot{r}(s)$ written above. Inside a region such as \mathcal{K} where r is small, one expects that the dominant term on the right hand side is the term $\frac{Q^2 \Omega^2}{4r^2}$, and (8.2) will yield upper and lower bounds of the form:

$$-C_{lower} r^{\beta^2-2\dot{r}} \lesssim -\frac{d}{ds}(-r\dot{r}) \lesssim -C_{upper} r^{\alpha^2-2\dot{r}}. \quad (8.3)$$

Integrating this expression, and ignoring the degenerate case where α or β are equal to 1, we have

$$|r^{\beta^2-1}(s) - r^{\beta^2-1}(s_i)| \lesssim r\dot{r}(s) - r\dot{r}(s_i) \lesssim |r^{\alpha^2-1}(s) - r^{\alpha^2-1}(s_i)|. \quad (8.4)$$

We can therefore make two observations:

- If $\beta < 1$, then $|r(s)^{\beta^2-1} - r(s_i)^{\beta^2-1}|$ is unbounded as $r(s) \rightarrow 0$, which suggests that $-r\dot{r}$ is unbounded. In fact, since this suggests $r\dot{r}(s)$ will at some point become positive, we have somehow exited the trapped region. So something must have gone wrong, either in our a priori assumptions or in assuming that $\beta < 1$. In our context, we shall show the latter issue arises; there must be a ‘bounce’ which forces $\beta \geq 1$.
- If $\alpha > 1$, then $|r(s)^{\alpha^2-1} - r(s_i)^{\alpha^2-1}|$ is bounded by a multiple of $r(s_i)^{\alpha^2-1}$, which in our case has order of magnitude $O(e^{-(\alpha-1)\delta_0\epsilon^{-2}}) \ll -r\dot{r}(s_i)$. So $-r\dot{r}$ changes little from its value at $s = s_i$. The insight is that if $\Psi(s_i) > 1$ initially, then there is a hope of closing estimates in a bootstrap argument, such that $-r\dot{r}$ only changes by this extremely small quantity, and thus allows for formation of a spacelike singularity.

In what follows, we formalize these observations in a quantitative manner, in order to obtain more *quantitative information* on the behavior of spacetime, both in cases when a bounce occurs, and when it does not.

8.2 The bootstraps, preliminary estimates and statement of Proposition 8.1

In this section, we state and initiate the proof of Proposition 8.1. As well as asserting the eventual formation of an $r = 0$ spacelike singularity, the key content of this proposition is that we can control the quantity $\Psi(s)$ via

a certain nonlinear ODE – which, as we show in Section 8.4, in turn allows us to control the other geometric quantities including $\Omega^2(s)$.

Proposition 8.1. Fix some $\eta \in \mathbb{R}$ with $0 < \eta < \min\{\frac{1}{2}\mathfrak{M}, \frac{1}{4}\}$. Then there exists some $\epsilon_0(\eta) > 0$ depending on η as well as the usual parameters $M, \mathbf{e}, \Lambda, m^2, q_0$, such that if both

$$0 < \epsilon \leq \epsilon_0(\eta) \quad \text{and} \quad |\Psi_i| := |\Psi(s_i)| \geq \eta, \quad (*)$$

then the solution of the system (2.36)–(2.46) exists in the interval $s \in (-\infty, s_\infty)$, with $s_i < s_\infty < +\infty$ and $r(s) \rightarrow 0$ as $s \rightarrow s_\infty$. In fact, for $s \in \mathcal{K} = \{s \geq s_i : r(s) > 0\}$, one obtains the following bounds on $-r\dot{r}(s)$.

$$-r\dot{r}(s) \geq 2|B|^2\mathfrak{M}^2r_-^2\omega_{RN}\eta^2\epsilon^2, \quad -r\dot{r}(s) \leq 8|B|^2\mathfrak{M}^2r_-^2\omega_{RN}\epsilon^2. \quad (8.5)$$

Regarding the quantity Ψ defined in (7.1), there exists some constant $D_K(\eta, M, \mathbf{e}, \Lambda, m^2, q_0) > 0$, a real number $\alpha = \alpha(\epsilon)$ and a function $\mathcal{F}(s)$ satisfying:

$$|\alpha - \Psi_i| \leq D_K \exp(-\delta_0\epsilon^{-2}), \quad |\mathcal{F}(s)| \leq D_K \exp(-\delta_0\epsilon^{-2})r(s) = D_K r_- e^{-\delta_0\epsilon^{-2}-R},$$

where we define $R = \log(r_-/r(s))$, so that $\Psi = \Psi(R)$ satisfies the following ODE in the region \mathcal{K} :

$$\frac{d\Psi}{dR} = -\Psi(\Psi - \alpha) \left(\Psi - \frac{1}{\alpha} \right) + \mathcal{F}. \quad (8.6)$$

Finally, one has the following upper and lower bounds for $|\Psi(s)|$ for $s \in \mathcal{K}$:

$$\min\{|\Psi_i|, |\Psi_i^{-1}|\} - D_K e^{-\delta_0\epsilon^{-2}} \leq |\Psi(s)| \leq \max\{|\Psi_i|, |\Psi_i^{-1}|\} + D_K e^{-\delta_0\epsilon^{-2}}. \quad (8.7)$$

Remark. We use the same notation $D_K = D_K(\eta, M, \mathbf{e}, \Lambda, m^2, q_0) > 0$ throughout the various lemmas and propositions of Section 8. Note that it is possible to track the dependence of D_K , and any constants implied by the notation \lesssim , on η , and thereby strengthen the result from having a fixed η in $(*)$ to allowing $\eta = \eta(\epsilon)$ to decay as $\epsilon \rightarrow 0$, for instance $\eta = \epsilon^{0.01}$. However, for the purpose of simpler exposition, we do not pursue that here.

The proof of Proposition 8.1 will be broken into several lemmas in Sections 8.2 and 8.3. We first list the three main bootstrap assumptions of the region \mathcal{K} :

$$|\Psi| \leq 4\eta^{-1}, \quad (\text{K1})$$

$$-r\dot{r}(s) \geq |B|^2\mathfrak{M}^2r_-^2\omega_{RN}\eta^2\epsilon^2, \quad (\text{K2})$$

$$\frac{|Q_\infty|}{2} \leq |Q(s)| \leq 2|Q_\infty|. \quad (\text{K3})$$

Here, $Q_\infty = Q_\infty(M, \mathbf{e}, \Lambda) \neq 0$ is defined in (5.13); by Lemma 5.7, Q_∞ lies strictly between $\mathbf{e}/2$ and \mathbf{e} . In light of Proposition 6.1 and Corollary 6.4, these bootstrap assumptions hold in a neighborhood of $s = s_i$.

In the remainder of Section 8.2, we state and prove two preliminary lemmas, the first of which provides estimates for the Maxwell quantities $\tilde{A}(s)$ and $Q(s)$, as well as the scalar field $\phi(s)$. The second lemma then produces a crucial lower bound for $|\Psi|$ as well as a useful preliminary upper bound on $\Omega^2(s)$.

Lemma 8.2. Assuming the bootstraps (K1), (K2), (K3), we have the following preliminary estimates on ϕ as

well as the Maxwell quantities Q and \tilde{A} :

$$|\phi(s)| \leq 2\eta^{-1} \log \left(\frac{8|B|^2 \mathfrak{W}^2 r_-^2 \epsilon^2}{r^2(s)} \right), \quad (8.8)$$

$$|Q(s) - Q(s_i)| \leq D_K \exp(-\delta_0 \epsilon^{-2}), \quad (8.9)$$

$$||q_0 \tilde{A}(s) - \omega_{RN}| \leq D_K \epsilon^2. \quad (8.10)$$

In particular, using (8.9), we immediately improve the bootstrap assumption (K3).

Lemma 8.3. Assuming the bootstraps (K1), (K2), (K3), we have the following upper bound on $-r\dot{r}$ and estimate on $r^2 \dot{\phi}$ which we use to get a corresponding lower bound on $|\Psi|$:

$$-r\dot{r}(s) \leq 4|B|^2 \mathfrak{W}^2 \omega_{RN} r_-^2 \epsilon^2 + D_K \epsilon^4 \log(\epsilon^{-1}), \quad (8.11)$$

$$\left| \frac{r^2 \dot{\phi}(s)}{r^2 \dot{\phi}(s_i)} - 1 \right| \leq D_K \exp(-\delta_0 \epsilon^{-2}), \quad (8.12)$$

$$|\Psi| \geq \eta - D_K \exp(-\delta_0 \epsilon^{-2}). \quad (8.13)$$

In particular, Ψ will never vanish, and thus never change sign, in the region \mathcal{K} . Moreover, we have the following initial upper bound for $\Omega^2(s)$:

$$\frac{\Omega^2}{-\dot{r}}(s) \leq \frac{\Omega^2}{-\dot{r}}(s_i) \leq \exp(-50\delta_0 \epsilon^{-2}). \quad (8.14)$$

Proof of Lemma 8.2. To prove the preliminary bound on ϕ , recall that we may rewrite Ψ as $-r \frac{d\phi}{dr}$. So we use (K1) as follows:

$$|\phi(s) - \phi(s_i)| \leq \int_{r(s)}^{r(s_i)} \frac{|\Psi(r)|}{r} dr \leq 4\eta^{-1} \log \left(\frac{r(s_i)}{r(s)} \right) \leq 2\eta^{-1} \log \left(\frac{r^2(s_i)}{r^2(s)} \right). \quad (8.15)$$

But, from (6.24) in Corollary 6.4,

$$|\phi(s_i)| \leq \frac{2}{\pi} C_{YK}(\epsilon) \mathfrak{W}^{-1} \log \left(\frac{r_-^2 \epsilon^2}{\xi_K r^2(s_i)} \right) + |c_1 C_{JK}(\epsilon)| + |c_2 C_{YK}(\epsilon)| \leq 2\eta^{-1} \log \left(\frac{8|B|^2 \mathfrak{W}^2 r_-^2 \epsilon^2}{r^2(s_i)} \right). \quad (8.16)$$

In the second step, we used $|C_{YK}(\epsilon)|, |C_{JK}(\epsilon)| \leq \sqrt{\pi} \mathfrak{W}$ from Propositions 5.5 and 6.1, as well as $\eta < \frac{1}{2} \mathfrak{W}$ and the definition (6.7). In particular, $r(s_i) = e^{-\delta_0 \epsilon^{-2}}$ is small enough that the contribution of $|c_1 C_{JK}(\epsilon)| + |c_2 C_{YK}(\epsilon)|$ is negligible. Combining the two inequalities (8.15) and (8.16) will clearly yield (8.8).

For the gauge field $\tilde{A}(s)$, we use the following trick: For $s \in \mathcal{K}$, we have $r(s) \leq \exp(-\delta_0 \epsilon^{-2}) r_- \leq \min \left\{ \frac{|Q_\infty|}{8}, \frac{1}{2\sqrt{|\Lambda|}} \right\}$, and $|m^2 r^2 |\phi|^2| < 1$ via (8.8), so

$$\frac{\Omega^2}{4} - \frac{\Omega^2 Q^2}{4r^2} - \frac{\Omega^2 r^2}{4} (m^2 |\phi|^2 + \Lambda) \leq -\frac{\Omega^2 Q^2}{8r^2}.$$

Thus, (2.40) tells us that $-r\dot{r}(s)$ is decreasing in \mathcal{K} , and one further has a bound on the integral

$$\int_{s_i}^s \frac{Q^2 \Omega^2}{4r^2}(\tilde{s}) d\tilde{s} \leq -2r\dot{r}(s_i). \quad (8.17)$$

Hence, using the lower bound of (K3) once more, the equation (2.44) yields

$$|q_0 \tilde{A}(s) - q_0 \tilde{A}(s_i)| \leq \int_{s_i}^s \frac{|Q| \Omega^2}{4r^2}(\tilde{s}) d\tilde{s} \leq \frac{2}{|Q_\infty|} \int_{s_i}^s \frac{Q^2 \Omega^2}{4r^2}(\tilde{s}) d\tilde{s} \leq \frac{-4r\dot{r}(s_i)}{|Q_\infty|}. \quad (8.18)$$

Thus, (6.3) and (6.4) of Proposition 6.1 allows one to deduce (8.10).

To close the estimate on Q , we simply integrate (2.43):

$$|Q(s) - Q(s_i)| \leq \int_{s_i}^s q_0^2 |\tilde{A}| r^2 |\phi|^2(\tilde{s}) d\tilde{s} \lesssim \int_{s_i}^s r^2(\tilde{s}) \log^2 \left(\frac{8|B|^2 \mathfrak{W}^2 r_-^2 \epsilon^2}{r^2(\tilde{s})} \right) d\tilde{s}. \quad (8.19)$$

But in the region \mathcal{K} , where $r(s) \leq e^{-\delta_0 \epsilon^{-2}} r_-$ and the interval of integration has length $|s - s_i| = O(\epsilon^{-2} e^{-2\delta_0 \epsilon^{-2}})$ by (K2), it is straightforward to determine (8.9) and improve the bootstrap (K3). \square

Proof of Lemma 8.3. The first estimate (8.11) is immediate by monotonicity. Indeed, as argued in the proof of Lemma 8.2, the quantity $-r\dot{r}(s)$ is decreasing in s . So the estimate (6.3) evaluated at $s = s_i$ yields (8.11).

For the lower bound on $|\Psi|$, we first produce the estimate (8.12) regarding $r^2 \dot{\phi}$. Using the monotonicity of $-\Omega^{-2} \dot{r}(s)$ from the Raychaudhuri equation (2.36), and Proposition 6.1, we first find the preliminary estimate

$$\frac{\Omega^2}{-\dot{r}}(s) \leq \frac{\Omega^2}{-\dot{r}}(s_i) \leq \frac{\Omega^2 r(s_i)}{-r\dot{r}(s_i)} \lesssim \exp(-50\delta_0 \epsilon^{-2}) \cdot \epsilon^{-2} \exp(-\delta_0 \epsilon^{-2}) \lesssim \exp(-50\delta_0 \epsilon^{-2}). \quad (8.20)$$

This is (8.14), and we use this together with (8.11) and the conclusions of Lemma 8.2 to yield from (2.46)

$$\left| \frac{d}{ds}(r^2 \dot{\phi})(s) \right| \lesssim \exp(-\delta_0 \epsilon^{-2}) \cdot r(s) \log \left(\frac{8|B|^2 \mathfrak{W}^2 r_-^2 \epsilon^2}{r^2(s)} \right) \lesssim \epsilon^2 \exp(-\delta_0 \epsilon^{-2}). \quad (8.21)$$

Integrating this up, and using once again that the interval of integration has length bounded by $O(\epsilon^{-2} e^{-2\delta_0 \epsilon^{-2}})$, we therefore find that

$$|r^2 \dot{\phi}(s) - r^2 \dot{\phi}(s_i)| \lesssim \exp(-3\delta_0 \epsilon^{-2}). \quad (8.22)$$

Finally, since $|\Psi(s_i)| \geq \eta$ and $-r\dot{r}(s_i)$ is bounded below using (5.18), we have $|r^2 \dot{\phi}(s_i)| = -r\dot{r}(s_i) \cdot |\Psi(s_i)| \gtrsim \epsilon^2$. Combining this with (8.22) we obtain (8.12).

Therefore, for ϵ sufficiently small, we see that

$$|\Psi(s)| = \frac{-r\dot{r}(s_i)}{-r\dot{r}(s)} \cdot \frac{r^2 \dot{\phi}(s)}{r^2 \dot{\phi}(s_i)} \cdot |\Psi(s_i)| \geq \eta - D_K \exp(-\delta_0 \epsilon^{-2}). \quad (8.23)$$

Here, we used (8.12) and that $-r\dot{r}(s)$ is decreasing for $s \in \mathcal{K}$, as well as the original assumption (*). \square

8.3 The dynamical system for Ψ and the proof of Proposition 8.1

In this section, we complete the proof of Proposition 8.1. The main step will be to find the ODE (8.6). For this purpose, we start with a lemma concerning the first and second derivatives of Ψ with respect to the timelike variable r .

Lemma 8.4. Assume that the bootstraps (K1), (K2), (K3) hold. If \mathcal{E} is defined such that

$$\frac{d\Psi}{dr} = \Psi \frac{1}{-r\dot{r}} \frac{\Omega^2}{-4\dot{r}} \left(1 - \frac{Q^2}{r^2} - m^2 r^2 |\phi|^2 - r^2 \Lambda \right) + \mathcal{E}, \quad (8.24)$$

then we have the following estimates in the region $s \in \mathcal{K}$:

$$|\mathcal{E}| \leq D_K \exp(-2\delta_0 \epsilon^{-2}) \cdot r, \quad \left| \frac{d\mathcal{E}}{dr} \right| \leq D_K \exp(-2\delta_0 \epsilon^{-2}) \cdot r^{-1}. \quad (8.25)$$

For the second derivative, if the error term \mathcal{F}_1 is defined such that

$$\frac{d^2\Psi}{dr^2} - 2\Psi^{-1} \left(\frac{d\Psi}{dr} \right)^2 - \frac{\Psi^2 - 2}{r} \frac{d\Psi}{dr} = \mathcal{F}_1, \quad (8.26)$$

then for $s \in \mathcal{K}$, the expression \mathcal{F}_1 satisfies the following bound:

$$\mathcal{F}_1 \leq D_K \exp(-2\delta_0 \epsilon^{-2}) r^{-1}. \quad (8.27)$$

Proof of Lemma 8.4. Assuming the bootstraps, the conclusions of Lemmas 8.2 and 8.3 will hold. In light of (2.40) and (2.46), differentiating Ψ in the variable r one yields:

$$\frac{d\Psi}{dr} = \frac{1}{\dot{r}} \frac{d\Psi}{ds} = \Psi \frac{1}{-r\dot{r}} \frac{\Omega^2}{-4\dot{r}} \left(1 - \frac{Q^2}{r^2} - m^2 r^2 |\phi|^2 - r^2 \Lambda \right) + \mathcal{E}, \quad (8.28)$$

where the error \mathcal{E} is given by

$$\mathcal{E} := \frac{1}{-r\dot{r}} \frac{d}{dr} (r^2 \dot{\phi}) = \frac{1}{-r\dot{r}} \left(\frac{q_0^2 |\tilde{A}|^2 r^3 \phi}{-r\dot{r}} + \frac{m^2 \Omega^2 r^2 \phi}{-4\dot{r}} \right). \quad (8.29)$$

We seek the estimates (8.25). Using Lemmas 8.2 and 8.3 together with (K2), it is straightforward to get

$$|\mathcal{E}| \lesssim \epsilon^{-4} r^3 \log \left(\frac{\epsilon^2}{\xi^* r^2} \right) + \exp(-2\delta_0 \epsilon^{-2}) \epsilon^{-2} r^2 \log \left(\frac{\epsilon^2}{\xi^* r^2} \right) \lesssim \exp(-2\delta_0 \epsilon^{-2}) r. \quad (8.30)$$

For the derivative estimate in (8.25), we simply differentiate the expression (8.29) term by term. This is rather cumbersome, and we simplify the exposition by merely considering the new multiplicative factors that arise when differentiating the various terms, noting that it is most crucial to keep track of the additional powers of r^{-1} that arise:

(i) Differentiating $(-r\dot{r})^{-1}$ in r will yield an extra multiplicative factor of

$$\frac{\Omega^2}{-4\dot{r}} \frac{1}{-r\dot{r}} \left(\frac{Q^2}{r^2} + m^2 r^2 |\phi|^2 + r^2 \Lambda - 1 \right).$$

Since $Q \neq 0$, this will contribute a multiplicative factor of r^{-2} . Note that though one could fear that additional powers of ϵ^{-1} will appear (e.g. in the $-r\dot{r}$ appearing in the denominator), these will be negated by the smallness of $\frac{\Omega^2}{-r\dot{r}}$, see (8.14).

(ii) Differentiating \tilde{A} in r will introduce a similar factor of

$$\frac{Q\Omega^2}{-4r^2\dot{r}}$$

which we treat in exactly the same way as (i).

(iii) Differentiating ϕ in r simply yields

$$\frac{d\phi}{dr} = -\Psi r^{-1},$$

so that in light of bootstrap (K1) providing an upper bound on $|\Psi|$, differentiating this term contributes only one power of r^{-1} .

(iv) Differentiating the $\frac{\Omega^2}{4r}$ in the second term of (8.29) introduces, by the Raychaudhuri equation (8.1), an extra multiplicative factor of

$$\frac{r}{\dot{r}^2}(|\dot{\phi}|^2 + q_0^2|\tilde{A}|^2\phi^2) = \frac{\Psi^2}{r} + \frac{r^3q_0^2|\tilde{A}|^2\phi^2}{(-r\dot{r})^2} \leq \frac{\Psi^2}{r} + 1,$$

where we used the bootstrap (K2) and Lemma 8.2. So differentiating this term contributes at worst one power of r^{-1} .

(v) Finally, differentiating any powers of r that arise in (8.29) will trivially only lose one power of r .

From (i)–(v) we get the estimate (8.25).

Due to (8.25), (8.8), (8.14) and the bootstrap assumptions, (8.24) yields the upper bound

$$\left| \frac{d\Psi}{dr} \right| \leq D_K \exp(-50\delta_0\epsilon^{-2})r^{-2} + D_K \exp(-2\delta_0\epsilon^{-2})r \leq D_K \exp(-5\delta_0\epsilon^{-2})r^{-2}. \quad (8.31)$$

We now treat the second derivative. We differentiate the expression (8.24) again in r , and find

$$\begin{aligned} \frac{d^2\Psi}{dr^2} &= \Psi^{-1} \left(2\frac{d\Psi}{dr} - \mathcal{E} \right) \left(\frac{d\Psi}{dr} - \mathcal{E} \right) + \left(\frac{d\Psi}{dr} - \mathcal{E} \right) \left(\frac{\Psi^2}{r} + \frac{r}{\dot{r}^2}q_0^2|\tilde{A}|^2\phi^2 \right) \\ &\quad + \left(\frac{d\Psi}{dr} - \mathcal{E} \right) \frac{d}{dr} \log \left| 1 - \frac{Q^2}{r^2} - m^2r^2\phi^2 - r^2\Lambda \right| + \frac{d\mathcal{E}}{dr}. \end{aligned} \quad (8.32)$$

To explain the derivation of the equation (8.32), we take (8.24), subtract \mathcal{E} from both sides, take a logarithm, and then finally differentiate, to write

$$\frac{d}{dr} \log \left| \frac{d\Psi}{dr} - \mathcal{E} \right| = \frac{d}{dr} \left(\log |\Psi| - \log(-r\dot{r}) + \log \left(\frac{\Omega^2}{-4\dot{r}} \right) + \log \left| 1 - \frac{Q^2}{r^2} - m^2r^2\phi^2 - r^2\Lambda \right| \right),$$

from which (8.32) follows after using the usual evolution equations (2.40) and (8.1).

We now wish to recover the ODE (8.26) along with (8.27) i.e. we just need to show that all error terms present within (8.32) are bounded by $\exp(-\delta_0\epsilon^{-2})r^{-1}$. This is mostly straightforward by (8.25) and (8.31), with the most complicated term being the one involving the log.

Firstly, using (8.31) and (8.25) as well as the lower bound (8.13) for $|\Psi|$, we see that

$$\left| \Psi^{-1} \left(2\frac{d\Psi}{dr} - \mathcal{E} \right) \left(\frac{d\Psi}{dr} - \mathcal{E} \right) - 2\Psi^{-1} \left(\frac{d\Psi}{dr} \right)^2 \right| \lesssim \exp(-2\delta_0\epsilon^{-2})r^{-1}. \quad (8.33)$$

Next, note that by (8.11), (8.8) and (8.10), the expression involving ϕ^2 can be bounded by

$$\frac{r}{\dot{r}^2} q_0^2 |\tilde{A}|^2 \phi^2 \lesssim \epsilon^{-4} r^3 \log(r^{-1}) \leq \exp(-\delta_0 \epsilon^{-2}) r^2 \leq \exp(-2\delta_0 \epsilon^{-2}) r,$$

from which we may also deduce

$$\left| \left(\frac{d\Psi}{dr} - \mathcal{E} \right) \left(\frac{\Psi^2}{r} + \frac{r}{\dot{r}^2} q_0^2 |\tilde{A}|^2 \phi^2 \right) - \frac{\Psi^2}{r} \frac{d\Psi}{dr} \right| \lesssim \exp(-2\delta_0 \epsilon^{-2}) r^{-1}. \quad (8.34)$$

We now move onto the more tedious term involving $\frac{d}{dr} \log(\cdots)$. Computing the derivative using the system of equations (2.36)–(2.46) one eventually finds

$$\frac{d}{dr} \log \left| 1 - \frac{Q^2}{r^2} - m^2 r^2 \phi^2 - r^2 \Lambda \right| = -\frac{2}{r} \frac{1-f}{1-g},$$

where the expressions f and g are given by

$$f = \frac{r^3}{Q^2} \left(-\frac{Q \tilde{A} q_0^2 \phi^2}{-\dot{r}} + m^2 r \phi^2 - m^2 r \phi \Psi + r \Lambda \right),$$

$$g = \frac{r^2}{Q^2} \cdot (1 - m^2 r^2 \phi^2 - r^2 \Lambda).$$

Using the bootstraps along with Lemmas 8.2 and 8.3, it is straightforward to deduce that $|f| + |g| \lesssim r^2$. The conclusion of this computation is therefore that

$$\left| \frac{d}{dr} \log \left| 1 - \frac{Q^2}{r^2} - m^2 r^2 \phi^2 \right| + \frac{2}{r} \right| \lesssim r, \quad (8.35)$$

which along with (8.31) and (8.25) finally yields the required estimate

$$\left| \left(\frac{d\Psi}{dr} - \mathcal{E} \right) \frac{d}{dr} \log \left| 1 - \frac{Q^2}{r^2} - m^2 r^2 \phi^2 \right| + \frac{2}{r} \frac{d\Psi}{dr} \right| \lesssim \exp(-2\delta_0 \epsilon^{-2}) r^{-1}. \quad (8.36)$$

The desired equation (8.26) is then found by combining the identity (8.32) with the estimates (8.33), (8.34), (8.36) and (8.25) to get the required error term \mathcal{F}_1 satisfying (8.27). \square

We have now finished all the preparation for the proof of Proposition 8.1. Before turning to the actual proof below, we first give a brief sketch for the benefit of the reader. After changing variables to $R = \log(r_-/r(s))$, we may integrate up the second-order ODE (8.26) to derive a first-order ODE of a similar form to (8.6). More precisely, one finds an equation of the form

$$-r \frac{d\Psi}{dr} = \frac{d\Psi}{dR} = -\Psi(\Psi^2 - K\Psi + 1) + \text{error}, \quad (8.37)$$

where the expression K appearing here is a constant of integration. By evaluating (8.37) at $s = s_i$ we find that $K \approx \Psi_i + \Psi_i^{-1}$.

We treat (8.37) as a one-dimensional dynamical system for the unknown $\Psi = \Psi(R)$, and consider what happens as $r \rightarrow 0$, i.e. $R \rightarrow +\infty$. Assuming the error to be negligible, the dynamical system (8.37) will prohibit Ψ from growing too large – in particular allowing us to improve the bootstrap (K1). This, in turn, will allow us

to improve the bootstrap (K2) due to the definition of Ψ and the upper bound on $r^2 \dot{\phi}$ from (8.12). Recall also that bootstrap (K3) has already been improved in Lemma 8.2.

Having improved all the bootstraps, the lower bound (K2) allows us to continue the solution all the way to some $s = s_\infty$ with $r(s_\infty) = 0$. To obtain (8.6), we again integrate up the second-order ODE (8.26), but by determining the constant of integration K teleologically at $R = +\infty$ (i.e. $r \rightarrow 0$), we get the precise bound for the error term \mathcal{F} as in Proposition 8.1.

Finally, some soft arguments using known upper and lower bounds for $|\Psi|$ will allow us to determine that $K \geq 2$, so that, writing $K = \alpha + \alpha^{-1}$, we get the required ODE (8.6). The remaining assertions are then straightforward. We now make this argument precise.

Proof of Proposition 8.1. Performing the change of variables $R = \log(r_-/r(s)) = \log r_- - \log r(s)$ on (8.26), one finds the ODE

$$\frac{d^2 \Psi}{dR^2} - 2\Psi^{-1} \left(\frac{d\Psi}{dR} \right)^2 + (\Psi^2 - 1) \frac{d\Psi}{dR} = r^2 \mathcal{F}_1. \quad (8.38)$$

Multiplying by the integrating factor Ψ^{-2} , we write the left hand side as a total derivative:

$$\frac{d}{dR} \left(\Psi^{-2} \frac{d\Psi}{dR} + \Psi + \frac{1}{\Psi} \right) = \Psi^{-2} r^2 \mathcal{F}_1. \quad (8.39)$$

Due to (8.13) and (8.27), the right hand side of (8.39) can be bounded by $4 D_K \eta^{-2} \exp(-2\delta_0 \epsilon^{-2}) r \leq \exp(-\delta_0 \epsilon^{-2}) e^{-R}$. So this error is integrable as $R \rightarrow +\infty$, and we proceed by integrating up (8.39).

For now, we can only integrate (8.39) in a finite bootstrap region; for $R_0 > R_i := \log(r_-/r(s_i)) = \delta_0 \epsilon^{-2}$ lying in our bootstrap region, there exists a constant of integration K_{R_0} and an error term $\mathcal{F}_{R_0}(R)$, such that, for $R \in [R_i, R_0]$, the following holds:

$$\Psi^{-2} \frac{d\Psi}{dR} + \Psi - K_{R_0} + \frac{1}{\Psi} = \mathcal{F}_{R_0}(R). \quad (8.40)$$

The choice of K_{R_0} is made such that $\mathcal{F}_{R_0}(R_0) = 0$ and hence from the aforementioned bound on \mathcal{F}_1 , one has $\mathcal{F}_{R_0}(R) \leq \exp(-\delta_0 \epsilon^{-2}) e^{-R}$. We also rewrite the above in the form

$$\frac{d\Psi}{dR} = -\Psi(\Psi^2 - K_{R_0} \Psi + 1) + \Psi^2 \mathcal{F}_{R_0}. \quad (8.41)$$

In order to proceed, we must estimate the constant of integration K_{R_0} . For this purpose, we evaluate (8.40) at $R = R_i$, and then apply Proposition 6.1 ((6.2) specifically). This proposition, together with (8.24), will give

$$\left| \Psi^{-2} \frac{d\Psi}{dR}(R_i) \right| \leq \exp(-2\delta_0 \epsilon^{-2}),$$

so that, when evaluating (8.40) at $R = R_i$, one finds the estimate

$$\left| K_{R_0} - \Psi_i - \frac{1}{\Psi_i} \right| \leq 2 \exp(-2\delta_0 \epsilon^{-2}). \quad (8.42)$$

In particular, for ϵ chosen sufficiently small one can get the key upper bound $|K_{R_0}| \leq \frac{5}{3} \eta^{-1}$. Here we used the estimate (6.26) at $s = s_i$ in Corollary 6.4 and that we chose $\eta \leq \min\{\frac{1}{2}\mathfrak{W}, \frac{1}{4}\}$, as well as $\pi^{-\frac{1}{2}} < \frac{2}{3}$. We can use this to improve the bootstraps (K1) and (K2). We first improve the upper bound (K1) on $|\Psi|$; we prove

$|\Psi| \leq \frac{5}{3}\eta^{-1}$. Without loss of generality, suppose that Ψ , and hence K_{R_0} , are positive for $s \in \mathcal{K}$, and suppose for contradiction that $\sup_{s \in \mathcal{K}} \Psi > \frac{5}{3}\eta^{-1}$.

So we may choose R_1 to be $R_1 = \inf\{R > R_i : \Psi(R) = \frac{5}{3}\eta^{-1}\}$. This trivially implies that $\frac{d\Psi}{dR}(R_1) \geq 0$. However, looking at (8.41) for any $R_0 \geq R_1$ we get

$$\frac{d\Psi}{dR}(R_1) = -\left(\frac{5}{3}\eta^{-1}\right)^2 \left(\frac{5}{3}\eta^{-1} - K_{R_0}\right) - \frac{5}{3}\eta^{-1} + \Psi^2 \mathcal{F}_{R_0}(R_1) < 0,$$

where the final step follows from $K_{R_0} \leq \frac{5}{3}\eta^{-1}$ and $\Psi^2 |\mathcal{F}_{R_0}(R_1)| \leq \Psi^2 \exp(-2\delta_0 \epsilon^{-2}) \leq \eta^{-1}$ for ϵ small. This is a contradiction, and thus ensures that $\sup_{s \in \mathcal{K}} |\Psi(s)| \leq \frac{5}{3}\eta^{-1}$. This improves the bootstrap (K1).

For the remaining bootstrap (K2), we combine the above with the estimate (8.12). To be precise, we have

$$-r\dot{r}(s) = -r\dot{r}(s_i) \cdot \frac{\Psi(s_i)}{\Psi(s)} \cdot \frac{r^2 \dot{\phi}(s)}{r^2 \dot{\phi}(s_i)} \geq \frac{3}{5}\eta^2 \cdot (-r\dot{r}(s_i)) \cdot \frac{r^2 \dot{\phi}(s)}{r^2 \dot{\phi}(s_i)}. \quad (8.43)$$

Thus, upon using Proposition 6.1 and (8.12), one finds (with D_K made larger if necessary) the lower bound

$$-r\dot{r}(s) \geq \frac{3}{5}\eta^2 \cdot [4|B|^2 \mathfrak{M}^2 \omega_{RN} r_-^2 \epsilon^2 - D_K \epsilon^4 \log(\epsilon^{-1})], \quad (8.44)$$

which clearly improves (K2) for ϵ sufficiently small. So the bootstrap argument is complete, and in light of (8.44), we conclude that the spacetime extends all the way to $r = 0$, i.e. $R = +\infty$.

To find the final one-dimensional dynamical system (8.6) we require a argument involving taking limits. Consider the identity (8.40); another consequence is that for $R_0 > R_1 \geq R_i$,

$$|K_{R_0} - K_{R_1}| = |\mathcal{F}_{R_0}(R_1)| \leq e^{-\delta_0 \epsilon^{-2}} e^{-R_1}.$$

In particular, if $(R_n)_{n \in \mathbb{N}}$ is a sequence with $R_n \rightarrow +\infty$, then the sequence $(K_{R_n})_{n \in \mathbb{N}}$ is Cauchy, and the limit is independent of the sequence taken. So there exists some $K \in \mathbb{R}$ such that $K_R \rightarrow K$ as $R \rightarrow +\infty$, which by (8.42) also satisfies

$$|K - \Psi_i - \Psi_i^{-1}| \leq 2 \exp(-2\delta_0 \epsilon^{-2}). \quad (8.45)$$

Hence we may take the limit in equation (8.41) where we fix R and take $R_0 \rightarrow +\infty$. We find that there will exist some function \mathcal{F} with $\Psi^2 \mathcal{F}_{R_0}(R) \rightarrow \mathcal{F}(R)$ as $R_0 \rightarrow +\infty$, also satisfying $|\mathcal{F}| \leq D_K e^{-\delta_0 \epsilon^{-2}} e^{-R}$, such that one has

$$\frac{d\Psi}{dR} = -\Psi(\Psi^2 - K\Psi + 1) + \mathcal{F}. \quad (8.46)$$

By construction, K has the same sign as $\Psi(s)$ in \mathcal{K} . We argue now that $|K| \geq 2$. Suppose otherwise that $|K| < 2$, which implies that $\Psi^2 - K\Psi + 1$ is bounded below by a positive constant β . Then (8.46) implies that

$$\frac{d|\Psi|}{dR} \leq -\beta|\Psi| + |\mathcal{F}|.$$

We then apply Grönwall's inequality, finding that

$$|\Psi(R)| \leq e^{-\beta(R-R^*)} |\Psi(R^*)| + \int_{R^*}^R e^{-\beta(R-\tilde{R})} |\mathcal{F}(\tilde{R})| d\tilde{R} \xrightarrow{R \rightarrow +\infty} 0.$$

But this is a contradiction to the lower bound (8.13)! Hence $|K| \geq 2$, and we may write $K = \alpha + \alpha^{-1}$ for some $\alpha \in \mathbb{R}$. By $|K| \leq \frac{5}{3}\eta^{-1}$, it is clear that $|\alpha| \leq \frac{5}{3}\eta^{-1}$ also. From (8.45), we can deduce that

$$|(\alpha - \Psi_i)(\alpha - \Psi_i^{-1})| \lesssim \exp(-2\delta_0\epsilon^{-2})\eta^{-1} \lesssim \exp(-2\delta_0\epsilon^{-2}),$$

so, interchanging $\alpha \leftrightarrow \alpha^{-1}$ if necessary, we may choose α accordingly such that $|\alpha - \Psi_i| \lesssim \exp(-\delta_0\epsilon^{-2})$ as required. Therefore, we have arrived at the ODE (8.6).

For the final statement in Proposition 8.1, note that the upper bound follows from rather straightforward analysis of this ODE, while the lower bound arises from a straightforward modification from the proof of (8.13) in Lemma 8.3. \square

8.4 Geometric features of the region \mathcal{K} in the bounce case $|\Psi_i| < 1$

In this section, we make use of Proposition 8.1 to derive more quantitative information regarding the quantities $r(s)$ and $\Omega^2(s)$ in the region $s \in \mathcal{K}$, focusing for now on the interesting case where $|\Psi_i| < 1$ and there is a Kasner bounce. In particular, we will estimate the value of $r(s)$ where the bounce occurs, and bound $\Omega^2(s)$ in such a way that we can infer quantitative closeness to Kasner-like spacetimes before and after the bounce.

To make precise statements about the closeness of these regions to Kasner-like geometries, we will have to assume further that Ψ_i , and therefore the quantities α and α^{-1} of Proposition 8.1, are bounded strictly away from 1 in absolute value, where several important quantities will begin to degenerate²¹.

So, for this section, we strengthen the condition (*) to the following assumption on Ψ_i , any $0 < \sigma < 1/4$:

$$\eta \leq |\Psi_i| \leq 1 - \sigma. \quad (**)$$

In light of Corollary 7.3, or more precisely the remark following it, the assumption (**) is not vacuous; for η sufficiently small and any choice of $\sigma \in (0, \frac{1}{4})$, there are certainly arbitrarily small ϵ such that (**) is satisfied, and in fact the measure of this set of ϵ is controlled, as claimed in Theorem 3.2.

Assuming (**), we make precise the region of spacetime where the bounce occurs in the following lemma.

Lemma 8.5. Given $n \in \mathbb{N}$ with $n \geq 2$, there exists $\epsilon_0(n, \eta, \sigma) > 0$ such that if $0 < |\epsilon| < \epsilon_0(n, \eta, \sigma)$ **and** the assumption (**) holds, then for any $z > 0$ such that $z \in [|\alpha| + \epsilon^n, |\alpha|^{-1} - \epsilon^n]$, there exists a unique $s_z \in \mathcal{K}$ such that $|\Psi(s_z)| = z$. For this domain of z , the function $z \mapsto s_z$ is increasing, smooth and invertible, we may define the inversion interval \mathcal{K}_{bo}^n to be $\{s_{in}(\epsilon) \leq s \leq s_{out}(\epsilon)\}$ with $|\Psi(s_{in})| = (|\alpha| + \epsilon^n)$ and $|\Psi(s_{out})| = (|\alpha|^{-1} - \epsilon^n)$.

Moreover there exists a constant $D_I(M, \mathbf{e}, \Lambda, m^2, q_0, \eta, \sigma, n) > 0$ depending on η and σ as well as the usual parameters $M, \mathbf{e}, \Lambda, m^2, q_0$ such that we have the following for all $s \in \mathcal{K}_{bo}^n$:

$$\left| \epsilon^2 \cdot \log \frac{r_-}{r(s)} - \frac{b_-^{-2}}{2(1 - \alpha^2)} \right| \leq D_I \epsilon^2 \log(\epsilon^{-1}). \quad (8.47)$$

Remark. The idea is that Lemma 8.5 identifies precisely the region where the quantity Ψ transitions from having absolute value smaller than 1 to having absolute value greater than 1, and that this transition occurs entirely within a region where $\log\left(\frac{r_-}{r(s)}\right)$ is of size $\sim \epsilon^{-2}$, but the $\log\left(\frac{r_-}{r(s)}\right)$ -difference within the region is only

²¹Assuming the Kasner correspondence of Section 1.5, having $|\alpha| = 1$ would imply a spacetime of Kasner exponents 0, 1/2 and 1/2, which already begins to display degenerate features in the BKL picture, see Section 1.5.

$O(\log(\epsilon^{-1}))$.

In what follows, we will, for the most part, take $n = 2$ and define $\mathcal{K}_{bo} := \mathcal{K}_{bo}^{n=2}$.

Proof. We shall prove Lemma 8.5 in three steps:

- First, we show using equations (8.1) and (2.40) that when $\log\left(\frac{r_-}{r(s)}\right) \leq \frac{1}{2}b_-^{-2}\epsilon^{-2}(1 - \alpha^2)^{-1} - O(\log(\epsilon^{-1}))$, we still have $-r\dot{r}(s) \approx -r\dot{r}(s_i)$ and $\Psi(s) \approx \Psi_i \approx \alpha$.
- Next we show using the same equations, that conversely, once we proceed to $\log\left(\frac{r_-}{r(s)}\right) \geq \frac{1}{2}b_-^{-2}\epsilon^{-2}(1 - \alpha^2)^{-1} + O(\log(\epsilon^{-1}))$, we must have that $\Psi(s) \geq |\alpha| + \epsilon^n$, hence identifying an $s = s_{in}(\epsilon)$ which satisfies (8.47).
- Now applying Proposition 8.1, particularly the ODE (8.6), we deduce that $\frac{d\Psi}{dR}$ is positive and bounded strictly away from 0 for $|\Psi| \in [|\alpha| + \epsilon^n, |\alpha|^{-1} - \epsilon^n]$. Using this, we then show that one proceeds from $|\Psi| = |\alpha| + \epsilon^n$ to $|\Psi| = |\alpha|^{-1} - \epsilon^n$ in an R -interval of length $O(\log(\epsilon^{-1}))$, thus proving (8.47) for $s \in \mathcal{K}_{bo}$, as well as the remaining assertions of the lemma.

For ease of notation we suppose, without loss of generality, that $\Psi, \alpha > 0$ in this proof.

By (8.7), we know that, $\Psi \geq \alpha - \epsilon^2$ in \mathcal{K} . Therefore, one has from (8.1) that

$$\frac{d}{ds} \log \left[\frac{\Omega^2(s)}{-\dot{r}} \left(\frac{r(s)}{r_-} \right)^{-(\alpha - \epsilon^2)^2} \right] \leq \frac{d}{ds} \log \left(\frac{\Omega^2(s)}{-\dot{r}(s)} \right) - \frac{\dot{r}}{r} \Psi^2 \leq 0.$$

So $\frac{\Omega^2}{-\dot{r}}(s) \left(\frac{r(s)}{r_-} \right)^{-(\alpha - \epsilon^2)^2}$ is decreasing. But by Corollary 6.4, specifically (6.29), and $|\alpha - \Psi_i| \lesssim \epsilon^2 \log(\epsilon^{-1})$, as well as the fact that $\frac{1}{|\dot{r}(s_i)|} \lesssim r(s_i) \cdot \epsilon^{-2} \lesssim \exp(2 \log(\epsilon^{-1}))$, we have

$$\frac{\Omega^2}{-\dot{r}}(s) \left(\frac{r(s)}{r_-} \right)^{-(\alpha - \epsilon^2)^2} \leq \frac{\Omega^2}{-\dot{r}}(s_i) \left(\frac{r(s_i)}{r_-} \right)^{-(\alpha - \epsilon^2)^2} \leq \exp \left(-\frac{1}{2}b_-^{-2}\epsilon^{-2} \right) \cdot \exp(D_K \log(\epsilon^{-1})). \quad (8.48)$$

Furthermore we used that, because $\Psi_i^2 - (\alpha - \epsilon^2)^2 = O(\epsilon^2)$, one has $\left(\frac{r(s_i)}{r_-} \right)^{\Psi_i^2 - (\alpha - \epsilon^2)^2} \lesssim e^{O(\epsilon^{-2}) \cdot O(\epsilon^2)} \lesssim 1$.

We now use this upper bound when integrating the equation (2.40). Due to Lemma 8.2, we can use the following estimate for the integral of the right hand side of (2.40):

$$\begin{aligned} | -r\dot{r}(s) + r\dot{r}(s_i) | &\leq \int_{s_i}^s \frac{Q_\infty^2 \Omega^2(\tilde{s})}{2r^2(\tilde{s})} d\tilde{s} + \int_{s_i}^s \frac{\Omega^2(\tilde{s})r^2(\tilde{s})}{4} (|\Lambda| + m^2|\phi|^2) d\tilde{s} + \int_{s_i}^s \frac{\Omega^2(\tilde{s})}{4} d\tilde{s} \\ &\lesssim \int_{r(s)}^{r(s_i)} \frac{\Omega^2}{-\dot{r}} \frac{1}{r^2} dr \\ &\lesssim \exp \left(-\frac{1}{2}b_-^{-2}\epsilon^{-2} \right) \cdot \exp(D_K \log(\epsilon^{-1})) \int_{r(s)}^{r(s_i)} \left(\frac{r}{r_-} \right)^{(\alpha - \epsilon^2)^2 - 2} dr \\ &\lesssim \left(\frac{r_-}{r(s)} \right)^{1 - (\alpha - \epsilon^2)^2} \cdot \exp \left(-\frac{1}{2}b_-^{-2}\epsilon^{-2} \right) \cdot \exp(D_K \log(\epsilon^{-1})). \end{aligned}$$

Here, the last step follows as $1 - (\alpha - \epsilon^2)^2 \geq \sigma > 0$ for sufficiently small ϵ depending on σ . If

$\frac{r(s)}{r_-} \geq \exp\left((1 - \alpha^2)^{-1} \left(-\frac{1}{2}b_-^2\epsilon^{-2} + (D_K + 6n)\log(\epsilon^{-1})\right)\right)$, then one finds

$$\begin{aligned} \left(\frac{r_-}{r(s)}\right)^{1-(\alpha-\epsilon^2)^2} &\leq \exp\left(-\frac{1-(\alpha-\epsilon^2)^2}{1-\alpha^2} \left(-\frac{1}{2}b_-^2\epsilon^{-2} + (D_K + 6n)\log(\epsilon^{-1})\right)\right) \\ &\lesssim \epsilon^{6n} \cdot \exp\left(\frac{1}{2}b_-^2\epsilon^{-2}\right) \cdot \exp(-D_K \log(\epsilon^{-1})). \end{aligned}$$

Putting this in the above one sees that $|-r\dot{r}(s) + r\dot{r}(s_i)| \lesssim \epsilon^{6n}$, or

$$\left|\frac{-r\dot{r}(s)}{-r\dot{r}(s_i)} - 1\right| \lesssim \epsilon^{6n-2}.$$

But $-r\dot{r}(s)$ changing little from its initial value means that $\Psi(s)$ also changes little from its initial value; to see this use also (8.12), which combined with the above implies $|\Psi(s) - \Psi_i| \lesssim \epsilon^{6n-2}$. As $|\alpha - \Psi_i| \lesssim e^{-\delta_0\epsilon^{-2}}$, we thus know that for $\log r(s) \geq -\frac{1}{2}(1 - \alpha^2)^{-1}b_-^2\epsilon^{-2} + O(\log(\epsilon^{-1}))$ as specified, we have not yet entered the regime \mathcal{K}_{bo} .

On the other hand, we show that for $s_{in} = \sup\{s \in \mathcal{K} : \Psi(s) \leq \alpha + \epsilon^n\}$, we must have $\log r(s_{in}) \geq -\frac{1}{2}(1 - \alpha^2)^{-1}b_-^2\epsilon^{-2} - O(\log(\epsilon^{-1}))$. For this purpose, we use the Raychaudhuri equation (8.1) to see that, for $s_i \leq s \leq s_{in}$, one has

$$\frac{d}{ds} \log \left[\frac{\Omega^2(s)}{-\dot{r}} \left(\frac{r(s)}{r_-} \right)^{-(\alpha+\epsilon^n)^2} \right] \geq \frac{d}{ds} \log \left(\frac{\Omega^2(s)}{-\dot{r}(s)} \right) - \frac{\dot{r}}{r} \Psi^2 \geq -\frac{r^2}{-r\dot{r}} |\tilde{A}|^2 q_0^2 |\phi|^2.$$

Since $r(s) \leq e^{-\delta_0\epsilon^{-2}}r_-$ for $s \in \mathcal{K}$, one sees using Proposition 8.1 and Lemma 8.2 that the integral of the right hand side is bounded below by $-\log 2$, say. Therefore a similar application of Corollary 6.4 will yield that

$$\frac{\Omega^2}{-\dot{r}} \left(\frac{r(s)}{r_-} \right)^{-(\alpha+\epsilon^n)^2} \geq \frac{1}{2} \exp\left(-\frac{1}{2}b_-^2\epsilon^{-2}\right) \cdot \exp(-D_K \log(\epsilon^{-1})).$$

One now again integrates the equation (2.40), or more precisely (8.17), getting now the upper bound

$$\begin{aligned} |-r\dot{r}(s) + r\dot{r}(s_i)| &\geq \int_{s_i}^s \frac{Q^2\Omega^2(\tilde{s})}{8r^2(\tilde{s})} d\tilde{s} \gtrsim \int_{r(s)}^{r(s_i)} \frac{\Omega^2}{-\dot{r}} \frac{1}{r^2} dr \\ &\gtrsim \exp\left(-\frac{1}{2}b_-^2\epsilon^{-2}\right) \cdot \exp(-D_K \log(\epsilon^{-1})) \int_{r(s)}^{r(s_i)} \left(\frac{r}{r_-}\right)^{(\alpha+\epsilon^n)^2-2} dr \\ &\gtrsim \left(\frac{r_-}{r(s)}\right)^{1-(\alpha+\epsilon^n)^2} \cdot \exp\left(-\frac{1}{2}b_-^2\epsilon^{-2}\right) \cdot \exp(-D_K \log(\epsilon^{-1})). \end{aligned}$$

But by Proposition 8.1, we always have $\epsilon^2 \lesssim -r\dot{r} \lesssim \epsilon^2$, so that

$$\left(\frac{r(s)}{r_-}\right)^{1-(\alpha+\epsilon^n)^2} \gtrsim \exp\left(-\frac{1}{2}b_-^2\epsilon^{-2}\right) \cdot \exp((2 - D_K) \log(\epsilon^{-1})).$$

Hence we do indeed find that for $s_i \leq s \leq s_{in}$, we must have $\log(r(s)/r_-) \geq -\frac{1}{2}(1 - \alpha^2)^{-1}b_-^2\epsilon^{-2} - O(\log(\epsilon^{-1}))$ as claimed. This identifies $s = s_{in}$ obeying (8.47).

The remainder of this proof then proceeds entirely using the ODE (8.6), which for $R = \log\left(\frac{r_-}{r(s)}\right)$ we record

again here as

$$\frac{d\Psi}{dR} = -\Psi(\Psi - \alpha)(\Psi - \alpha^{-1}) + \mathcal{F}, \quad |\mathcal{F}(R)| \leq D_K e^{-\delta_0 \epsilon^{-2} - R}. \quad (8.49)$$

We have identified $R_{in} = R(s_{in}) = \frac{1}{2}(1 - \alpha^2)^{-1}b_-^{-2}\epsilon^{-2} + O(\log(\epsilon^{-1}))$ such that $\Psi(R_{in}) = \alpha + \epsilon^n$. We want to use that α is an unstable fixed point and α^{-1} a stable fixed point of this one-dimensional dynamical system.

Note that for $\Psi(s) \in [\alpha + \epsilon^n, \alpha^{-1} - \epsilon^n]$, one knows that (i) $\Psi \geq \eta$, and (ii) $\alpha^{-1} - 1 \geq 1 - \alpha \geq \sigma - O(e^{-\delta_0 \epsilon^{-2}})$, so we absorb the error term \mathcal{F} and quantify the stability and instability of the fixed points to find

$$\frac{d}{dR}(\Psi - \alpha) \geq \frac{\eta\sigma}{2}(\Psi - \alpha) \quad \text{if } \Psi \in [\alpha + \epsilon^n, 1], \quad (8.50)$$

$$\frac{d}{dR}(\alpha^{-1} - \Psi) \leq -\frac{\sigma}{2}(\alpha^{-1} - \Psi) \quad \text{if } \Psi \in [1, \alpha^{-1} - \epsilon^n]. \quad (8.51)$$

In particular, $\frac{d\Psi}{dR} > 0$ as long as $\Psi \in [\alpha + \epsilon^n, \alpha^{-1} - \epsilon^n]$. From (8.50), one finds that $\Psi - \alpha$ proceeds from ϵ^n to $1 - \alpha$ in $O(\log(\epsilon^{-1}))$ time in R , and from (8.51) that $\alpha^{-1} - \Psi$ proceeds from $\alpha^{-1} - 1$ to ϵ^n also in $O(\log(\epsilon^{-1}))$ time in R . Therefore defining R_{out} to be the minimal R such that $\Psi(R_{out}) = \alpha^{-1} - \epsilon^n$, one finds $R_{out} = R_{in} + O(\log(\epsilon^{-1})) = \frac{1}{2}(1 - \alpha^2)^{-1}b_-^{-2}\epsilon^{-2} + O(\log(\epsilon^{-1}))$ also.

Finally, since $\frac{d\Psi}{dR} \geq \frac{1}{2}\epsilon^n\eta\sigma > 0$ when $\Psi \in [\alpha + \epsilon^n, \alpha^{-1} - \epsilon^n]$, we have that, upon entering this region of Ψ , it is impossible to return, and the remaining claims of the lemma are immediate. \square

9 Quantitative Kasner-like asymptotics

Let us recapitulate the various regions so far:

1. In Section 6, we worked in the Proto-Kasner region $\mathcal{PK} = \{s_{PK} \leq s \leq s_i\} = \{2|B|\mathfrak{W}\epsilon \geq \frac{r}{r_-} \geq e^{-\delta_0 \epsilon^{-2}}\}$.
We now also define the restricted region $\mathcal{PK}' = \{s_{K_1} \leq s \leq s_i\} = \{2|B|\mathfrak{W}\epsilon^2 \geq \frac{r}{r_-} \geq e^{-\delta_0 \epsilon^{-2}}\}$.
2. In Section 8, we have worked in the Kasner region $\mathcal{K} = \{s_i \leq s < s_\infty\} = \{0 < \frac{r}{r_-} \leq e^{-\delta_0 \epsilon^{-2}}\}$ and showed that $\lim_{s \rightarrow s_\infty} r(s) = 0$.

In what follows, we prove quantitative estimates on the ‘‘Kasner-like behavior’’ of the metric; for this, we will first have to restrict \mathcal{PK} to its aforementioned subset \mathcal{PK}' on which $r \gtrsim \epsilon^2$ (recall that $r(s_{K_1}) = 2|B|\mathfrak{W}r_- \epsilon^2$). While in the previous sections, the analysis was so far oblivious to the absence/presence of a Kasner bounce, we will now also be obliged to distinguish both cases and treat them differently.

As we will soon show, the ‘‘No Kasner bounce’’ condition will be that, for some $0 < \sigma < 1$,

$$|\Psi(s_i)| \geq 1 + \sigma, \quad (***)$$

whereas the ‘‘Kasner bounce’’ condition will be that, for some $0 < \sigma < 1$ and $\eta > 0$,

$$\eta \leq |\Psi(s_i)| \leq 1 - \sigma. \quad (**)$$

We note that even combining (***) and (**) does not cover the range of $\Psi(s_i)$ included in (*). In particular, we do not say anything further in the case where $\Psi(s_i) = 1$. In each of these two cases, we will further sub-divide $\mathcal{PK} \cup \mathcal{K}$ as follows:

i. If the “No Kasner bounce” condition (***) is satisfied, we define the first Kasner region by

$$\mathcal{K}_1 = \mathcal{PK}' \cup \mathcal{K}. \quad (9.1)$$

Because there is no bounce in that case, we show indeed that the metric is close to a single Kasner spacetime on the whole of $\mathcal{K}_1 = \mathcal{PK}' \cup \mathcal{K}$ in Theorem 9.1.

ii. If the “Kasner bounce” condition (**) is satisfied, we define the first Kasner region by

$$\mathcal{K}_1 = \{s_{K_1} \leq s \leq s_{in}\} \supset \mathcal{PK}', \quad (9.2)$$

where $s_{in} \in \mathcal{K}$ will be defined shortly. We also define

$$\mathcal{K}_{bo} = \{s_{in} \leq s \leq s_{out}\} \quad (9.3)$$

to be the Kasner bounce region, and

$$\mathcal{K}_2 = \{s_{out} \leq s < s_\infty\} \quad (9.4)$$

to be the second Kasner region, where $s_{in}, s_{out} \in \mathcal{K}$ given by Lemma 8.5 (applied to $n = 2$) are defined such that (8.47) is satisfied on \mathcal{K}_{bo} . Because of the Kasner bounce, we show that the metric is close to a first Kasner spacetime in \mathcal{K}_1 , and close to a second, different Kasner spacetime in \mathcal{K}_2 in Theorem 9.2. By (8.47), the transition region \mathcal{K}_{bo} will be shown to be small in an appropriate sense.

We now state the two main theorems of this section, Theorem 9.1 and 9.2.

Theorem 9.1. Let $(r, \Omega^2, \phi, Q, \tilde{A})$ be a solution to the system (2.36)–(2.46), which, by Proposition 6.1, exists at least up to the value $s = s_i = \frac{b_-^{-2}\epsilon^{-2}}{4|K_-|} + O(\log(\epsilon^{-1}))$ at which $r(s) = e^{-\delta_0\epsilon^{-2}}r_-$ (see Proposition 4.5 for a definition of b_-). Suppose that for some given $0 < \sigma < 1$, (***) is satisfied.

Then there exists some $\epsilon_0(M, \mathbf{e}, \Lambda, m^2, q_0, \sigma) > 0$, such that, if $0 < |\epsilon| < \epsilon_0$, then there exists some $s_\infty > s_i$ such that the solution of (2.36)–(2.46) exists for $s \in (-\infty, s_\infty)$ with $\lim_{s \rightarrow s_\infty} r(s) = 0$.

Furthermore, we have the following Kasner-like asymptotics: denote s_{K_1} such that $r(s_{K_1}) = 2|B|\mathfrak{W}\epsilon^2r_-$, then in the region $\mathcal{K}_1 = \{s_{K_1} \leq s < s_\infty\}$, one may write the metric in the following form, where α is as determined in Proposition 8.1:

$$g = -d\tau^2 + \mathcal{X}_1 \cdot (1 + \mathfrak{E}_{X,1}(\tau)) \tau^{\frac{2(\alpha^2-1)}{\alpha^2+3}} dt^2 + \mathcal{R}_1 \cdot (1 + \mathfrak{E}_{R,1}(\tau)) r_-^2 \tau^{\frac{4}{\alpha^2+3}} d\sigma_{\mathbb{S}^2}. \quad (9.5)$$

Here, \mathcal{X}_1 and \mathcal{R}_1 are constants, and $\mathfrak{E}_{X,1}(\tau)$ and $\mathfrak{E}_{R,1}(\tau)$ are small functions of τ satisfying the following bounds for $\beta = \min\{\frac{1}{2}, 1 - \alpha^2\}$

$$\left| \log \mathcal{X}_1 + \frac{\alpha^2 + 1}{\alpha^2 + 3} b_-^{-2} \epsilon^{-2} \right| + \left| \log \mathcal{R}_1 - \frac{1}{\alpha^2 + 3} b_-^{-2} \epsilon^{-2} \right| \leq C_K \log(\epsilon^{-1}), \quad (9.6)$$

$$|\mathfrak{E}_{X,1}(\tau)| + |\mathfrak{E}_{R,1}(\tau)| \leq C_K \epsilon^2 \cdot \left(\frac{\tau}{\tau(s_{K_1})} \right)^{\frac{2\beta}{\alpha^2+3}}. \quad (9.7)$$

Hence, the spacetime corresponds to a Kasner-like spacetime, in the sense of (1.16), with Kasner exponents

$$p_1 = \frac{\alpha^2-1}{\alpha^2+3}, p_2 = p_3 = \frac{2}{\alpha^2+3}.$$

Theorem 9.2. Let $(r, \Omega^2, \phi, Q, \tilde{A})$ be a solution to the system (2.36)–(2.46), which by Proposition 8.1 exists at least up to the value $s = s_i = \frac{b_-^{-2}\epsilon^{-2}}{4|K_-|} + O(\log(\epsilon^{-1}))$ at which $r(s) = e^{-\delta_0\epsilon^{-2}}r_-$. Suppose that for given $\eta > 0$ and $0 < \sigma < 1$, (**) is satisfied.

Then there exists some $\epsilon_0(M, e, \Lambda, m^2, q_0, \eta, \sigma) > 0$, such that, if $0 < |\epsilon| < \epsilon_0$, then there exists some $s_\infty > s_i$ such that the solution of (2.36)–(2.46) exists for $s \in (-\infty, s_\infty)$ with $\lim_{s \rightarrow s_\infty} r(s) = 0$. We further single out two different regions with Kasner-like asymptotics, between which there is an *intermediate region* where the Kasner bounce occurs. Letting s_{K_1} be such that $r(s_{K_1}) = 2|B|\mathfrak{M}\epsilon^2r_-$, we define the following three regions:

$$\mathcal{K}_1 = \{s_{K_1} \leq s \leq s_{in}\}, \mathcal{K}_{bo} = \{s_{in} \leq s \leq s_{out}\}, \mathcal{K}_2 = \{s_{out} \leq s \leq s_\infty\}.$$

We will describe Kasner-like asymptotics for the two regions \mathcal{K}_1 and \mathcal{K}_2 .

In the region \mathcal{K}_1 , one writes the metric in the following form, for α as in Proposition 8.1:

$$g = -d\tau^2 + \mathcal{X}_1 \cdot (1 + \mathfrak{E}_{X,1}(\tau)) (\tau - \tau_0)^{\frac{2(\alpha^2-1)}{\alpha^2+3}} dt^2 + \mathcal{R}_1 \cdot (1 + \mathfrak{E}_{R,1}(\tau)) r_-^2 (\tau - \tau_0)^{\frac{4}{\alpha^2+3}} d\sigma_{\mathbb{S}^2}. \quad (9.8)$$

Here $\tau_0 > 0$, \mathcal{X}_1 and \mathcal{R}_1 are constants, and $\mathfrak{E}_{X,1}(\tau)$ and $\mathfrak{E}_{R,1}(\tau)$ are functions of τ satisfying

$$\left| \log \mathcal{X}_1 + \frac{\alpha^2 + 1}{\alpha^2 + 3} b_-^{-2} \epsilon^{-2} \right| + \left| \log \mathcal{R}_1 - \frac{1}{\alpha^2 + 3} b_-^{-2} \epsilon^{-2} \right| \leq C_K \log(\epsilon^{-1}), \quad (9.9)$$

$$|\mathfrak{E}_{X,1}(\tau)| + |\mathfrak{E}_{R,1}(\tau)| \leq C_K \epsilon^2. \quad (9.10)$$

On the other hand, in the region \mathcal{K}_2 , one instead has the following form for the metric

$$g = -d\tau^2 + \mathcal{X}_2 \cdot (1 + \mathfrak{E}_{X,2}(\tau)) \tau^{\frac{2(1-\alpha^2)}{1+3\alpha^2}} dt^2 + \mathcal{R}_2 \cdot (1 + \mathfrak{E}_{R,2}(\tau)) r_-^2 \tau^{\frac{4\alpha^2}{1+3\alpha^2}} d\sigma_{\mathbb{S}^2}. \quad (9.11)$$

The constants \mathcal{X}_2 and \mathcal{R}_2 are constants, and the functions $\mathfrak{E}_{X,2}(\tau)$ and $\mathfrak{E}_{R,2}(\tau)$ now satisfying the following bounds for $\beta = \min\{\frac{1}{2}, 1 - \alpha^2\}$

$$\left| \log \mathcal{X}_2 + \frac{1 + \alpha^{-2}}{1 + 3\alpha^2} b_-^{-2} \epsilon^{-2} \right| + \left| \log \mathcal{R}_2 - \frac{1}{1 + 3\alpha^2} b_-^{-2} \epsilon^{-2} \right| \leq C_K \log(\epsilon^{-1}), \quad (9.12)$$

$$|\mathfrak{E}_{X,2}(\tau)| + |\mathfrak{E}_{R,2}(\tau)| \leq C_K \epsilon^2 \cdot \left(\frac{\tau}{\tau(s_{out})} \right)^{\frac{2\beta}{\alpha^{-2}+3}}. \quad (9.13)$$

One sees that the spacetime exhibits a Kasner bounce from the Kasner-like region \mathcal{K}_1 (in the sense of (1.16)) with Kasner exponents of $p_1 = \frac{\alpha^2-1}{\alpha^2+3}, p_2 = p_3 = \frac{2}{\alpha^2+3}$ to another Kasner-like region \mathcal{K}_2 with exponents of $p_1 = \frac{1-\alpha^2}{1+3\alpha^2}, p_2 = p_3 = \frac{2\alpha^2}{1+3\alpha^2}$. We further provide the following estimates regarding the proper time length of the regions \mathcal{K}_2 and \mathcal{K}_{bo} . For \mathcal{K}_2 , the proper time τ from the singularity varies between 0 and $\tau(s_{out})$, obeying

$$\left| \log \tau(s_{out}) - \frac{1}{2} \frac{\alpha^{-2} + 1}{1 - \alpha^2} \cdot b_-^{-2} \epsilon^{-2} \right| \leq C_K \log(\epsilon^{-1}). \quad (9.14)$$

On the other hand, we have the following (non-sharp) upper bound for the size of $\mathcal{K}_{bo} = [s_{in}, s_{out}]$, where the

proper time variable $\tau = \tau(s)$ satisfies $\frac{d\tau}{ds} = -\frac{\Omega(s)}{2}$.

$$0 \leq \tau(s_{in}) - \tau(s_{out}) \leq \exp\left(-\frac{b_-^{-2}\epsilon^{-2}}{1-\alpha^2}\right) \cdot \exp(C_K \log(\epsilon^{-1})). \quad (9.15)$$

9.1 Asymptotics for Ψ near the $\{r = 0\}$ singularity

The first step in proving that the $\{r = 0\}$ singularity has Kasner-like asymptotics relies on showing that Ψ tends to the appropriate constant α or α^{-1} sufficiently quickly near the singularity. The aim will be to show that $\Psi = \alpha + O((\frac{r}{r_-})^\beta)$ or $\Psi = \alpha^{-1} + O((\frac{r}{r_-})^\beta)$ for some positive exponent $\beta > 0$.

After the usual change of coordinates $r = e^{-R} r_-$, this translates to showing that Ψ decays exponentially to α or α^{-1} in the variable R . For this purpose, we shall need to use the ODE (8.6) from Proposition 8.1. By standard dynamical systems theory, one expects that Ψ tends towards its stable fixed point at an exponential rate. We quantify this in the following lemma:

Lemma 9.3. Fix constants $0 < \sigma, \eta < \frac{1}{2}$. For all $\alpha \in \mathbb{R}$ satisfying $1 + \sigma \leq |\alpha| \leq \eta^{-1}$, consider the following ODE for the function $\Psi = \Psi(R)$:

$$\frac{d\Psi}{dR} = -\Psi(\Psi - \alpha)(\Psi - \alpha^{-1}) + \mathcal{F}(R), \quad |\mathcal{F}(R)| \leq e^{-R}. \quad (9.16)$$

Define $\beta = \min\{\frac{1}{2}, \alpha^2 - 1\} \geq \sigma$. Then there exists some $\nu_0 = \nu_0(\sigma, \eta) > 0$ such that, for all $|\nu| < \nu_0$ and R_* satisfying both

$$|\Psi(R_*) - \alpha| \leq \nu^2 \quad \text{and} \quad e^{-R_*} \leq \nu^2, \quad (9.17)$$

one finds that, for $R \geq R_*$, $\Psi(R)$ decays to α at the following exponential rate

$$|\Psi(R) - \alpha| \leq 8\nu^2 e^{-\beta(R-R_*)}. \quad (9.18)$$

The above lemma will be applied with $\nu \sim \epsilon^n$ or $\nu \sim e^{-\frac{\delta_0}{2}\epsilon^{-2}}$ in what follows.

Proof. We use a bootstrap argument along with Grönwall's inequality. We take the bootstrap assumption to be the desired estimate (9.18). Assuming this holds in some bootstrap region, we have

$$\Psi(\Psi - \alpha^{-1}) \geq \alpha^2 - 1 - |2\alpha - \alpha^{-1}| \cdot 8\nu^2 e^{-\beta(R-R_*)}.$$

Therefore, for R and \tilde{R} in the bootstrap region, one computes that, for ν small enough,

$$\begin{aligned} -\int_{\tilde{R}}^R \Psi(R')(\Psi(R') - \alpha^{-1}) dR' &\leq -(\alpha^2 - 1)(R - \tilde{R}) + \beta^{-1}|2\alpha - \alpha^{-1}| \cdot 8\nu^2 e^{-\beta(\tilde{R}-R_*)} \\ &\leq -\beta(R - \tilde{R}) + \log 2. \end{aligned}$$

Hence, after finding from (9.16) the differential inequality

$$\frac{d}{dR} |\Psi - \alpha| \leq -\Psi(\Psi - \alpha^{-1}) |\Psi - \alpha| + e^{-R},$$

one uses Grönwall to deduce that

$$|\Psi(R) - \alpha| \leq 2\nu^2 e^{-\beta(R-R_*)} + \int_{R_*}^R 2e^{-\tilde{R}} e^{-\beta(R-\tilde{R})} d\tilde{R} \leq 2(\nu^2 + (1-\beta)^{-1} e^{-R_*}) e^{-\beta(R-R_*)}.$$

So taking into account the second assumption of (9.17) and $\beta \leq 1/2$, we improve the bootstrap assumption (9.18). So this estimate is true for all $R \geq R_*$. \square

9.2 First case: absence of Kasner bounce

In this subsection, assuming that (***) holds, we prove the quantitative Kasner asymptotics in the region $\mathcal{K}_1 = \{s_{K_1} \leq s < s_\infty\}$. The essential ingredient is the following lemma:

Lemma 9.4. Consider a solution $(r, \Omega^2, \phi, Q, \tilde{A})$ to the system (2.36)–(2.46) as in Proposition 8.1. Assuming also (***), one finds that there exists some $\mathcal{Y}_1 > 0$ satisfying, for $s_{K_1} \leq s < s_\infty$:

$$\left| \log \left(\frac{\Omega^2}{-\dot{r}} \left(\frac{r}{r_-} \right)^{-\alpha^2} \right) (s) - \log \mathcal{Y}_1 \right| \leq D_1 \epsilon^2 \left(\frac{r(s)}{r_-} \right)^\beta, \quad (9.19)$$

with \mathcal{Y}_1 satisfying

$$\left| \log \mathcal{Y}_1 + \frac{1}{2} b_-^{-2} \epsilon^{-2} \right| \leq D_1 \cdot \log(\epsilon^{-1}). \quad (9.20)$$

Furthermore, one may find a constant $\mathcal{Z}_1 > 0$ such that

$$|-r\dot{r}(s) - \mathcal{Z}_1| \leq D_1 \epsilon^4 \left(\frac{r(s)}{r_-} \right)^\beta, \quad (9.21)$$

with \mathcal{Z}_1 satisfying

$$|\mathcal{Z}_1 - 4|B|^2 \mathfrak{W}^2 \omega_{RN} r_-^2 \epsilon^2| \leq D_1 \cdot \epsilon^4 \log(\epsilon^{-1}). \quad (9.22)$$

Proof. We will use the Raychaudhuri equation (8.1). In light of Lemma 9.3, it is preferable to change variables once again, now to the R -coordinate:

$$\frac{d}{dR} \log \left(\frac{\Omega^2}{-\dot{r}} \right) = -\Psi^2 - \frac{r^4 q_0^2 \tilde{A}^2 \phi^2}{(-r\dot{r})^2}. \quad (9.23)$$

Proposition 8.1 and Lemma 8.2 tell us that the second term on the right hand side of this expression is $O(\epsilon^{-4} e^{-4R} R^2)$. Adding α^2 to both sides and using that Ψ is bounded, we have

$$\left| \frac{d}{dR} \log \left(\frac{\Omega^2}{-\dot{r}} \right) + \alpha^2 \right| \lesssim |\Psi - \alpha| + \epsilon^{-4} e^{-4R} R^2. \quad (9.24)$$

The crucial observation is that the right-hand side will be integrable (and with small integral) in the region \mathcal{K}_1 . Indeed, we claim that if $R_{K_1} = -\log \left(\frac{r_{K_1}}{r_-} \right) = -\log(2|B|\mathfrak{W}\epsilon^2)$, then for $R_{K_1} \leq R < +\infty$, we have

$$\int_R^{+\infty} |\Psi(\tilde{R}) - \alpha| d\tilde{R} + \int_R^{+\infty} \epsilon^{-4} e^{-4\tilde{R}} \tilde{R}^2 d\tilde{R} \lesssim \epsilon^2 e^{-\beta R}. \quad (9.25)$$

The bound for the latter integral follows by straightforward calculus, using also $\beta < 1/2$ and $e^{-R} \leq e^{-R_{K_1}} \sim \epsilon^2$ to get the correct dependence on ϵ . For the former integral, we proceed in two steps; first we use Lemma 9.3

to deal with the region \mathcal{K} , then use Corollary 6.4 to handle the remaining part $\mathcal{PK} \cap \mathcal{K}_1$.

Note that, for the region \mathcal{K} , where we have access to the ODE (8.6), we have the bound $|\Psi(R_i) - \alpha| \lesssim e^{-\delta_0 \epsilon^{-2}}$ from Proposition 8.1. Hence, by Lemma 9.3 with $\nu^2 \sim e^{-\delta_0 \epsilon^{-2}}$, we know that, for $R \geq R_i$, we have $|\Psi - \alpha| \lesssim e^{-\delta_0 \epsilon^{-2}} e^{-\beta(R-R_i)}$. Thus, for $R \geq R_i$, one has

$$\int_R^{+\infty} |\Psi(\tilde{R}) - \alpha| d\tilde{R} \lesssim e^{-\delta_0 \epsilon^{-2}} e^{-\beta(R-R_i)} \lesssim e^{-(1-\beta)\delta_0 \epsilon^{-2}} e^{-\beta R}.$$

The last line here follows from the definition $R_i = \delta_0 \epsilon^{-2}$. The smallness of the expression $e^{-(1-\beta)\delta_0 \epsilon^{-2}}$ thus proves (9.25) for $R \geq R_i$.

For the remaining portion $R \in [R_{K_1}, R_i]$, we use Corollary 6.4. The point is that, in this region, we have $|\Psi - \alpha| \leq |\Psi - \Psi_i| + |\Psi_i - \alpha| \lesssim e^{-2R} \log(\epsilon^{-1}) + e^{-\delta_0 \epsilon^{-2}}$. Therefore, one finds that

$$\int_R^{R_i} |\Psi(\tilde{R}) - \alpha| d\tilde{R} \lesssim e^{-2R} \log(\epsilon^{-1}) + e^{-\delta_0 \epsilon^{-2}} R_i \lesssim \epsilon^2 e^{-\beta R}.$$

(We also note here that (3.23) follows straightforwardly from the $|\Psi - \alpha|$ estimates here.)

So we have proved the estimate (9.25). From (9.24), this shows that the expression

$$\log\left(\frac{\Omega^2}{-\dot{r}}\right) + \alpha^2 R = \log\left(\frac{\Omega^2}{-\dot{r}} \left(\frac{r}{r_-}\right)^{-\alpha^2}\right) \quad (9.26)$$

indeed has a finite limit $\log \mathcal{Y}_1$ as $R \rightarrow \infty$, and moreover satisfies the estimate (9.19).

We next estimate the constant $\log \mathcal{Y}_1$. To do this, we evaluate (9.19) at $r = r_{K_1}$ i.e. $s = s_{K_1}$ and use the estimate (6.29) from Corollary 6.4. As $|\log r(s_{K_1})|, |\log(-\dot{r}(s_{K_1}))| = O(\log(\epsilon^{-1}))$ here, we find that

$$\left| \log \mathcal{Y}_1 + \frac{1}{2} b_-^2 \epsilon^{-2} \right| \lesssim \log(\epsilon^{-1}). \quad (9.27)$$

Finally, we show the estimate (9.21) by considering the equation (2.40) after changing variables to r ; Propositions 6.1 and 8.1 and then the now-known (9.19) tell us that for $s \in \mathcal{K}_1$, we have

$$\left| \frac{d}{dr}(-r\dot{r}) \right| \lesssim \frac{\Omega^2}{-r^2 \dot{r}} \lesssim \mathcal{Y}_1 \cdot \left(\frac{r}{r_-}\right)^{\alpha^2 - 2}.$$

Integrating this expression then yields (9.21) – of course it is essential here that $\alpha^2 - 1 \geq \frac{\sigma}{2} > 0$, and we have the smallness (9.27) for the expression \mathcal{Y}_1 . \square

9.3 Second case: presence of a Kasner bounce

Assuming instead that $(**)$ holds, Proposition 8.1 and Lemma 8.5 (for $n = 2$) show that the spacetime must exhibit a Kasner bounce. We proceed to show that if we define \mathcal{K}_1 and \mathcal{K}_2 as in (9.2), (9.4), there are Kasner-like asymptotics in both regimes. As in Section 9.2, we first find the precise asymptotics for the lapse Ω^2 , as well as $-\dot{r}$.

9.3.1 The pre-bounce Kasner regime

We start to look at the region \mathcal{K}_1 (pre-bounce regime).

Lemma 9.5. Consider a solution $(r, \Omega^2, \phi, Q, \tilde{A})$ to the system (2.36)–(2.40) as in Proposition 8.1. Assuming now the condition $(**)$ on the value of Ψ at $s = s_i$, there will exist some \mathcal{Y}_1 satisfying, for $s_{K_1} \leq s \leq s_{in}$,

$$\left| \log \left(\frac{\Omega^2}{-\dot{r}} \left(\frac{r}{r_-} \right)^{-\alpha^2} \right) (s) - \log \mathcal{Y}_1 \right| \leq D_1 \epsilon^2, \quad (9.28)$$

with \mathcal{Y}_1 satisfying

$$\left| \log \mathcal{Y}_1 + \frac{1}{2} b_-^{-2} \epsilon^{-2} \right| \lesssim \log(\epsilon^{-1}). \quad (9.29)$$

Furthermore, one may find a constant $\mathcal{Z}_1 > 0$ such that

$$|-r\dot{r}(s) - \mathcal{Z}_1| \leq D_1 \epsilon^4, \quad (9.30)$$

with \mathcal{Z}_1 satisfying

$$|\mathcal{Z}_1 - 4|B|^2 \mathfrak{W}^2 \omega_{RN} r_-^2 \epsilon^2| \lesssim \epsilon^4 \log(\epsilon^{-1}). \quad (9.31)$$

Proof. We follow a similar template to the proof of Lemma 9.4, though unlike in that case, we do not need $(\frac{r}{r_-})^\beta$ decay rates. In particular, we are able to integrate from $R = R_{K_1}$ rather than backwards from $R = +\infty$. Using the same Raychaudhuri equation (9.23), we need to prove the analogue of (9.25), i.e. for $R \geq R_{K_1}$,

$$\int_{R_{K_1}}^R |\Psi(\tilde{R}) - \alpha| d\tilde{R} + \int_{R_{K_1}}^R \epsilon^{-4} e^{-4\tilde{R}} \tilde{R}^2 d\tilde{R} \lesssim \epsilon^2. \quad (9.32)$$

As in Lemma 9.4, the latter integral is straightforward, and we focus on the former. Following Corollary 6.4 and Proposition 8.1, we know that for $s \in \mathcal{PK}' = \mathcal{PK} \cap \mathcal{K}_1$, where $R \in [R_{K_1}, R_i]$, we have $|\Psi(R) - \alpha| \leq |\Psi(R) - \Psi_i| + |\Psi_i - \alpha| \lesssim e^{-2R} \log(\epsilon^{-1}) + e^{-\delta_0 \epsilon^{-2}}$. So we know as before that

$$\int_{R_{K_1}}^{R_i} |\Psi(\tilde{R}) - \alpha| d\tilde{R} \lesssim \epsilon^2. \quad (9.33)$$

On the other hand, when integrating between R_i and R_{in} , Ψ is growing away from α exponentially as opposed to exponentially decaying, so we need a new tactic. The key observation is that following the definition of R_{in} from Lemma 8.5 for $n = 2$, we know a priori that $|\Psi(R) - \alpha| \leq \epsilon^2$ when $R \in [R_i, R_{in}]$. The same lemma also tells us that $|R_i - R_{K_1}| \lesssim \epsilon^{-2}$, so these two observations combined tell us that $\int_{R_i}^{R_{in}} |\Psi(\tilde{R}) - \alpha| d\tilde{R} \lesssim 1$.

This is not quite the claimed estimate (9.32). To improve the $O(1)$ bound to $O(\epsilon^2)$, we apply Lemma 8.5 with $n = 4$. Defining R'_{in} to instead be the unique $R > R_i$ with $|\Psi(R'_{in}) - \alpha| = \epsilon^4$, we find that, for $R \in [R'_{in}, R_{in}]$, we have $|\Psi(R) - \alpha| \leq e^{\frac{\eta\sigma}{2}(R-R_{in})} \epsilon^2$. This is because, within this region, (8.50) holds and may be “integrated backwards” from $R = R_{in}$. Furthermore, for $R \in [R_i, R'_{in}]$, we know a priori that $|\Psi(R) - \alpha| \leq \epsilon^4$. So

$$\int_{R_i}^{R_{in}} |\Psi(\tilde{R}) - \alpha| d\tilde{R} \leq \int_{R_i}^{R'_{in}} \epsilon^4 d\tilde{R} + \int_{R'_{in}}^{R_{in}} e^{\frac{\eta\sigma}{2}(\tilde{R}-R_{in})} \epsilon^2 d\tilde{R} \lesssim \epsilon^2. \quad (9.34)$$

Combining this with (9.33) yields the desired (9.32). The estimate (9.28) then follows exactly as in the proof of (9.19), as does the estimate (9.29) on \mathcal{Y}_1 .

For the estimate (9.30), let us define \mathcal{Z}_1 as $-r\dot{r}(s_i)$. By Proposition 6.1, it is easy to integrate (2.40) and deduce (9.30) in the region $s \in [s_{K_1}, s_i]$. The difficulty lies in showing (9.30) in the region $s \in [s_i, s_{in}]$, not least

because $-r\dot{r}$ is expected to change value during the inversion process.

What helps us here is that $-r\dot{r}$ is approximately inversely proportional to the quantity Ψ , given that $r^2\dot{\phi} = -r\dot{r} \cdot \Psi$ is approximately constant. To be quantitatively precise, we combine the estimate (8.12) with the trivial a priori observation that $\left| \frac{\Psi(s)}{\Psi_i} - 1 \right| \lesssim \epsilon^2$ for $s \in [s_i, s_{in}]$ to get

$$\left| \frac{-r\dot{r}(s)}{-r\dot{r}(s_i)} - 1 \right| = \left| \frac{\Psi(s_i)}{\Psi(s)} \cdot \frac{r^2\dot{\phi}(s)}{r^2\dot{\phi}(s_i)} - 1 \right| \lesssim \epsilon^2. \quad (9.35)$$

Since $-r\dot{r}(s_i) \sim \epsilon^2$, the estimate (9.30) follows immediately. \square

9.3.2 The post-bounce Kasner regime

Finally, we consider the post-bounce regime, i.e. the region $\mathcal{K}_2 = \{s_{out} \leq s < s_\infty\}$.

Lemma 9.6. Consider a solution $(r, \Omega^2, \phi, Q, \tilde{A})$ to the system (2.36)–(2.40) as in Proposition 8.1. Assuming the condition $(**)$ on the value of Ψ at $s = s_i$, then for $s_{out} \leq s \leq s_\infty$, there exists some constant \mathcal{Y}_2 such that

$$\left| \log \left(\frac{\Omega^2}{-\dot{r}} \left(\frac{r}{r_-} \right)^{-\alpha^{-2}} \right) (s) - \log \mathcal{Y}_2 \right| \leq D_2 \epsilon^2 \cdot \left(\frac{r(s)}{r(s_{out})} \right)^\beta, \quad (9.36)$$

with $\mathcal{Y}_2 > 0$ satisfying

$$\left| \log \mathcal{Y}_2 - \frac{1}{2} \alpha^{-2} b_-^{-2} \epsilon^{-2} \right| \leq D_2 \cdot \log(\epsilon^{-1}). \quad (9.37)$$

Here $\beta = \min\{\alpha^{-2} - 1, \frac{1}{2}\}$. One may also find a constant $\mathcal{Z}_2 > 0$ with $|\mathcal{Z}_2| \sim \epsilon^2$ such that, in the same region,

$$|-r\dot{r}(s) - \mathcal{Z}_2| \leq D_2 \epsilon^4 \cdot \left(\frac{r(s)}{r(s_{out})} \right)^\beta. \quad (9.38)$$

Proof. We again begin the proof of (9.36) by using the Raychaudhuri equation (9.23). In this case, this equation alongside Proposition 8.1 will tell us that

$$\left| \frac{d}{dR} \log \left(\frac{\Omega^2}{-\dot{r}} \right) - \alpha^{-2} \right| \lesssim |\Psi(R) - \alpha^{-1}| + \epsilon^{-4} e^{-4R} R^2. \quad (9.39)$$

To estimate $|\Psi - \alpha^{-1}|$ in (9.39), we apply Lemma 9.3 with $R_* = R_{out}$, $\nu = \epsilon$ and α replaced by α^{-1} [note that $\alpha^{-1} > 1 + \sigma > 0$ assuming $(**)$]. The lemma thus tells us that, for ϵ chosen sufficiently small, we have $|\Psi - \alpha^{-1}| \leq 8\epsilon^2 e^{-\beta(R-R_{out})}$ for all $R \geq R_{out}$. Hence, using that $R \geq R_{out} \gtrsim \epsilon^{-2}$ which in turn yields $\epsilon^{-4} e^{-4R} R^2 \lesssim e^{-\beta R} \epsilon^2$, the inequality (9.39) implies that

$$\left| \frac{d}{dR} \log \left(\frac{\Omega^2}{-\dot{r}} \left(\frac{r}{r_-} \right)^{\alpha^{-2}} \right) \right| \lesssim \epsilon^2 e^{-\beta(R-R_{out})}.$$

As the right hand side is integrable, $\frac{\Omega^2}{-\dot{r}} \left(\frac{r}{r_-} \right)^{\alpha^{-2}}$ has a well defined limit \mathcal{Y}_2 as $R \rightarrow +\infty$, and we obtain (9.36).

For (9.38), we will not estimate $-r\dot{r}(s)$ directly but instead use Ψ and $r^2\dot{\phi} = -r\dot{r} \cdot \Psi$. We already have $|\Psi - \alpha^{-1}| \lesssim \epsilon^2 e^{-\beta(R-R_{out})}$, while we integrate (2.46) backwards from $R = +\infty$ to find that

$$|r^2\dot{\phi}(s) - \lim_{\tilde{s} \rightarrow s_\infty} r^2\dot{\phi}(\tilde{s})| \lesssim \int_s^{s_\infty} r^2 |\phi|(\tilde{s}) + \Omega^2 r^2 |\phi|(\tilde{s}) d\tilde{s} \lesssim \int_0^{r(s)} \frac{r^3 |\phi|}{-r\dot{r}} + \frac{\Omega^2}{-\dot{r}} r^2 |\phi| dr.$$

Using Proposition 8.1 and that $\frac{\Omega^2}{-\dot{r}}$ is monotonically decreasing in s and thus uniformly small (see e.g. (8.14)), it is straightforward to find that defining $\mathcal{P}_2 = \lim_{s \rightarrow s_\infty} r^2 \dot{\phi}(s) \sim \epsilon^2$, one (easily, since the RHS is $O(r^{4-})$) has

$$|r^2 \dot{\phi}(s) - \mathcal{P}_2| \lesssim \epsilon^4 e^{-\beta(R-R_{out})}. \quad (9.40)$$

Combining this with the aforementioned $|\Psi - \alpha^{-1}| \lesssim \epsilon^2 e^{-\beta(R-R_{out})}$, we deduce (9.38) for $\mathcal{Z}_2 = \alpha \mathcal{P}_2$.

Finally, we provide the estimate (9.37) for $\log \mathcal{Y}_2$. Note that (9.39) is valid in the whole region $\mathcal{K} = \{R_i \leq R < +\infty\}$, so that, in particular, we may integrate in the interval $R \in [R_{in}, +\infty)$ to find

$$\left| \log \mathcal{Y}_2 - \log \left(\frac{\Omega^2}{-\dot{r}} \left(\frac{r}{r_-} \right)^{-\alpha^{-2}} \right) (R_{in}) \right| \lesssim \epsilon^2 + \int_{R_{in}}^{R_{out}} |\Psi(R) - \alpha^{-1}| dR. \quad (9.41)$$

We now compare this to the estimate (9.28) evaluated at $R = R_{in}$. As we are changing the exponent from α^{-2} to α^2 , we generate an extra term on the left hand side:

$$|\log \mathcal{Y}_2 - \log \mathcal{Y}_1 - (\alpha^{-2} - \alpha^2) R_{in}| \lesssim \epsilon^2 + \int_{R_{in}}^{R_{out}} |\Psi(R) - \alpha^{-1}| dR. \quad (9.42)$$

Now we appeal to Lemma 8.5. By this lemma, we know that $|R_{out} - R_{in}| \lesssim \log(\epsilon^{-1})$, so the integral on the RHS is $O(\log(\epsilon^{-1}))$. Using also (8.47) to estimate R_{in} and the estimate (9.27) for $\log \mathcal{Y}_1$, we find that

$$\left| \log \mathcal{Y}_2 - \frac{1}{2} \alpha^{-2} b_-^{-2} \epsilon^{-2} \right| \lesssim \log(\epsilon^{-1}). \quad (9.43)$$

This completes the proof of the lemma. \square

9.4 Kasner-like asymptotics in synchronous coordinates in both cases

To complete the proofs of Theorems 9.1 and 9.2, we simply need to use the estimates of Lemmas 9.4, 9.5 and 9.6 to put the metric g in the Kasner-like form stated. The following lemma will justify the change of coordinates.

Lemma 9.7. Let (M, g) be a spherically symmetric spacetime with metric (2.1). Defining the coordinates $s = u + v$, $t = v - u$, suppose further that $T = \partial_t = \frac{1}{2}(\partial_v - \partial_u)$ is a Killing field for the metric, i.e. $r(s)$ and $\Omega^2(s)$ are functions of s , and that we are in a trapped region with $\dot{r}(s) < 0$.

Suppose that for some interval $J \subset \mathbb{R}$, there exist constants $\mathcal{Y}, \mathcal{Z} > 0$ and an exponent $\gamma \geq 0$, as well as sufficiently small “lower-order terms” $\mathfrak{E}(s)$, such that we have the following asymptotics for the expressions $\frac{\Omega^2}{-\dot{r}}$ and $-r\dot{r}$ when $s \in J$:

$$\frac{\Omega^2}{-\dot{r}}(s) = \mathcal{Y} \cdot \left(\frac{r(s)}{r_-} \right)^\gamma \cdot (1 + \mathfrak{E}(s)), \quad (9.44)$$

$$-r\dot{r}(s) = \mathcal{Z} \cdot (1 + \mathfrak{E}(s)). \quad (9.45)$$

We quantify the required smallness of \mathfrak{E} in the following way: there exists $\epsilon_* > 0$ small and a non-increasing function $\bar{\mathfrak{E}}(s)$ such that $|\mathfrak{E}(s)| \leq \bar{\mathfrak{E}}(s) \leq \epsilon_*$.

Upon defining (up to translation) the past-directed proper time coordinate τ such that

$$\frac{d\tau}{ds} = -\frac{\Omega(s)}{2}, \quad (9.46)$$

then there exist constants \mathcal{X} and \mathcal{R} depending on $\mathcal{Y}, \mathcal{Z}, \gamma, r_-,$ and $\tau_0 \in \mathbb{R}$, such that one has the following asymptotics for Ω^2 and r^2 with respect to τ :

$$\Omega^2(\tau) = 4\mathcal{X} \cdot (\tau - \tau_0)^{\frac{2(\gamma-1)}{\gamma+3}} \cdot (1 + \mathfrak{E}_X(\tau)), \quad (9.47)$$

$$r^2(\tau) = \mathcal{R} \cdot r_-^2 \cdot (\tau - \tau_0)^{\frac{4}{\gamma+3}} \cdot (1 + \mathfrak{E}_R(\tau)). \quad (9.48)$$

Here, there exists some $C = C(\gamma) > 0$ such that $|\mathfrak{E}_X(\tau)|, |\mathfrak{E}_R(\tau)| \leq C\bar{\mathfrak{E}}(s(\tau))$.

In particular, the metric g can be written in the form

$$g = -d\tau^2 + \mathcal{X} \cdot (\tau - \tau_0)^{\frac{2(\gamma-1)}{\gamma+3}} \cdot (1 + \mathfrak{E}_X(\tau)) dt^2 + \mathcal{R} \cdot (\tau - \tau_0)^{\frac{4}{\gamma+3}} \cdot (1 + \mathfrak{E}_R(\tau)) \cdot r_-^2 d\sigma_{\mathbb{S}^2}. \quad (9.49)$$

Finally, one can find the following relationships between \mathcal{X}, \mathcal{R} and \mathcal{Y} :

$$\left| \log \mathcal{X} - \frac{2(\gamma+1)}{\gamma+3} \log \mathcal{Y} \right| \lesssim 1 + |\log \mathcal{Z}|, \quad (9.50)$$

$$\left| \log \mathcal{R} + \frac{2}{\gamma+3} \log \mathcal{Y} \right| \lesssim 1 + |\log \mathcal{Z}|. \quad (9.51)$$

Proof. In this proof we schematically write all lower-order terms as \mathfrak{E} , leaving the precise claims on these errors to the reader. The crucial estimate is to find an expression for τ in terms of r . Using (9.46), (9.44) and (9.45), we find

$$\frac{d\tau}{dr} = \frac{\Omega}{-2\dot{r}} = \frac{\mathcal{Y}^{1/2} r_-^{1/2}}{2\mathcal{Z}^{1/2}} \cdot \left(\frac{r}{r_-} \right)^{\frac{\gamma+1}{2}} \cdot (1 + \mathfrak{E}). \quad (9.52)$$

Although $\inf_{s \in J} r(s)$ is not necessarily 0, we may artificially extend the interval J to an interval \tilde{J} , and the functions $r(s), \tau(s)$ on \tilde{J} so that $\inf_{s \in \tilde{J}} r(s) = 0$ and (9.52) holds for all $s \in \tilde{J}$. After doing so, we may normalize τ_0 so that $r(\tau_0) = 0$, and find that, for $s \in \tilde{J}$,

$$\tau - \tau_0 = \frac{\mathcal{Y}^{1/2} r_-^{3/2}}{(\gamma+3)\mathcal{Z}^{1/2}} \cdot \left(\frac{r}{r_-} \right)^{\frac{\gamma+3}{2}} \cdot (1 + \mathfrak{E}). \quad (9.53)$$

The remaining assertions are immediate upon combining (9.53) with the assumptions (9.44) and (9.45). \square

Conclusion of the proof of Theorem 9.1 and 9.2. Theorem 9.1 follows immediately from combining Lemmas 9.4 and 9.7, taking $\tau_0 = 0$ (note indeed that, in the No Kasner bounce case (**), (9.52) is true up to $\{r = 0\}$, so $\tau_0 = 0$). Here $\gamma = \alpha^2$, and in order to obtain the final error estimate (9.7), we also need (9.52) to change variables from r to τ .

For the proof of Theorem 9.2 in case (**), we first run the proof in \mathcal{K}_1 and apply Lemma 9.5 to show that (9.44) and (9.45) with $\mathcal{Y} = \mathcal{Y}_1, \mathcal{Z} = \mathcal{Z}_1, \gamma = \alpha^2$ are true for $J = \mathcal{K}_1$. Unlike in case (**), we are not able to continue these estimates all the way up to $r = 0$, so we take $\tau_0 \neq 0$ to account for the fact that the proper time variable with respect to which \mathcal{K}_1 is Kasner-like must be modified. Thus, we can apply Lemma 9.7 to deduce the Kasner-like behavior of \mathcal{K}_1 claimed in Theorem 9.2. On the other hand, Lemma 9.6 and Lemma 9.7, applied to $\mathcal{Y} = \mathcal{Y}_2, \mathcal{Z} = \mathcal{Z}_2, \gamma = \alpha^{-2}$ determine the Kasner-like behavior of $J = \mathcal{K}_2$ (where here we take $\tau = 0$).

Finally, we prove the proper time estimates (9.14) and (9.15). For the former, taking the logarithm of (9.53)

in the context of the region \mathcal{K}_2 (where $\tau_0 = 0$) yields:

$$\log \tau = \frac{1}{2} \log \mathcal{Y}_2 - \frac{1}{2} \log \mathcal{Z}_2 + \frac{\alpha^{-2} + 3}{2} \log r + O(1).$$

In particular, evaluating this at $s = s_{out}$, then using Lemma 8.5 to estimate $r(s_{out}) = r_{out}$ yields

$$\log \tau^{-1}(s_{out}) = \frac{1}{4} \alpha^{-2} b_-^{-2} \epsilon^{-2} + \frac{\alpha^{-2} + 3}{4(1 - \alpha^2)} b_-^{-2} \epsilon^{-2} + O(\log(\epsilon^{-1})) = b_-^{-2} \frac{\alpha^{-2} + 1}{2(1 - \alpha^2)} + O(\log(\epsilon^{-1})).$$

For the final estimate (9.15), we shall use the fact that $\frac{d\tau}{dr} = \frac{\Omega}{-2\dot{r}}$ to find that

$$|\tau(s_{in}) - \tau(s_{out})| \leq (r_{in} - r_{out}) \cdot \max_{s \in \mathcal{K}_{bo}} \frac{\Omega}{-2\dot{r}} \leq r_{in}^{3/2} \cdot \max_{s \in \mathcal{K}_{bo}} \left(\frac{\Omega^2}{-4\dot{r} - r\ddot{r}} \right)^{1/2}.$$

Now applying the estimate (8.48) and then (8.47) again (as $-r\ddot{r} \sim \epsilon^2$ it is absorbed into the $\exp(D \log(\epsilon^{-1}))$ term in the next line), one obtains

$$\begin{aligned} |\tau(s_{in}) - \tau(s_{out})| &\leq \left(\frac{r_{in}}{r_-} \right)^{\frac{3+(\alpha-\epsilon^2)^2}{2}} \cdot \exp\left(-\frac{1}{4} b_-^{-2} \epsilon^{-2}\right) \cdot \exp(D \log(\epsilon^{-1})), \\ &\leq \exp\left(-\frac{1}{4} b_-^{-2} \epsilon^{-2} \left[\frac{3 + \alpha^2}{1 - \alpha^2} + 1 \right]\right) \cdot \exp(D \log(\epsilon^{-1})), \end{aligned}$$

yielding (9.15) as required. This completes the proof of Theorem 9.2, and also Theorem 3.2.

A Bessel functions

In this appendix, we record several basic facts about Bessel functions, which are used widely in Section 5. For further details, refer to Chapter 10 of [35]. We start by recalling *Bessel's equation of order $\nu \in \mathbb{C}$* :

$$z^2 \frac{d^2 f}{dz^2} + z \frac{df}{dz} + (z^2 - \nu^2) f = 0. \quad (\text{A.1})$$

Solutions to this equation are known as *Bessel functions of order ν* . Within the appendix, we shall always assume ν to be a nonnegative integer, and our applications will always be in the cases $\nu = 0, 1$.

As (A.1) is a second order linear homogeneous ODE, there are two linearly independent solutions, denoted $J_\nu(z)$ and $Y_\nu(z)$. These have the following properties.

Fact A.1. The function $J_\nu(z)$, known as the *Bessel function of the first kind*, is an entire function given by the following Taylor expansion:

$$J_\nu(z) = \left(\frac{1}{2}z\right)^\nu \sum_{k=0}^{\infty} \frac{\left(-\frac{1}{4}z^2\right)^k}{k! \Gamma(\nu + k + 1)}. \quad (\text{A.2})$$

In particular, as $z \rightarrow 0$, $J_0(z) \rightarrow 1$ and $z^{-1} J_1(z) \rightarrow 1/2$. Furthermore, for $0 < z \leq 1$, one has $z|J_0(z)| \leq 1$.

Fact A.2. The function $Y_\nu(z)$, known as the *Bessel function of the second kind*, can be defined via the following

Fuchsian asymptotic expansion for $\nu = n \in \mathbb{N} \cup \{0\}$ and $z \in \mathbb{R}^+$:

$$Y_n(z) = -\frac{(\frac{1}{2}z)^{-n}}{\pi} \sum_{k=0}^{n-1} \frac{(n-k-1)!}{k!} \left(\frac{1}{4}z^2\right)^k + \frac{2}{\pi} \ln\left(\frac{1}{2}z\right) J_n(z) - \frac{(\frac{1}{2}z)^n}{\pi} \sum_{k=0}^{\infty} (\psi(k+1) + \psi(n+k+1)) \frac{(-\frac{1}{4}z^2)^k}{k!(n+k)!}, \quad (\text{A.3})$$

where $\psi(z) = \Gamma'(z)/\Gamma(z)$ and $\gamma \approx 0.577$ is the Euler-Mascheroni constant. In particular, one has the following asymptotics for $Y_0(z)$ and $Y_1(z)$:

$$\left| Y_0(z) - \frac{2}{\pi} (\log(\frac{1}{2}z) + \gamma) \right| \lesssim z^2, \quad \left| Y_1(z) + \frac{2}{\pi z} \right| \lesssim |z \log z|. \quad (\text{A.4})$$

Furthermore, for $0 < z \leq 1$, one has the quantitative estimate $z|Y_0(z)| \leq 1$.

Fact A.3. By studying the expansions (A.2) and (A.3),

$$J'_0(z) = -J_1(z) \quad \text{and} \quad Y'_0(z) = -Y_1(z). \quad (\text{A.5})$$

Fact A.4. As $z \rightarrow \infty$, we have the following asymptotics for $J_\nu(z)$ and $Y_\nu(z)$:

$$J_\nu(z) = \sqrt{\frac{2}{\pi z}} \left(\cos\left(z - \frac{\nu\pi}{2} - \frac{\pi}{4}\right) + O(z^{-1}) \right), \quad (\text{A.6})$$

$$Y_\nu(z) = \sqrt{\frac{2}{\pi z}} \left(\sin\left(z - \frac{\nu\pi}{2} - \frac{\pi}{4}\right) + O(z^{-1}) \right). \quad (\text{A.7})$$

We finish this appendix with two lemmas concerning Bessel's equation (A.1). These will be useful when studying Bessel-type equations with inhomogeneous error terms, as in Section 5.

Lemma A.5. Consider Bessel's equation (A.1), where ν is a nonnegative integer. We define the usual *Wronskian*, normalized by the Bessel functions of the first and second kind, by

$$\mathcal{W}_\nu(z) := \det \begin{vmatrix} J_\nu(z) & Y_\nu(z) \\ J'_\nu(z) & Y'_\nu(z) \end{vmatrix} = J_\nu(z)Y'_\nu(z) - Y_\nu(z)J'_\nu(z). \quad (\text{A.8})$$

Then

$$\mathcal{W}_\nu(z) = \frac{2}{\pi z}. \quad (\text{A.9})$$

Proof. A standard manipulation of the second order ODE (A.1) gives

$$\frac{d}{dz} \mathcal{W}_\nu(z) = -\frac{1}{z} \mathcal{W}_\nu(z).$$

Integrating for $z \in \mathbb{R}^+$ therefore yields $\mathcal{W}_\nu(z) = Cz^{-1}$ for some constant of integration C .

To determine C , simply use the asymptotics of Facts A.1 and A.2. This yields $C = \frac{2}{\pi}$, as required. (This computation is more straightforward in our case $\nu = 0$.) \square

For the next lemma, we consider Bessel's equation of order 0 as a first-order system in $(f_1, f_2) = (f, \frac{df}{dz})$:

$$\frac{d}{dz} \begin{bmatrix} f_1 \\ f_2 \end{bmatrix} = \begin{bmatrix} f_2 \\ -f_1 - \frac{1}{z}f_2 \end{bmatrix} = \begin{bmatrix} 0 & 1 \\ -1 & -\frac{1}{z} \end{bmatrix} \begin{bmatrix} f_1 \\ f_2 \end{bmatrix}. \quad (\text{A.10})$$

So for any $z_0, z_1 > 0$, we may define the solution operator²² $\mathbf{S}(z_1; z_0)$ as a linear operator $\mathbf{S}(z_1; z_0) : \mathbb{R}^2 \rightarrow \mathbb{R}^2$ in the following manner: if $(f_1(z_0), f_2(z_0))$ is considered as data for the linear ODE (A.10), then $\mathbf{S}(z_1; z_0)$ maps this data $(f_1(z_0), f_2(z_0))$ to the value of the solution at $z = z_1$, namely $(f_1(z_1), f_2(z_1))$. As an equation:

$$\begin{bmatrix} f_1(z_1) \\ f_2(z_1) \end{bmatrix} = \mathbf{S}(z_1; z_0) \begin{bmatrix} f_1(z_0) \\ f_2(z_0) \end{bmatrix}. \quad (\text{A.11})$$

The following lemma then asserts how to use this linear operator in solving Bessel's equation with inhomogeneous terms, as well as an explicit formula and estimates for the operator $\mathbf{S}(z_1; z_0)$.

Lemma A.6. Consider Bessel's equation (A.1) with $\nu = 0$, but with an inhomogeneous term $F(z)$, i.e.

$$\frac{d^2 f}{dz^2} + \frac{1}{z} \frac{df}{dz} + f = F. \quad (\text{A.12})$$

Then, for $z_0, z_1 \in \mathbb{R}^+$ and the solution operator $\mathbf{S}(z; w)$ defined as before, we have the following expression:

$$\begin{bmatrix} f(z_1) \\ \frac{df}{dz}(z_1) \end{bmatrix} = \mathbf{S}(z_1; z_0) \begin{bmatrix} f(z_0) \\ \frac{df}{dz}(z_0) \end{bmatrix} + \int_{z_0}^{z_1} \mathbf{S}(z_1; \tilde{z}) \begin{bmatrix} 0 \\ F(\tilde{z}) \end{bmatrix} d\tilde{z}. \quad (\text{A.13})$$

Furthermore, we have the following results regarding the linear operator $\mathbf{S}(z_1; z_0)$:

(1) In terms of the Bessel functions $J_\nu(z)$, $Y_\nu(z)$, one may write

$$\mathbf{S}(z_1; z_0) = \begin{bmatrix} J_0(z_1) & Y_0(z_1) \\ -J_1(z_1) & -Y_1(z_1) \end{bmatrix} \cdot \begin{bmatrix} J_0(z_0) & Y_0(z_0) \\ -J_1(z_0) & -Y_1(z_0) \end{bmatrix}^{-1}, \quad (\text{A.14})$$

$$= \frac{\pi z_0}{2} \begin{bmatrix} J_0(z_1) & Y_0(z_1) \\ -J_1(z_1) & -Y_1(z_1) \end{bmatrix} \cdot \begin{bmatrix} -Y_1(z_0) & -Y_0(z_0) \\ J_1(z_0) & J_0(z_0) \end{bmatrix}. \quad (\text{A.15})$$

(2) Using the usual l^2 norm on \mathbb{R}^2 , defined as $\|(x, y)\|_{l^2} = \sqrt{x^2 + y^2}$, and defining $\|\mathbf{A}\|_{l^2 \rightarrow l^2} := \sup_{x \in \mathbb{R}^2, \|x\|_{l^2}=1} \|\mathbf{A}x\|_{l^2}$ to be the l^2 operator norm of a linear map \mathbf{A} , we have that, for all $z_0, z_1 > 0$,

$$\|\mathbf{S}(z_1; z_0)\|_{l^2 \rightarrow l^2} \leq \max \left\{ \frac{z_0}{z_1}, 1 \right\}. \quad (\text{A.16})$$

Proof. Once again letting $(f_1, f_2) = (f, \frac{df}{dz})$, we have now the first-order system:

$$\frac{d}{dz} \begin{bmatrix} f_1(z) \\ f_2(z) \end{bmatrix} = \begin{bmatrix} 0 & 1 \\ -1 & -\frac{1}{z} \end{bmatrix} \begin{bmatrix} f_1(z) \\ f_2(z) \end{bmatrix} + \begin{bmatrix} 0 \\ F(z) \end{bmatrix}.$$

²²This can be viewed as a “non-autonomous” semigroup, also commonly known as a propagator. In particular, it follows that $\mathbf{S}(z_2; z_1) \circ \mathbf{S}(z_1; z_0) = \mathbf{S}(z_2; z_0)$.

Then the expression (A.13) follows from the standard theory of first-order systems and Duhamel's principle.

To get (1), we recall that in light of Fact A.3, the most general solution to the first-order system with no inhomogeneous term is:

$$\begin{bmatrix} f_1(z) \\ f_2(z) \end{bmatrix} = \begin{bmatrix} c_J J_0(z) + c_Y Y_0(z) \\ -c_J J_1(z) - c_Y Y_1(z) \end{bmatrix} = \begin{bmatrix} J_0(z) & Y_0(z) \\ -J_1(z) & -Y_1(z) \end{bmatrix} \begin{bmatrix} c_J \\ c_Y \end{bmatrix}, \quad (\text{A.17})$$

where c_J, c_Y are coefficients in \mathbb{R} . Plugging this into (A.11) and allowing c_J, c_Y to vary will yield (A.14). The expression (A.15) then follows by using Lemma A.5 to compute the inverse.

Finally, for (2), suppose $f(z)$ is a solution to the homogeneous Bessel's equation of order 0. Then we directly compute

$$\frac{d}{dz}(f(z)^2 + f'(z)^2) = -\frac{2}{z}f'(z)^2.$$

Therefore, if $z_1 \geq z_0$, then it is clear that $f(z_1)^2 + f'(z_1)^2 \leq f(z_0)^2 + f'(z_0)^2$, while if $z_1 < z_0$, then Grönwall's inequality gives

$$f(z_1)^2 + f'(z_1)^2 \leq \exp\left(\int_{z_0}^{z_1} -\frac{2}{z} dz\right)(f(z_0)^2 + f'(z_0)^2) = \left(\frac{z_0}{z_1}\right)^2 (f(z_0)^2 + f'(z_0)^2).$$

This yields exactly the required estimate on $\|\mathbf{S}(z_1; z_0)\|_{l^2 \rightarrow l^2}$. \square

In this paper, we will often encounter rescaled versions of Bessel's equation: let $\chi > 0$ be a constant, then consider the equation:

$$\frac{d^2 f}{dx^2} + \frac{1}{x} \frac{df}{dx} + \chi^2 f = F(x). \quad (\text{A.18})$$

Using Lemma A.6, it is then straightforward to deduce the following corollary.

Corollary A.7. Let $f = f(x)$ be a solution to (A.18). Then, if we denote by \mathbf{Q}_χ the scaling matrix

$$\mathbf{Q}_\chi := \begin{bmatrix} 1 & 0 \\ 0 & \chi \end{bmatrix},$$

and define $\mathbf{S}_\chi(x_1; x_0) = \mathbf{Q}_\chi \circ \mathbf{S}(\chi x_1; \chi x_0) \circ \mathbf{Q}_\chi^{-1}$, then for any $x_0, x_1 > 0$ we have

$$\begin{bmatrix} f(x_1) \\ \frac{df}{dx}(x_1) \end{bmatrix} = \mathbf{S}_\chi(x_1; x_0) \begin{bmatrix} f(x_0) \\ \frac{df}{dx}(x_0) \end{bmatrix} + \int_{x_0}^{x_1} \mathbf{S}_\chi(x_1; \tilde{x}) \begin{bmatrix} 0 \\ F(\tilde{x}) \end{bmatrix} d\tilde{x}. \quad (\text{A.19})$$

Furthermore, we have the following results regarding $\mathbf{S}_\chi(x_1; x_0)$:

(1) An explicit formula is given by:

$$\mathbf{S}_\chi(x_1; x_0) = \begin{bmatrix} J_0(\chi x_1) & Y_0(\chi x_1) \\ -\chi J_1(\chi x_1) & -\chi Y_1(\chi x_1) \end{bmatrix} \cdot \begin{bmatrix} J_0(\chi x_0) & Y_0(\chi x_0) \\ -\chi J_1(\chi x_0) & -\chi Y_1(\chi x_0) \end{bmatrix}^{-1}, \quad (\text{A.20})$$

$$= \frac{\pi x_0}{2} \begin{bmatrix} J_0(\chi x_1) & Y_0(\chi x_1) \\ -\chi J_0(\chi x_1) & -\chi Y_1(\chi x_1) \end{bmatrix} \cdot \begin{bmatrix} -\chi Y_1(\chi x_0) & -Y_0(\chi x_0) \\ \chi J_1(\chi x_0) & J_0(\chi x_0) \end{bmatrix}. \quad (\text{A.21})$$

(2) The following estimate holds on the operator norm of $\mathbf{S}_\chi(x_1; x_0)$:

$$\|\mathbf{S}_\chi(x_1; x_0)\|_{l^2 \rightarrow l^2} \leq \max\{\chi, \chi^{-1}\} \cdot \max\left\{1, \frac{x_0}{x_1}\right\}. \quad (\text{A.22})$$

Proof. Simply use the substitution $z = \chi x$ in (A.18), and apply Lemma A.6. Details are left to the reader. \square

References

- [1] X. An and D. Gajic. “Curvature Blow-up and Mass Inflation in Spherically Symmetric Collapse to a Schwarzschild Black Hole”. In: *Arch. Ration. Mech. Anal.* 247.3 (2023), p. 51.
- [2] X. An and R. Zhang. “Polynomial blow-up upper bounds for the Einstein-scalar field system under spherical symmetry”. In: *Comm. Math. Phys.* 376.2 (2020), pp. 1671–1704.
- [3] L. Andersson and A. Rendall. “Quiescent Cosmological Singularities”. In: *Comm. Math. Phys.* 218.3 (2001), pp. 479–511.
- [4] F. Béguin and T. Dutilleul. “Chaotic Dynamics of Spatially Homogeneous Spacetimes”. In: *Comm. Math. Phys.* 399.2 (2023), pp. 737–927.
- [5] J. Bekenstein. “Nonexistence of baryon number for static black holes. I”. In: *Phys. Rev. D (3)* 5 (1972), pp. 1239–1246.
- [6] V. Belinski and M. Henneaux. *The Cosmological Singularity*. Cambridge Monographs on Mathematical Physics. Cambridge University Press, 2017.
- [7] V. Belinski and I. Khalatnikov. “Effect of Scalar and Vector Fields on the Nature of the Cosmological Singularity”. In: *Sov. Phys. JETP* 36.4 (1973), pp. 591–597.
- [8] V. Belinski and I. Khalatnikov. “On the influence of the spinor and electromagnetic fields on the cosmological singularity”. In: *Rend. Sem. Mat. Univ. e Politec. Torino* 35 (1976), pp. 159–180.
- [9] V. Belinski, I. Khalatnikov, and E. Lifshitz. “Oscillatory approach to a singular point in relativistic cosmology”. In: *Sov. Phys. Usp.* 13.6 (1971), pp. 745–765.
- [10] V. Belinski, I. Khalatnikov, and E. Lifshitz. “A general solution of the Einstein equations with a time singularity”. In: *Adv. Phys.* 31.6 (1982), pp. 639–667.
- [11] N. Besset and D. Häfner. “Existence of exponentially growing finite energy solutions for the charged Klein-Gordon equation on the de Sitter-Kerr-Newman metric”. In: *J. Hyperbolic Differ. Equ.* 18.02 (2024/11/11 2021), pp. 293–310.
- [12] F. Beyer and T. Oliynyk. “Localized Big Bang Stability for the Einstein-Scalar Field Equations”. In: *Arch Ration Mech Anal* 248.1 (2024), p. 3.
- [13] P. Bizoń. “Colored black holes”. In: *Phys. Rev. Lett.* 64.24 (1990), pp. 2844–2847.
- [14] P. Breitenlohner, G. Lavrelashvili, and D. Maison. “Mass inflation and chaotic behaviour inside hairy black holes”. In: *Nuclear Phys. B* 524.1-2 (1998), pp. 427–443.
- [15] R.-G. Cai, L. Li, and R.-Q. Yang. “No inner-horizon theorem for black holes with charged scalar hairs”. In: *J. High Energy Phys.* 3 (2021).

- [16] Y. Chen, J. Du, and S.-T. Yau. “Existence of black hole solutions for the Einstein-Yang-Mills equations”. In: *Comm. Math. Phys.* 154.2 (1993), pp. 377–401.
- [17] O. Chodosh and Y. Shlapentokh-Rothman. “Time-periodic Einstein-Klein-Gordon bifurcations of Kerr”. In: *Comm. Math. Phys.* 356.3 (2017), pp. 1155–1250.
- [18] D. Christodoulou. “Violation of cosmic censorship in the gravitational collapse of a dust cloud”. In: *Comm. Math. Phys.* 93.2 (1984), pp. 171–195.
- [19] D. Christodoulou. “The formation of black holes and singularities in spherically symmetric gravitational collapse”. In: *Comm. Pure Appl. Math.* 44.3 (1991), pp. 339–373.
- [20] D. Christodoulou. “Bounded variation solutions of the spherically symmetric Einstein-scalar field equations”. In: *Comm. Pure Appl. Math.* 46.8 (1993), pp. 1131–1220.
- [21] D. Christodoulou. “Examples of naked singularity formation in the gravitational collapse of a scalar field”. In: *Ann. of Math.* 140.3 (1994), pp. 607–653.
- [22] D. Christodoulou. “The instability of naked singularities in the gravitational collapse of a scalar field”. In: *Ann. of Math.* 149.1 (1999), pp. 183–217.
- [23] P. Chruściel, J. Costa, and M. Heusler. “Stationary Black Holes: Uniqueness and Beyond”. In: *Living Rev. Relativ.* 15.1 (2012).
- [24] M. Dafermos. “Stability and instability of the Cauchy horizon for the spherically symmetric Einstein-Maxwell-scalar field equations”. In: *Ann. of Math. (2)* 158.3 (2003), pp. 875–928.
- [25] M. Dafermos. “Black holes without spacelike singularities”. In: *Comm. Math. Phys.* 332.2 (2014), pp. 729–757.
- [26] M. Dafermos and J. Luk. “The interior of dynamical vacuum black holes I: The C^0 -stability of the Kerr Cauchy horizon”. In: *Ann. of Math. (Accepted)* (2024).
- [27] M. Dafermos and I. Rodnianski. “A proof of Price’s law for the collapse of a self-gravitating scalar field”. In: *Invent. Math.* 162.2 (2005), pp. 381–457.
- [28] M. Dafermos and I. Rodnianski. “The red-shift effect and radiation decay on black hole spacetimes”. In: *Comm. Pure Appl. Math.* 62.7 (2009), pp. 859–919.
- [29] M. Dafermos, I. Rodnianski, and Y. Shlapentokh-Rothman. “Decay for solutions of the wave equation on Kerr exterior spacetimes III: The full subextremal case $|a| < M$ ”. In: *Ann. of Math. (2)* 183.3 (2016), pp. 787–913.
- [30] T. Damour, M. Henneaux, and H. Nicolai. “Cosmological billiards”. In: *Class. Quantum Grav.* 20.9 (2003).
- [31] J. Demaret, M. Henneaux, and P. Spindel. “Non-oscillatory behaviour in vacuum Kaluza-Klein cosmologies”. In: *Phys. Lett. B* 164.1 (1985), pp. 27–30.
- [32] Ó. Dias, G. Horowitz, and J. Santos. “Inside an asymptotically flat hairy black hole”. In: *J. High Energy Phys.* 12 (2021).
- [33] Ó. Dias, G. Horowitz, and J. Santos. “Extremal black holes that are not extremal: maximal warm holes”. In: *J. High Energy Phys.* 1 (2022).

- [34] Ó. Dias, R. Monteiro, H. Reall, and J. Santos. “A scalar field condensation instability of rotating anti-de Sitter black holes”. In: *J. High Energy Phys.* 11 (2010).
- [35] *NIST Digital Library of Mathematical Functions*. <http://dlmf.nist.gov/>, Release 1.1.6 of 2022-06-30. F. Olver, A. Olde Daalhuis, D. Lozier, B. Schneider, R. Boisvert, C. Clark, B. Miller, B. Saunders, H. Cohl, and M. McClain, eds.
- [36] E. Donets, D. Galtsov, and M. Zotov. “Internal structures of Einstein-Yang-Mills black holes”. In: *Phys. Rev. D* (3) 56.6 (1997), pp. 3459–3465.
- [37] D. Fajman and L. Urban. *Cosmic Censorship near FLRW spacetimes with negative spatial curvature*. ArXiv preprint: <https://arxiv.org/abs/2211.08052>. To be published in Analysis & PDE. 2022.
- [38] G. Fournodavlos and J. Luk. “Asymptotically Kasner-like singularities”. In: *Amer. J. Math.* 145.4 (2023), pp. 1182–1272.
- [39] G. Fournodavlos, I. Rodnianski, and J. Speck. “Stable Big Bang formation for Einstein’s equations: The complete sub-critical regime”. In: *J. Amer. Math. Soc.* 36.3 (2023), pp. 827–916.
- [40] A. Frenkel, S. Hartnoll, J. Kruthoff, and Z. Shi. “Holographic flows from CFT to the Kasner universe”. In: *J. High Energy Phys.* 8 (2020).
- [41] N. Grandi and I. Landea. “Diving inside a hairy black hole”. In: *J. High Energy Phys.* 5 (2021).
- [42] H. Groeniger, O. Petersen, and H. Ringström. *Formation of quiescent big bang singularities*. ArXiv preprint: <https://arxiv.org/abs/2309.11370>. 2023.
- [43] S. Gubser. “Breaking an Abelian gauge symmetry near a black hole horizon”. In: *Phys. Rev. D* 78.6 (2008).
- [44] S. Hartnoll, C. Herzog, and G. Horowitz. “Building a Holographic Superconductor”. In: *Phys. Rev. Lett.* 101 (2008).
- [45] S. Hartnoll, C. Herzog, and G. Horowitz. “Holographic superconductors”. In: *J. High Energy Phys.* 12 (2008).
- [46] S. Hartnoll, G. Horowitz, J. Kruthoff, and J. Santos. “Gravitational duals to the grand canonical ensemble abhor Cauchy horizons”. In: *J. High Energy Phys.* 10 (2020).
- [47] S. Hartnoll, G. Horowitz, J. Kruthoff, and J. Santos. “Diving into a holographic superconductor”. In: *SciPost Phys.* 10.1 (2021).
- [48] S. Hartnoll and N. Neogi. “AdS black holes with a bouncing interior”. In: *SciPost Phys.* 14 (2023), p. 074.
- [49] S. A. Hartnoll, A. Lucas, and S. Sachdev. *Holographic quantum matter*. MIT Press, Cambridge, MA, 2018, pp. xvi+390.
- [50] M. Henneaux. “The final Kasner regime inside black holes with scalar or vector hair”. In: *J. High Energy Phys.* 3 (2022).
- [51] C. Herdeiro and E. Radu. “Kerr Black Holes with Scalar Hair”. In: *Phys. Rev. Lett.* 112 (2014).
- [52] C. Herdeiro and E. Radu. “Asymptotically flat black holes with scalar hair: a review”. In: *Internat. J. Modern Phys. D* 24.9 (2015).
- [53] G. T. Horowitz. “Introduction to holographic superconductors”. In: *From gravity to thermal gauge theories: the Ads/CFT correspondence*. Vol. 828. Lecture Notes in Phys. Springer, Heidelberg, 2011, pp. 313–347.

- [54] B. Josephson. “Possible new effects in superconductive tunnelling”. In: *Phys. Lett. A* 1.7 (1962), pp. 251–253.
- [55] B. Josephson. “The discovery of tunnelling supercurrents”. In: *Rev. Mod. Phys.* 46 (1974), pp. 251–254.
- [56] E. Kasner. “Geometrical theorems on Einstein’s cosmological equations”. In: *Gen. Relativity Gravitation* 40.4 (2008), pp. 865–876.
- [57] C. Kehle and Y. Shlapentokh-Rothman. “A scattering theory for linear waves on the interior of Reissner-Nordström black holes”. In: *Ann. Henri Poincaré* 20.5 (2019), pp. 1583–1650.
- [58] C. Kehle and M. Van de Moortel. “The null contraction singularity at the Cauchy horizon of dynamical black holes”. In: *In preparation* (2023).
- [59] C. Kehle and M. Van de Moortel. “Strong cosmic censorship in the presence of matter: the decisive effect of horizon oscillations on the black hole interior geometry”. In: *Anal. PDE* 17.5 (2024), pp. 1501–1592.
- [60] J. Kommemi. “The global structure of spherically symmetric charged scalar field spacetimes”. In: *Comm. Math. Phys.* 323.1 (2013), pp. 35–106.
- [61] W. Li. *Kasner-like description of spacelike singularities in spherically symmetric spacetimes with scalar matter*. ArXiv preprint: <https://arxiv.org/abs/2304.04802>. 2023.
- [62] W. Li. *BKL bounces outside homogeneity: Einstein-Maxwell-scalar field in surface symmetry*. ArXiv preprint: <https://arxiv.org/abs/2408.12434>. 2024.
- [63] W. Li. *BKL bounces outside homogeneity: Gowdy symmetric spacetimes*. ArXiv preprint: <https://arxiv.org/abs/2408.12427>. 2024.
- [64] E. Lifshitz and I. Khalatnikov. “Investigations in relativistic cosmology”. In: *Adv. Phys.* 12.46 (Apr. 1, 1963), pp. 185–249.
- [65] J. Luk. “Singularities in General Relativity”. In: *Proceedings of the International Congress of Mathematicians* (2022).
- [66] J. Luk and S.-J. Oh. “Strong cosmic censorship in spherical symmetry for two-ended asymptotically flat initial data II: the exterior of the black hole region”. In: *Ann. PDE* 5.1 (2019).
- [67] A. Ori. “Inner structure of a charged black hole: an exact mass-inflation solution”. In: *Phys. Rev. Lett.* 67.7 (1991), pp. 789–792.
- [68] H. Ringström. “The Bianchi IX Attractor”. In: *Ann. Henri Poincaré* 2.3 (June 1, 2001), pp. 405–500.
- [69] I. Rodnianski and Y. Shlapentokh-Rothman. “Naked singularities for the Einstein vacuum equations: the exterior solution”. In: *Ann. of Math. (2)* 198.1 (2023), pp. 231–391.
- [70] I. Rodnianski and J. Speck. “On the nature of Hawking’s incompleteness for the Einstein-vacuum equations: The regime of moderately spatially anisotropic initial data”. In: *J. Eur. Math. Soc.* 24 (2018), pp. 167–273.
- [71] I. Rodnianski and J. Speck. “Stable Big Bang formation in near-FLRW solutions to the Einstein-scalar field and Einstein-stiff fluid systems”. In: *Sel. Math.* 24.5 (2018), pp. 4293–4459.
- [72] O. Sarbach, N. Straumann, and M. Volkov. “Internal structure of Einstein-Yang-Mills-dilaton black holes”. In: *Ann. Isr. Phys. Soc.* 13 (1997), pp. 163–171.

- [73] J. Smoller, A. Wasserman, and S.-T. Yau. “Existence of black hole solutions for the Einstein-Yang-Mills equations”. In: *Comm. Math. Phys.* 154.2 (1993), pp. 377–401.
- [74] J. Speck. “The Maximal Development of Near-FLRW Data for the Einstein-Scalar Field System with Spatial Topology \mathbb{S}^3 ”. In: *Comm. Math. Phys.* 364.3 (2018), pp. 879–979.
- [75] M. Van De Moortel. “Decay of weakly charged solutions for the spherically symmetric Maxwell-Charged-Scalar-Field equations on a Reissner-Nordström exterior space-time”. In: *Ann. Sci. Éc. Norm. Supér.* 55.2 (2022).
- [76] M. Van de Moortel. “Stability and instability of the sub-extremal Reissner-Nordström black hole interior for the Einstein-Maxwell-Klein-Gordon equations in spherical symmetry”. In: *Comm. Math. Phys.* 360.1 (2018), pp. 103–168.
- [77] M. Van de Moortel. “*Charged scalar fields on Black Hole space-times*, University of Cambridge”. University of Cambridge. PhD Thesis. 2019.
- [78] M. Van de Moortel. “Mass inflation and the C^2 -inextendibility of spherically symmetric charged scalar field dynamical black holes”. In: *Comm. Math. Phys.* 382.2 (2021), pp. 1263–1341.
- [79] M. Van de Moortel. “The breakdown of weak null singularities inside black holes”. In: *Duke Math. J.* 172.15 (2023), pp. 2957–3012.
- [80] M. Van de Moortel. *The Strong Cosmic Censorship Conjecture*. To be published in *Comptes Rendus. Mécanique*. Special issue for the 100th birthday of Yvonne Choquet-Bruhat. 2024.
- [81] M. Van de Moortel. “Violent Nonlinear Collapse in the Interior of Charged Hairy Black Holes”. In: *Arch. Ration. Mech. Anal.* 248.5 (2024), Paper No. 89.
- [82] M. Volkov and D. Galtsov. “Gravitating non-abelian solitons and black holes with Yang-Mills fields”. In: *Phys. Rep.* 319.1-2 (1999), pp. 1–83.
- [83] W. Zheng. *Asymptotically Anti-de-Sitter hairy black holes*. ArXiv preprint: <https://arxiv.org/abs/2410.04758>. 2024.
- [84] W. Zheng. *Exponentially-growing Mode Instability on Reissner–Nordström–Anti-de-Sitter black holes*. ArXiv preprint: <https://arxiv.org/abs/2410.04750>. 2024.